NATIONAL AERONAUTICS AND SPACE ADMINISTRATION

Technical Report 32-1302

The Surveyor V, VI, and VII Flight Paths and Their Determination From Tracking Data

R. G. Labrum
S. K. Wong
G. W. Reynolds

JET PROPULSION LABORATORY
CALIFORNIA INSTITUTE OF TECHNOLOGY
PASADENA, CALIFORNIA

December 1, 1968

NATIONAL AERONAUTICS AND SPACE ADMINISTRATION

Technical Report 32-1302

The Surveyor V, VI, and VII Flight Paths and Their Determination From Tracking Data

R. G. Labrum
S. K. Wong
G. W. Reynolds

JET PROPULSION LABORATORY
CALIFORNIA INSTITUTE OF TECHNOLOGY
PASADENA, CALIFORNIA
December 1, 1968

TECHNICAL REPORT 32-1302

Prepared Under Contract No. NAS 7-100
National Aeronautics and Space Administration

Preface

The work described in this report was performed by the Systems Division of the Jet Propulsion Laboratory under the cognizance of the *Surveyor* Project.

Foreword

This report is the third in a series of reports concerning the determination of the flight path of each of the seven *Surveyor* spacecraft. Related information for the *Surveyor I* and *II* spacecraft is contained in Technical Report 32-1285; and data for *Surveyors III* and *IV* are recorded in Technical Report 32-1292. This document describes the current best estimates of the *Surveyor V*, *VI*, and *VII* flight paths and the way in which they were determined. Postflight analysis of the tracking data has verified the adequacy of the inflight orbit determinations and provided valuable information regarding tracking station locations and physical constants.

Surveyors V, *VI*, and *VII* were launched from Cape Kennedy at two-month intervals during the period from September 1967 through January 1968. They successfully soft-landed on the moon at their prime targets which were, respectively, Mare Tranquillitatis, Sinus Medii, and the northern Tycho blanket. The science instrument payload of each of the *Surveyors* included, in addition to a survey television camera, an alpha scattering device for performing chemical analysis of the lunar surface. *Surveyor VII* also carried a soil mechanics/surface sampler instrument similar to those carried on *Surveyors III* and *IV*. A tremendous amount of data was obtained with each of these instruments.

The *Surveyor V* flight became nonstandard when, 18 hours after launch, the propellant pressurant gas began leaking, following the midcourse maneuver. Five additional midcourse maneuvers were performed which, ultimately, readjusted critical spacecraft and trajectory parameters so that an abbreviated terminal descent, compatible with the degraded propulsion system capability, was possible. The multiplicity of maneuvers and stringent timing requirements for nonstandard ground commanding during the terminal descent made the inflight orbit determination function particularly demanding for *Surveyor V*. The *Surveyor VI* and *VII* flights were very close to nominal in all respects.

This report is divided into four major parts. Discussion in the first part (Sections I through IV) applies, generally, to all three of the subject *Surveyors*, and it describes the basic orbit determination process, the tracking stations, and the inflight computational sequence. Other sections pertain to *Surveyors V*, *VI*, and *VII*, individually. Material covered includes the inflight orbit solutions, the postflight analysis, the comparison of the inflight and postflight results, and the analysis of the Air Force Eastern Test Range tracking data for the respective *Surveyor* flight.

The orbit determination group for *Surveyors V*, *VI*, and *VII*, headed by S. K. Wong, included R. G. Labrum, C. J. Vegos, S. J. Reinbold, and G. W. Reynolds. Mr. Labrum, the principal author of this report, coordinated all of the contributions and was co-author, with Mr. Wong, of Sections I through IV.

Foreword (contd)

Discussion of the inflight analysis for each flight (Sections V, IX, and XIII) was provided by Mr. Wong, Mr. Labrum, and Mr. Reynolds. Discussion of the post-flight analysis (Sections VI, X, and XIV) was provided by Mr. Wong and Mr. Labrum. Mr. Labrum also provided the Observations and Conclusions for each flight (Sections VII, XI, XV). The analysis of AFETR tracking data (Sections VIII, XII, XVI) was provided by Mr. Reynolds.

W. J. O'Neil

Contents

Contents (contd)

Contents (contd)

Tables

Contents (contd)

Tables (contd)

Contents (contd)

Tables (contd)

Figures

Contents (contd)

Figures (contd)

Contents (contd)

Figures (contd)

Contents (contd)

Figures (contd)

Abstract

To determine the current best estimates of the *Surveyor V*, *Surveyor VI*, and *Surveyor VII* flight paths, tracking data from DSS 11, DSS 42, DSS 51, DSS 61, and DSS 72 were analyzed. Significant blocks of bad data were detected and eliminated from the final solutions. Various combinations of parameters were estimated to achieve the best possible fit of the data with realistic orbit parameters. The current best estimates indicate that *Surveyors V*, *VI*, and *VII* landed 31.7 km, 6.9 km, and 4.2 km, respectively, from the final aim points. Landed locations estimated by analysis of post-touchdown data and *Lunar Orbiter* photographs are also presented for comparison. Deep Space Station locations, $GM_{\oplus}$, and $GM_{\leftmoon}$ were also determined from *Surveyor* tracking data. These solutions agree quite well with the solutions obtained from analysis of *Ranger* data. JPL postflight analysis of AFETR tracking data supplied during the near-earth phase of the *Surveyor* missions confirms the adequacy of the solutions provided inflight.

The *Surveyor V, VI,* and *VII* Flight Paths and Their Determination From Tracking Data

I. Introduction

This report describes the current best estimate of the *Surveyor V, VI,* and *VII* flight paths and the way in which they were determined. Postflight analysis of the Deep Space Instrumentation Facility (DSIF) tracking data has verified the adequacy of the inflight orbit determinations. For example, the current best estimates of the pre-midcourse maneuver unbraked lunar impact points differ from those obtained inflight by only 1.7, 1.2, and 0.9 km for *Surveyors V, VI,* and *VII,* respectively.

The *Surveyor* Project objectives are: (1) To accomplish successful soft landings on the moon as demonstrated by operations of the spacecraft subsequent to landing; (2) To provide basic data in support of *Apollo*; and (3) To perform operations on the lunar surface which will contribute new scientific knowledge about the moon and provide further information in support of *Apollo.*

Surveyors V, VI, and *VII* were launched from Cape Kennedy on September 8, 1967, November 7, 1967 and January 7, 1968, respectively; these last three spacecraft in the series more than fulfilled Project objectives. Although the *Surveyor V* mission was a nonstandard one—a helium leak in the vernier propellant pressurization system ultimately resulted in six midcourse maneuvers—all flight path functions were completed successfully, and lunar soft landing was achieved.

Surveyor inflight flight path analysis was the responsibility of the *Surveyor* flight path analysis and command (FPAC) team, which was staffed jointly by personnel affiliated with Hughes Aircraft Company and the Jet Propulsion Laboratory. The FPAC team comprised the following functional groups: tracking data analysis (TDA); orbit determination (OD), maneuver analysis (MA), trajectory (TRAJ) and computer support (CS). The FPAC activities for *Surveyors V, VI,* and *VII* are described in Refs. 1, 2, and 3, respectively. The purpose of this report is to give additional insight into the overall performance of the orbit determination function, specifically.

Data taken during free flight, only, is used for orbit solutions. This limitation resulted in a discontinuity at the midcourse maneuver epoch and led to a logical division of the tracking data into two blocks: (1) data taken prior to midcourse maneuver execution and (2) data taken after midcourse maneuver execution. Results of the inflight orbit solutions, based on these two blocks of data, were used primarily by the MA group to compute the midcourse and terminal maneuvers and to provide the best estimate of the time at which a ground command should be sent to initiate the terminal retroignition sequence in the event the onboard altitude marking radar (AMR) did not function. The solutions were also used by the trajectory group to obtain spacecraft trajectory information and view-period summaries, as well as by the TDA

group to generate observable predictions for the DSIF stations.

II. Computational Philosophy

A. Orbit Determination Program

The single-precision orbit determination program (SPODP) of the Jet Propulsion Laboratory (Ref. 4) is the principal analysis tool used for *Surveyor* orbit determination. This program utilizes an iterative, modified-least-squares technique to find that set of initial conditions at a given epoch which causes the weighted sum of squares of the tracking data residuals (defined as observed values minus computed values [O − C]) to be minimized. Here the term *modified* is used to indicate that the weighting of individual data types was accomplished in a different manner from that in the usual least-squares method. The single-precision Cowell trajectory program (SPACE) (Ref. 5) and the double-precision JPL development ephemeris 19 (DE-19) are used in conjunction with the SPODP.

The weighted-least-squares technique used for the parameter estimates has the refinement that *a priori* information on the parameters together with their statistics influence the estimate. The basic equations are:

$$\Delta \mathbf{q}_i = [\mathbf{A}^T\mathbf{W}\mathbf{A} + \tilde{\mathbf{\Gamma}}^{-1}]^{-1}\,[\mathbf{A}^T\mathbf{W}(\mathbf{O}-\mathbf{C}) + \tilde{\mathbf{\Gamma}}^{-1}\,\Delta\tilde{\mathbf{q}}_i]$$

and

$$\mathbf{q}_{i+1} = \mathbf{q}_i + \Delta\mathbf{q}_i$$

where

$\mathbf{q}_i$ = the estimate of the solution parameter vector $(m \times 1)$ on the ith iteration

$\mathbf{A}$ = the matrix of first order partial derivatives on each observable with respect to each solution parameter $(m \times n)$

$\mathbf{W}$ = the diagonal weighting matrix formed by taking the reciprocal of the *a priori* estimated effective variance on each observable $(n \times n)$

$\tilde{\mathbf{\Gamma}}$ = the *a priori* covariance matrix on the solution parameters $(m \times m)$

$\mathbf{O} - \mathbf{C}$ = the vector of differences between the observed data and the calculated data $(n \times 1)$

$\Delta\tilde{\mathbf{q}}_i$ = the difference between the *a priori* solution estimate and the ith iteration estimate $(m \times 1)$

The statistics associated with the parameter estimates are given in the covariance matrix $[\mathbf{A}^T\mathbf{W}\mathbf{A} + \tilde{\mathbf{\Gamma}}^{-1}]^{-1}$. From this expression, it can be seen that the statistics are a direct reflection of the data weights.

Trajectory perturbations caused by gas leaks in the attitude control systems were observed during the *Mariner IV* and *Pioneer VI* missions. Based on the post-flight analysis of *Mariner IV* data by G. Null (JPL), an improved model for handling nongravitational, non-drag trajectory perturbations was included in the Mod II version of the SPODP. The equations for this model are as follows:

$$\Delta\ddot{\mathbf{r}} = \left[f_1(1-\alpha_1\tau-\alpha_2\tau^2) + \frac{A_p}{m_p}\frac{(SC)}{r^2_{\odot,S/C}}(1+G+\Delta G)\right]\mathbf{U}_{SP}$$
$$+\left[f_2(1-\alpha_1\tau-\alpha_2\tau^2) + \frac{A_p}{m_p}\frac{(SC)}{r^2_{\odot,S/C}}(G_T+\Delta G_T)\right]\mathbf{T}$$
$$+\left[f_3(1-\alpha_1\tau-\alpha_2\tau^2) + \frac{A_p}{m_p}\frac{(SC)}{r^2_{\odot,S/C}}(G_N+\Delta G_N)\right]\mathbf{N} \qquad (1)$$

= change of acceleration of probe resulting from solar radiation pressure and such small forces as gas leaks in the attitude control system and non-coupled attitude-control jets.

where the solve-for parameters are:

f_1, f_2, f_3 = accelerations caused by gas leaks

α_1, α_2 = coefficients of polynomial in τ

G, G_T, G_N = solar radiation coefficients in the radial, tangential, and normal directions

and where the constants, or not-solve-for parameters, are:

$\tau = T_C - T_0$ where T_C = current time, T_0 = initial epoch

A_p = nominal area of spacecraft projected onto plane normal to sun–probe line, m^2

m_p = instantaneous mass of probe, kg

$r_{\odot,S/C}$ = distance from sun to probe, km

(SC) = spacecraft solar radiation constant

$$= \frac{J(\mathrm{AU})^2}{c} \times \frac{1\,\mathrm{km}^2}{10^6\mathrm{m}^2}$$

$$= 1.031 \times 10^8 \frac{\mathrm{km}^3\mathrm{kg}}{\mathrm{s}^2\mathrm{m}^2}$$

where

J = solar radiation constant

$= 1.383 \times 10^3\ \mathrm{W/m}^2$

$= 1.383 \times 10^3\ \mathrm{kg/s}^2$

AU = astronomical unit

$= 1.496 \times 10^8$ km

c = speed of light

$= 2.997925 \times 10^5$ km/s

$\mathbf{U}_{SP}$ = a unit vector directed out from the sun as in the case of a radiation pressure force. For *Surveyor*, this corresponds to the spacecraft $+Z$ direction (roll axis)

$\mathbf{T}$ = a unit vector in the direction of the projection of the spacecraft–Canopus vector in the plane normal to $\mathbf{U}_{SP}$. For *Surveyor* this corresponds to the spacecraft $-X$ direction (pitch axis)

$\mathbf{N}$ = a unit vector in the direction required to make T, N, U a right-handed orthogonal system. For *Surveyor*, this corresponds to the spacecraft $+Y$ direction (yaw axis)

$\Delta G, \Delta G_T, \Delta G_N$ = input values specified at up to 100 time points with linear interpolation between points

The portion of the trajectory during which these accelerations are estimated is under option control. That is, during a given orbit computation, the acceleration can be estimated either for specific parts of the trajectory or for the entire trajectory.

B. Data Weighting and Error Sources

The philosophy used for weighting data in the SPODP is to calculate a weight value based on the effective (or expected) variance of a given data type. The effective variance for a given data type is determined by summing up the variances caused by all known error sources. For two-way doppler data,[1] the error sources were divided into two general classes: (1) hardware or station equipment errors, and (2) software—i.e., computing and model errors. For the first class of errors, such items as transmitter reference oscillator stability, doppler counter roundoff error or quantization, and doppler counter error caused by dropped or added cycles in the presence of a low signal-to-noise ratio were considered. Of these, the major contributor is counter quantization error, which is estimated to be 0.017 Hz (equivalent to a velocity error of 0.0011 m/s) for a data sample rate of 60 s. For the second class of errors, it is known that certain model errors exist that are not adequately accounted for in the SPODP and are not sufficiently known so that they may be reflected in the effective variance. Among these are planetary and earth–moon ephemerides errors. The planetary ephemerides errors are negligible for a lunar trajectory, but earth–moon ephemerides errors will affect such quantities as predicted unbraked impact time, the unbraked time of arrival. This influence is evidenced by the fact that the predicted time tends to vary as more near-moon tracking data is included in the orbit solution. The error in the refraction correction model used to correct low-elevation data contributes a maximum of 1.07×10^{-4} m/s for a 60-s sample rate. In the ODP, statistics are based upon 1σ data weights, modified by an empirical refraction formula to account for varying elevation angles. Computing errors incurred within the program are the major contributors to the two-way doppler data weight. These errors (approximately 0.012 m/s for a 60-s sample rate) arise from the fact that most of the computations are done in single precision, which results in interpolation errors and the build up of roundoff errors. Based on the above error sources, the effective two-way doppler data weight is 0.013 m/s, which corresponds to 0.2 Hz for S-band stations.

The error sources associated with angular rate–hour angle (HA) and declination angle (dec) or azimuth angle (az) and elevation angle (el)—are:

(1) Angle jitter or variation about the aiming point caused by antenna drive servomechanisms.

(2) Angle correction errors caused by differences between the empirical correction model which is based on the antenna optical axis, and the RF pointing axis.

(3) Angular encoder readout errors caused by inaccuracies in the compensation cams. Resolution of the encoder is ± 1 count, which corresponds to 0.002 deg.

(4) Refraction correction errors caused by the difference between the atmospheric model used in the SPODP and the actual atmosphere at a given time.

[1]See Appendix A for a definition of tracking data types.

Of these, the dominant error sources are angle correction errors, which contribute an estimated variance of 0.033 deg^2 for a sample rate of 60 s. Based on this, an effective data weight of 0.18 deg was used for HA–dec and az–el data. In past missions, it was observed that a bias remained after applying the corrections to the angular data. Therefore, these data are usually omitted from the orbit solution as soon as enough two-way doppler data are available to obtain a good solution. An idea of the biases for both uncorrected and corrected angular data can be obtained by examining the residual plots for *Surveyor* V DSS 51 premaneuver angle data in Figs. 1 and 2. These residuals were obtained by passing a converged set of initial conditions through the angular data. This set of initial conditions was obtained from an orbit solution that used all premaneuver two-way doppler data in the fit; no angular data were used to obtain the conditions. The residuals are plotted vs HA, rather than time. Thus, the shape of the uncorrected residual plots (Fig. 1) will show the total deflection or pointing error (main antenna structure deflection plus quadripod deflection) as the antenna moves from one horizon to the other. Figure 2 shows the residuals of the same angular data after corrections that were intended to remove the systematic pointing errors were applied. These corrections are in the form of polynomial coefficients based on optical horizon-to-horizon star tracks. That is, a polynomial curve fit is made to the optical pointing errors[2] resulting from a given horizon-to-horizon star track. The results of a number of such star tracks, using different stars, are combined to obtain the actual polynomial coefficients used in the orbit data generator program (ODG) to correct the angular data prior to use in the ODP. Star tracks of stars which were not used in the polynomial curve fits are periodically conducted to validate the coefficients. A comparison between the corrected residuals (Fig. 2) and the uncorrected residuals (Fig. 1) shows that a large percentage of the skew and curvature has been removed by the angle corrections, but some bias still exists. Similar biases have been observed in all previous lunar and planetary missions. These biases are most likely effects of a difference between the antenna optical axis and the antenna RF axis. An optical ray path is from the source directly to a small telescope mounted near the bottom of the main paraboloidal reflector. On the other hand, the RF signal path is more complex. In general terms, an RF signal arriving at the main disk is reflected to a hyperboloidal reflector (part of the cassegrain feed system) located essentially at the apex (focal point of the paraboloid) of a quadripod structure approximately 36 ft above the bottom of the paraboloidal reflector. From the hyperboloid, the signal is reflected back to the cassegrain cone, which supports the cassegrain tracking feed. The net result is that another deflection has been introduced—namely, that of the quadripod structure. Efforts are now under way to use such RF sources as postlanding *Surveyor* tracking to generate more accurate correction coefficients. Even though the present corrections do not completely remove the systematic pointing errors, the corrected angular data are extremely valuable in converging to an orbit solution during the early part of a mission.

[2]The optical pointing error is defined as the difference between the known star position (in terms of topocentric hour angle and declination) at a given time and the corresponding antenna position at the same time.

C. Data Sample Rate

The sample spacing to be used at the tracking station is determined by the tradeoff between doppler counter rounding errors and truncation errors occurring in the doppler frequency computations. The expression used in the SPODP for the computations is

$$f(t_{ob}) = \int_{T-1/2\tau}^{T+1/2\tau} \ddot{F}(t)\, dt$$

where

$f(t_{ob})$ = the integrated doppler frequency which should be observed by a station at time t_{ob}

$T = t_{ob} - 1/2\,\tau$

τ = sample spacing

$F(t)$ = the instantaneous frequency of the doppler shift which should have been observed at time t.

This integral is evaluated by expanding a Taylor series about T and integrating term by term leading to

$$f(t_{ob}) = \tau \ddot{F}(t) + \frac{\tau^3}{24} F(t) + 0(F^{iv})$$

Thus, the truncation error is a function of τ and the fourth derivative of the frequency (which is dependent on the fifth derivative of range). Sample spacing has to be reduced during two phases of flight: (1) near earth, and (2) during midcourse maneuver. For these phases, a sample spacing of 10 s was used. At all other times a sample spacing of 60 s was used.

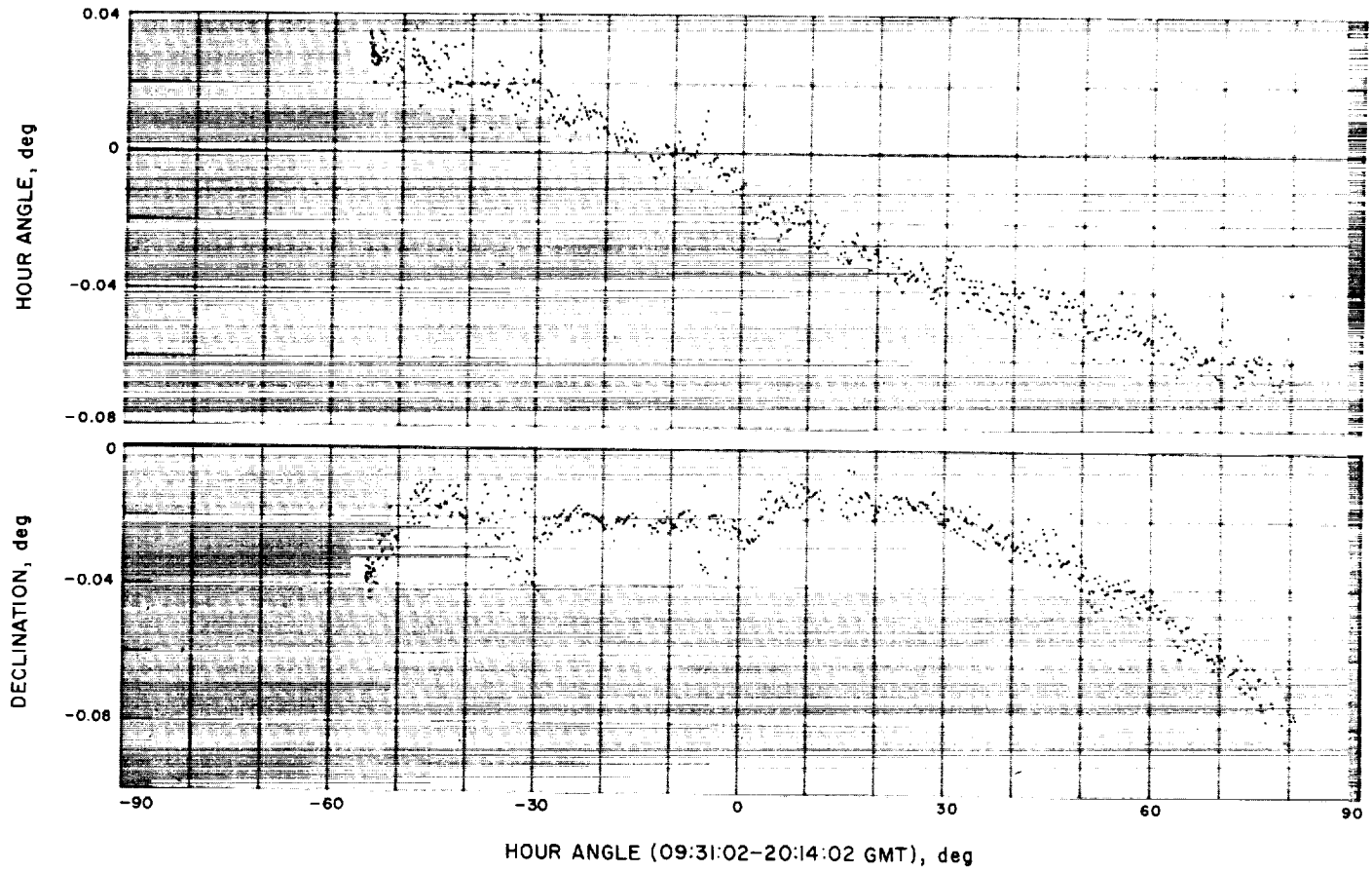

Fig. 1. DSS 51 uncorrected premaneuver angle residuals, *Surveyor V*

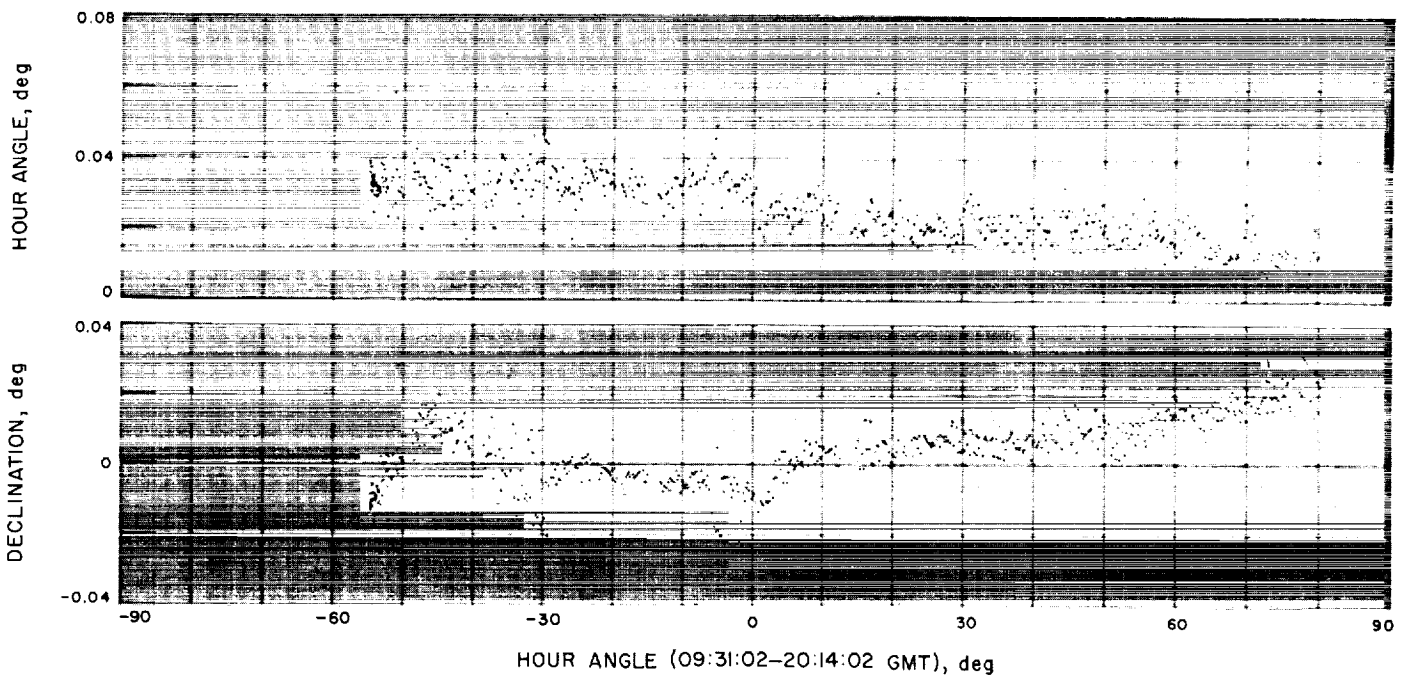

Fig. 2. DSS 51 corrected premaneuver angle residuals, *Surveyor V*

D. Data Editing

The JPL tracking data processor (TDP) and orbit data generator (ODG) programs are used to edit all incoming tracking data and to prepare a data file for input to the SPODP. Data points are first read into the TDP, which checks each data sample for acceptable format[3] to determine (1) if it is one of 30 acceptable message formats, (2) if each time in the sample is the proper field, and (3) if any item contains a missing or illegal character. It should be noted that, during flight operations, time does not permit reconstruction of data points that were rejected for bad format. The next item the TDP checks is the data condition code. A data point is given in bad data condition code when automatic detectors, at the station, sense that the data would be unusable. These detectors have manual overrides that are used whenever an equipment malfunction is suspected and, also, during periods when the transmitter is being retuned prior to transferring transmitting assignment to another station. A coarse in-range value check is made by the TDP to determine if each data type is within an acceptable limit—i.e., 360 deg for angle data and 10^4 Hz for doppler data. All data that either have passed these checks or is not rejected by a user option is time-sorted and written on disk and magnetic tape for access by the ODG. The ODG reads the data file and, if it includes angular data from DSS 42 or DSS 51, the values are corrected to remove systematic antenna pointing errors.

Next, the doppler data are checked for monotonicity, valid tracking mode, valid sample rate, and are converted from cycles to cycles per second by differencing adjacent samples, then dividing by the sample time. Pertinent transmitter and receiver frequencies are entered on the file with each doppler sample. These frequencies either are read in by the user or, in some formats, may be included with the data sample. The information is then written on disk and magnetic tape for access by the SPODP.

Blunder points are the data points rejected either by the TDP and ODG during validity checks or by applying the user rejection limits during the orbit computation. These limits are based on experience gained in previous missions and on the philosophy that it is better immediately to reject questionable points—if they could create difficulties in converging to an orbit—than it is to attempt to salvage every point. This choice is particularly preferable when very few data points are available during the early phase of the mission.

[3]See Appendix B for tracking data formats.

III. Description of DSIF Tracking Stations

Four DSIF stations provided tracking data for *Surveyors V, VI* and *VII*: the Pioneer Deep Space Station (DSS 11) at Goldstone, California; the Tidbinbilla Deep Space Station (DSS 42) at Canberra, Australia; the Johannesburg Deep Space Station (DSS 51) at Johannesburg, South Africa; and Robledo Deep Space Station (DSS 61) near Madrid, Spain. The Ascension Island Deep Space Station (DSS 72) participated as a backup facility for all three missions and supplied tracking data for *Surveyor V*. The locations[4] of these stations as used for *Surveyors V, VI*, and *VII* are given in Tables 1, 2, and 3, respectively. The locations are mission dependent because of the correction for polar motion, which is time dependent. Figure 3 is a simplified functional diagram of the prime tracking stations.

[4]Locations given here are values used in flight. For solved-for values, see parts F in Sections VI, X, and XIV.

Table 1. Deep Space Station locations for *Surveyor V*

Station	Geocentric radius, km	Geocentric latitude, deg	Geocentric longitude, deg
DSS 11	6372.0107	35.208362N	243.150980E
DSS 42	6371.6771	35.219199S	148.981630E
DSS 51	6375.5063	25.739237S	27.685668E
DSS 61	6369.9995	40.238790N	355.751300E
DSS 72	6378.2390	7.899938S	345.67362E

Table 2. Deep Space Station locations for *Surveyor VI*

Station	Geocentric radius, km	Geocentric latitude, deg	Geocentric longitude, deg
DSS 11	6372.0107	35.208368N	243.150980E
DSS 42	6371.6771	35.219204S	148.981640E
DSS 51	6375.5063	25.739290S	27.685660E
DSS 61	6369.9955	40.238792N	355.751310E
DSS 72	6378.2390	7.899925S	345.67363E

Table 3. Deep Space Station locations for *Surveyor VII*

Station	Geocentric radius, km	Geocentric latitude, deg	Geocentric longitude, deg
DSS 11	6372.0107	35.208390N	243.150950E
DSS 42	6371.6771	35.219236S	148.981660E
DSS 51	6375.5063	25.739291S	27.685646E
DSS 61	6369.9955	40.238810N	355.751340E
DSS 72	6378.2390	7.899901S	345.673620E

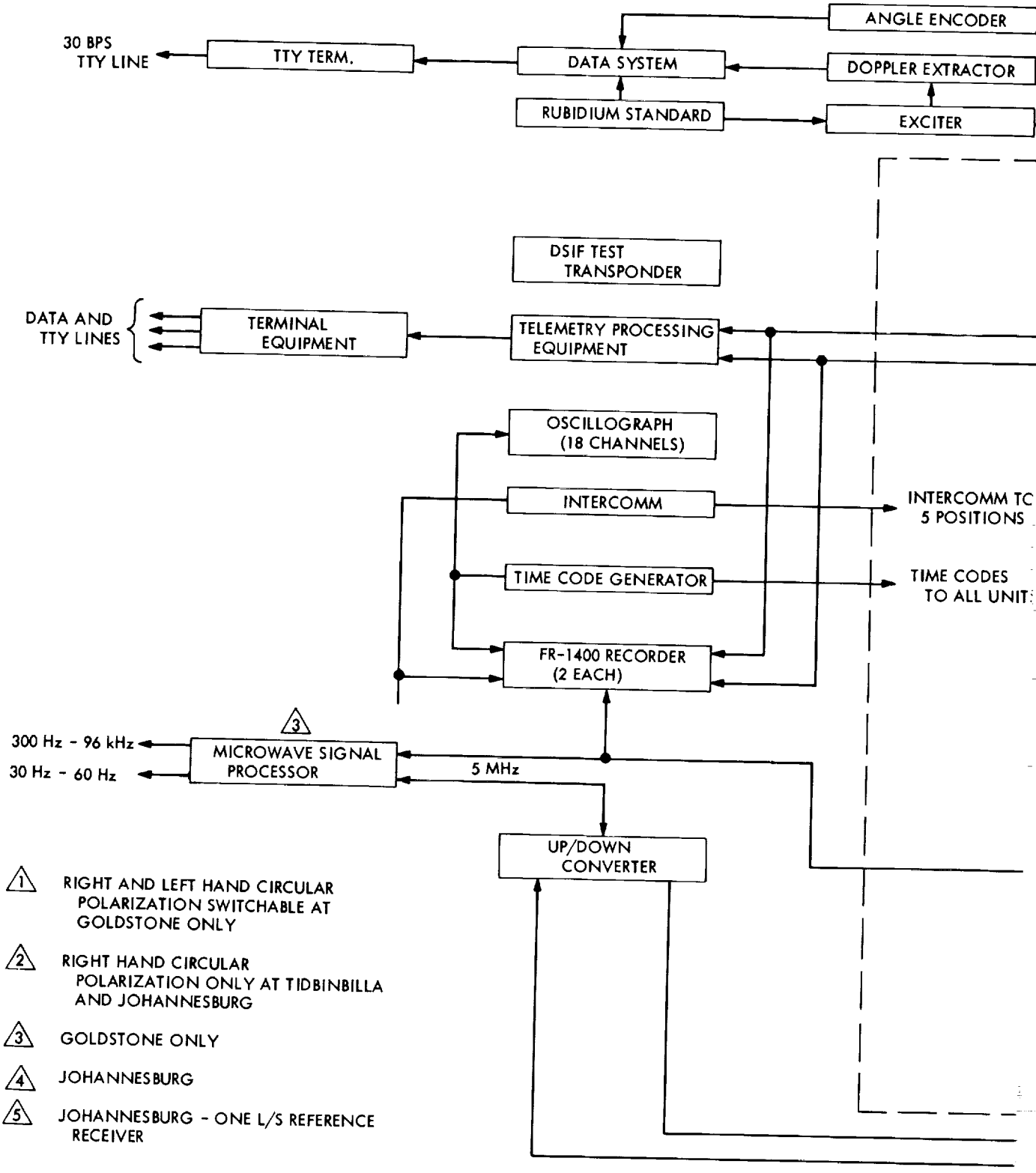
30 BPS
TTY LINE
TTY TERM.
DATA SYSTEM
ANGLE ENCODER
DOPPLER EXTRACTOR
RUBIDIUM STANDARD
EXCITER
DSIF TEST
TRANSPONDER
DATA AND
TTY LINES
TERMINAL
EQUIPMENT
TELEMETRY PROCESSING
EQUIPMENT
OSCILLOGRAPH
(18 CHANNELS)
INTERCOMM
INTERCOMM TC
5 POSITIONS
TIME CODE GENERATOR
TIME CODES
TO ALL UNIT
FR-1400 RECORDER
(2 EACH)
3
300 Hz - 96 kHz
30 Hz - 60 Hz
MICROWAVE SIGNAL
PROCESSOR
5 MHz
UP/DOWN
CONVERTER
1 RIGHT AND LEFT HAND CIRCULAR POLARIZATION SWITCHABLE AT GOLDSTONE ONLY
2 RIGHT HAND CIRCULAR POLARIZATION ONLY AT TIDBINBILLA AND JOHANNESBURG
3 GOLDSTONE ONLY
4 JOHANNESBURG
5 JOHANNESBURG - ONE L/S REFERENCE RECEIVER

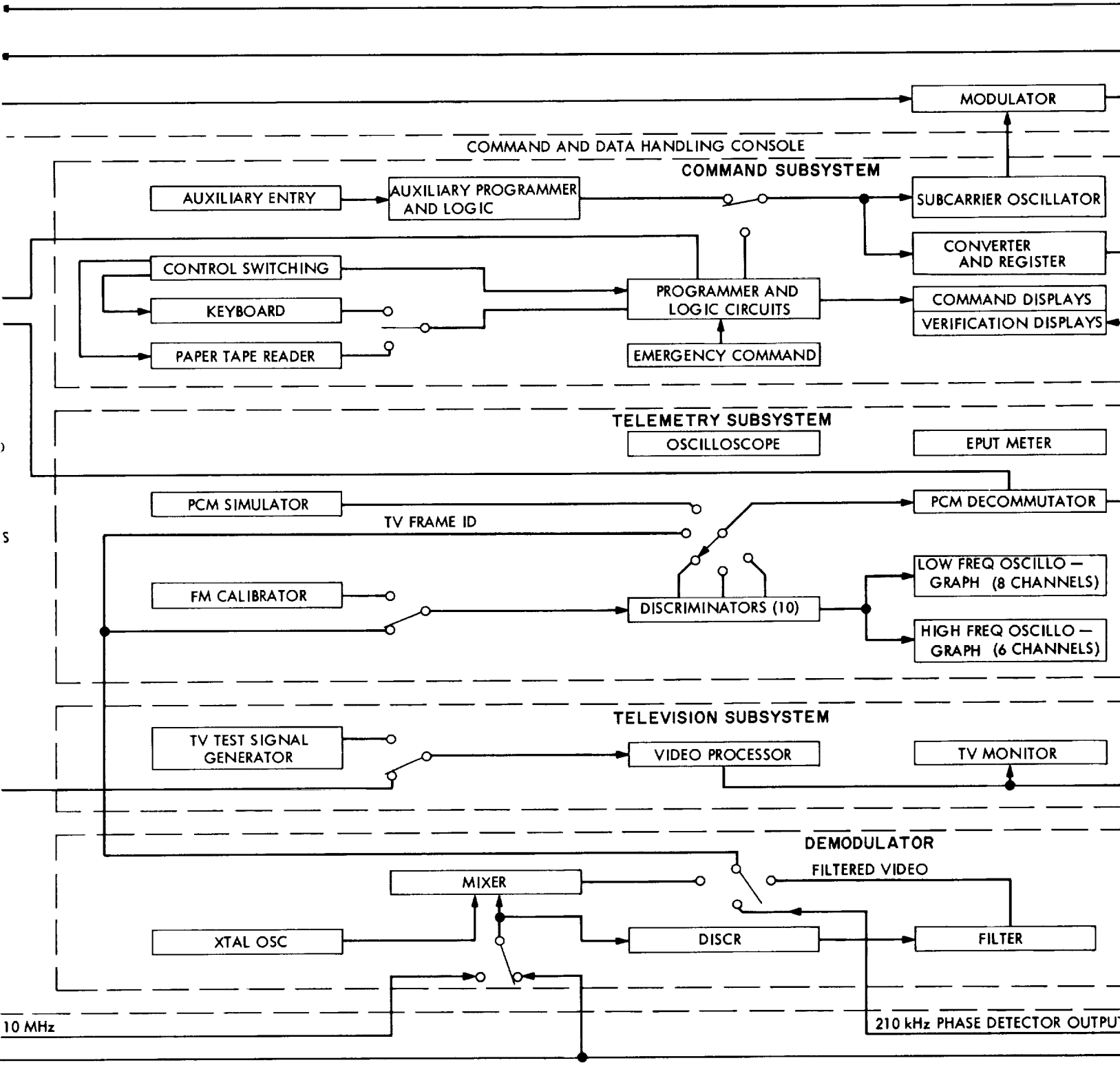

DEEP SPACE INSTRUMENTATION FACILITY, SURVEYOR CONFIGURATION

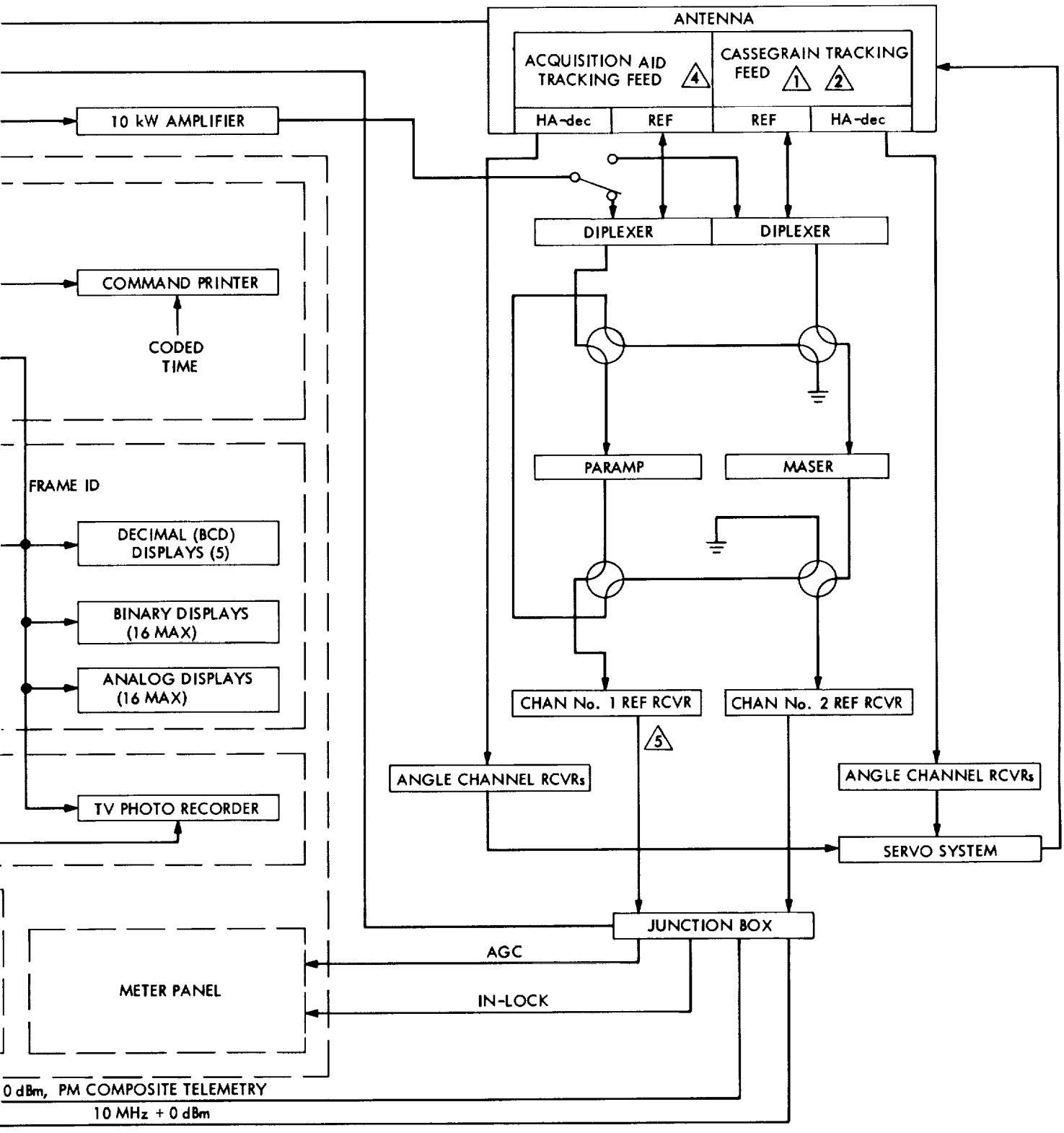

Fig. 3. S-band station block diagram

IV. Inflight Sequence and Solution Types

During the flight, the orbit solution is periodically updated as new tracking data becomes available. The nominal schedule on which these computations are made, together with the purpose of each computation, is given in Table 4. Because of the helium leak and subsequent midcourse maneuvers experienced with *Surveyor V*, the nominal schedule was not followed after the nominal LAPM orbit time. Since the computers are heavily loaded (it was necessitated that a number of different engineering programs be run at various intervals) throughout most of the mission, the type of orbit solution had to be held to a minimum; the number of parameters estimated in a solution were restricted to the minimum set that would still allow the orbit determination accuracy goals to be met.[5] Based on preflight, inflight and postflight analysis of data for *Surveyors I* through *IV* and *Ranger* Block III, it was determined that, in general, estimating only the position and velocity of the spacecraft at a given epoch is the best compromise between accuracy and computer time for inflight *Surveyor* orbit determination.[6] This conclusion is based on the assumption that the improved physical constants and station location parameter solutions obtained from the *Ranger* Block III and *Mariner II* and *IV* tracking data be used as nominal values. Numerical values of these, plus other critical constants, are given in Tables 1, 2, 3, and 5.

In the pre-midcourse maneuver phase, all orbit solutions are obtained by estimating only the standard six parameters. After midcourse maneuver execution, all pre-midcourse tracking data acquired between the initial DSS acquisition and the start of the premaneuver roll turn, are used to obtain a best-estimate pre-midcourse 6×6 orbit

[5]The *Surveyor* guaranteed orbit determination accuracy capabilities are given in Ref. 4.

[6]This type of orbit solution is commonly referred to as a 6×6 or *standard six*.

Table 4. Nominal schedule for orbit computations

Orbit ID	Time[a] of computation		Type solution	Purpose of computation
	Start	End		
ETR	L^a + 18 min	L + 1 h	6 × 6	Back up AFETR orbit computation, using AFETR C-band *Centaur* tracking data.
PROR	L + 1 h, 10 min	L + 1 h, 40 min	6 × 6	Estimate initial spacecraft orbit, based on DSS data-orbital elements used to generate acquisition predictions for DSS stations.
ICEV	L + 2 h, 10 min	L + 2 h, 55 min	6 × 6	Evaluate initial injection conditions.
PREL	L + 3 h, 20 min	L + 4 h, 10 min	6 × 6	Provide orbital and target information for preliminary midcourse study, and elements for updating acquisition predictions.
DACO	M^b − 10 h, 10 min	M − 7 h	6 × 6	Check data consistency and computations; validate consistency of all available data.
LAPM	M − 3 h, 45 min	M − 2 h, 45 min	6 × 6	Compute final pre-midcourse orbit to be used for determining midcourse maneuver corrections.
PRE M/C CLEANUP	M + 2 h	M + 4 h	6 × 6	Clean up orbit to generate *a priori* covariance matrix for post-midcourse orbit computations.
1 POM	M + 7 h	M + 9 h, 40 min	6 × 6	Make preliminary evaluation of midcourse maneuver execution; provide orbital elements to generate acquisition predictions for DSS stations.
2 POM	M + 12 h, 30 min	M + 14 h, 30 min	6 × 6	Update post-midcourse orbit solution based on post-midcourse data only.
3 POM	R^c − 24 h	R − 21 h, 30 min	6 × 6	Update post-midcourse orbit solution.
4 POM	R − 14 h, 5 min	R − 11 h, 5 min	6 × 6	Update post-midcourse orbit solution.
5 POM	R − 5 h, 40 min	R − 2 h, 50 min	6 × 6	Solve final post-midcourse orbit for determining terminal spacecraft altitude maneuvers.
FINAL OD	R − 2 h	R − 40 min	10 × 10	Obtain best estimate of unbraked impact time for AMR backup.

[a]Time reference to launch.
[b]Time reference to midcourse.
[c]Time reference to retromaneuver.

Table 5. Physical constants used for *Surveyor V, VI,* and *VII* missions

Constant	Value	SPODP symbolic designation	Space symbolic designation	Basic source
Earth gravitational coefficient, km^3/s^2	398601.27	KE	GME	*Ranger* Block III (Ref. 4)
Moon gravitational coefficient, km^3/s^2	4902.6309	KM	GMM	Ref. 4
Earth radius to convert lunar ephemeris to km, km	6378.1495	RE	REM	DE-19 ephemeris development
Earth radius to be used in the earth's oblate potential, km	6378.1650	—	RE	Ref. 4
Ephemeris–Universal Time reduction $\Delta T = ET - UT$, s	38.1	DUT	DUT	Internal document
Earth–moon mass ratio $GM_\oplus/GM_\leftmoon$	81.304389	—	—	*Ranger* Block III (Ref. 4)
Moments of inertia of moon for lunar oblate potential, kg-km^2	$0.88778216 \times 10^{29}$	—	A	Derived from *Ranger* Block III value of KM
	$0.88796612 \times 10^{29}$	—	B	
	$0.88833394 \times 10^{29}$	—	C	
Coefficient of second harmonic in earth's oblateness	0.00162345	J	J	Ref. 4
Coefficient of third harmonic in earth's oblateness	−0.00000575	H	H	Ref. 4
Coefficient of fourth harmonic in earth's oblateness	0.000007875	D	D	Ref. 4
Speed of light, km/s	299792.5	—	—	Ref. 4
Lunar radius at aim point, *Surveyor V*, km	1734.9	RSTOP	—	ACIC Lunar Charts, *Ranger, Surveyor,* and *Lunar Orbiter*
Lunar radius at aim point, *Surveyor VI*, km	1736.0	—	—	
Lunar radius at aim point, *Surveyor VII*, km	1736.6	—	—	

solution. The state vector (probe position and velocity) at injection epoch is integrated forward to the end of midcourse motor burn and incremented by the commanded midcourse velocity change. The resulting vector is then used as the initial estimate of the spacecraft post-midcourse orbit.

During the post-midcourse maneuver phase, from end of midcourse motor burn until lunar encounter (E) minus 5 h 40 min the orbit solutions are based on estimating only the standard six parameters. The spacecraft terminal attitude maneuvers are computed from the final 6×6 orbit solution. The rationale here is the same as that used for the premaneuver 6×6 solutions. That is, even though model and ephemerides errors exist, and errors might occur from differences between the assumed values of physical constants and station locations and the *true* values, the orbit determination accuracy goal can be achieved by estimating only the standard six orbital parameters.

To provide an effective backup for the *Surveyor* altitude marking radar, the type of orbit solution must be changed during the last few hours of the mission. The backup consists of transmitting a retroignition sequence turn-on command (from a ground station) at a time such that if a turn-on pulse has not been generated by the AMR by the time the backup command reaches the spacecraft, it will initiate the sequence. Operationally, the transmission time is intentionally biased late enough for the AMR to have ample opportunity to function but yet in time to save a significant percentage of missions in the event the AMR does not function. This biasing requires that the SPODP be capable of predicting the unbraked impact time to within an uncertainty of approximately 0.5 s (1σ). The uncertainty must include all error sources. Error sources, exclusive of tracking data errors, that significantly affect the predicted unbraked impact time are: (1) assumed value of lunar elevation at the impact point; (2) errors in earth–moon ephemerides, and (3) timing errors. The lunar elevation was obtained from NASA Langley Research Center; it is in close agreement with the elevation based on the Air Force Aeronautical Chart and Information Center (ACIC) lunar charts, less 2.4 km. The 2.4 km is the amount by which elevations based on the appropriate ACIC lunar charts exceed elevations obtained from the *Ranger VI, VII,* and *VIII* tracking data. An *a priori* 1σ uncertainty of ± 1 km

(roughly equivalent to ±0.4 s) is assigned to the elevation. A study using *Ranger* Block III tracking data indicated that the remaining two error sources could be adequately reduced by relying heavily on the near-moon tracking data and processing the data in the following manner:

(1) Process all available two-way doppler data from the midcourse epoch to approximately encounter $E-5$ h, 40 min and map the resulting solution, plus the covariance matrix, to the time of the last data point. There is nothing significant about the $E-5$ h, 40 min epoch, other than the fact that it is consistent with nominal sequence of events items. Degrade the diagonal elements of the mapped covariance matrix by 0.25 km² on position components and by 1×10^{-10} km²/s² on velocity components.

(2) Expand the estimate list to include geocentric radius and longitude of the two observing stations. That is, the type solution is expanded to a 10×10. *A priori* uncertainties of 12 m in spin axis distance, 40 m in station longitude, and 25 m in longitude difference between the two stations are added to the mapped covariance matrix.

(3) Reduce the effective data weight to 0.003 m/s (0.0195 Hz) to obtain realistic statistics on predicted unbraked impact time. This reduction is valid, since computational errors are no longer a major error source, the trajectory being integrated over a 6-h period, only. Also, the model errors have been taken into account by degrading the covariance matrix and by adding the station parameters to the estimate list.

V. *Surveyor V* Inflight Orbit Determination Analysis

A. View Periods and Tracking Patterns

Figure 4 summarizes the tracking station view periods and their data coverage for the period from launch to lunar touchdown. Figures 5 through 9 are tracking station stereographic projections that show the trace of the spacecraft trajectory for the view periods in Fig. 4. Table 6 summarizes the tracking data used for both inflight and postflight orbital calculations and analyses. This table provides a general picture of the performance of the data recording and handling systems.

B. Pre (First) Maneuver Orbit Estimates

The first estimate of the spacecraft orbit (PROR XA) based on DSS data only was completed at $L+1$ h, 45 min, based on 35 min of DSS 51 two-way doppler and angle (HA–dec) data. Although it was based on only 35 min

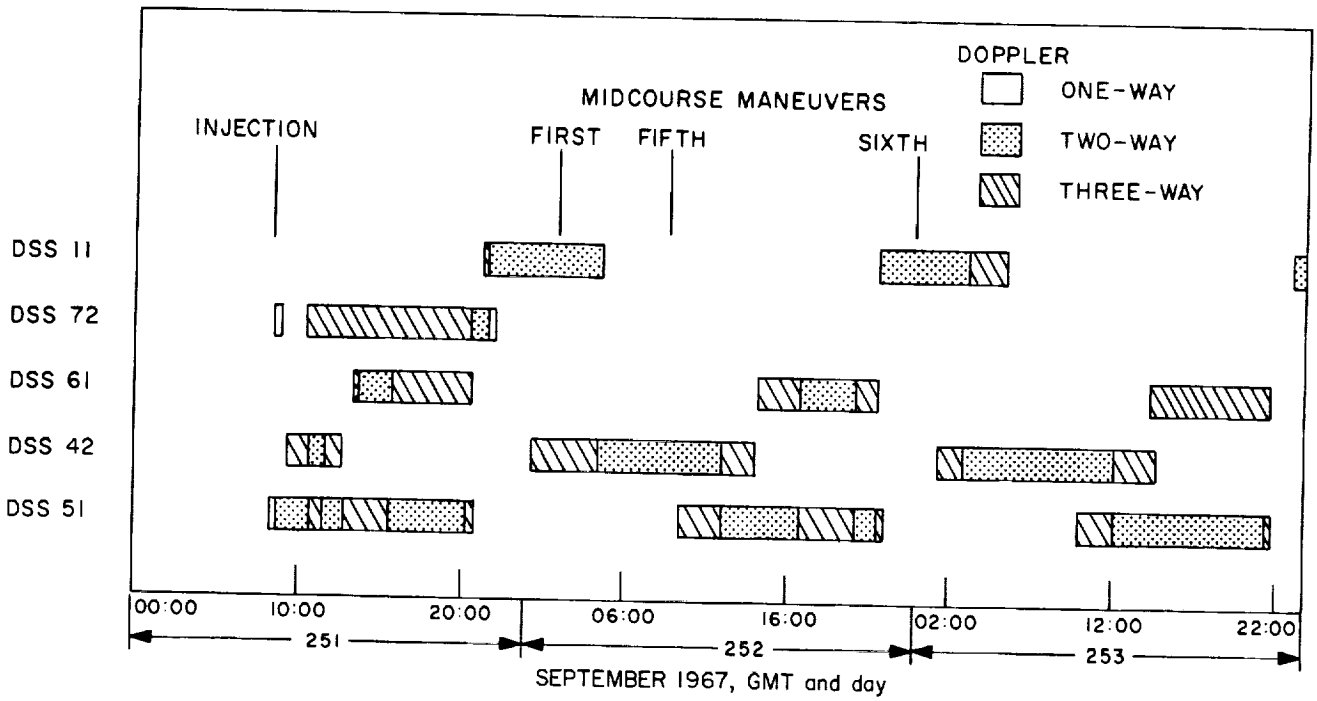

Fig. 4. DSS tracking coverage for *Surveyor V*

Table 6. Summaries of data used in orbit determination, *Surveyor V*

Station	Data type	Points recd	Points used in real time		Bad format		Bad data condition code		Blunder points		Rejection limits on blunder points	Points used in postflight analysis, best estimate orbit
			Number	% of recd	Number	% of recd	Number	% of recd	Number	% of recd		
Pre (first) maneuver data												
DSS 11	CC3	375	317	84.5	2	0.5	2	0.5	27	7.2	CC3, Hz 0.12 for 10-s sample rate 0.03 for 60-s sample rate Angles, deg 0.1	206
DSS 42	CC3	60	46	76.7	0	0.0	9	15.0	51	85.0		0
DSS 42	HA	267	78	29.2	0	0.0	11	4.1	36	13.5		0
DSS 42	Dec	267	78	29.2	0	0.0	11	4.1	58	21.7		0
DSS 51	CC3	669	573	85.7	15	2.2	18	2.7	12	1.8		554
DSS 51	HA	943	261	27.7	17	1.8	26	2.8	18	1.9		0
DSS 51	Dec	943	261	27.7	17	1.8	26	2.8	20	2.1		0
DSS 61	CC3	156	38	24.4	0	0.0	8	5.1	20	2.1		46
DSS 72	CC3	59	35	59.3	0	0.0	9	15.3	0	0.0		39
Pre (sixth) maneuver data												
DSS 11	CC3	387	120	31.0	1	0.3	12	3.1	38	9.8		120
DSS 42	CC3	226	158	69.9	0	0.0	7	3.1	219	96.9		0
DSS 51	CC3	364	309	84.9	0	0.0	18	5.0	5	11.4		309
DSS 61	CC3	207	108	52.2	0	0.0	6	2.9	0	0.0		191
Post (sixth) maneuver data												
DSS 11	CC3	244	220	90.2	8	3.3	12	4.9	5	2.0		213
DSS 42	CC3	534	448	83.9	0	0.0	5	0.9	0	0.0		448
DSS 51	CC3	571	448	78.5	1	0.2	13	2.4	27	4.7		444

of data, this orbit indicated that a lunar encounter would be achieved and that the correction required to hit the prelaunch aim point was well within the nominal midcourse correction capability. These results were further verified by the second (ICEV) and third (PREL) orbit computations completed at $L + 3$ h and $L + 3$ h, 52 min, respectively.

When sufficient data were received, the angle data were weighted out of the orbit solution. This was done first during the ICEV XB orbit. The resulting change of 0.8 km in the **B** vector indicates an unusually good agreement between the doppler and angle data.

During the data consistency (DACO) orbit computation period, data were received from DSS 61 and DSS 72. Data from all DSS stations received up to this time seemed to be consistent, i.e., no significant biases were discovered. The first pass of DSS 61 data had a maximum elevation angle of 16.9 deg. However, DSS 61 data was of much better quality than it had been for the past three *Surveyor* missions.

By the end of the DACO orbit computations ($L + 11$ h, 10 min), it had been decided to execute the maneuver at approximately $L + 18$ h. All indications were that a small maneuver (approximately 14 m/s) would be required.

At the beginning of the last pre-midcourse (LAPM) orbit computation period, the following amount of usable two-way doppler data were available: 1 h, 18 min from DSS 11; 49 min from DSS 42; 8 h, 33 min from DSS 51; 53 min from DSS 61; and 48 min from DSS 72.

The LAPM orbit solutions indicated that data from DSS 11 were consistent with the other DSS data. After updating the ODP data file, the pre-midcourse orbit (LAPM XB)—on which the first maneuver was based—was run. This orbit utilized all the two-way doppler data to midcourse minus 3 h 16 min, except DSS 61, which was eliminated because of low elevation angles. When mapped to target, this solution predicted an unbraked impact point at 2.34° N lat and 23.74° E lon. The numerical results of the inflight pre (first) maneuver orbit computations are presented in Tables 7 and 8. Amounts and types of tracking data used in the various orbit computations, together with the associated noise statistics, are given in Table 9. Epochs used in all inflight solutions are given in Table 10.

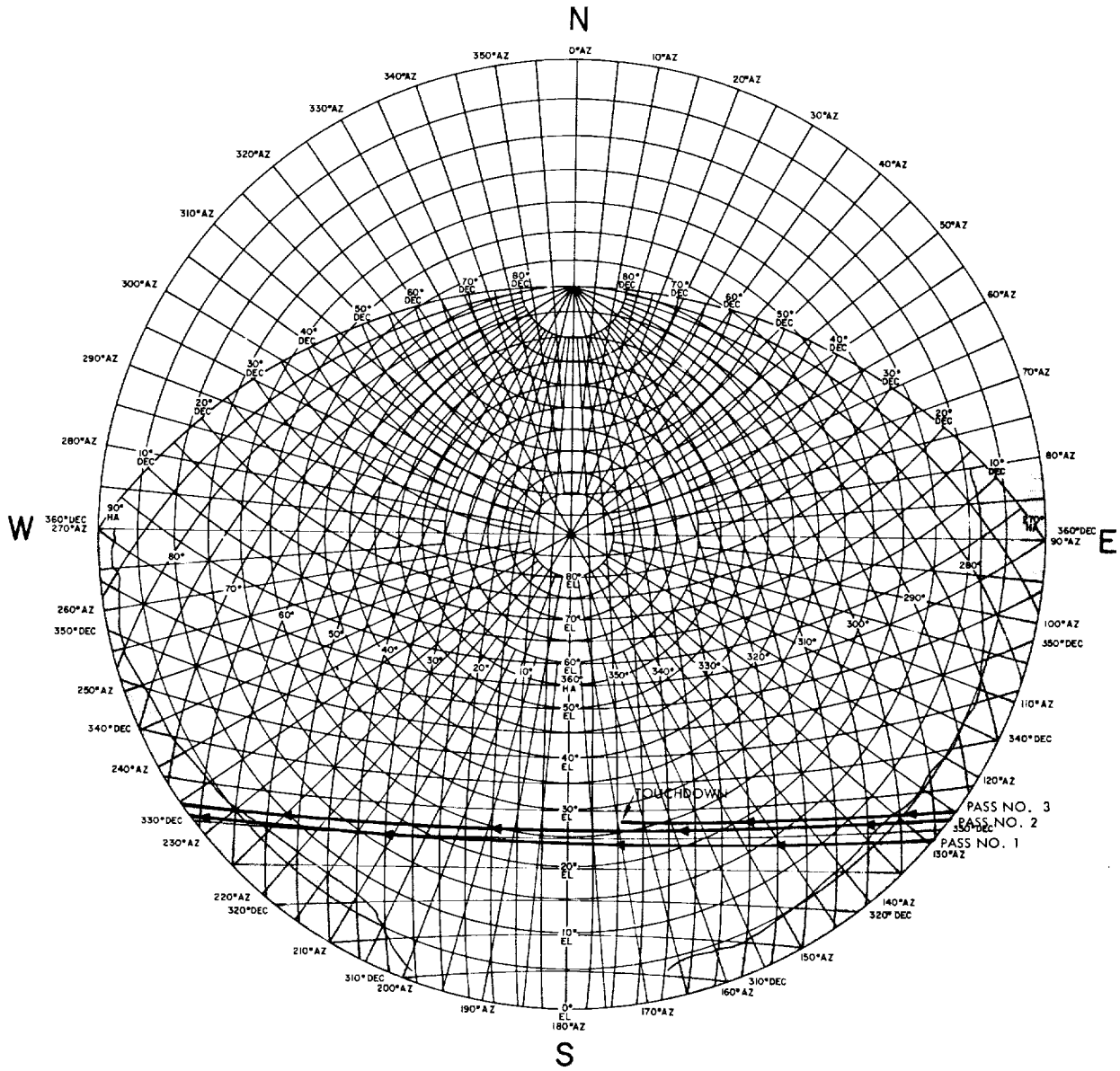

Fig. 5. DSS 11 stereographic projection, *Surveyor V*

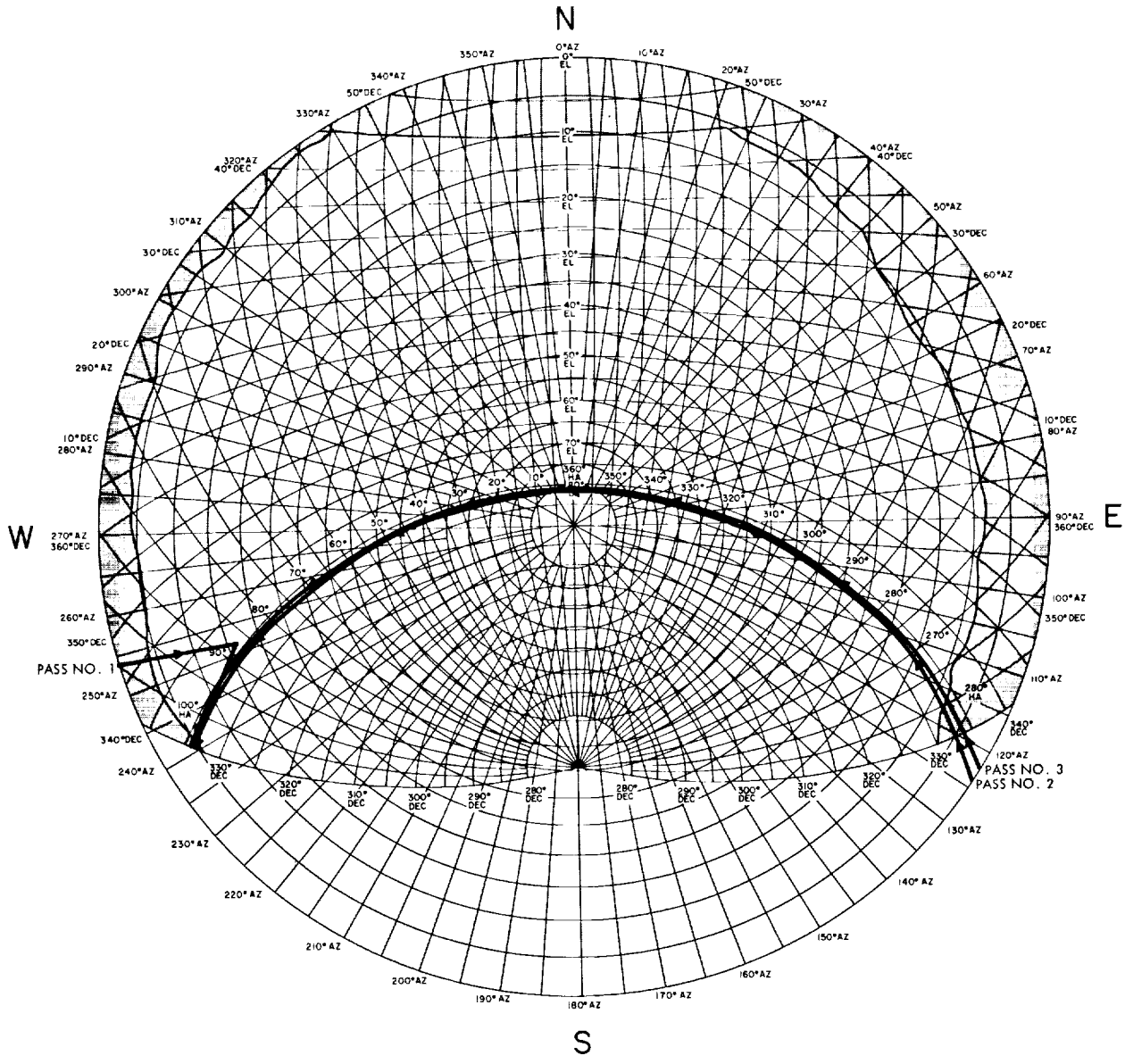

Fig. 6. DSS 42 stereographic projection, *Surveyor V*

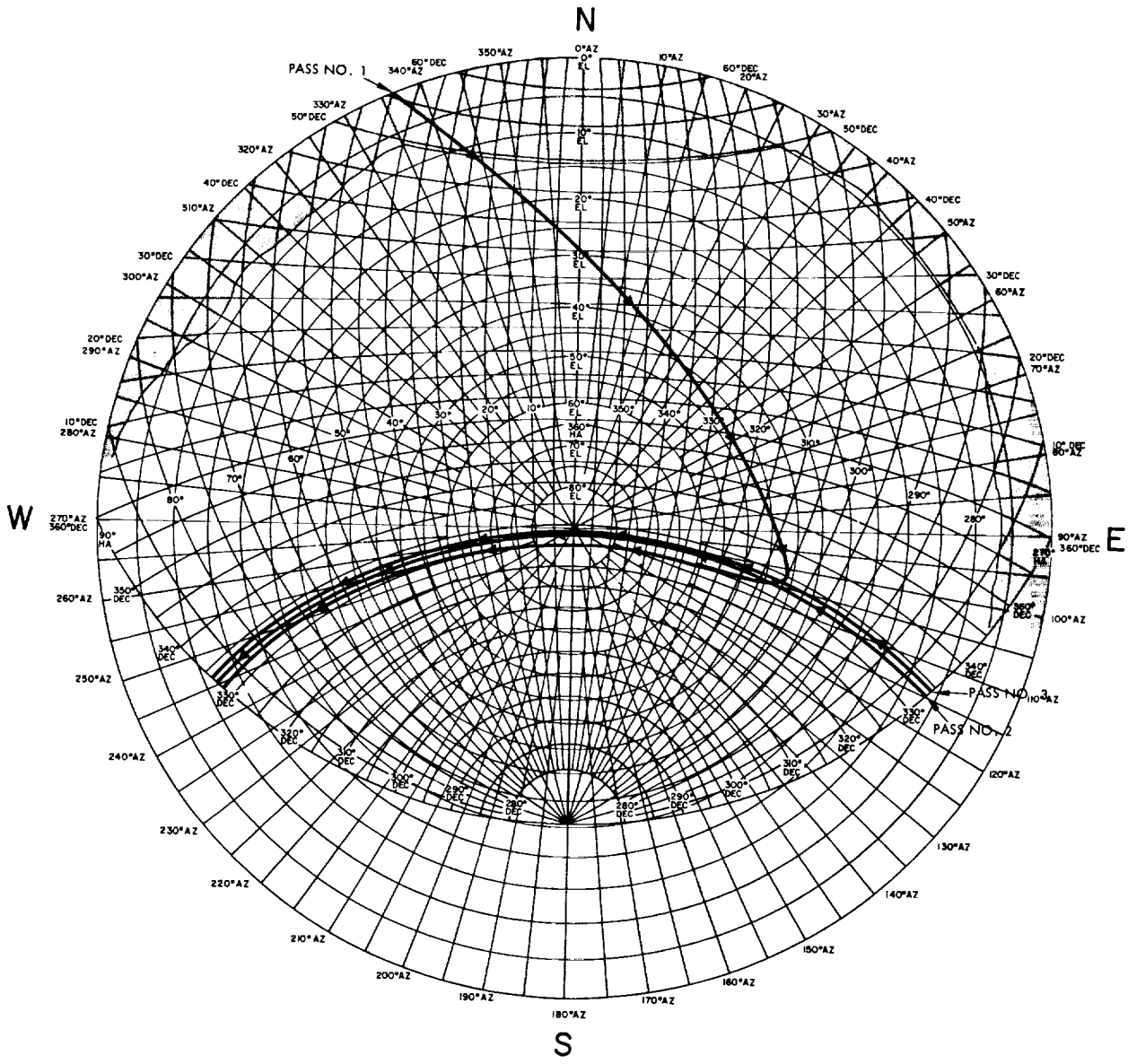

Fig. 7. DSS 51 stereographic projection, *Surveyor V*

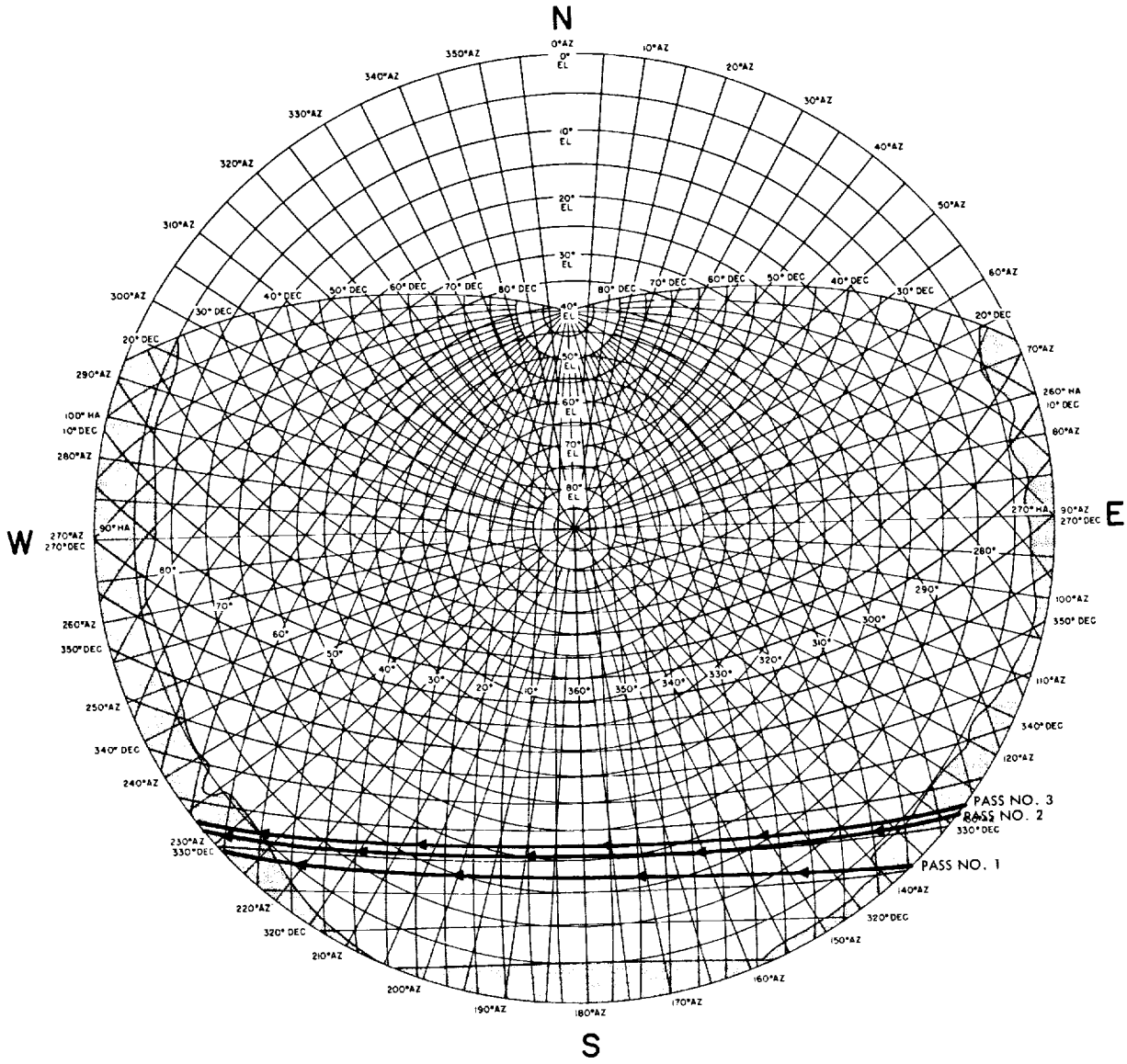

Fig. 8. DSS 61 stereographic projection, *Surveyor V*

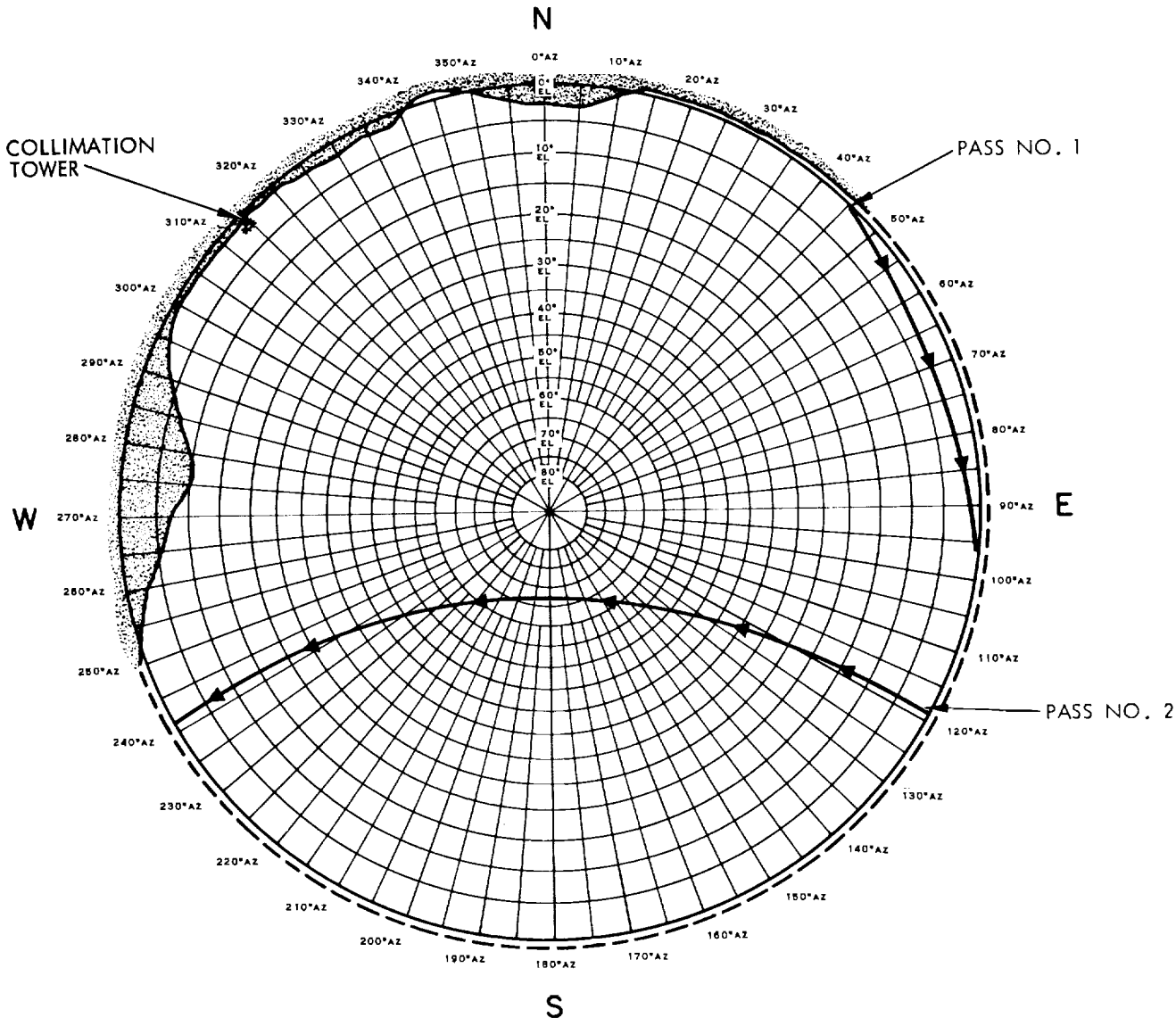

Fig. 9. DSS 72 stereographic projection, *Surveyor V*

Table 7. *Surveyor V* premaneuver computations

Orbit ID	Time computed, GMT		Target statistics[a]								
	Start	Stop	B, km	B • TT, km	B • RT, km	TL, h	SMAA, km (1σ)	SMIA, km (1σ)	THETA, deg	$\sigma_{T,impact}$, s (1σ)	PHI_{99}, deg
PROR XA	09:12	09:42	2866.8	2823.5	−496.8	63.12	123.19	27.63	98.15	48.184	3.927
PROR YA	09:13	10:47	2895.4	2878.1	−315.9	63.12	98.90	15.40	91.65	44.267	3.561
ICEV XA	10:20	10:36	2903.9	2891.5	−268.4	63.12	81.93	8.58	92.15	34.388	2.753
ICEV YA	11:11	11:33	2908.7	2896.9	−262.6	63.12	26.77	6.704	97.34	6.7095	0.6320
ICEV XB	10:36	10:55	2904.7	2896.3	−220.8	63.12	25.08	6.868	95.99	6.5323	0.6125
PREL YA	11:37	11:55	2904.6	2896.2	−221.1	63.12	17.92	6.866	95.23	4.8304	0.4728
DACO XA	13:57	14:20	2904.3	2896.3	−215.7	63.12	13.69	3.245	94.95	3.4506	0.3212
DACO YA	14:46	15:45	2904.7	2896.4	−220.3	63.12	30.76	5.249	97.94	7.8936	0.6938
DACO YB	16:50	17:33	2904.9	2897.2	−211.2	63.12	22.31	3.792	104.3	6.2880	0.4887
DACO XG	17:34	17:53	2904.3	2895.8	−221.8	63.12	4.615	2.894	113.8	0.94885	0.0907
DACO XI	18:05	18:17	2904.1	2895.5	−222.7	63.12	3.269	2.195	69.38	0.70757	0.0819
DACO XJ	18:52	19:07	2903.8	2895.3	−222.2	63.12	3.172	2.071	67.87	0.68499	0.0789
LAPM XA	22:10	22:23	2903.5	2895.0	−221.7	63.12	2.971	2.063	69.41	0.68097	0.0754
LAPM XB[b]	22:43	22:59	2903.2	2894.9	−219.7	63.12	8.811	3.651	78.00	1.7105	0.2268
LAPM YA	22:09	22:18	2903.2	2894.8	−221.2	63.12	2.752	2.154	71.70	0.67634	0.0727
LAPM YB	22:24	23:22	2903.4	2894.9	−221.8	63.12	2.862	2.161	72.51	0.69898	0.0757
LAPM XC	23:08	23:27	2902.9	2894.6	−219.3	63.12	8.792	3.593	78.32	1.6869	0.2241
PRCL YA	06:43	07:09	2903.2	2894.7	−221.1	63.12	2.515	2.037	69.98	0.67145	0.0692
PRCL YC	08:19	08:39	2903.3	2894.7	−220.7	63.12	2.373	2.010	61.62	0.66585	0.0678
PRCL YD[c]	10:29	10:53	2903.0	2894.7	−218.9	63.12	7.053	3.143	77.51	1.4345	0.1848
PRCL YE	11:31	11:45	2902.9	2894.6	−219.5	63.12	7.896	3.368	82.77	1.4383	0.1889

[a]Statistics are defined as follows:
SMAA = Semi-major axis of dispersion ellipse.
SMIA = Semi-minor axis of dispersion ellipse.
THETA = Orientation angle of dispersion ellipse measured counterclockwise from B • TT axis.
$\sigma_{T,impact}$ = Uncertainty in predicted unbraked impact time.
[b]Orbit used for first midcourse maneuver computations.
[c]Inflight best estimate, premaneuver.

Table 7 (contd)

Orbit ID	Target statistics[a] (contd)		Selenocentric conditions at unbraked impact		Solution type	Data type and source
	SVFIXR, m/s (1σ)	Latitude, deg (Positive N)	Longitude, deg (East)	Time, Sept. 10, 1967, GMT		
PROR XA	0.6309	7.26	22.087	23:25:02.413	6 × 6	DSS 51, CC3 and angles
PROR YA	0.6270	4.04	23.34	23:24:58.089	6 × 6	DSS 51, CC3 and angles; DSS 42, angles
ICEV XA	0.6233	3.21	23.68	23:25:07.173	6 × 6	DSS 51, CC3 and angles; DSS 42, angles
ICEV YA	0.6187	3.11	23.84	23:25:02.078	6 × 6	DSS 51 and DSS 42, CC3 and angles
ICEV XB	0.6187	2.36	23.78	23:25:13.901	6 × 6	DSS 51 and DSS 42, CC3
PREL YA	0.6186	2.36	23.78	23:25:13.842	6 × 6	DSS 51 and DSS 42, CC3
DACO XA	0.6186	2.27	23.78	23:25:15.121	6 × 6	DSS 51, DSS 42, DSS 61, CC3
DACO YA	0.6187	2.35	23.78	23:25:14.074	6 × 6	DSS 51, CC3
DACO YB	0.6186	2.19	23.80	23:25:16.389	6 × 6	DSS 51 and DSS 61, CC3
DACO XG	0.6185	2.37	23.77	23:25:13.647	6 × 6	DSS 51, DSS 42, DSS 61, CC3
DACO XI	0.6185	2.39	23.76	23:25:13.550	6 × 6	DSS 51 and DSS 42, CC3
DACO XJ	0.6185	2.38	23.75	23:25:13.621	6 × 6	DSS 51, DSS 42, and DSS 72, CC3
LAPM XA	0.6185	2.37	23.74	23:25:13.662	6 × 6	DSS 51, DSS 42, DSS 72, and DSS 11, CC3
LAPM XB[b]	0.6186	2.34	23.74	23:25:13.907	6 × 6	DSS 51, DSS 42, DSS 72, and DSS 11, CC3
LAPM YA	0.6185	2.36	23.74	23:25:13.669	6 × 6	DSS 51, DSS 42, DSS 72, and DSS 11, CC3
LAPM YB	0.6185	2.37	23.74	23:25:13.514	6 × 6	DSS 51, DSS 42, and DSS 11, CC3
LAPM XC	0.6186	2.33	23.73	23:25:14.028	14 × 14	DSS 51, DSS 42, DSS 72, and DSS 11, CC3; estimate radius and longitude
PRCL YA	0.6185	2.36	23.74	23:25:13.689	6 × 6	DSS 51, DSS 42, DSS 72, DSS 11, CC3
PRCL YC	0.6185	2.35	23.73	23:25:13.703	6 × 6	DSS 51, DSS 42, DSS 72, DSS 11, DSS 61, CC3
PRCL YD[c]	0.6185	2.32	23.73	23:25:14.005	16 × 16	DSS 51, DSS 42, DSS 72, DSS 11, DSS 61, CC3; estimate radius and longitude
PRCL YE	0.6185	2.33	23.73	23:25:13.947	14 × 14	DSS 51, DSS 42, DSS 72, DSS 11, CC3; estimate radius and longitude

Table 8. *Surveyor V* premaneuver position and velocity at injection epoch[a]

Orbit ID	Geocentric space-fixed position			Geocentric space-fixed velocity			Uncertainties, 1σ					
							Position			Velocity		
	x, km	y, km	z, km	Dx, km/s	Dy, km/s	Dz, km/s	σ_x, km	σ_y, km	σ_z, km	σ_{Dx}, m/s	σ_{Dy}, m/s	σ_{Dz}, m/s
PROR XA	197.43497	6028.8303	2566.5860	−10.268759	2.0937569	−3.2190433	1.0450	2.0215	1.6344	1.1824	1.7390	1.4700
PROR YA	198.12558	6025.4960	2568.6301	−10.270642	2.0968803	−3.2174597	0.7979	1.5273	1.4609	0.8598	0.7955	1.1072
ICEV XA	198.06001	6024.7962	2569.1682	−10.270870	2.0975514	−3.2175267	0.51803	1.2832	1.2098	0.70875	0.53805	0.79002
ICEV YA	198.39291	6024.4151	2569.2686	−10.271321	2.0978217	−3.2167871	0.15259	0.60944	0.42157	0.47989	0.34132	0.57765
ICEV XB	198.53009	6023.4483	2569.9849	−10.272125	2.0980412	−3.2158007	0.14949	0.58116	0.40449	0.46878	0.32050	0.57427
PREL YA	198.52798	6023.4562	2569.9799	−10.272119	2.0980366	−3.2158078	0.12970	0.42481	0.29753	0.35354	0.27456	0.44497
DACO XA	198.55084	6023.3296	2570.0699	−10.272225	2.0980722	−3.2156752	0.09770	0.33106	0.22477	0.27676	0.15586	0.35135
DACO YA	198.52667	6023.4444	2569.9896	−10.272124	2.0980454	−3.2158079	0.17865	0.70354	0.47947	0.58392	0.33989	0.76024
DACO YB	198.56863	6023.2296	2570.1380	−10.272295	2.0981272	−3.2156000	0.10333	0.42467	0.29755	0.28738	0.30310	0.34448
DACO XG	198.52018	6023.4745	2569.9708	−10.272107	2.0980197	−3.2158223	0.07618	0.12642	0.07046	0.11552	0.11492	0.16543
DACO XI	198.51059	6023.4984	2569.9578	−10.272086	2.0980047	−3.2158490	0.05679	0.08666	0.05842	0.09103	0.07296	0.13738
DACO XJ	198.50906	6023.4892	2569.9668	−10.272095	2.0980009	−3.2158381	0.055318	0.08373	0.05663	0.08910	0.06948	0.13521
LAPM XA	198.50555	6023.4818	2569.9754	−10.272101	2.0979962	−3.2158313	0.05474	0.08239	0.05399	0.08817	0.06869	0.1345
LAPM XB[b]	198.48952	6023.4509	2570.0017	−10.272125	2.0979927	−3.2158118	0.11824	0.15859	0.13055	0.14819	0.15105	0.18664
LAPM YA	198.50152	6023.4759	2569.9830	−10.272107	2.0979908	−3.2158256	0.05543	0.08173	0.05118	0.08758	0.07107	0.13424
LAPM YB	198.50191	6023.4864	2569.9737	−10.272097	2.0979930	−3.2158378	0.05550	0.08349	0.05308	0.08891	0.07125	0.13563
LAPM XC	198.48262	6023.4435	2570.0085	−10.272132	2.0979852	−3.2158061	0.11647	0.15842	0.13027	0.14778	0.14804	0.18657
PRCL YA	198.50166	6023.4728	2569.9853	−10.272109	2.0979918	−3.2158237	0.05389	0.07915	0.04845	0.08617	0.06725	0.13298
PRCL YC	198.50587	6023.4610	2569.9931	−10.272120	2.0979941	−3.2158075	0.05334	0.07509	0.04570	0.08257	0.06703	0.12839
PRCL YD[c]	198.48565	6023.4381	2570.0137	−10.272135	2.0979910	−3.2158004	0.10161	0.13285	0.10540	0.12976	0.12647	0.17209
PRCL YE	198.48389	6023.4484	2570.0052	−10.272128	2.0979847	−3.2158098	0.10289	0.14697	0.11762	0.13642	0.13459	0.18109

[a]See Table 10 for epoch used.
[b]Orbit used for (first) midcourse maneuver computations.
[c]Inflight best estimate.

Table 9. Summary of premaneuver DSS tracking data used in *Surveyor V* orbit computations

Orbit ID	Station	Data type	Begin data, time		End data, time		Number of points	Standard deviation	Root mean square	Mean error	Data sample rate, s
			Date 1967	GMT	Date 1967	GMT					
PROR XA	DSS 51	CC3	9/08	08:30:26	9/08	09:05:32	175	0.754	0.754	−0.00101	10
		HA	9/08	08:30:21	9/08	09:06:02	162	0.0221	0.0353	0.0275	10
		Dec	9/08	08:30:21	9/08	09:06:02	161	0.0221	0.0238	−0.00878	10
PROR YA	DSS 42	HA	9/08	09:14:02	9/08	09:36:02	7	0.00370	0.00741	0.00643	60
		Dec	9/08	09:14:02	9/08	09:36:02	7	0.00195	0.0361	−0.0360	60
	DSS 51	CC3	9/08	08:30:36	9/08	09:35:32	203	0.703	0.703	0.0107	10
		HA	9/08	08:30:41	9/08	09:36:02	188	0.0111	0.0345	0.0327	10
		Dec	9/08	08:30:41	9/08	09:36:02	188	0.0126	0.0189	−0.0141	10
ICEV XA	DSS 42	HA	9/08	09:14:02	9/08	10:08:02	37	0.00330	0.00665	0.00578	60
		Dec	9/08	09:14:02	9/08	10:08:02	37	0.00318	0.0327	−0.0326	60
	DSS 51	CC3	9/08	08:30:26	9/08	10:08:32	234	0.0645	0.0656	0.0121	10
		HA	9/08	08:30:21	9/08	10:09:02	223	0.00911	0.0326	0.0313	10
		Dec	9/08	08:30:21	9/08	10:09:02	223	0.0114	0.0155	−0.0105	10
ICEV YA	DSS 42	HA	9/08	09:14:02	9/08	10:25:02	51	0.00472	0.00609	0.00385	60
		Dec	9/08	09:14:02	9/08	10:25:02	51	0.00542	0.0379	−0.0375	60
		CC3	9/08	10:34:32	9/08	11:00:32	25	0.0406	0.0407	0.00373	60
		HA	9/08	10:34:02	9/08	11:01:02	27	0.00568	0.00718	−0.00440	60
		Dec	9/08	10:34:02	9/08	11:01:02	27	0.00601	0.0483	−0.0480	60
	DSS 51	CC3	9/08	08:30:26	9/08	10:23:32	242	0.0539	0.0545	0.00797	10
		HA	9/08	08:30:21	9/08	11:01:02	261	0.00811	0.0336	0.0326	10
		Dec	9/08	08:30:21	9/08	11:01:02	261	0.0127	0.0176	−0.0122	10
ICEV XB	DSS 42	CC3	9/08	10:34:32	9/08	11:09:32	32	0.0160	0.0160	0.000549	60
	DSS 51	CC3	9/08	08:30:26	9/08	10:23:32	242	0.0378	0.0378	0.000107	10
PREL YA	DSS 42	CC3	9/08	10:34:32	9/08	11:23:32	46	0.00847	0.00848	−0.000467	60
	DSS 51	CC3	9/08	08:30:26	9/08	10:23:32	240	0.0379	0.0379	−0.000130	10
DACO XA	DSS 42	CC3	9/08	10:34:32	9/08	11:23:32	46	0.0182	0.0182	−0.000573	60
	DSS 51	CC3	9/08	08:30:26	9/08	10:23:32	240	0.0382	0.0382	−0.00119	10
	DSS 51	CC3	9/08	11:33:32	9/08	13:23:32	104	0.00749	0.00760	−0.00131	60
	DSS 61	CC3	9/08	13:34:32	9/08	13:46:32	13	0.0168	0.0435	0.0401	60
DACO YA	DSS 42	CC3	9/08	10:34:32	9/08	11:23:32	232	0.0337	0.0338	−0.000467	60
	DSS 51	CC3	9/08	11:33:32	9/08	13:23:32	104	0.00717	0.00717	0.000178	60
DACO YB	DSS 42	CC3	9/08	10:34:32	9/08	11:23:32	232	0.0341	0.0341	−0.00174	60
	DSS 51	CC3	9/08	11:33:32	9/08	13:23:32	104	0.0830	0.0830	0.0000563	60
	DSS 61	CC3	9/08	13:34:32	9/08	14:31:32	52	0.108	0.108	0.00465	60
DACO XG	DSS 42	CC3	9/08	10:34:32	9/08	11:23:32	46	0.0162	0.0163	−0.00144	60
	DSS 51	CC3	9/08	08:30:26	9/08	10:23:32	226	0.0314	0.0314	0.000568	10
	DSS 51	CC3	9/08	11:33:32	9/08	13:23:32	104	0.00718	0.00719	−0.000254	60
	DSS 51	CC3	9/08	15:33:32	9/08	17:43:32	120	0.00800	0.00804	0.000875	60
	DSS 61	CC3	9/08	14:30:32	9/08	15:23:32	38	0.0155	0.0167	0.00617	60

Table 9 (contd)

Orbit ID	Station	Data type	Begin data, time		End data, time		Number of points	Standard deviation	Root mean square	Mean error	Data sample rate, s
			Date 1967	GMT	Date 1967	GMT					
DACO XI	DSS 42	CC3	9/08	10:34:32	9/08	11:23:32	46	0.00883	0.00886	−0.000701	60
	DSS 51	CC3	9/08	08:30:26	9/08	10:23:32	225	0.0311	0.0311	−0.0000152	10
	DSS 51	CC3	9/08	11:33:32	9/08	13:23:32	104	0.00715	0.00740	0.00193	60
	DSS 51	CC3	9/08	15:33:32	9/08	20:09:32	234	0.00788	0.00788	−0.0000793	60
	DSS 72	CC3	9/08	20:35:32	9/08	21:19:32	31	0.00931	0.0239	−0.0220	60
	DSS 42	CC3	9/08	10:34:32	9/08	11:23:32	46	0.00867	0.00903	−0.00253	60
	DSS 51	CC3	9/08	08:30:26	9/08	10:23:32	226	0.0310	0.0318	−0.00119	10
	DSS 51	CC3	9/08	11:33:32	8/08	13:23:32	104	0.00713	0.00718	0.000883	60
	DSS 51	CC3	9/08	15:33:32	9/08	20:23:32	243	0.00808	0.00823	0.00158	60
LAPM XA	DSS 72	CC3	9/08	20:35:32	9/08	21:23:32	35	0.00905	0.0209	−0.0189	60
	DSS 11	CC3	9/08	21:35:32	9/08	21:53:32	13	0.00766	0.0291	0.0281	60
	DSS 42	CC3	9/08	10:34:32	9/08	11:23:32	46	0.00867	0.00942	−0.00367	60
	DSS 51	CC3	9/08	08:30:26	9/08	10:23:32	226	0.0321	0.0321	−0.000369	10
	DSS 51	CC3	9/08	11:33:32	9/08	13:23:32	104	0.00727	0.00727	−0.000329	60
	DSS 51	CC3	9/08	15:33:32	9/08	20:23:32	243	0.00806	0.00868	0.00322	60
LAPM XB	DSS 72	CC3	9/08	20:35:32	9/08	21:23:32	35	0.00936	0.00936	−0.000237	60
	DSS 11	CC3	9/08	21:35:32	9/08	22:29:32	45	0.00848	0.00869	0.00188	60
	DSS 42	CC3	9/08	10:34:32	9/08	11:23:32	46	0.00832	0.00833	−0.000435	60
	DSS 51	CC3	9/08	08:30:26	9/08	10:23:32	229	0.0338	0.0338	−0.000533	10
	DSS 51	CC3	9/08	11:33:32	9/08	13:23:32	104	0.00718	0.00723	0.00850	60
	DSS 51	CC3	9/08	15:33:32	9/08	20:23:32	243	0.00791	0.00792	0.000332	60
LAPM YA	DSS 72	CC3	9/08	20:35:32	9/08	21:23:32	39	0.00904	0.0202	−0.0181	60
	DSS 11	CC3	9/08	21:35:32	9/08	22:11:32	33	0.00806	0.0216	0.0200	60
	DSS 42	CC3	9/08	10:34:32	9/08	11:23:32	46	0.00847	0.00970	−0.00473	60
	DSS 51	CC3	9/08	08:30:26	9/08	10:23:32	226	0.0335	0.0335	0.000417	10
	DSS 51	CC3	9/08	11:33:32	9/08	13:23:32	104	0.00718	0.00739	−0.00176	60
	DSS 51	CC3	9/08	15:33:32	9/08	20:13:32	242	0.00797	0.00898	0.00414	60
LAPM YB	DSS 11	CC3	9/08	20:35:32	9/08	22:11:32	33	0.00807	0.0209	0.0192	60
	DSS 42	CC3	9/08	10:34:32	9/08	11:23:32	46	0.00871	0.00988	−0.00467	60
	DSS 51	CC3	9/08	08:30:26	9/08	10:23:32	226	0.0332	0.0332	0.000115	10
	DSS 51	CC3	9/08	11:33:32	9/08	13:23:32	104	0.00717	0.00771	−0.00283	60
	DSS 51	CC3	9/08	15:33:32	9/08	20:13:32	242	0.00784	0.00787	−0.000777	60
LAPM XC	DSS 72	CC3	9/08	20:35:32	9/08	21:23:32	35	0.00941	0.00945	−0.000949	60
	DSS 11	CC3	9/08	21:35:32	9/08	22:50:32	64	0.0129	0.0129	−0.00108	60
	DSS 42	CC3	9/08	10:34:32	9/08	11:23:32	46	0.00829	0.00831	−0.000637	60
	DSS 51	CC3	9/08	08:30:26	9/08	10:23:32	229	0.0337	0.0337	−0.000333	10
	DSS 51	CC3	9/08	11:33:32	9/08	13:23:32	104	0.00717	0.00718	0.000263	60
	DSS 51	CC3	9/08	15:33:32	9/08	20:23:32	243	0.00790	0.00791	−0.000364	60

Table 9 (contd)

Orbit ID	Station	Data type	Begin data, time		End data, time		Number of points	Standard deviation	Root mean square	Mean error	Data sample rate, s
			Date 1967	GMT	Date 1967	GMT					
PRCL YA	DSS 72	CC3	9/08	20:35:32	9/08	21:23:32	35	0.00912	0.0216	−0.0196	60
	DSS 11	CC3	9/08	21:23:32	9/09	01:45:00	316	0.0405	0.0409	0.00544	60
	DSS 42	CC3	9/08	10:34:32	9/08	11:23:32	46	0.00853	0.0111	−0.00704	60
	DSS 51	CC3	9/08	08:30:26	9/08	10:23:32	228	0.0346	0.0346	−0.00131	10
	DSS 51	CC3	9/08	11:33:32	9/08	13:23:32	104	0.00728	0.00853	−0.00446	60
	DSS 51	CC3	9/08	15:33:32	9/08	20:23:32	241	0.00805	0.00826	0.00185	60
PRCL YC	DSS 72	CC3	9/08	20:35:32	9/08	21:23:32	35	0.00921	0.0192	−0.0169	60
	DSS 11	CC3	9/08	21:35:32	9/09	01:45:00	317	0.0421	0.0424	0.00543	60
	DSS 42	CC3	9/08	10:34:32	9/08	11:23:32	46	0.00841	0.0125	−0.00931	60
	DSS 51	CC3	9/08	08:30:26	9/08	10:23:32	228	0.0347	0.0347	−0.000707	10
	DSS 51	CC3	9/08	11:33:32	9:08	13:23:32	104	0.00725	0.00870	−0.00481	60
	DSS 51	CC3	9/08	15:33:32	9/08	20:23:32	241	0.00825	0.00913	0.00392	60
	DSS 61	CC3	9/08	14:30:32	9/08	15:23:32	38	0.00892	0.0187	0.0164	60
PRCL YD	DSS 72	CC3	9/08	20:35:32	9/08	21:23:32	35	0.00936	0.00937	0.000321	60
	DSS 11	CC3	9/08	21:35:32	9/09	01:45:00	316	0.0410	0.0413	0.00544	60
	DSS 42	CC3	9/08	10:34:32	9/08	11:23:32	46	0.00826	0.00829	−0.000743	60
	DSS 51	CC3	9/08	08:30:26	9/08	10:23:32	228	0.0330	0.0330	−0.000171	10
	DSS 51	CC3	9/08	11:33:32	9/08	13:23:32	104	0.00720	0.00721	0.000465	60
	DSS 51	CC3	9/08	15:33:32	9/08	20:23:32	241	0.00793	0.00793	0.000294	60
	DSS 61	CC3	9/08	14:30:32	9/08	15:23:32	38	0.00869	0.00902	0.000240	60
PRCL YE	DSS 11	CC3	9/08	21:35:32	9/09	01:45:00	316	0.0410	0.0414	0.00616	60
	DSS 42	CC3	9/08	10:34:32	9/08	11:23:32	46	0.00834	0.00834	−0.000287	60
	DSS 51	CC3	9/08	08:30:26	9/08	10:23:32	228	0.0332	0.0332	−0.0000921	10
	DSS 51	CC3	9/08	11:33:32	9/08	13:23:32	104	0.00724	0.00736	0.00131	60
	DSS 51	CC3	9/08	15:33:32	9/08	20:23:32	241	0.00792	0.00797	0.000875	60
	DSS 72	CC3	9/08	20:35:32	9/08	21:23:32	35	0.00919	0.00923	0.000837	60

Table 10. Epochs used in orbit solutions

Epoch	Orbits using given epoch	Remarks
670900808, 1512951	PROR, ICEV, PREL, DACO, LAPM, PRCL	Nominal transfer orbit injection (MECO 2)
670900904, 1916000	1POM after three maneuvers	End of third burn
670900908, 2503000	1POM, 2POM	Epoch used after fifth maneuver
670900823, 4900000	1PM6, 2PM6, 3POM, 4POM, 5POM, POST	Epoch used after sixth maneuver
670901019, 0400000	FINAL	R − 5 h 40 min
670900911, 5700000	Postflight 2 POM	After biased DSS 42 data between fifth and sixth midcourse maneuver

C. Pre (Sixth) Maneuver Orbit Estimates

Immediately after the first midcourse maneuver, a leak in the helium supply was detected. In an attempt to reseat the faulty valve causing the leak and to maximize chances of soft landing under nonstandard conditions if the valve would not reseat, additional vernier firings of various durations were executed. There were not sufficient data received between burns to reestablish the orbit until after the fifth maneuver execution.

After the fifth maneuver was executed, it was decided to perform another maneuver in an attempt to hit near the prelaunch aim point and further optimize the terminal descent parameters. Based on the 2 POM XD orbit solution, a sixth maneuver was designed and executed. This orbit solution contained the following amounts of two-way doppler data: 3 h, 20 min from DSS 42; 9 h, 18 min from DSS 51; and 3 h, 15 min from DSS 61. When mapped to impact, this solution indicated an unbraked impact point of 4.24° S lat and 16.828° E lon.

The numerical results of the pre (sixth) maneuver orbit computations are listed in Tables 11 and 12, identified as 1 POM and 2 POM orbits. Amounts and types of tracking data used in these orbits with the associated statistics are given in Table 13. For the pre-midcourse estimates of the unbraked impact point see Figs. 10 and 11. Epochs used are given in Table 10.

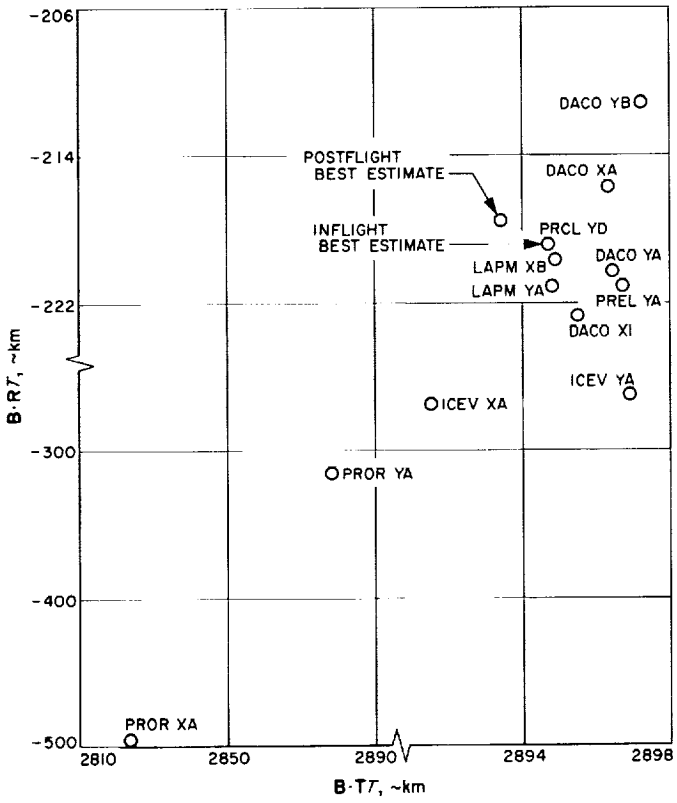

Fig. 10. Estimated pre (first) midcourse unbraked impact point, *Surveyor V*

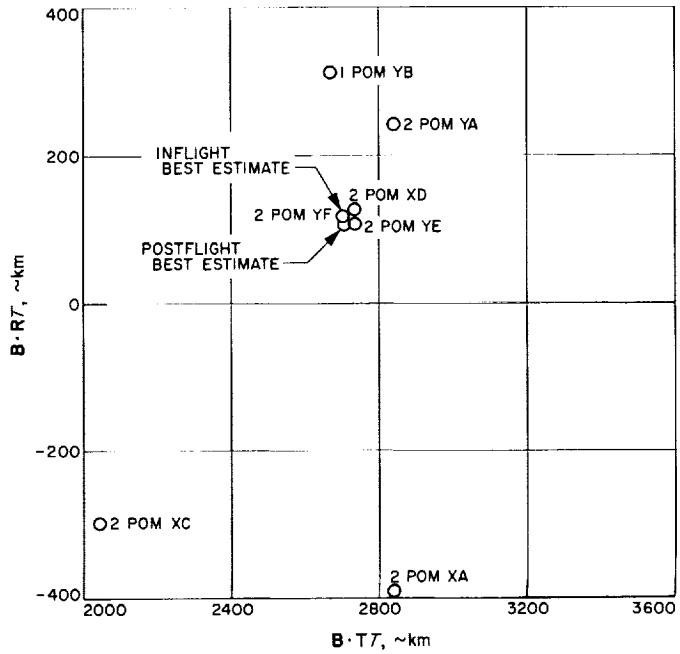

Fig. 11. Estimated pre (sixth) midcourse unbraked impact point, *Surveyor V*

D. Postmaneuver Orbit Estimates

The first post (sixth) midcourse orbit computations were completed approximately 8 h after maneuver execution. During this period, 1 PM 6, 2 PM 6, and 3 POM orbits were computed. For the final (3 POM XC) orbit computation during this period, approximately 3 h of DSS 11 data and 5 h of DSS 42 data were used. The initial values used for the orbit estimate were provided by the trajectory group assuming a nominal maneuver mapped to the post-midcourse epoch.

When these conditions were passed through the initial post-midcourse two-way doppler data from DSS 11, residuals of <1 Hz were computed which was an early indication of a near-nominal maneuver execution. When the 3 POM XC orbit was mapped to the moon, it indicated an unbraked impact point 25.8 km west and 14.8 km north of the aim point. This was later refined to be 17.6 km north and 26.8 km west of the revised aim point.

Orbit ID	Time computed		B, km	B•TT, km	B•RT, km	TL, h	SMAA, km (1σ)
	Start	Stop					
1 POM after three maneuvers	These orbits all computed between fifth and sixth maneuver with epoch at end of fifth burn.		4423.4	3975.2	−1940.2	43.00	86.71
1 POM YB			2681.0	2662.8	312.16	40.21	138.5
2 POM YA			2846.6	2836.3	242.27	40.16	108.6
2 POM XA			2866.9	2840.2	−390.6	40.14	7598.6
2 POM XC			2062.6	2041.0	−298.4	40.26	1277.6
2 POM XD[a]			2738.3	2735.3	127.8	40.19	10.40
2 POM YE			2733.8	2731.6	108.1	40.19	11.28
2 POM YF[b]			2703.8	2701.3	118.0	40.20	23.03
1 PM6 YA	01:57	02:15	3125.8	3125.66	−27.51	24.85	0.355×10^{5}
1 PM6 YB	02:42	03:15	3029.16	3027.9	−86.74	24.86	0.102×10^{10}
1 PM6 XA	04:18	04:28	2989.1	2984.5	−165.9	24.88	1839.7
2 PM6 XA	04:30	04:45	2995.1	2990.8	−159.8	24.88	1637.8
3 POM XB	06:20	06 30	2996.9	2991.5	−179.9	24.88	819.09
3 POM XC	07:14	07:31	2997.5	2993.5	−172.8	24.88	332.7
4 POM XA	10:40	11:00	2997.5	2992.6	−171.1	24.88	61.41
4 POM XC	12:50	13:17	2998.1	2993.0	−175.1	24.88	21.11
4 POM XF	14:40	15:06	2999.1	2993.8	−177.3	24.88	36.69
4 POM YE	14:38	15:10	2998.8	2993.7	−175.0	24.88	8.338
4 POM XG	16:15	16:37	2998.4	2993.3	−175.0	24.88	8.315
5 POM XA	19:18	19:34	2998.2	2993.1	−175.0	24.88	8.314
5 POM YA	19:11	19:15	2998.2	2993.1	−175.0	24.88	8.331
5 POM XD[c]	21:13	21:31	2997.7	2992.4	−177.5	24.88	7.773
FINAL YA	22:38	22:48	2997.8	2992.4	−180.2	56.34	2.849
FINAL XA	22:41	22:55	2997.7	2992.3	−180.2	56.33	2.937
FINAL YB	22:57	23:08	2996.8	2991.4	−179.3	56.33	2.465
FINAL XB	23:04	23:15	2997.3	2991.9	−179.8	56.34	2.673
FINAL YC	23:36	23:46	2995.4	2990.2	−178.4	56.34	1.664
FINAL XC	23:32	23 45	2995.7	2990.4	−178.7	56.34	1.695
FINAL YD	23:56	00:04	2996.8	2991.4	−179.4	56.34	1.544
FINAL XD	23:51	00:03	2997.1	2991.7	−179.7	56.34	1.567
FINAL XE	00:09	00:15	2996.4	2991.1	−179.2	56.34	1.539
FINAL YE[d]	00:11	00:17	2996.3	2990.9	−179.0	56.34	1.527
POST 1	[f]		2996.5	2991.2	−179.4	24.88	2.301
POST 2[c]	[f]		2996.7	2991.3	−178.3	24.88	9.385

[a]Orbit used for sixth midcourse maneuver computations.
[b]Inflight best estimate of pre (sixth) maneuver.
[c]O
[d]C

ainties, 1σ			
	Velocity		
	σ_{Dx_f} m/s	σ_{Dy_f} m/s	σ_{Dz_f} m/s
92	0.53777	0.10239	0.47058
	1.2914	0.56412	0.54572
	0.80500	0.45323	0.21761
	16.565	16.693	37.222
	3.2677	2.0394	1.6225
7	0.13786	0.04790	0.04710
1	0.14840	0.04934	0.06199
	0.26842	0.08490	0.18646
	0.121633	0.16847	0.34593
	20.423	15.691	17.756
	12.029	9.1170	10.250
	7.531	7.915	9.896
	4.557	4.056	4.597
	2.2870	1.6894	1.7175
	0.65999	0.33689	0.33052
5	0.32579	0.11969	0.07704
0	0.20601	0.27021	0.40341
0	0.08204	0.05541	0.06594
4	0.07697	0.05528	0.06507
7	0.07455	0.05514	0.06498
6	0.07514	0.05518	0.06521
0	0.05764	0.05022	0.06289
7	0.01626	0.01688	0.02957
3	0.01909	0.01750	0.02981
7	0.01052	0.01499	0.02831
8	0.01400	0.01597	0.02902
6	0.00832	0.01251	0.02442
9	0.00857	0.01256	0.02468
5	0.00764	0.01213	0.02293
2	0.00801	0.01219	0.02327
9	0.00736	0.01209	0.02268
9	0.00688	0.01206	0.02242
6	0.01345	0.01463	0.02835
3	0.03107	0.04518	0.08253

Table 11. *Surveyor V* postmaneuver computations

Target statistics					Selenocentric conditions at unbraked impact			Solution type	Data type and source
SMIA, km (1σ)	THETA, deg	$\sigma_{T,\ impact}$, s (1σ)	PHI_{IMP}, deg	SVFIXR, m/s (1σ)	Latitude, deg (Negative S)	Longitude, deg (East)	GMT		
Orbits computed after three maneuvers									
23.83	48.94	4.1×10^{10}	0.9454	0.5103	2.23	90.92	23:43:07.133	6 × 6	DSS 42 and DSS 72, CC3
73.87	140.8	56.625	5.884	0.7372	−7.62	15.32	00:38:28.324	6 × 6	DSS 42 and DSS 51, CC3
9.646	132.0	28.925	3.729	0.6671	−6.07	19.831	00:36:56.193	6 × 6	DSS 42, DSS 51, and DSS 61, CC3
2729.0	138.6	1350.81	120.0	30.78	4.95	19.72	00:35:45.938	9 × 9	DSS 42 and DSS 51, CC3; estimate gas jets
287.0	135.0	77.256	20.12	3.7531	2.519	359.82	00:37:35.228	9 × 9	DSS 42, DSS 51, and DSS 61, CC3; estimate gas jets
10.13	170.0	7.9421	0.6943	0.6244	−4.24	16.828	00:37:38.795	6 × 6	DSS 42, DSS 51, and DSS 61, CC3
7.67	156.9	8.5850	0.7421	0.6246	−3.89	16.69	00:37:42.527	6 × 6	DSS 11, DSS 42, DSS 51, and DSS 61, CC3
18.84	47.84	16.407	1.394	0.6293	−4.12	15.90	00:38:06.637	14 × 14	DSS 11, DSS 42, DSS 51, and DSS 61, CC3; estimate radius and longitude
Orbits computed after the sixth maneuver									
0.46×10^4	72.45	7948.6	770.6	50.78	−0.863	27.30	00:44:46.966	6 × 6	DSS 11, CC3; 1×10^N diagonal *a priori*
0.99×10^0	9.92	0.88×10^0	0.488×10^0	0.446×10^4	−0.025	24.33	00:44:42.024	6 × 6	DSS 11 and DSS 42, CC3
378.7	98.17	531.35	48.84	0.0372	1.275	23.05	00:45:13.612	6 × 6	DSS 11 and DSS 42, CC3
150.3	92.5	423.75	37.58	2.284	1.180	23.23	00:45:10.371	6 × 6	DSS 11 and DSS 42, CC3
45.88	96.7	226.82	20.39	1.491	1.528	23.26	00:45:15.288	6 × 6	DSS 11 and DSS 42, CC3
33.09	101.3	96.742	9.010	0.933	1.409	23.28	00:45:13.321	6 × 6	DSS 11 and DSS 42, CC3
28.63	107.6	21.446	2.013	0.657	1.378	23.29	00:45:12.821	6 × 6	DSS 11 and DSS 42, CC3
8.42	132.8	7.742	0.8335	0.6319	1.447	23.298	00:45:14.240	6 × 6	DSS 11, DSS 42, and DSS 51, CC3
6.06	93.26	5.1213	0.6222	0.6256	1.487	23.323	00:45:14.435	6 × 6	DSS 42 and DSS 51, CC3
2.98	81.98	3.3317	0.2125	0.6237	1.447	23.317	00:45:14.158	6 × 6	DSS 11, DSS 42, and DSS 51, CC3
2.62	82.54	3.3204	0.2086	0.6236	1.446	23.307	00:45:14.213	6 × 6	DSS 11, DSS 42, and DSS 51, CC3
2.50	82.46	3.3108	0.2065	0.6236	1.447	23.301	00:45:14.297	6 × 6	DSS 11, DSS 42, and DSS 51, CC3
2.51	82.32	3.3149	0.2071	0.6236	1.447	23.301	00:45:14.290	6 × 6	DSS 11, DSS 42, DSS 51, CC3
2.20	79.49	3.0671	0.1800	0.6234	1.488	23.28	00:45:15.325	6 × 6	DSS 11, DSS 42, DSS 51, CC3
1.23	46.93	1.6392	0.0557	0.6231	1.534	23.28	00:45:16.359	6 × 6	DSS 11, DSS 51, CC3
1.25	46.37	1.7151	0.0589	0.6231	1.535	23.28	00:45:16.284	6 × 6	
1.22	50.59	1.3563	0.0464	0.6231	1.519	23.25	00:45:15.528	6 × 6	
1.24	48.03	1.5146	0.0504	0.6231	1.527	23.27	00:45:15.926	6 × 6	
0.8535	81.60	0.75028	0.0266	0.6231	1.501	23.22	00:45:14.667	6 × 6	
0.8726	79.95	0.76321	0.0271	0.6231	1.505	23.22	00:45:14.791	6 × 6	
0.4511	93.90	0.59426	0.0242	0.6231	1.520	23.25	00:45:15.431	6 × 6	
0.5420	91.85	0.61729	0.0246	0.6321	1.526	23.26	00:45:15.590	6 × 6	
0.3430	95.11	0.57330	0.0240	0.6231	1.516	23.24	00:45:15.251	6 × 6	
0.2345	96.12	0.55949	0.0238	0.6231	1.513	23.24	00:45:15.162	6 × 6	
0.8925	84.46	0.74352	0.0359	0.6231	1.519	23.25	00:45:15.306	6 × 6	DSS 11, DSS 42, DSS 51, CC3
1.743	96.19	0.99209	0.1515	0.6232	1.502	23.25	00:45:15.315	15 × 15	DSS 11, DSS 42, DSS 51, CC3; estimate radius, latitude, longitude

[a] used for terminal computations.
[b] used to obtain unbraked impact time on which to base the final pre-touchdown sequence.
[c] Inflight best estimate, postmaneuver.
[f] Computed immediately following touchdown.

Table 12. *Surveyor V* postmaneuver position and velocity at injection epoch

Orbit ID	Geocentric space-fixed position			Geocentric space-fixed velocity			Uncer		
							Position		
	x, km	y, km	z, km	Dx, km/s	Dy, km/s	Dz, km/s	σ_x, km	σ_y, km	σ_z, km
1 POM after three maneuvers	−69048.391	−149943.46	−89421.304	−0.27498649	−1.4863208	−0.70885803	1.1036	0.59671	0.90
1 POM YB[a]	−72606.876	−171021.54	−99543.451	−0.18307785	−1.3516489	−0.65083634	18.083	12.723	54.66
2 POM YA[a]	−72584.368	−171010.80	−99626.065	−0.18499922	−1.3515042	−0.64982576	12.536	9.7071	33.50
2 POM XA[a]	−72589.524	−171040.72	−99531.464	−0.18282308	−1.3500515	−0.65387234	919.30	1287.0	1411.9
2 POM XC[a]	−72636.263	−171129.82	−99655.876	−0.18491362	−1.3514863	−0.64988294	33.888	133.10	142.23
2 POM XD[a]	−72600.441	−170995.89	−99581.413	−0.18388801	−1.3521487	−0.64951797	3.3274	2.5451	6.68
2 POM YE[a]	−72605.152	−170992.47	−99574.464	−0.18380670	−1.3522285	−0.64944171	3.5749	2.7230	7.41
2 POM YF[a]	−72608.498	−170992.66	−99552.311	−0.18341952	−1.3522585	−0.64966586	6.0485	4.7213	15.83
1 PM 6 YA	−79388.298	−263876.52	−130376.99	−0.078710280	−1.0497002	−0.47568803	5761.12	8521.09	9706.02
1 PM 6 YB	−79393.537	−236891.57	−130373.41	−0.077577611	−1.0502395	−0.47539210	263.88	625.29	1224.0
1 PM 6 XA	−79400.919	−236880.92	−130330.66	−0.076634921	−1.0506863	−0.47514116	160.89	366.89	705.18
2 PM 6 XA	−79400.068	−236881.33	−130334.94	−0.076752463	−1.0506466	−0.47514446	136.11	348.60	566.95
3 POM XB	−79401.501	−236876.76	−130328.52	−0.076688633	−1.0507407	−0.47501501	77.107	165.83	300.48
3 POM XC	−79400.820	−236878.18	−130331.13	−0.076729054	−1.0507056	−0.47505403	37.377	64.541	128.9
4 POM XA	−79400.680	−236878.54	−130331.79	−0.076738213	−1.0506967	−0.47506445	12.158	17.698	23.94
4 POM XC	−79401.130	−236877.12	−130330.48	−0.076721337	−1.0507173	−0.47503797	7.553	5.6886	9.6
4 POM XF	−79401.553	−236875.98	−130331.15	−0.076723887	−1.0507322	−0.47500961	10.856	14.944	7.7
4 POM YE	−79401.006	−236876.99	−130330.70	−0.076730814	−1.0507159	−0.47503511	4.5159	4.9742	2.8
4 POM XG	−79401.201	−236877.01	−130330.57	−0.076724226	−1.0507165	−0.47503753	4.4342	4.9691	2.8
5 POM XA	−79401.428	−236876.96	−130330.44	−0.076718430	−1.0507179	−0.47503830	4.3753	4.9670	2.7
5 POM YA	−79401.421	−236876.96	−130330.45	−0.076718646	−1.0507178	−0.47503838	4.3840	4.9712	2.8
5 POM XD	−79403.345	−236875.71	−130329.34	−0.076678412	−1.0507364	−0.47503436	3.7260	4.7125	2.4
FINAL YA	−83695.798	−301901.53	−15877.125	−0.089503807	−0.86413118	−0.36212195	0.54256	1.6802	1.9
FINAL XA	−83695.763	−301901.63	−15877.128	−0.089506119	−0.86413051	−0.36212190	0.56745	1.7623	1.9
FINAL YB	−83695.534	−301902.38	−158772.11	−0.089514922	−0.86412407	−0.36212994	0.45394	1.3834	1.6
FINAL XB	−83695.656	−301901.98	−158771.67	−0.089511352	−0.86412726	−0.36212543	0.05795	1.5569	1.7
FINAL YC	−83695.249	−301903.29	−158773.02	−0.089518667	−0.86411779	−0.36214089	0.25745	0.72315	1.1
FINAL XC	−83695.275	−301903.18	−158772.82	−0.089520404	−0.86411865	−0.36213797	0.25891	0.73149	1.2
FINAL YD	−83695.491	−301902.50	−158772.15	−0.08523236	−0.86412287	−0.36212727	0.21332	0.54817	1.0
FINAL XD	−83685.522	−301902.37	−158771.89	−0.089525644	−0.86412398	−0.36212338	0.21836	0.57124	1.0
FINAL XE	−83695.424	−301902.72	−158772.29	−0.089520812	−0.86412171	−0.36213115	0.20722	0.52094	1.0
FINAL YE	−83695.407	−301902.79	−158772.43	−0.089519076	−0.86412111	−0.36213354	0.20421	0.50282	1.0
POST 1	−79403.979	−236875.91	−130328.71	−0.076657137	−1.0507477	−0.47501800	0.96365	1.22705	1.4
POST 2	−79403.172	−236876.78	−130327.68	−0.076667989	−1.0507343	−0.47503747	1.9898	4.01193	7.

[a]Solutions using end of fifth maneuver as epoch.
All other PM 6, POM, and POST orbits used end of sixth burn as epoch. (See Table 10 for epochs.)
All FINAL orbits have epoch at approximately unbraked impact minus 5 h, 40 min.

Table 13. Summary of postmaneuver DSS tracking data used in *Surveyor V* orbit computations

Orbit ID	Station	Data type	Begin data, time		End data, time		Number of points	Standard deviation	Root mean square	Mean error
			Date 1967	GMT	Date 1967	GMT				
1 POM[a]	DSS 72	CC3	9/09	04:19:23	9/09	04:23:32	6	0.0433	0.0433	0.00142
	DSS 42	CC3	9/09	05:44:32	9/09	07:31:32	103	0.0760	0.0760	0.000133
1 POM YB[b]	DSS 42	CC3	9/09	08:36:32	9/09	11:56:32	173	0.0148	0.0148	−0.000312
	DSS 51	CC3	9/09	12:03:32	9/09	16:47:32	253	0.00879	0.00880	−0.000520
2 POM YA	DSS 42	CC3	9/09	08:36:32	9/09	11:56:32	173	0.0184	0.0184	0.000806
	DSS 51	CC3	9/09	12:03:32	9/09	16:47:32	252	0.0294	0.0294	0.000920
	DSS 61	CC3	9/09	16:52:32	9/09	18:45:32	83	0.0109	0.0120	−0.000497
2 POM XA	DSS 42	CC3	9/09	08:25:07	9/09	11:56:32	189	0.0170	0.0171	0.00186
	DSS 51	CC3	9/09	12:03:32	9/09	16:47:32	234	0.00697	0.00698	0.0000534
2 POM XC	DSS 42	CC3	9/09	08:25:07	9/09	11:56:32	189	0.0160	0.0160	0.00115
	DSS 51	CC3	9/09	12:03:32	9/09	16:47:32	233	0.00791	0.00791	0.0000409
	DSS 61	CC3	9/09	16:52:32	9/09	19:09:32	131	0.0102	0.0102	−0.0000671
2 POM XD	DSS 42	CC3	9/09	08:36:32	9/09	11:56:32	173	0.0274	0.0275	0.00103
	DSS 51	CC3	9/09	12:03:32	9/09	20:23:32	253	0.0316	0.0317	0.00199
	DSS 51	CC3	9/09	20:25:32	9/09	21:23:32	56	0.0177	0.0192	0.00729
	DSS 61	CC3	9/09	16:58:32	9/09	20:13:32	108	0.0307	0.0326	−0.0111
2 POM YE	DSS 11	CC3	9/09	21:39:32	9/09	22:01:32	21	0.0167	0.0735	−0.0716
	DSS 42	CC3	9/09	08:56:32	9/09	11:56:32	158	0.0244	0.0244	−0.00138
	DSS 51	CC3	9/09	12:03:32	9/09	20:23:32	253	0.0280	0.0280	−0.000277
	DSS 51	CC3	9/09	20:25:32	9/09	21:23:32	56	0.0170	0.0171	0.00117
	DSS 61	CC3	9/09	16:58:32	9/09	20:13:32	108	0.0393	0.0398	0.00600
2 POM YF	DSS 11	CC3	9/09	21:39:32	9/09	22:54:32	25	0.0200	0.0275	−0.0189
	DSS 42	CC3	9/09	08:56:32	9/09	11:56:32	158	0.0172	0.0172	−0.000144
	DSS 51	CC3	9/09	12:03:32	9/09	20:23:32	253	0.0185	0.0185	0.00111
	DSS 51	CC3	9/09	20:25:32	9/09	21:23:32	56	0.00882	0.00906	0.00209
	DSS 61	CC3	9/09	16:58:32	9/09	20:13:32	108	0.0181	0.0181	0.00101
1 PM6 YA[c]	DSS 11	CC3	9/09	23:49:09	9/10	01:47:32	87	0.0168	0.0168	0.000208
1 PM6 YB	DSS 11	CC3	9/09	23:49:09	9/10	02:32:32	120	0.0147	0.0147	0.000240
	DSS 42	CC3	9/10	03:03:32	9/10	03:36:32	28	0.00657	0.00657	−0.000140
1 PM6 XA	DSS 11	CC3	9/09	23:49:09	9/10	02:53:32	138	0.0110	0.0110	−0.000478
	DSS 42	CC3	9/10	03:03:32	9/10	04:08:32	58	0.00662	0.00662	0.0000421
2 PM6 XA	DSS 11	CC3	9/09	23:49:09	9/10	02:53:32	138	0.0110	0.0110	−0.000419
	DSS 42	CC3	9/10	03:03:32	9/10	05:13:32	114	0.00672	0.00672	0.0000814
3 POM XB	DSS 11	CC3	9/09	23:49:14	9/10	02:53:32	138	0.00804	0.00805	0.000110
	DSS 42	CC3	9/10	03:03:32	9/10	07:03:32	206	0.00917	0.00917	0.474×10^{-5}
3 POM XC	DSS 11	CC3	9/09	23:49:14	9/10	02:53:32	138	0.00807	0.00808	0.000142
	DSS 42	CC3	9/10	03:03:32	9/10	08:00:32	257	0.0104	0.0104	0.0000636

[a]After three maneuvers.

[b]Five maneuvers.

[c]After six maneuvers.

Table 13 (contd)

Orbit ID	Station	Data type	Begin data, time		End data, time		Number of points	Standard deviation	Root mean square	Mean error
			Date 1967	GMT	Date 1967	GMT				
4 POM XA	DSS 11	CC3	9/09	23:49:14	9/10	02:53:32	136	0.00803	0.00803	0.0000413
	DSS 42	CC3	9/10	03:03:32	9/10	10:18:32	369	0.00683	0.00683	−0.0000
4 POM XC	DSS 11	CC3	9/09	23:49:14	9/10	02:53:32	136	0.00810	0.00810	0.628×10^{-5}
	DSS 42	CC3	9/10	03:03:32	9/10	11:55:32	448	0.00663	0.00663	0.0000749
	DSS 51	CC3	9/10	12:03:32	9/10	12:41:32	34	0.00845	0.00847	−0.000470
4 POM XF	DSS 42	CC3	9/09	03:03:32	9/10	11:55:32	448	0.00663	0.00663	0.0000106
	DSS 51	CC3	9/10	12:03:32	9/10	15:01:32	151	0.00778	0.00779	0.000134
4 POM YE	DSS 11	CC3	9/09	23:49:14	9/10	02:48:32	133	0.00804	0.00804	−0.000136
	DSS 42	CC3	9/10	03:03:32	9/10	11:55:32	448	0.00665	0.00665	0.000108
	DSS 51	CC3	9/10	12:03:32	9/10	17:21:32	273	0.00759	0.00759	−0.0000286
4 POM XG	DSS 11	CC3	9/09	23:49:14	9/10	02:48:32	133	0.00805	0.00805	−0.000293
	DSS 42	CC3	9/10	03:03:32	9/10	11:55:32	448	0.00664	0.00664	0.000178
	DSS 51	CC3	9/10	12:03:32	9/10	17:21:32	327	0.00860	0.00860	0.0000180
5 POM XA	DSS 11	CC3	9/09	23:49:14	9/10	02:48:32	133	0.00808	0.00809	−0.000461
	DSS 42	CC3	9/10	03:03:32	9/10	11:55:32	448	0.00666	0.00666	0.000144
	DSS 51	CC3	9/10	12:03:32	9/10	19:03:32	348	0.00903	0.00903	0.0000281
5 POM YA	DSS 11	CC3	9/09	23:49:14	9/09	02:48:32	133	0.00804	0.00805	−0.000446
	DSS 42	CC3	9/10	03:03:32	9/10	11:55:32	448	0.00667	0.00668	0.000157
	DSS 51	CC3	9/10	12:03:32	9/10	19:03:32	324	0.00852	0.00852	0.0000765
5 POM XD	DSS 11	CC3	9/09	23:49:14	9/10	02:48:32	133	0.00831	0.00832	0.000312
	DSS 42	CC3	9/10	03:03:32	9/10	19:24:32	448	0.00803	0.00809	−0.000984
	DSS 51	CC3	9/10	12:03:32	9/10	20:45:32	409	0.0106	0.0106	0.00102
FINAL YA	DSS 11	CC3	9/10	21:48:32	9/10	22:26:32	33	0.00677	0.00677	0.000163
	DSS 51	CC3	9/10	19:04:32	9/10	21:28:32	124	0.00763	0.00763	0.0000256
FINAL XA	DSS 11	CC3	9/10	21:48:32	9/10	22:22:32	24	0.00733	0.00733	−0.0000356
	DSS 51	CC3	9/10	19:04:32	9/10	21:28:32	122	0.00746	0.00746	0.0000780
FINAL YB	DSS 11	CC3	9/10	21:48:32	9/10	22:44:32	41	0.00592	0.00592	0.000131
	DSS 51	CC3	9/10	19:04:32	9/10	21:28:32	124	0.00766	0.00766	0.0000453
FINAL XB	DSS 11	CC3	9/10	21:53:32	9/10	22:35:32	29	0.00619	0.00619	0.0000673
	DSS 51	CC3	9/10	19:04:32	9/10	21:28:32	122	0.00745	0.00745	0.0000921
FINAL YC	DSS 11	CC3	9/10	21:53:32	9/10	23:22:32	61	0.00632	0.00633	0.000358
	DSS 51	CC3	9/10	19:04:32	9/10	21:28:32	124	0.00767	0.00767	0.0000256
FINAL XC	DSS 11	CC3	9/10	21:53:32	9/10	23:22:32	56	0.0100	0.0100	0.000251
	DSS 51	CC3	9/10	19:04:32	9/10	21:28:32	122	0.00746	0.00746	0.0000360
FINAL YD	DSS 11	CC3	9/10	21:48:32	9/10	23:46:32	78	0.00920	0.00920	0.000171
	DSS 51	CC3	9/10	19:04:32	9/10	21:28:32	124	0.00765	0.00765	0.0000118
FINAL XD	DSS 11	CC3	9/10	21:53:32	9/10	23:41:32	70	0.0128	0.0128	−0.0000209
	DSS 51	CC3	9/10	19:04:32	9/10	21:28:32	122	0.00752	0.00752	−0.0000200

Table 13 (contd)

Orbit ID	Station	Data type	Begin data, time		End data, time		Number of points	Standard deviation	Root mean square	Mean error
			Date 1967	GMT	Date 1967	GMT				
FINAL XE	DSS 11	CC3	9/10	21:53:32	9/10	23:54:32	79	0.0157	0.0160	0.00270
	DSS 51	CC3	9/10	19:04:32	9/10	21:28:32	122	0.00752	0.00752	0.0000200
FINAL YE	DSS 11	CC3	9/10	21:48:32	9/11	00:03:32	87	0.0105	0.0105	−0.0000814
	DSS 51	CC3	9/10	19:04:32	9/10	21:28:32	124	0.00761	0.00761	0.0000512
POST 1 and 2	DSS 11	CC3	9/09	23:49:14	9/10	02:48:32	133	0.00810	0.0103	0.00632
	DSS 11	CC3	9/10	21:48:32	9/11	00:04:32	87	0.0106	0.0110	−0.00279
	DSS 42	CC3	9/10	03:03:32	9/10	11:55:32	448	0.0101	0.0107	−0.00363
	DSS 51	CC3	9/10	12:03:32	9/10	21:28:32	448	0.0106	0.0108	0.00233

Prior to retrofire $R - 5$ h, 40 min, a decision had to be made on which station–DSS 51 or DSS 61–was to be used with DSS 11 for the terminal phase (FINAL) orbit computations. Since DSS 61 would have relatively low elevation angles, it was decided that DSS 51 would probably yield the better data; therefore, the Johannesburg station was used. The final terminal maneuver computations were based on the 5 POM XD orbit solution.

Numerical results of the inflight post-midcourse orbit solutions are presented in Tables 11 and 12. Figure 12 is a plot of the indicated unbraked impact point for post-midcourse solutions. The inflight best estimate of the location of the landed *Surveyor V* spacecraft was 17.6 km north and 26.8 km west of the revised aim point. The amounts of tracking data used in the post-midcourse orbit computations and their associated statistics are given in Table 13. Epochs used are given in Table 10.

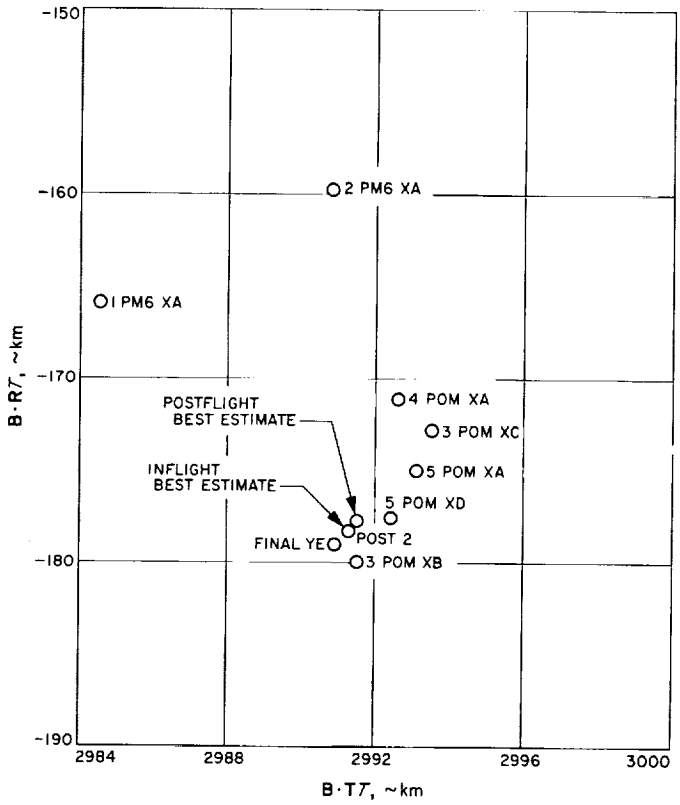

Fig. 12. Estimated postmidcourse unbraked impact point, *Surveyor V*

E. Terminal Computations

After the 5 POM XD computation, primary emphasis was placed on obtaining an estimate of unbraked impact time. Normally, the estimate of unbraked impact time is used in calculating a backup signal for the onboard altitude marking radar. However, as a result of the helium leak detected after the first midcourse maneuver, a nonstandard sequence of terminal events had been designed that precluded the use of the traditional AMR backup. Critical to this sequence of events was the unbraked impact time estimate provided by OD group. This time was used as the basis on which to compute the time to trigger the explosive bolts on the retromotor and start the final sequence of retromotor–spacecraft separation and vernier firing, which led to the successful soft landing. The unbraked impact time used as the basis on which the final sequence of events was triggered was obtained from the FINAL YE orbit computation. This solution was based on 2 h, 15 min of two-way doppler data from DSS 11 and 2 h, 24 min from DSS 51. Also, *a priori* was used in the form of a covariance matrix based on data from the end of the sixth maneuver to $R - 5$ h, 40 min. The covariance matrix was degraded and expanded, as discussed in Section II-A. In addition to being able to account for the SPODP model errors by use of this method, working from the updated epoch results in a

considerable saving in program running time, which is very important, since the basic philosophy is that the near-moon data will yield the best estimate of unbraked impact time. This requires as much near-moon data as possible to be included in the orbit solution while still being able to provide the results at $R - 40$ min, which is the nominal lead time required to implement the backup command transmission.

For the terminal computations, a lunar elevation of 1734.9 km at the predicted unbraked impact point was used. This lunar elevation was obtained from NASA Langley Research Center and was in close agreement with the elevation based on the appropriate Air Force Aeronautical Chart and Information Center (ACIC) lunar chart less 2.4 km. The 2.4 km is the amount by which the elevation figures that are based on the ACIC charts exceed the elevations obtained from the *Ranger VI, VII,* and *VIII* tracking data. An *a priori* 1σ uncertainty of ± 1 km (roughly equivalent to ± 0.4 s) was assigned to the elevation.

Table 14. Inflight results of orbit determination terminal computations

Orbit solution data span, time		Predicted selenocentric conditions at unbraked impact on September 11, 1967		
From	To	Latitude, deg (South)	Longitude, deg (East)	GMT
Initial post-midcourse epoch	$E - 5$ h, 40 min	1.447	23.301	00:45:14.297[a]
	$E - 2$ h, 21 min	1.535	23.281	16.359
	$E - 1$ h, 59 min	1.519	23.252	15.528
$E - 5$ h, 40 min	$E - 1$ h, 21 min	1.501	23.216	14.667
	$E - 57$ min	1.520	23.252	15.431
	$E - 40$ min	1.513	23.238	00:45:15.162
Best estimate of unbraked impact time				00:45:15.318

[a]Solution used for initial estimate of AMR mark time.

The FINAL YE orbit computation predicted an unbraked impact time of 00:45:15.162 GMT on September 11, 1967. Based on this time, the predicted AMR mark time was 00:44:37.73 GMT. Based on telemetry records, the actual AMR mark time was determined to be 00:44:37.85 GMT, just 0.12 s later than the predicted time, well within the desired 0.5 s, 1σ uncertainty. The inflight results of the terminal orbit computations are given in Table 14. A comparison of the inflight and postflight results is presented in Table 15.

Terminal orbit computations were performed to determine a best estimate of unbraked impact time. As observed during other *Surveyor* missions, the unbraked impact time changed significantly as near-moon data were used in the solution. However, the terminal data fit well and was consistent with all the post-midcourse data when combined in postflight analyses. The last orbit (5 POM XD) computation made before changing to the terminal epoch ($R - 5$ h, 40 min) indicated an unbraked impact time of 00:45:15.325 GMT on September 11, 1967. Impact time predicted during the terminal orbit phase varied from 00:45:14.667 to 00:45:16.641 GMT. The inflight best estimate of the post-midcourse orbit, based on all the data from the sixth maneuver to approximately $R - 40$ min, gives an impact time of 00:45:15.315 GMT, which is very consistent with the inflight orbit computations.

As detected on *Surveyors III* and *IV*, DSS 11 again changed transmitter frequency during the terminal phase. This change, which went undetected during flight, resulted in an incorrect frequency being used for the final few points of DSS 11 data. The effect of this frequency error was negligible, as can be seen by comparing the FINAL YE orbit that includes the frequency error, with

Table 15. Comparisons of inflight and postflight terminal computations

Orbit solution data span, time from encounter		Unbraked impact time, GMT		Difference between inflight and postflight computations, s
From	To	Inflight computations	Postflight computations[a]	
Midcourse maneuver[b]	5 h, 40 min	00:45:14.297	00:45:14:444	0.147
	2 h, 21 min	16.359	15.965	−0.394
	1 h, 59 min	15.528	15.344	−0.176
5 h, 40 min	1 h, 21 min	14.667	14.710	0.043
	57 min	15.431	15.016	−0.415
	40 min	00:45:15.162	00:45:15.079	−0.083

[a]With corrected DSS 11 and DSS 51 frequencies.
[b]Post-midcourse epoch at end of sixth maneuver.

the POST 2 orbit, which has the frequency error corrected. The difference in unbraked impact time is only 0.153 s, well within the desired OD accuracy of 0.5 s. A plot of the one-way doppler data taken during main retroengine burn is given in Fig. 13.

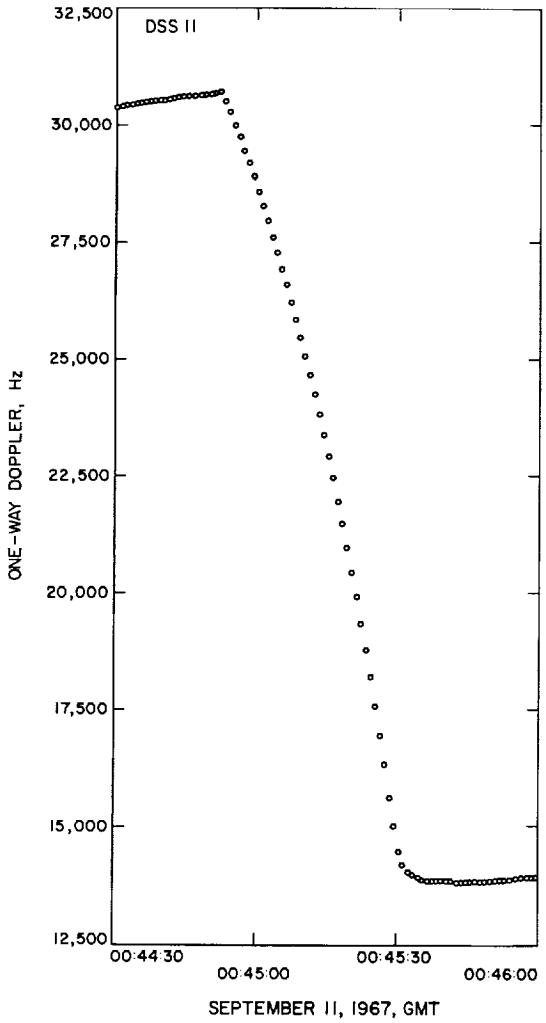

Fig. 13. Main retroengine-burn phase doppler, *Surveyor V*

VI. *Surveyor V* Postflight Orbit Determination Analysis

Presented in this section are the best estimate of the *Surveyor V* flight path and other significant results obtained from the DSS tracking data. The analysis verified that the premaneuver and postmaneuver inflight orbit solutions were within the *Surveyor* guaranteed orbit determination accuracy. The inflight philosophy of estimating only a minimum parameter set (i.e., spacecraft position and velocity vectors) for the orbit computations was again proven valid.

The tracking data was divided into three logical blocks:

(1) Pre (first) maneuver data taken between transfer orbit injection and first attitude maneuver prior to first midcourse thrust

(2) pre (sixth) maneuver data taken from Canopus reacquisition (after fifth midcourse thrust) to the first attitude maneuver prior to the sixth midcourse thrust

(3) postmaneuver data taken from Canopus reacquisition (after sixth midcourse thrust) to last two way doppler data point prior to terminal maneuvers

The *Surveyor* version (Mod II) of the single-precision orbit determination program, or SPODP—which is often referred to as simply the ODP—of the Jet Propulsion Laboratory (Ref. 1) was the principal analysis tool.

For the postflight orbital computations and analysis, only two-way doppler data were used. The rightmost column of Table 6, summarizes the data used for the final orbit computations used in the postflight analyses. Also in Table 6, comparison between the data in the columns recording information used inflight and postflight shows that a smaller amount of two-way doppler data points were used for the postflight computations. This was the result of removing some bad data points and points taken at low elevation angles. (See Section VII-A for the tracking data evaluation.)

A. Pre (First) Maneuver Orbit Estimates

All the known bad data points were removed in the orbit data generator program (ODG) before the start of the postflight analysis. After the data file was prepared a 6×6 type orbit solution was computed on all the data from initial acquisition to the first maneuver burn. Examination of the residual plots revealed four problem areas: (1) the DSS 42 data appeared to be biased; (2) part of the DSS 61 data was excessively noisy and biased; (3) the DSS 72 data (1 h) was biased; and (4) the 10-s sample rate data from DSS 11 taken just prior to maneuver execution was excessively noisy (Fig. 14).

A close examination of spacecraft event records revealed the source of problems listed under items 2 and 4 above. The DSS 61 data were bad because maneuvers were performed prior to, and during, Canopus acquisition. The actual roll search effect on the doppler data can

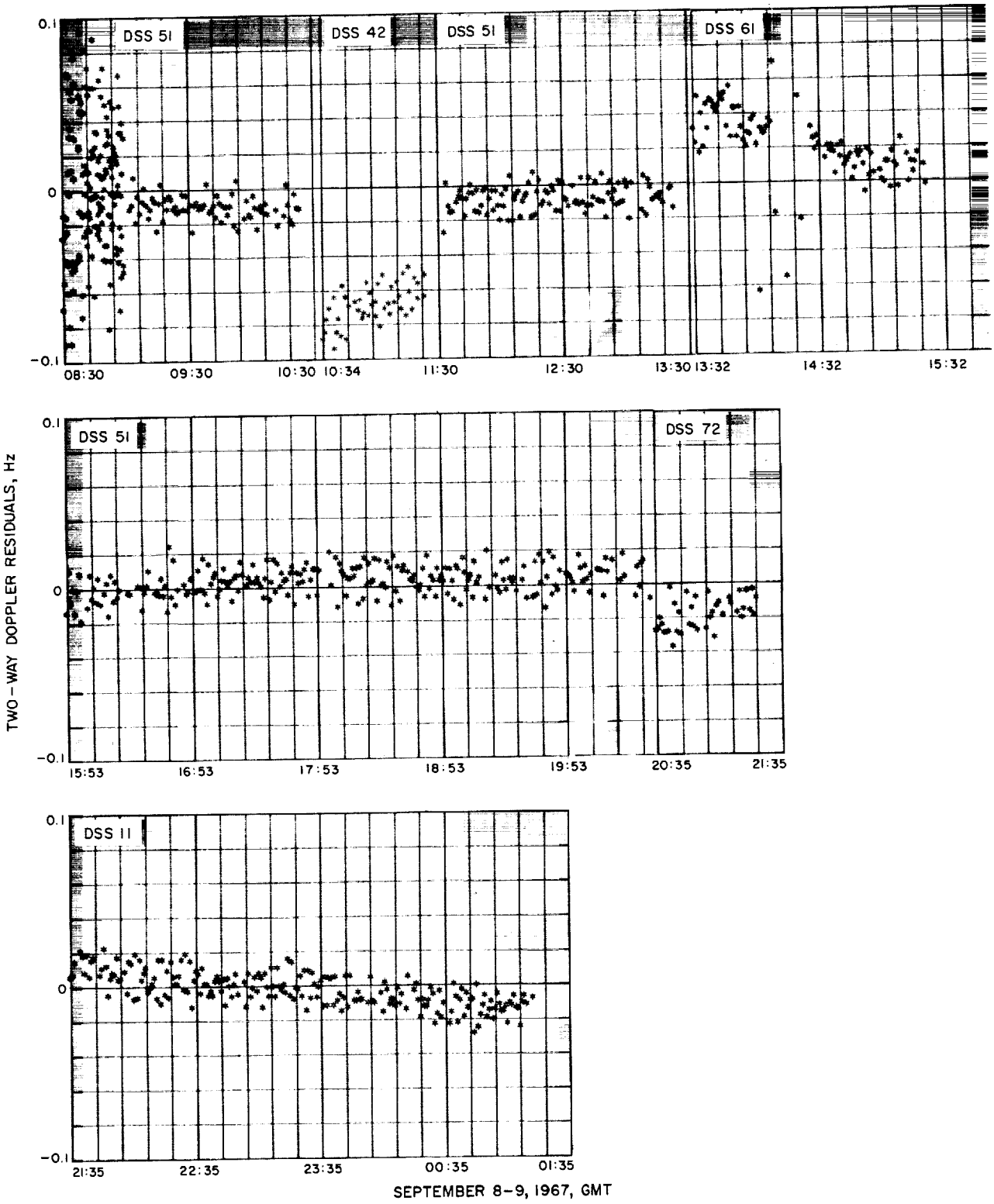

Fig. 14. Pre (first) maneuver two-way doppler residuals, *Surveyor V* (trajectory *not* corrected for perturbations)

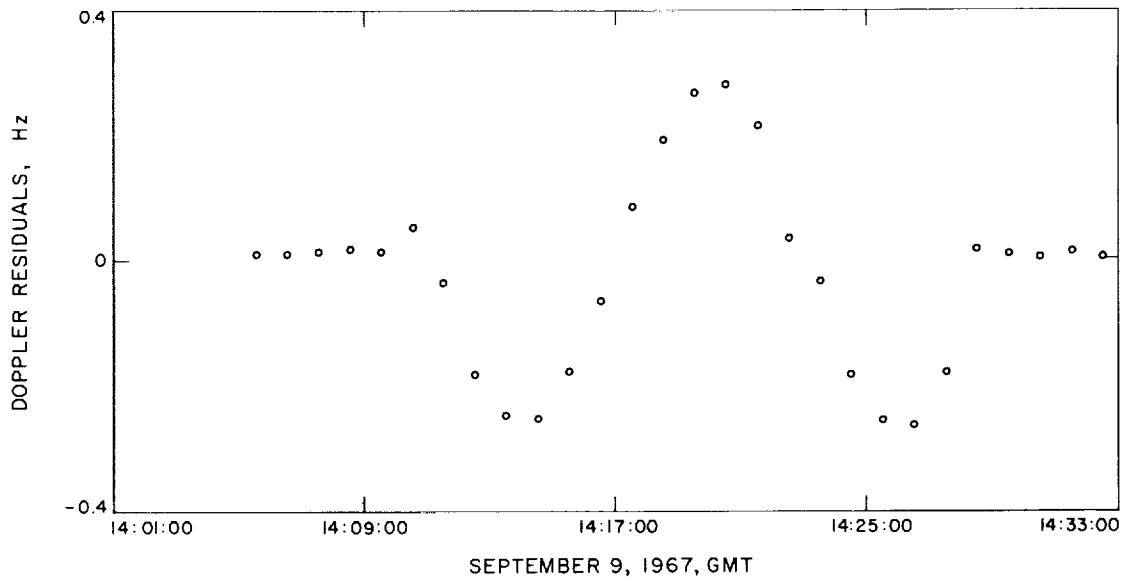

Fig. 15. Doppler residuals during Canopus acquisition (DSS 61), *Surveyor V*

be seen in Fig. 15. The questionable DSS 11 data were bad because of a similar problem resulting from orientation maneuvers performed prior to the actual firing of the engines for the midcourse maneuver. After removing the bad DSS 11 and DSS 61 data from the solution, another 6×6 orbit computation was run. This solution still showed DSS 42 and DSS 72 as biased from the other data. In an attempt to compensate for these biases, the estimate list was expanded to 12 to include the station location parameters – radius, latitude, longitude – for DSS 42 and DSS 72. The resulting fit was improved but not satisfactory. Another solution was computed with the DSS 72 data weighted out of the fit, and station location parameters for DSS 11, DSS 42, DSS 51 and DSS 61 were estimated. Again, the fit was unsatisfactory. Finally, the DSS 42 data were weighted out and station locations were estimated for DSS 11, DSS 51, DSS 61 and DSS 72. The resulting solution yielded an excellent fit on the data (Fig. 16), and the results were consistent with those achieved inflight. This final 18×18 solution yielded a maximum change of 10 m from the nominal station locations. This change was in the radius of DSS 51. All other station location parameters changed <10 m, well within the expected uncertainty of ± 15 m as determined by analysis of *Ranger* data. The difference in the predicted impact point of the final 18×18 solution, when compared with the inflight solution used to compute the maneuver, is 0.04 deg in latitude and 0.05 deg in longitude.

The 18×18 solution is considered to be the best estimate of the spacecraft pre (first) maneuver orbit. The uncorrected, unbraked impact point predicted by this solution (2.30° N lat, 23.69° E lat) was 1.442 deg north and 0.725 deg west of the prelaunch unbraked aim point, which was 0.858° N lat and 24.415° E lon. Other numerical values from this solution are presented in Table 16, and the number of data points, together with data noise statistics, are given in Table 17. A graphical comparison between the predicted unbraked impact (in the **B**-plane) of this solution and the inflight solutions may be seen in Fig. 10. The residual plots for this solution are presented in Fig. 16.

B. Pre (Sixth) Maneuver Orbit[†] Estimates

Inflight results of processing the data between the fifth and sixth maneuvers indicated something wrong with the data. Successive solutions varied so much that a 1σ uncertainty of 100 km was used for the final maneuver.

Initial postflight attempts to fit the data by estimating station location parameters and nongravitational perturbations were futile. The effect of the problem, as shown in the doppler residuals, may be seen by examining Fig. 17. Several data consistency orbits were run with various combination of data, deleting one station at a time. When deleting DSS 42 or DSS 51, the fit improved and the residuals from DSS 42 and DSS 51 indicated a large bias. At first examination, it was felt that DSS 51 data were responsible, but deletion of DSS 51 did not improve the fit as much as did the deletion of DSS 42.

[†]May also be referred to as the post (fifth) maneuver orbit.

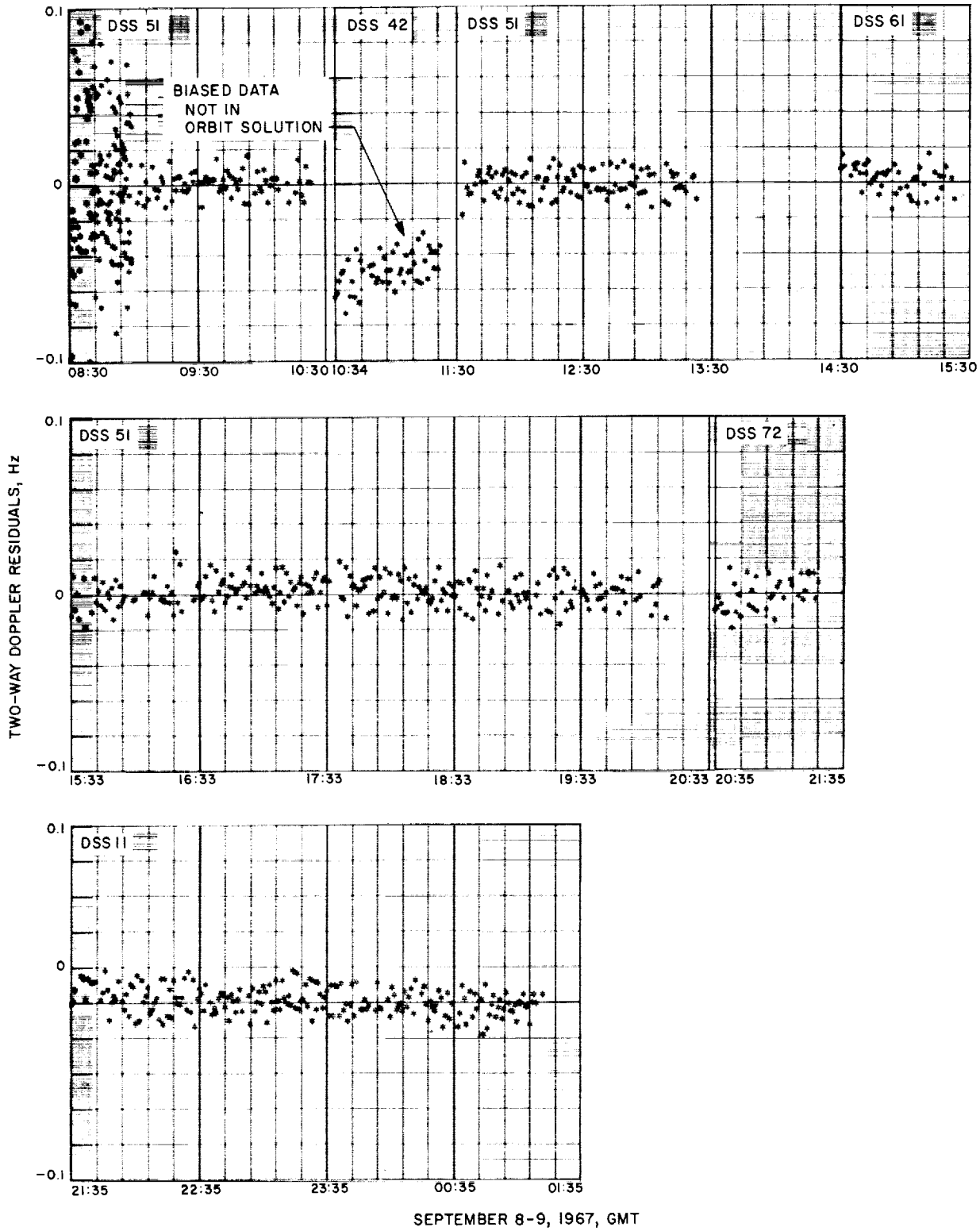

Fig. 16. Pre (first) maneuver two-way doppler residuals, *Surveyor V* (trajectory *corrected* for perturbations)

Table 16. Summary of postflight orbit parameters[a]

Parameter	Pre (first) midcourse	Pre (sixth) midcourse	Post-midcourse
Epoch, GMT	9/08/67, 08:15:12.951	9/09/67, 11:57:00.000	9/09/67, 23:49:00.000
Geocentric position and velocity at epoch			
x, km ($\pm 1\sigma$)	198.52578 ±0.14209	−74742.568 ±31.848	−79402.842 ±2.110
y, km	6023.3581 ±0.2400	−187664.93 ±99.232	−236876.73 ±4.28
z, km	2570.0625 ±0.1376	−107508.26 ±97.234	−130328.07 ±7.56
Dx, km/s	−10.272247 ±0.000302	−0.14916366 ±0.00058350	−0.076673517 ±0.000035285
Dy, km/s	2.0979605 ±0.0001003	−1.2675173 ±0.00042779	−1.0507320 ±0.0000459
Dz, km/s	−3.2156173 ±0.0004718	−0.60024406 ±0.00062883	−0.47503885 ±0.00008542
Target statistics			
B, km	2901.5595	2709.4959	2996.8192
B • TT, km	2893.3789	2707.3054	2991.5441
B • RT, km	−217.75480	108.97284	−177.75626
1σ SMAA, km	6.02	68.0	2.50
1σ SMIA, km	2.81	55.0	1.00
THETA, deg	66.26	179.24	93.98
σ_T IMPACT, s	1.172	15.000	0.600
PHI_{99}, deg	0.164221	3.830032	0.154138
1σ SVFIXR, m/s	0.618553	0.743556	0.623216
Latitude, deg	2.2985465	−3.9436889	1.4917731
Longitude, deg	23.692446	16.037533	23.255754
Impact time, GMT	9/10/67, 23:25:14.318	9/11/67, 00:37:27.924	9/11/67, 00:45:15.318

[a]Current best estimate, as of February 1, 1968.

Table 17. Summary of data[a] used in postflight (current best estimate) orbit solutions

Station	Begin data, time		End data, time		Number of points	Standard deviation	Root mean square	Mean error
	Date 1967	GMT	Date 1967	GMT				
Pre(first)midcourse								
DSS 72	9/08	20:35:32	9/08	21:23:32	39	0.00890	0.00897	−0.00115
11	9/08	21:35:32	9/09	01:17:32	206	0.00749	0.00755	0.000964
51	9/08	08:30:26	9/08	10:23:32	210	0.0293	0.0293	−0.000630
51	9/08	11:33:32	9/08	13:23:32	104	0.00717	0.00718	−0.000254
51	9/08	15:33:32	9/08	20:13:32	240	0.00787	0.00799	0.00134
DSS 61	9/08	14:30:32	9/08	15:23:32	46	0.00756	0.00769	0.00143
Pre(sixth)midcourse								
DSS 11	9/09	21:39:32	9/09	22:54:32	120	0.0306	0.0306	−0.00115
51	9/09	12:03:32	9/09	20:23:32	253	0.00705	0.00705	−0.0000145
51	9/09	20:25:32	9/09	21:23:32	56	0.00748	0.00749	−0.000231
DSS 61	9/09	16:52:32	9/09	20:13:32	191	0.00820	0.00820	0.000151
Post-midcourse								
DSS 11	9/09	23:53:32	9/10	02:48:32	131	0.00811	0.00814	−0.000620
11	9/10	21:48:32	9/10	23:53:32	82	0.00775	0.00806	0.00219
42	9/10	03:03:32	9/10	11:55:32	448	0.00688	0.00688	0.000206
DSS 51	9/10	12:04:32	9/10	21:28:32	443	0.00721	0.00721	−0.000198

[a]Two-way doppler data, only, was used in postflight analysis.

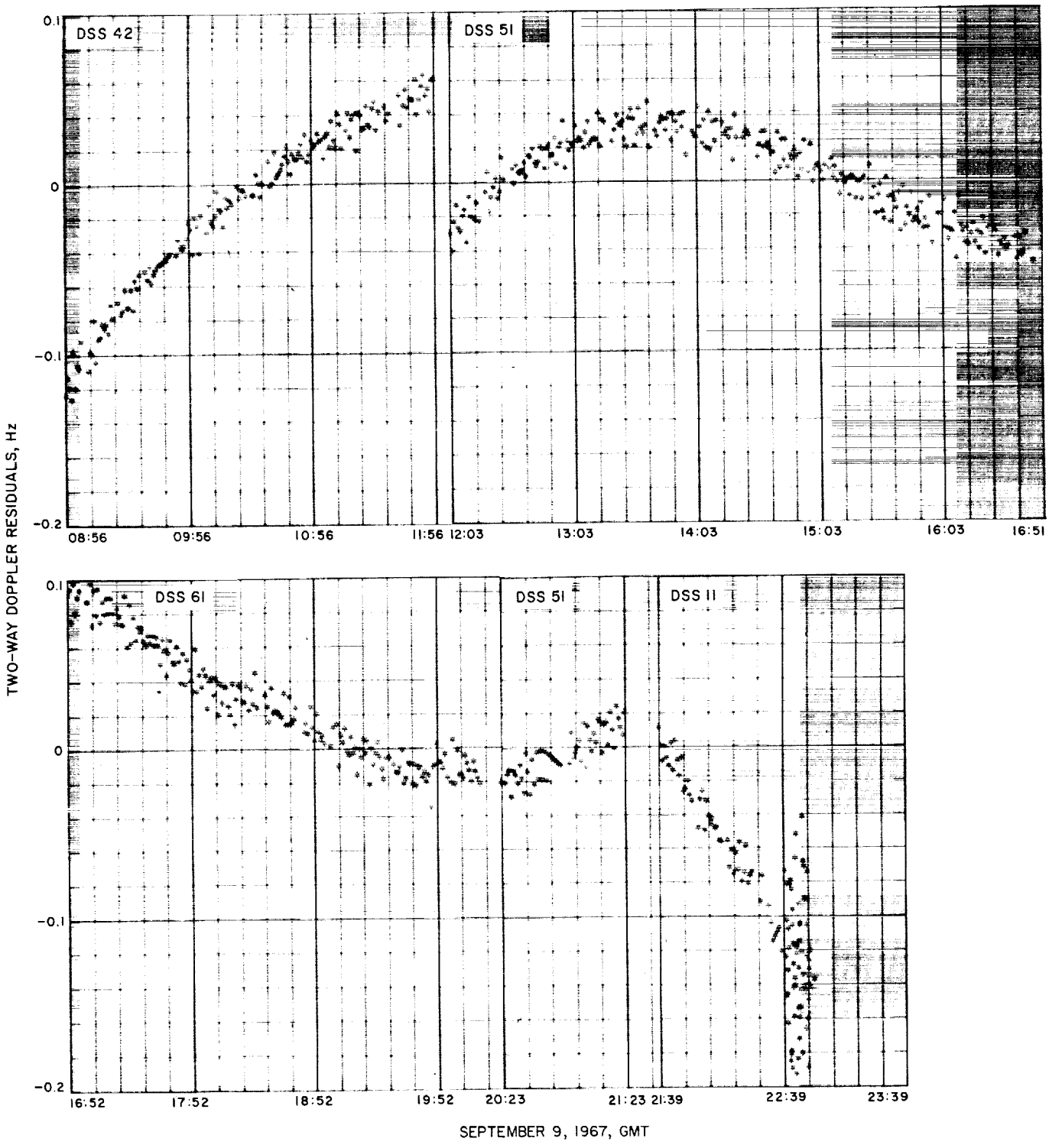

Fig. 17. Pre (sixth) maneuver two-way doppler residuals, *Surveyor V* (trajectory *not* corrected for perturbations)

Several attempts to fit the data without DSS 51 data in the solution resulted in good fits with *unreasonable* target parameters when mapped to impact. When the DSS 42 data were deleted, a good fit was possible by expanding the estimated parameter list to 15 to include nongravitational[8] forces (f_1, f_2, f_3) and radius and longitude station location parameters for DSS 11, DSS 51 and DSS 61. The resulting impact parameters were consistent with expected values, and the orbit data fit was excellent (Fig. 18).

[8]A discussion of the model used to estimate these parameters is found in Section II-A.

The accelerations resulting from nongravitational perturbations estimated in the final 15×15 solution are as follows:

$$f_1 = -0.113 \times 10^{-7}\ \text{km/s}^2$$

$$f_2 = 0.344 \times 10^{-8}\ \text{km/s}^2$$

$$f_3 = 0.702 \times 10^{-9}\ \text{km/s}^2$$

$$\Delta\ddot{\mathbf{r}} \cong 0.118 \times 10^{-7}\ \text{km/s}^2$$

The 15×15 solution discussed above is considered to be the best estimate of spacecraft pre (sixth) maneuver orbit. The uncorrected, unbraked impact point predicted

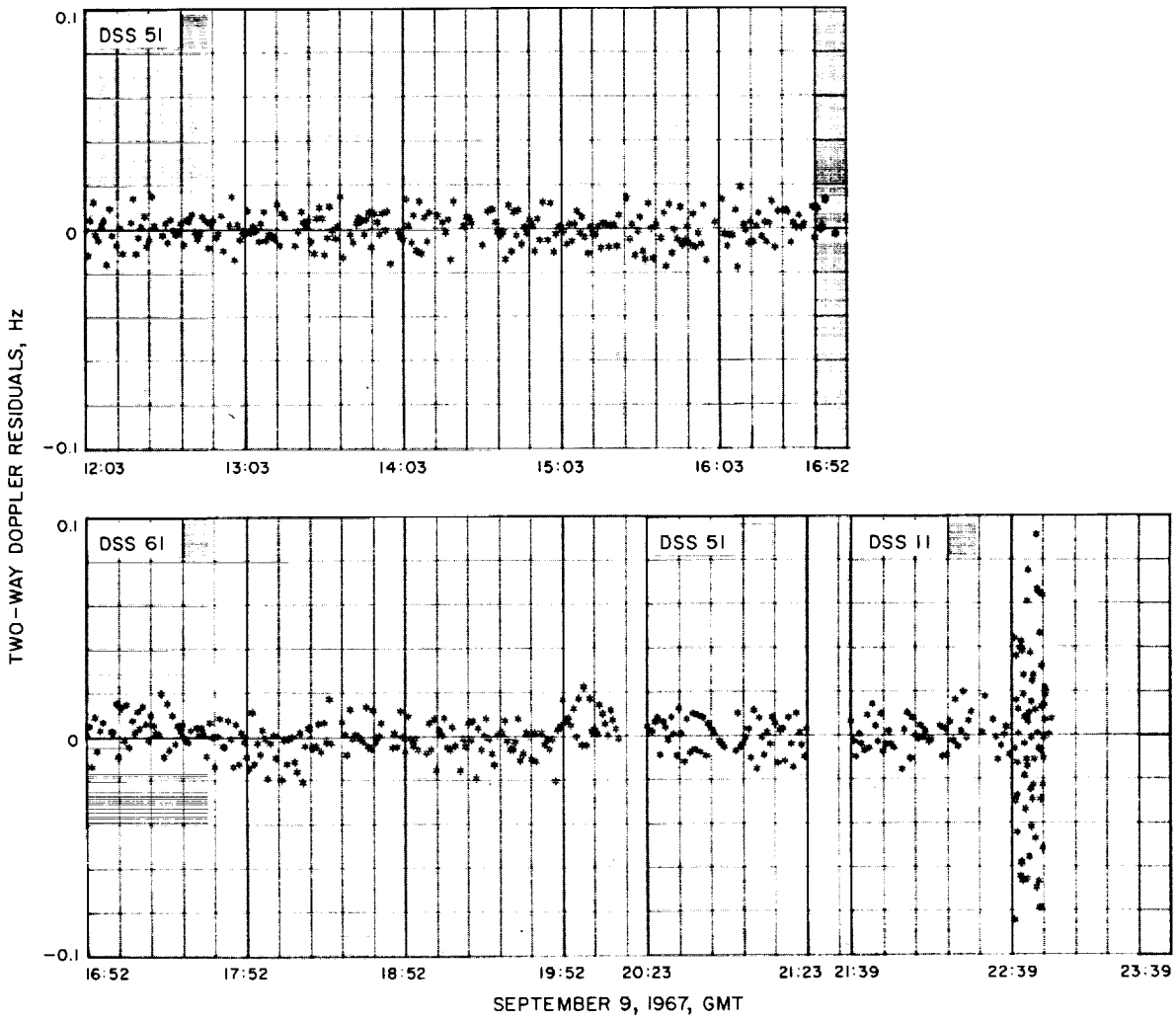

Fig. 18. Pre (sixth) maneuver two-way doppler residuals, *Surveyor V* (trajectory *corrected* for perturbations)

by this solution (3.94° S lat, 16.04° E lon), is approximately 4.8 deg south and 8.4 deg west of the prelaunch aim point. The large miss is from the unprecedented five maneuvers executed prior to this orbit. Other numerical values from this solution are presented in Table 16, and the number of data points, together with associated statistics, are given in Table 17. A graphical comparison between this solution and inflight solutions mapped to encounter (in the **B**-plane) is presented in Fig. 10. The residual plots are presented in Fig. 18.

C. Postmaneuver Orbit Estimates

Prior to starting the analysis of the postmaneuver tracking data, all known or suspected bad data points were removed. The objective of the analysis in this section was to obtain an orbit solution based on processing all postmaneuver tracking data in one block. This differed from the inflight computations, which required that the data be processed in two blocks to meet the AMR backup requirements. The lunar radius was not changed from 1734.9 for final postflight orbit computations. This value was obtained by subtracting 2.4 km from the elevation, based on the Air Force Aeronautical Chart and Information Center (ACIC) lunar chart. The 2.4 km is the difference between the elevation based on the ACIC and elevation obtained from *Ranger VI, VII,* and *VIII* tracking data (the ACIC figure is higher).

A close examination of the post-midcourse data revealed two minor discrepancies in the data: (1) a discontinuity of 0.02 Hz in the residuals[9] for DSS 51 at 14:27 GMT on September 10, 1967 (Day 253), and (2) a similar discontinuity in the data from DSS 11 at 23:31 GMT during the same day. Inflight, these jumps were believed to be caused by gyro drift checks and, therefore, were not alarming. However, a study of the tracking data teletype messages revealed that both of these problems were caused by an unnoticed change in frequency.

After the frequencies were corrected and a new ODP data tape (B-2) was made, a 6×6 orbit solution based on all postmaneuver data was obtained and mapped forward to target. Examination of residual plots indicated a fairly good fit with some slight biases. This solution agreed very well with the inflight solutions, which indicated that the frequency errors had little effect. The predicted impact time for this 6×6 solution was only 0.10 s from the *observed*[10] value. In an attempt to remove the remaining disturbances from the data fit, the estimated parameter list was expanded to 15 to include the radius, latitude, and longitude station location parameters from DSS 11, DSS 42 and DSS 51. The residual plots from this fit (Fig. 20) indicated an improved fit, with the impact parameters still in good agreement with inflight and observed results. The impact time from the 15×15 was now only 0.036 s from the observed. This 15×15 solution is considered to be the current best estimate of the *Surveyor V* postmaneuver orbit. Numerical values from the best estimate postmaneuver orbit solution are presented in Table 16. Amounts of data used in this solution, together with the associated noise statistics, are shown in Table 17. A **B**-plane comparison between this solution and inflight solutions may be seen in Fig. 14.

Based on the current best estimate, the *Surveyor V* spacecraft is estimated to be at 1.4918° N lat and 23.256° E lon. This is 0.827 deg ($\approx$24.8 km) north and 0.887 deg ($\approx$26.6 km) west of the final soft-landing aim point.

D. Evaluation of Sixth Midcourse Maneuver Based on DSIF Tracking Data

The *Surveyor V* sixth midcourse maneuver can be evaluated by examining the velocity changes at midcourse epoch and by comparing the maneuver aim point with the target parameters from the best estimate postmidcourse orbit solution. There was not sufficient data between maneuvers to evaluate the first maneuver.

The observed velocity changes resulting from midcourse thrust (applied by igniting the vernier engines) are determined by differencing the velocity components of best estimate orbit solutions based on postmaneuver data only and those based on premaneuver data only. These solutions are independent—i.e., *a priori* information from premaneuver data is not used during the processing of postmaneuver data. The estimated maneuver execution errors at midcourse epoch are determined by differencing the observed velocity changes and the commanded maneuver velocity increments. The remaining major contribution to the total maneuver error is made by the orbit determination process. This error source includes ODP computational and model errors, and errors in tracking data. These errors may be obtained by differencing the velocity components, at midcourse epoch, of the best estimate premaneuver orbit and the inflight orbit solution used for the maneuver computations. Numerical results of this part of the evaluation are presented in Table 18. In the table, it can be seen that the execution errors in Dx, Dy and Dz were only $+0.2195$ m/s, -0.0120 m/s, and -0.0580 m/s, respectively. Total maneuver errors for *Surveyor V* were well within specifications.

[9]See Fig. 19.

[10]Observed values are based on telemetry records analyzed postflight.

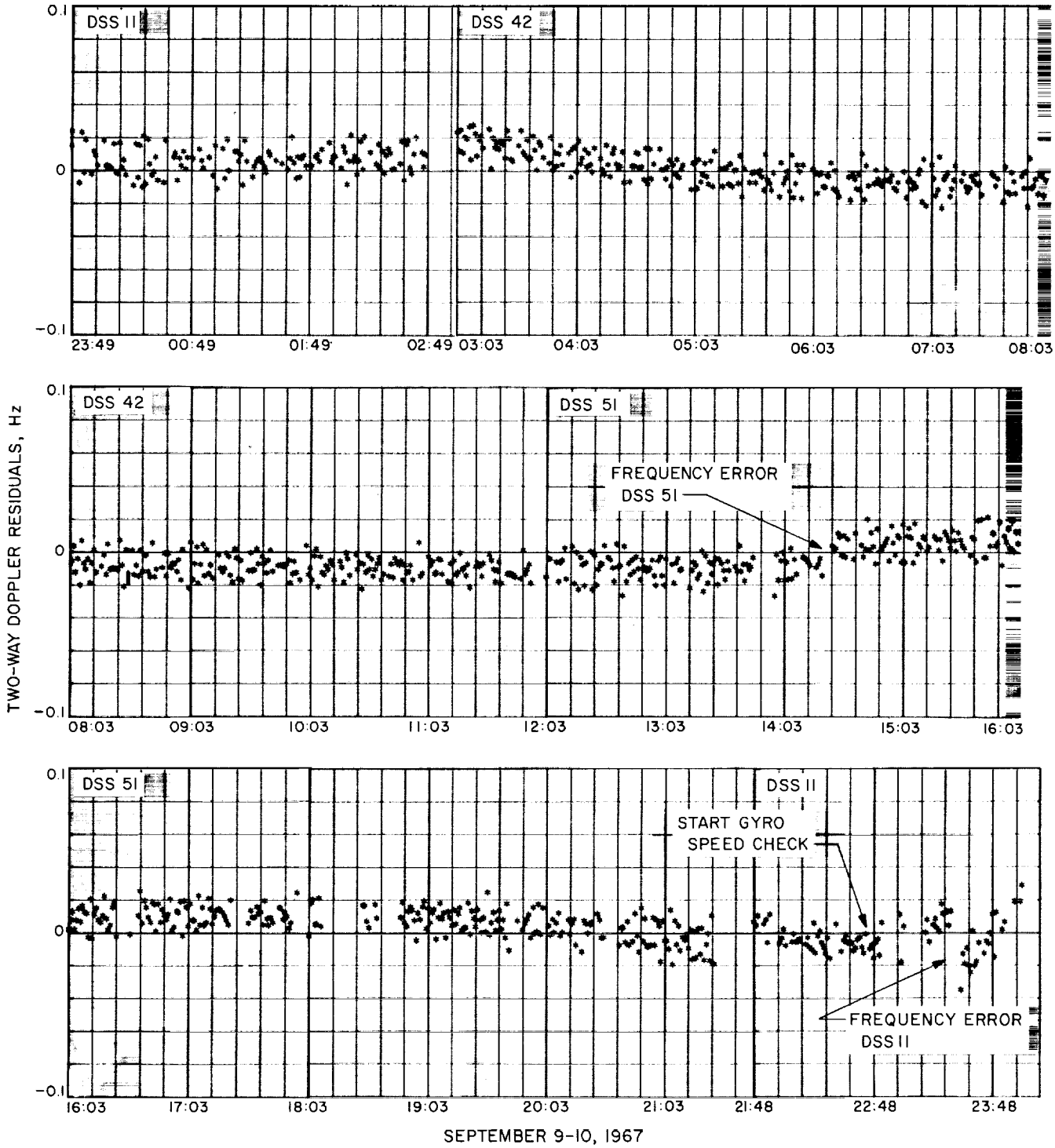

Fig. 19. Post (sixth) maneuver two-way doppler residuals, *Surveyor V* (trajectory *not* corrected for perturbations)

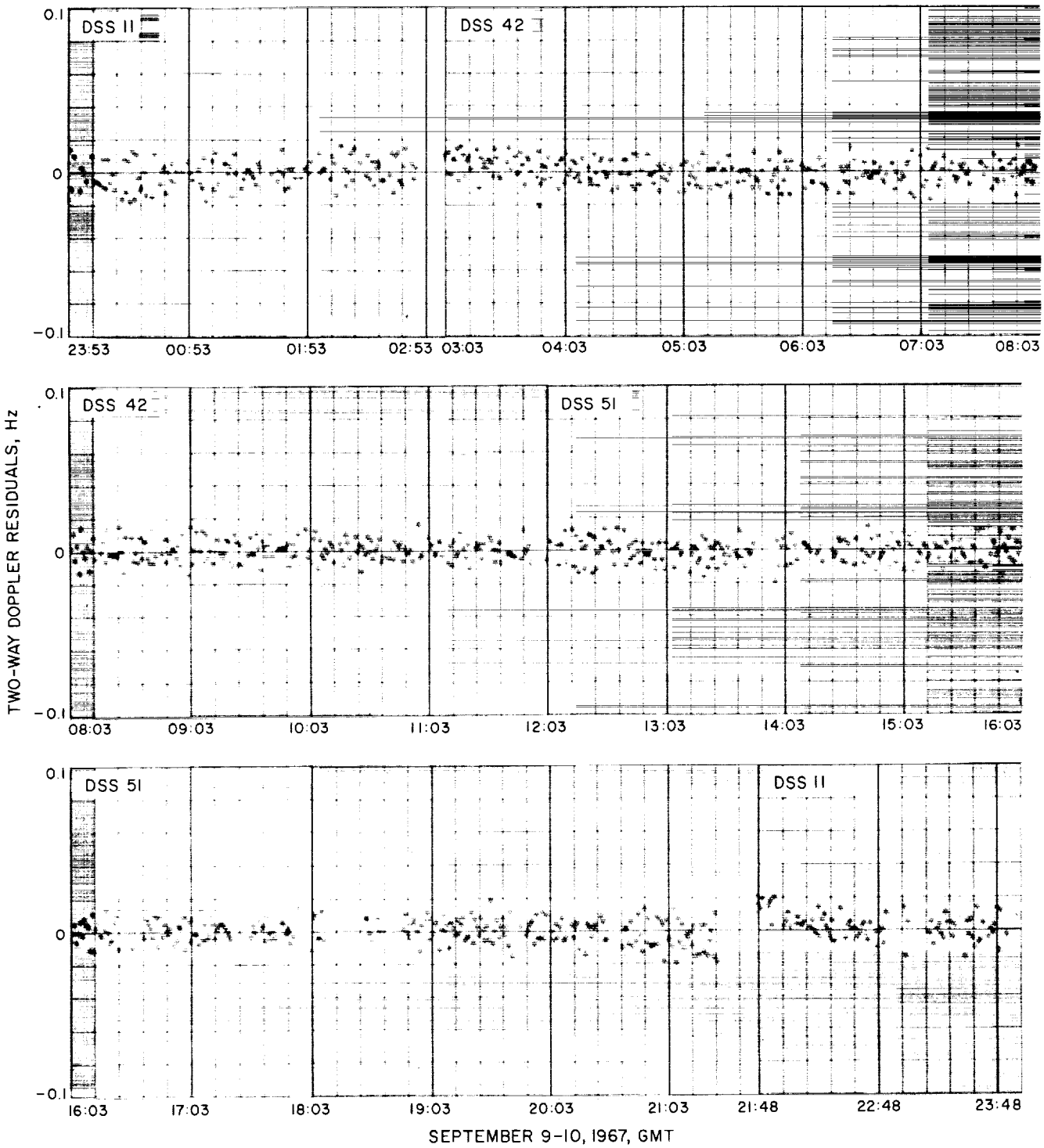

Fig. 20. Postmaneuver two-way doppler residuals, *Surveyor V* (trajectory *corrected* for perturbations)

Table 18. *Surveyor V* midcourse maneuver evaluated[a] at midcourse epoch[b]

Current best estimate of premaneuver velocity, m/s (mapped to midcourse epoch[b])	Inflight[c] estimate of premaneuver velocity, m/s (mapped to midcourse epoch[b])	Current best estimate of postmaneuver velocity, m/s	Observed velocity change due to maneuver (best post *minus* best pre), m/s	Commanded[c] maneuver velocity change, m/s	Total maneuver errors	
					Execution errors[d] (observed change *minus* commanded change), m/s	OD errors (best pre *minus* inflight), m/s
$Dx = -78.9373$	−79.5158	−76.6735	$\Delta Dx = +2.2638$	+2.0443	+0.2195	+0.5785
$Dy = -1053.7509$	−1053.6142	−1050.7320	$\Delta Dy = +3.0189$	+3.0309	−0.0120	−0.1367
$Dz = -478.8446$	−478.7959	−475.0389	$\Delta Dz = 3.8057$	+3.8637	−0.0580	−0.0487

[a]All velocity components are given in geocentric space-fixed cartesian coordinates.
[b]Midcourse epoch = end of sixth motor burn = September 9, 1967, 08:25:03.000 GMT.
[c]Based on inflight premaneuver orbit solution (2 POM XD) used for final midcourse maneuver computations.
[d]Based on difference of best pre-midcourse and post-midcourse orbit estimates. The 1σ uncertainties associated with these determinations of midcourse velocity errors are of the same order as the errors, themselves. However, these determinations have particular merit because of their independence of the spacecraft system.

A more meaningful evaluation can be made by examining certain critical target parameters. Since the primary objective of the midcourse maneuver is to achieve lunar encounter at a selected landing site, the maneuver unbraked aim point is used as the basic reference for this evaluation. The aim point for *Surveyor V* was 0.9167° N lat and 24.143° E lon. Based on the predicted unbraked impact point from the best estimate inflight orbit solution (2 POM XD), trajectory corrections were computed to achieve landing at the desired site. To evaluate the total maneuver error at the target, the maneuver aim point is compared with the predicted unbraked impact point from the current best estimate postmaneuver orbit solution. The OD errors can be obtained by differencing the unbraked target parameters of the current best estimate premaneuver orbit solution and the inflight orbit solution used for maneuver computations. Execution errors, consisting of both attitude maneuver errors and engine system errors, are then determined by differencing the total and OD errors. Numerical results of these computations are presented in Table 19. In the table, it can be seen that landing was achieved within +0.575 deg latitude and −0.887 deg longitude of the desired aiming point. These differences in latitude and longitude are roughly equivalent to 17.3 km and −26.6 km, respectively, on the lunar surface. OD position errors ($\Delta\mathbf{B}\cdot\mathbf{T}Q = 50.25$ km, $\Delta\mathbf{B}\cdot\mathbf{R}Q = -19.53$ km) are well within the 100 km, one standard deviation OD accuracy stated inflight. This high uncertainty was due to orbit changes observed because of bad data and spacecraft perturbations. In general, the accuracy of the *Surveyor V* midcourse maneuver was well within *Surveyor* Project specifications. It should be noted that these results cannot be used to evaluate the *Centaur* injection accuracy, since the final aim point was not the same as the prelaunch aim point.

Table 19. Impact points, *Surveyor V*

a. Unbraked impact points

Source	Latitude, deg (Negative s)	Longitude, deg
Best estimate of premidcourse	−3.944	16.038
Inflight orbit (2 POM XD)	−4.235	16.828
Best estimate of post midcourse	1.492	23.256
Maneuver unbraked aim point	0.917	24.143

b. Estimated midcourse errors mapped to unbraked impact point

Source	Δ Latitude (Lunar)		Δ Longitude (Lunar)	
	deg	km	deg	km
OD errors[a]	+0.291	+8.73	−0.790	−23.70
Maneuver error[b]	+0.284	+8.52	−0.097	−2.91
Overall errors[c]	+0.575	+17.25	−0.887	−26.61

[a]OD errors = Current best premaneuver estimate *minus* orbit used for maneuver computations (2 POM XD).
[b]Maneuver errors = Overall errors *minus* OD errors.
[c]Overall errors = Current best postmaneuver estimate *minus* aiming point.

E. Estimated Tracking Station Locations and Physical Constants

1. Method of analysis. Computations were made to determine the best estimate of $GM_\oplus$, GM_ζ and station location parameters for the *Surveyor V* mission. The total parameters estimated in these computations were: the spacecraft position and velocity at an epoch; $GM_\oplus$; GM_ζ; spacecraft acceleration perturbations, f_1, f_2, and f_3; the solar radiation constant, G; and two components (geocentric radius and longitude) of station locations for each of DSS 11, DSS 42, DSS 51, and DSS 61. These solutions were computed using only two-way doppler data. Data were available for both pre-midcourse and post-midcourse phases from DSS 11 and DSS 51. For DSS 42, post-midcourse data were available; for DSS 61, only pre-midcourse data were available. To obtain the best

Table 20. Station locations and statistics, *Surveyor V* (referenced to 1903.0 pole)

Station	Data source	Distance off spin axis r_s, km	1σ r_s standard deviation, m	Geocentric longitude, deg	1σ longitude standard deviation, m	Geocentric radius, deg	Geocentric latitude,[a] deg
DSS 11	*Mariner II*	5206.3357	3.9	243.15058	8.8	6372.0044	35.208035
	Mariner IV, cruise	404	10.0	067	20.0	2.0188	08144
	Mariner IV, post-encounter	378	37.0	072	40.0	2.0161	08151
	Pioneer VI, Dec. 1965–June 1966	359	9.6	092	10.3	2.0286	08030
	Goddard Land Survey, Aug. 1966	718	29.0	094	35.0	2.0640	08230
	Surveyor I, post-touchdown	276	2.9	085	23.8	2.6446	16317
	Surveyor I, inflight, post-midcourse, only	200	50.8	098	59.4	1.9975	08192
	Surveyor III, inflight	408	29.7	100	49.0	2.0230	08192
	Surveyor IV, inflight	326	41.1	097	49.0	2.0129	08192
	Surveyor V, inflight	256	47.0	092	39.0	2.0043	08192
DSS 42	*Mariner IV*, cruise	5205.3478	10.0	136	20.0	6371.6882	−35.219410
	Mariner IV, post-encounter	.3480	28.0	134	29.0	.6824	19333
	Pioneer VI, Dec. 1965–June 1966	.3384	5.0	151	8.1	.6932	19620
	Goddard Land Survey, Aug. 1966	.2740	52.0	000	61.0	.7030	20750
	Surveyor I, post-touchdown	.3474	3.5	130	22.1	.6651	19123
	Surveyor I, inflight, post-midcourse, only	.3465	32.7	166	41.1	.6834	19372
	Surveyor III, inflight	.3522	26.5	146	45.0	.6905	19372
	Surveyor IV, inflight	.3487	34.8	161	49.0	.6861	19372
	Surveyor V, inflight post-midcourse, only	.3448	33.9	156	35.0	.6814	19372
DSS 51	Combined *Rangers*, LE3[b]	5742.9315	8.5	27.68572	22.2	6375.5072	−25.739169
	Ranger VI, LE3	203	19.7	72	69.3	.4972	9215
	Ranger VII, LE3	211	25.5	83	61.3	.4950	9157
	Ranger VIII, LE3	372	22.3	48	85.0	.5130	9159
	Ranger IX, LE3	626	56.6	80	49.5	.5322	8993
	Mariner IV, cruise	363	10.0	40	20.0	.5120	9148
	Mariner IV, post-encounter	365	40.0	57	38.0	.5143	9198
	Pioneer VI, Dec. 1965–June 1966	332	11.6	69	12.0	.5094	9176
	Goddard Land Survey, Aug. 1966	706	39.0	86	43.0	.5410	8990
	Surveyor I, inflight	380	38.3	78	41.0	.5144	9169
	Surveyor III, inflight	312	35.0	74	46.2	.5069	9169
	Surveyor IV, inflight	337	39.3	75	46.8	.5096	9169
	Surveyor V, inflight	355	44.1	74	31.5	.5116	9169
DSS 61	*Lunar Orbiter II*, doppler	4862.6067	9.6	355.75115	44.4	6369.9932	40.238566
	Lunar Orbiter II, doppler and ranging	.6118	3.4	138	4.0	69.9999	8566
	Mariner IV, post-encounter	.6063	14.0	099	24.0	70.0009	8655
	Pioneer VI, Dec. 1965–June 1966	.6059	8.8	103	10.4	70.0060	8715
	Surveyor III, inflight	.6054	24.5	126	47.0	70.0046	8701
	Surveyor V, inflight, pre-midcourse, only	.5962	72.2	125	75.0	69.9921	8701

[a]Latitude was not estimated for *Surveyor* inflight solutions.
[b]Lunar ephemeris 3 (development ephemeres 15); all *Surveyor* inflight solutions used LE 4 (DE 19).

estimate of the solved-for parameters, the pre-midcourse data block was combined with the post-midcourse data block. The procedure of combining the two data blocks is to fit only the pre-midcourse data, accumulate the normal equations at the injection epoch, and map the converged estimate to the midcourse epoch with a linear mapping of the inverted normal equation matrix (i.e., covariance matrix). The estimate is then incremented with the best estimate of the maneuver, and the mapped covariance matrix is corrupted in the velocity increment and used as *a priori* for the post-midcourse data fit. The ephemerides used in the reduction was one of the latest JPL ephemerides (DE-19) with the updated mass ratios and Eckert's corrections.

2. *Results.* The results of these computations are presented in Table 20 in an unnatural station coordinate system (geocentric radius, latitude, and longitude) and in a natural coordinate system (r_s, λ, Z) where r_s is the distance off the spin axis (in the station meridian), λ is the longitude, and Z is along the earth spin axis (Fig. 21).

The numerical results indicate that the values obtained for r_s for DSS 11, DSS 42, and DSS 61 are a few meters smaller than most of the previous *Surveyor* solutions listed. All other station location parameters are consistent with previous solutions. As with previous *Surveyor* solutions the improved values[11] of DSS indices of refraction were used in the solution. The new indices improved the data fit for all stations that took low elevation data. Previous to the availability of new indices, a value of 340 was used for all DSS.

Solutions of *Surveyors I* to *V* for the longitude of DSS 42 are a few meters higher than previous solutions. However, these values are consistent with all the other *Surveyor* solutions that have been computed in postflight analysis of the tracking data. Therefore, it is felt that the estimate for DSS 42 longitude is a good one. All other station locations estimated for *Surveyor V* are within the range of the previous solutions listed. The statistics obtained with the station locations are higher than most other missions because (1) larger effective data weights were used for *Surveyor* missions and (2) the amount of data available is generally smaller.

The solved-for $GM_\oplus$ and $GM_\mathfrak{c}$ for *Surveyor V* are given in Table 21 along with previous solutions. The value for

[11]Indices of refraction obtained from A. S. Liu, Navigation Accuracy Group, JPL: DSS 11 = 240, DSS 42 = 310, DSS 51 = 240, DSS 61 = 300.

Table 21. Physical constants and statistics, *Surveyor V*

Data source	$GM_\oplus$, km^3/s^2	1σ standard deviation, km^3/s^2	$GM_\mathfrak{c}$, km^3/s^2	1σ standard deviation, km^3/s^2
Lunar Orbiter II, doppler	398600.88	2.14	4902.6605	0.29
Lunar Orbiter II, doppler and ranging	398600.37	0.68	4902.7562	0.13
Combined *Rangers*	398601.22	0.37	4902.6309	0.074
Ranger VI	398600.69	1.13	4902.6576	0.185
Ranger VII	398601.34	1.55	4902.5371	0.167
Ranger VIII	398601.14	0.72	4902.6304	0.119
Ranger IX	398601.42	0.60	4902.7073	0.299
Surveyor I	398601.27	0.78	4902.6492	0.237
Surveyor III	398601.11	0.84	4902.6420	0.246
Surveyor IV	398601.19	0.99	4902.6297	0.247
Surveyor V	398601.10	0.61	4902.6298	0.236

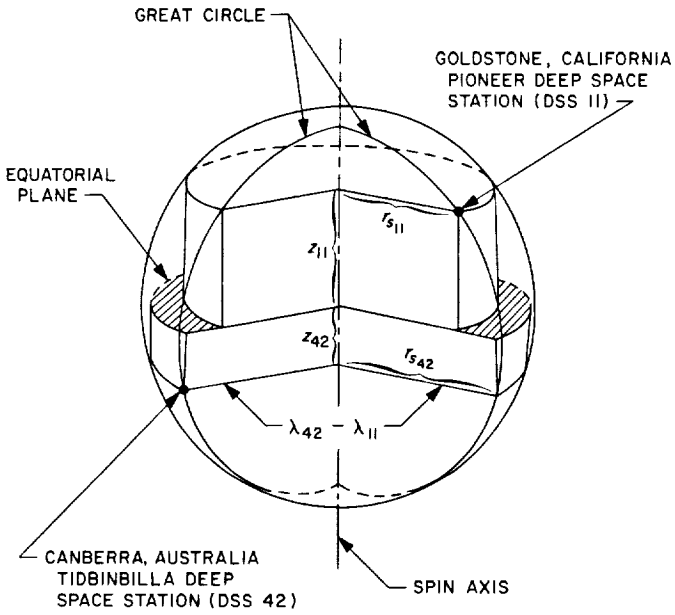

Fig. 21. Tracking station coordinate system

$GM_\oplus$ is slightly higher than the *Lunar Orbiter II* solutions. However, it is within the range of previous *Surveyor* and *Ranger* solutions, and is less than ½σ from the combined *Ranger* solution. The value obtained for $GM_\mathfrak{c}$ is consistent with previous solutions and is almost identical to the *Surveyor IV* solution. It is slightly lower than the solutions obtained from *Surveyors I* and *III*, but is within 1σ of the combined *Ranger* solution. The correlation matrix on postmaneuver data with premaneuver data as *a priori* is given in Table 22.

Table 22. Correlation matrix of estimated parameters, *Surveyor V* (postmaneuver data with premaneuver data as *a priori*)

Standard deviation		x	y	z	Dx	Dy	Dz	$GM_\oplus$	G	GM_ζ	f_1	f_2	f_3	R_{11}	Lon_{11}	R_{42}	Lon_{42}	R_{51}	Lon_{51}
x	1.40	1.000	0.060	−0.340	0.965	0.284	−0.360	0.448	0.002	0.498	−0.872	0.168	−0.232	0.082	0.587	0.123	0.284	0.354	0.336
y	1.72		1.000	−0.953	−0.007	0.827	−0.845	−0.005	−0.003	0.032	−0.416	0.019	−0.058	0.690	−0.205	0.814	−0.284	0.805	−0.418
z	3.34			1.000	−0.263	−0.849	0.910	−0.127	0.003	−0.192	0.634	−0.081	0.130	−0.670	0.092	−0.823	0.258	−0.856	0.350
Dx	0.007				1.000	0.339	−0.373	0.589	0.024	0.411	−0.826	0.050	−0.141	0.063	0.664	0.002	0.359	0.226	0.292
Dy	0.009					1.000	−0.966	0.324	−0.007	0.151	−0.508	−0.239	0.153	0.619	0.113	0.594	0.004	0.552	−0.317
Dz	0.017						1.000	−0.271	0.002	−0.251	0.571	0.151	−0.084	−0.618	0.008	−0.691	0.148	−0.623	0.369
$GM_\oplus$	0.610							1.000	0.000	0.088	−0.447	0.050	−0.163	0.220	0.414	−0.124	0.189	0.083	−0.191
G	0.100								1.000	0.000	−0.009	0.005	−0.005	−0.001	0.001	−0.003	−0.002	0.000	−0.002
GM_ζ	0.236									1.000	−0.245	0.037	0.024	0.082	0.183	0.220	0.248	0.058	0.322
f_1	0.71×10^{-9}										1.000	−0.380	0.471	−0.368	−0.425	−0.380	−0.061	−0.696	−0.056
f_2	0.45×10^{-9}											1.000	−0.986	0.170	−0.114	0.148	−0.307	0.441	−0.102
f_3	0.94×10^{-9}												1.000	−0.216	0.032	−0.139	0.281	−0.483	0.138
R_{11}	0.058													1.000	0.031	0.539	−0.199	0.581	−0.395
Lon_{11}	0.00039														1.000	−0.311	0.732	−0.062	0.574
R_{42}	0.041															1.000	−0.354	0.724	−0.316
Lon_{42}	0.00035																1.000	−0.286	0.719
R_{51}	0.049																	1.000	−0.260
Lon_{51}	0.00031																		1.000

3. Conclusion. The $GM_{\oplus}$ and GM_{ζ} estimates were well within the standard deviation of the combined *Ranger* and previous *Surveyor* estimates. The Pioneer Deep Space Station r_s is felt to be a little low, however all other station location solutions are consistent with *Ranger*, *Mariner*, *Pioneer* and previous *Surveyor* solutions. The results of successive *Surveyor* estimates, *Surveyors VI* and *VII*, are presented in Sections X-E and XIV-E, respectively.

VII. Observations and Conclusions From *Surveyor V*

A. Tracking Data Evaluation

In general, DSIF station operations during the *Surveyor V* mission were effectively implemented. From the time of first two-way acquisition of the spacecraft over DSS 51 until shortly before retroignition, the spacecraft was almost continuously in two-way lock, and station transfers were rapid and efficiently executed. The most serious loss of two-way doppler data inflight occurred during the second pass of DSS 42 when the uplink was lost during transfer from DSS 11. For 70 min, DSS 42 tracked *Surveyor V* in the one-way mode, unaware of the loss of two-way lock. It was supposed that the large doppler deviations reported by the near-real-time tracking data monitor were the result of the four midcourse maneuvers that the spacecraft had undergone by this time. For this reason the error was not discovered sooner and the data were not acquired. During the third pass of DSS 11, approximately 2 h before retroignition, the most significant digit of the doppler counter was lost for 32 min. These data were quickly recovered by hand-restoring the missing digit on punched cards. The Johannesburg Deep Space Station mislabeled approximately 2½ minutes of data at initial two-way acquisition during the launch pass. This data was mislabeled three-way, but the data was recovered by changing the data condition code from three-way to two-way. The resultant effect from these data losses on the mission was negligible.

1. Pre-midcourse phase angular tracking. In general, doppler data yields far greater accuracy in the determination of a spacecraft orbit than does angular data and is, therefore, used almost exclusively in the orbit determination process during most of the mission. The one exception is the launch phase, when a small amount of doppler data is available; since quick determination of the orbit is necessitated at this time, both doppler and angle data are used. During the *Surveyor V* mission, angle data from DSS 51 and DSS 42 were used in the orbit determination program during the first passes of these two stations. To improve the quality of the angular data to be used in the ODP, it is first corrected for antenna optical pointing error, as discussed in Section II-B.

Experience gained in past missions has shown that the correction coefficients do not remove all systematic pointing errors. Since DSS 51 was the initial acquisition station, the angular data taken by this station was the most important angular data for use in the early orbits. These data, when fit through the final postflight orbit, show a bias of +0.029 deg HA and −0.012 deg dec. These values are reasonable and correlate well with past experience on the *Surveyor* Project. First-pass angular residuals at DSS 51 are presented in Figs. 1 and 2 to show the effect of the angle correction applied.

2. Pre (first) midcourse phase doppler tracking. The Johannesburg Deep Space Station, the first prime station to view the spacecraft continuously after injection, began taking good two-way, 10-s count doppler data at 08:30:21 GMT on September 8, 1967. The sample rate was changed to 60 s at 08:59:51, and the spacecraft was transferred to DSS 42 at 10:34:02 GMT. These early data from DSS 51, which showed a standard deviation of 0.029 Hz, were quite acceptable. The two-way doppler residuals for this initial pass over DSS 51 may be seen in Figs. 14 and 16. The Tidbinbilla Deep Space Station returned 60-s count two-way doppler data from 10:34:02 to 11:24:02 GMT on September 8, 1967. Data from DSS 42 for this first pass showed a bias from the other DSS data. The cause of this bias has not been determined. First-pass DSS 61 two-way doppler data show a standard deviation of 0.046 Hz. This unusually high noise is attributed to star acquisition from 14:09:00 to 14:28:27 GMT. Figure 15 more clearly shows the star acquisition phase, which was deleted from the final postflight analyses. The Ascension Island Deep Space Station tracked the *Surveyor V* spacecraft in the two-way mode from 20:35:02 to 21:24:02 GMT. Residuals from these data show a standard deviation of 0.009 Hz. Two-way doppler data residuals from DSS 11 from rise until first midcourse maneuver are presented in Figs. 14 and 16.

Early analysis of the *Surveyor V* trajectory indicated a midcourse maneuver during the first pass of DSS 11 would be advantageous; therefore, the first such maneuver was executed during this pass. A spacecraft malfunction occurred as a result of the midcourse maneuver, and in an attempt to correct the malfunction, four more maneuvers were executed. Two-way doppler data from these maneuvers are presented in Figs. 22 through 26.

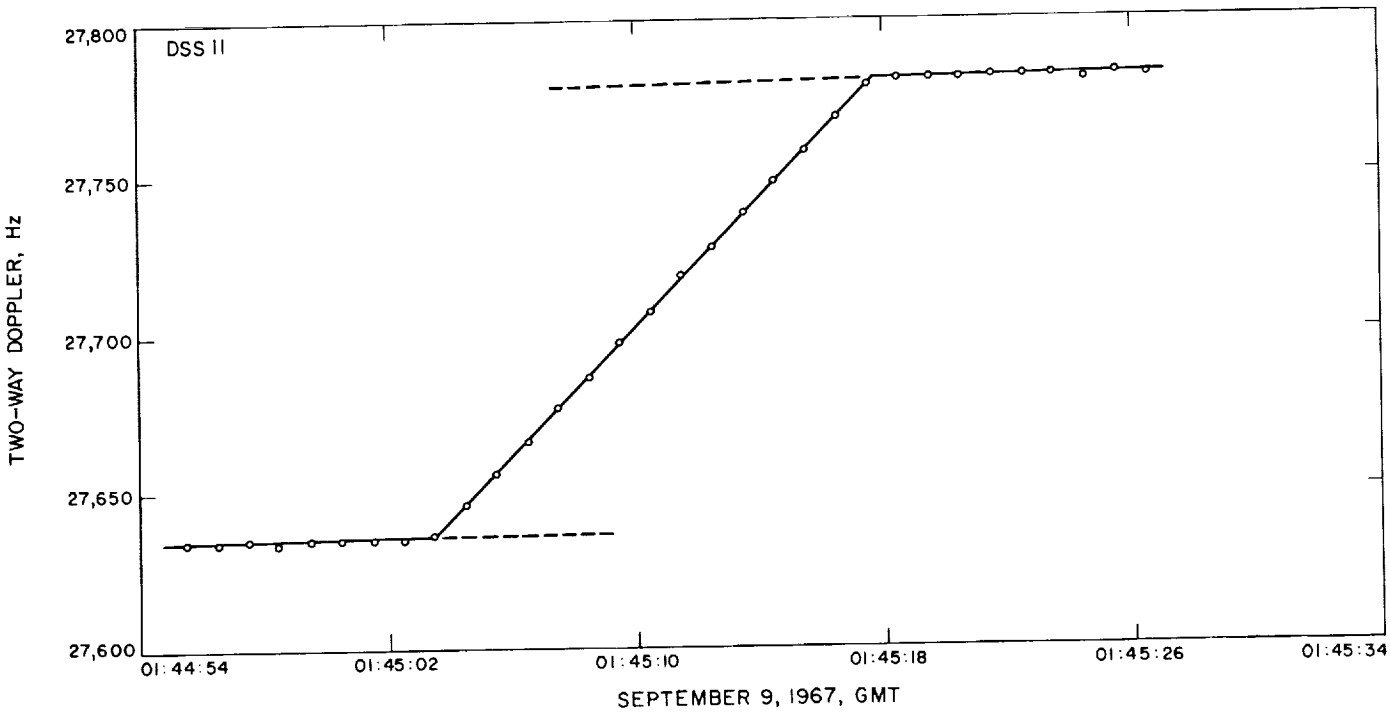

Fig. 22. First midcourse maneuver doppler data, *Surveyor V*

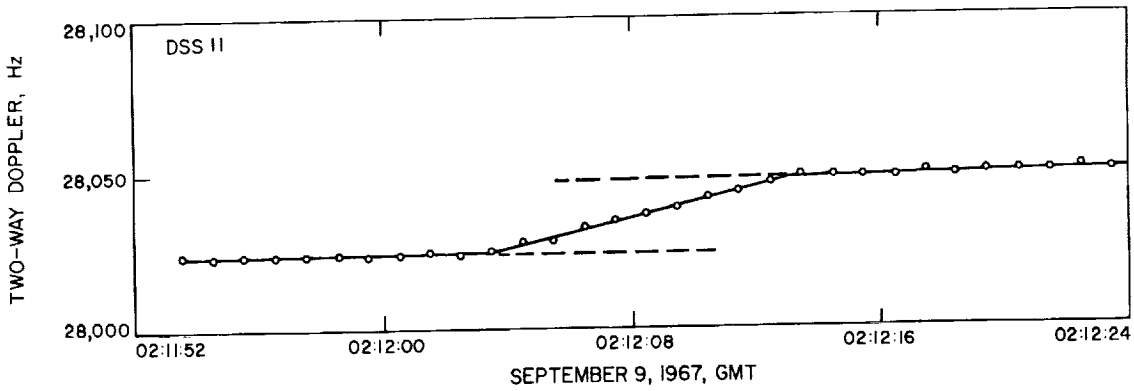

Fig. 23. Second midcourse maneuver doppler data, *Surveyor V*

For comparison, these data were plotted to identical vertical scales.

3. Pre (sixth) midcourse phase doppler data. No usable data was taken between the first maneuver at 01:45:03 GMT on September 9, and the fifth maneuver at 08:24:38 of the same day. The data taken from DSS 11, DSS 42, DSS 51 and DSS 61 after the fifth maneuver were inconsistent with each other. Inflight orbit computations failed to reveal the problem. Postflight analysis indicates that all the data from DSS 42 taken before the final maneuver is biased. The cause of this bias has not been determined. Therefore, for the final postflight pre (sixth) maneuver orbit computation, the DSS 42 data were deleted. Figures 7, 18, and 19 show the residual plots for the orbit computations with and without the DSS 42 data, respectively. Two-way doppler data taken during the sixth maneuver are shown in Fig. 27.

4. Post-midcourse phase doppler data. Very good two-way doppler data were obtained from after the sixth maneuver until the start of the retrograde phase, without exception. The doppler data from all stations indicated a standard deviation of < 0.008 Hz during this period,

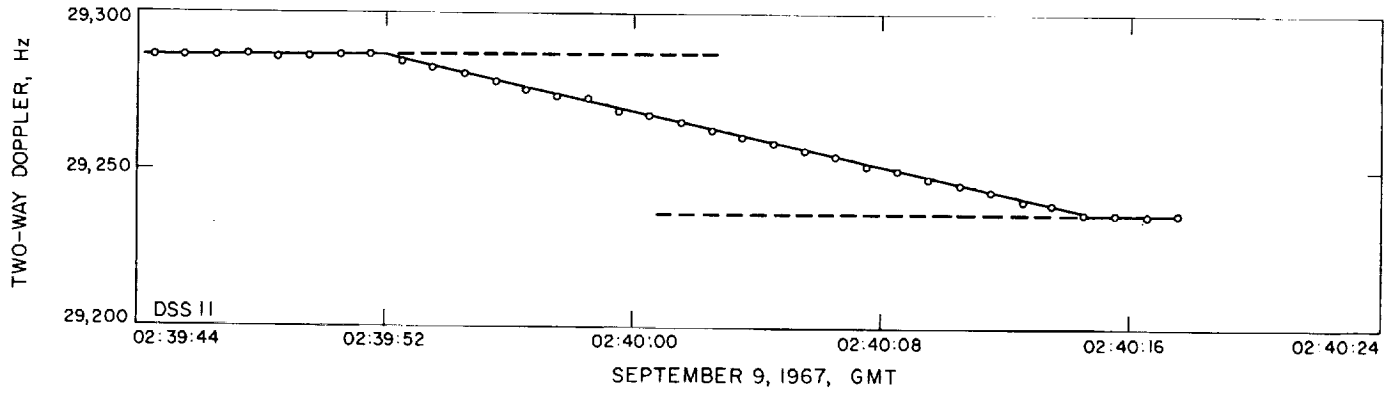

Fig. 24. Third midcourse maneuver doppler data, *Surveyor V*

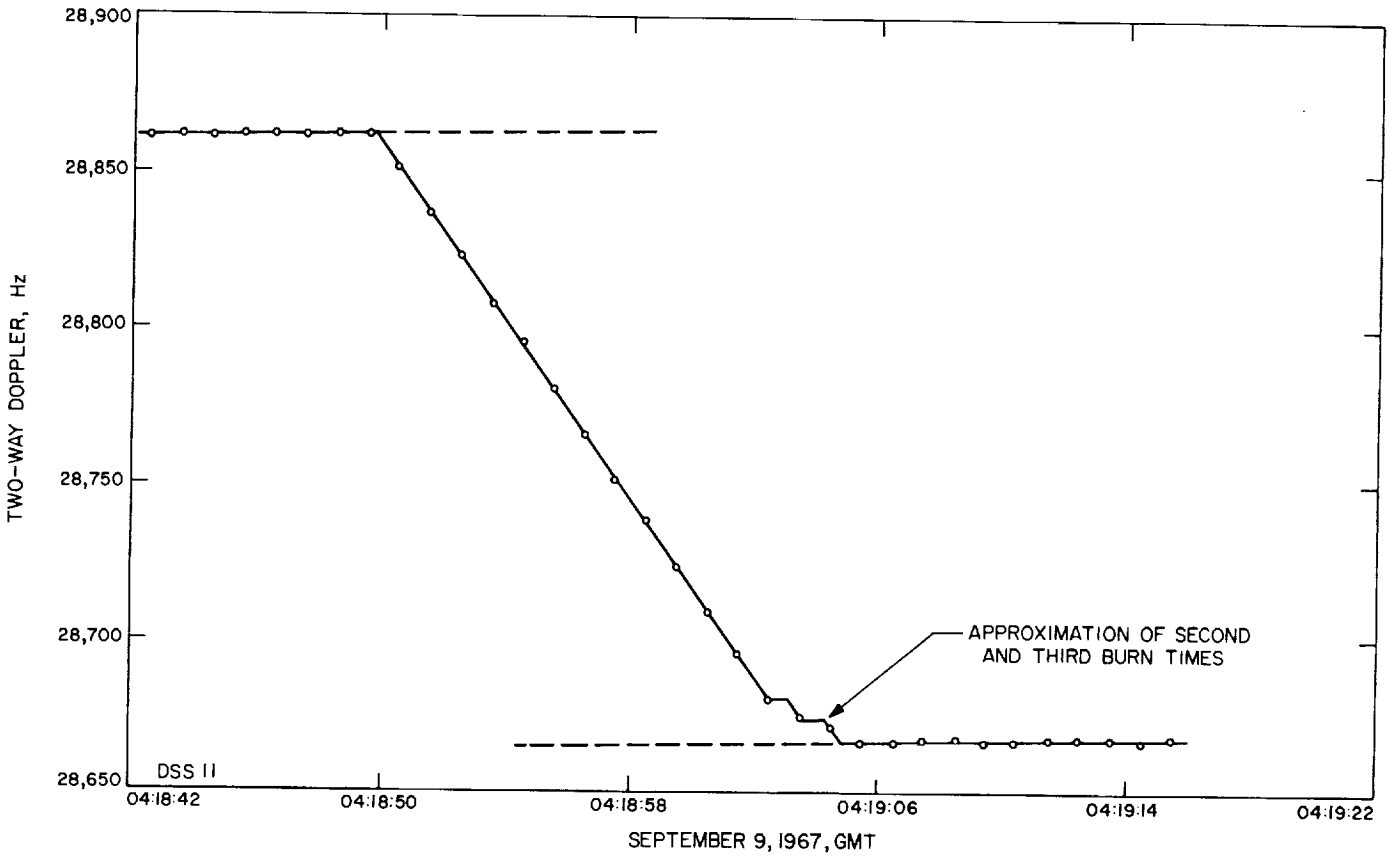

Fig. 25. Fourth midcourse maneuver doppler data, *Surveyor V*

and any biases in the data were negligible. Tidbinbilla Deep Space Station residuals during this phase are shown in Figs. 19 and 20. Johannesburg Deep Space Station residuals may be seen in Figs. 19 and 20, while two-way doppler residuals from DSS 11 are presented in Figs. 19 and 20.

5. Touchdown phase. Final inflight calculations indicated a retroignition time of 00:44:54.6 GMT on September 11, 1967, and touchdown at 00:46:46 GMT. The results of the retroengine burn, as seen in the one-way doppler data at DSS 11, are presented in Fig. 13.

B. Comparison of Inflight and Postflight Results

The orbit determination inflight results can be evaluated by comparing them to the results obtained from the postflight computations. The degree to which these

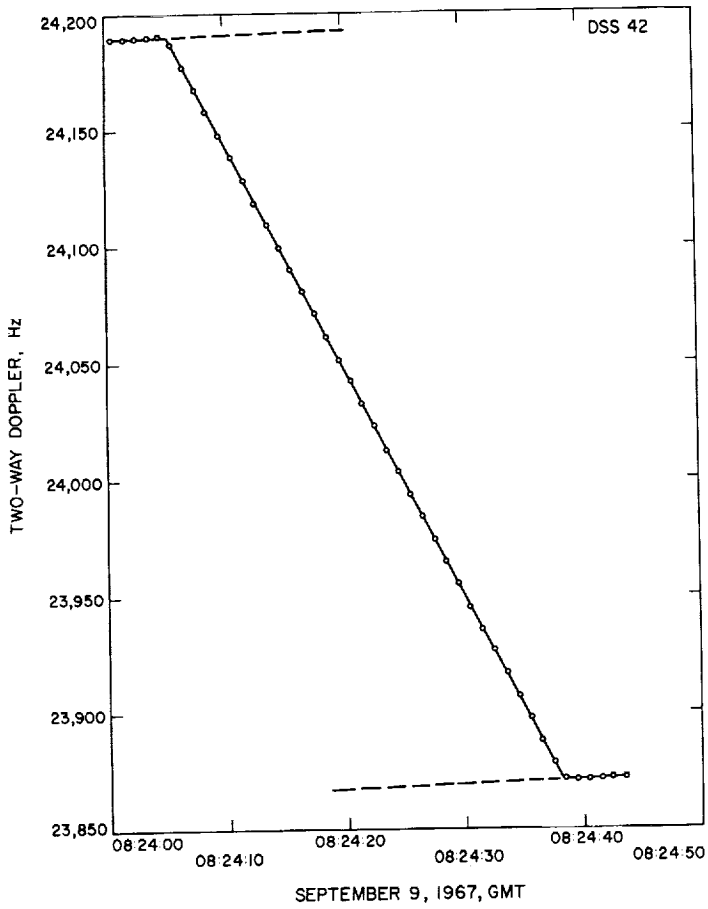

Fig. 26. Fifth midcourse maneuver doppler data, *Surveyor V*

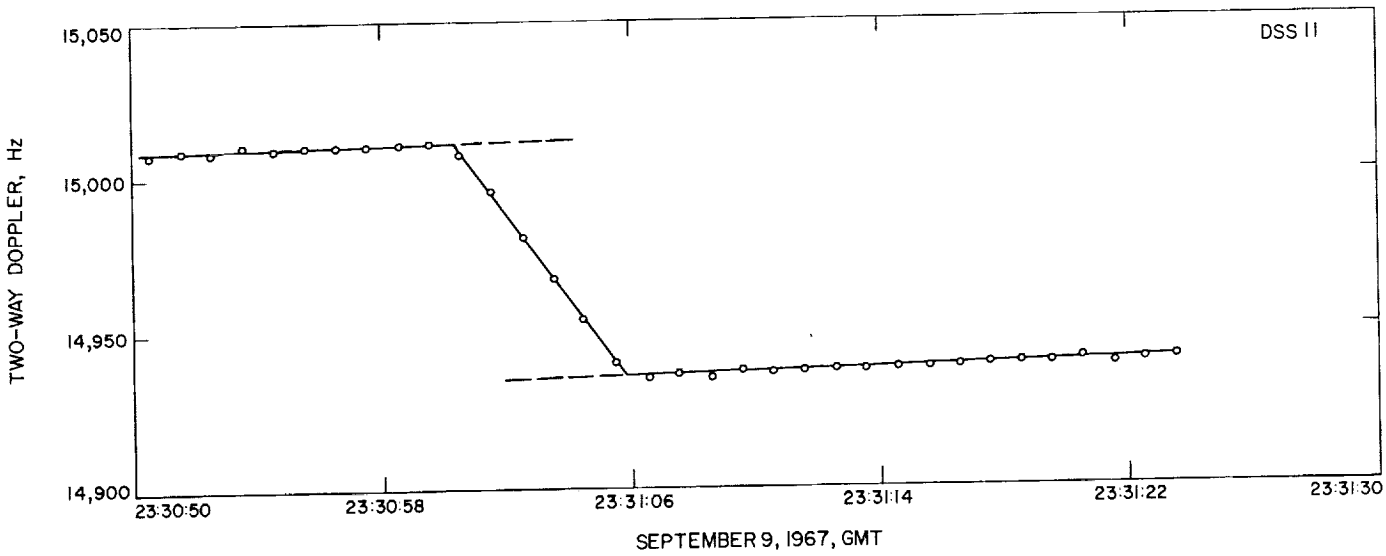

Fig. 27. Sixth midcourse maneuver doppler data, *Surveyor V*

results agree is primarily influenced by the success attained in detecting and eliminating bad, or questionable, tracking data from the inflight computations, and accounting for all trajectory perturbations. Of these, the largest variations are usually caused by bad or questionable data that results from equipment malfunction, incorrect time information, and incorrect frequency information. Other than gross blunder points, these are not easily detected. For *Surveyor V*, an added perturbation was experienced because of the helium leak and the resulting number of maneuvers performed. In general, the pre-midcourse data fit fairly well and the post-midcourse data was excellent. However, the data taken between maneuvers is highly questionable and is examined more closely in the postflight analyses in Section VI.

The most meaningful comparison between inflight and postflight orbit determination results can be made by examining the critical target parameters—namely, the unbraked impact time and impact location. These results are summarized in Table 23. In this table, it can be seen that the inflight pre (first) maneuver impact point was in error by 0.04 deg lat and 0.05 deg lon. Both were well within the uncertainty associated with the inflight estimate. The pre (sixth) maneuver inflight predicted impact point was in error by 0.30 deg lat and 0.79 deg lon. These values are within the uncertainty of 100 km given inflight. This high uncertainty was the result of the limited amount of data available and the effect of the biased data from DSS 42, which caused the orbit solution to move as more data came in. The inflight postmaneuver impact point associated with the orbit solution (5 POM XD) used for the terminal attitude maneuver computations was in error by 0.0 deg lat and 0.02 deg lon. It should be noted that these errors are also within the stated uncertainties associated with the inflight estimates. The inflight predicted unbraked impact time used as a basis to trigger the terminal sequence was in error by 0.120 s, which was within the 1σ uncertainty of 0.500 s. Part of this error is attributable to an incorrect input of DSS 11 and DSS 51 station frequencies. However, had the correct frequencies been used, this error would have been increased to 0.203 s, still within the stated uncertainty.

The estimated landing point determined by transit tracking data (i.e., current best postmaneuver orbit) and the landing point determined by post touchdown data are presented in Table 23. In this table, it can be seen

Table 23. Summary of target impact parameters

Source	Estimated impact or landed location		Uncertainty about estimated impact point, 1σ dispersion ellipse			Estimated unbraked impact time, GMT	1σ uncertainty in estimated unbraked impact time, s
	Latitude, deg	Longitude, deg	SMAA, km	SMIA, km	THETA, deg		
Pre (first) maneuver, *uncorrected*							
Inflight OD	2.34	23.74	9.0	4.0	78.0	23:25:13.907	1.71
Postflight OD	2.30	23.69	6.0	3.0	66.3	23:25:14.318	1.17
Pre (sixth) maneuver, *uncorrected*							
Inflight OD	−4.24	16.83	100.0	75.0	170.0	00:37:38.795	25.00
Postflight OD	−3.94	16.04	68.0	55.0	179.2	00:37:27.924	15.00
Postmaneuver transit							
Inflight OD	1.49	23.28	8.0	3.0	79.5	00:45:15.325	3.07
Postflight OD	1.49	23.26	2.5	1.0	94.0	00:45:15.318	0.60
Observed unbraked impact time	—	—	—	—	—	00:45:15.282	0.05
Post landing							
Postflight OD, adjusted	1.49	23.20	—	—	—	—	—
Post-touchdown OD	1.41	23.15	—	—	—	—	—

that the estimated location based on the preliminary analysis of the landed spacecraft tracking data falls well within the 1σ dispersion ellipse associated with the transit location (Fig. 28). The *observed* unbraked impact time and impact time predicted by the current best post-maneuver orbit solution (based on a lunar elevation of 1734.9 km) differ by only 0.036 s.

Based on the results of the comparison between inflight and postflight results, the following conclusions may be made: (1) the expected OD accuracy was achieved for the first maneuver; (2) although plagued with biased data and a short supply of data, the pre (sixth) maneuver orbit computations and subsequent maneuver achieved sufficient accuracy to place the spacecraft within 32 km of the aim point; and (3) postmaneuver data were very good, and all expected OD accuracies were achieved.

VIII. Analysis of Air Force Eastern Test Range (AFETR) Tracking Data, *Surveyor V*

The AFETR supported the *Surveyor* missions by computing injection conditions for both the spacecraft transfer orbit and the *Centaur* post-retromaneuver orbit. The AFETR injection conditions were relayed to the SFOF in Pasadena, where they were used as the initial values for early JPL orbit computations. The AFETR also transmitted initial acquisition information to the SFOF, which could be relayed to the Deep Space Stations. The input for the AFETR calculations was the *Centaur* C-band tracking data obtained from various AFETR and Manned Space Flight Network (MSFN) tracking stations. The locations of these stations are given in Table 24.

In addition to fulfilling these requirements, the AFETR transmitted the C-band tracking data taken during the

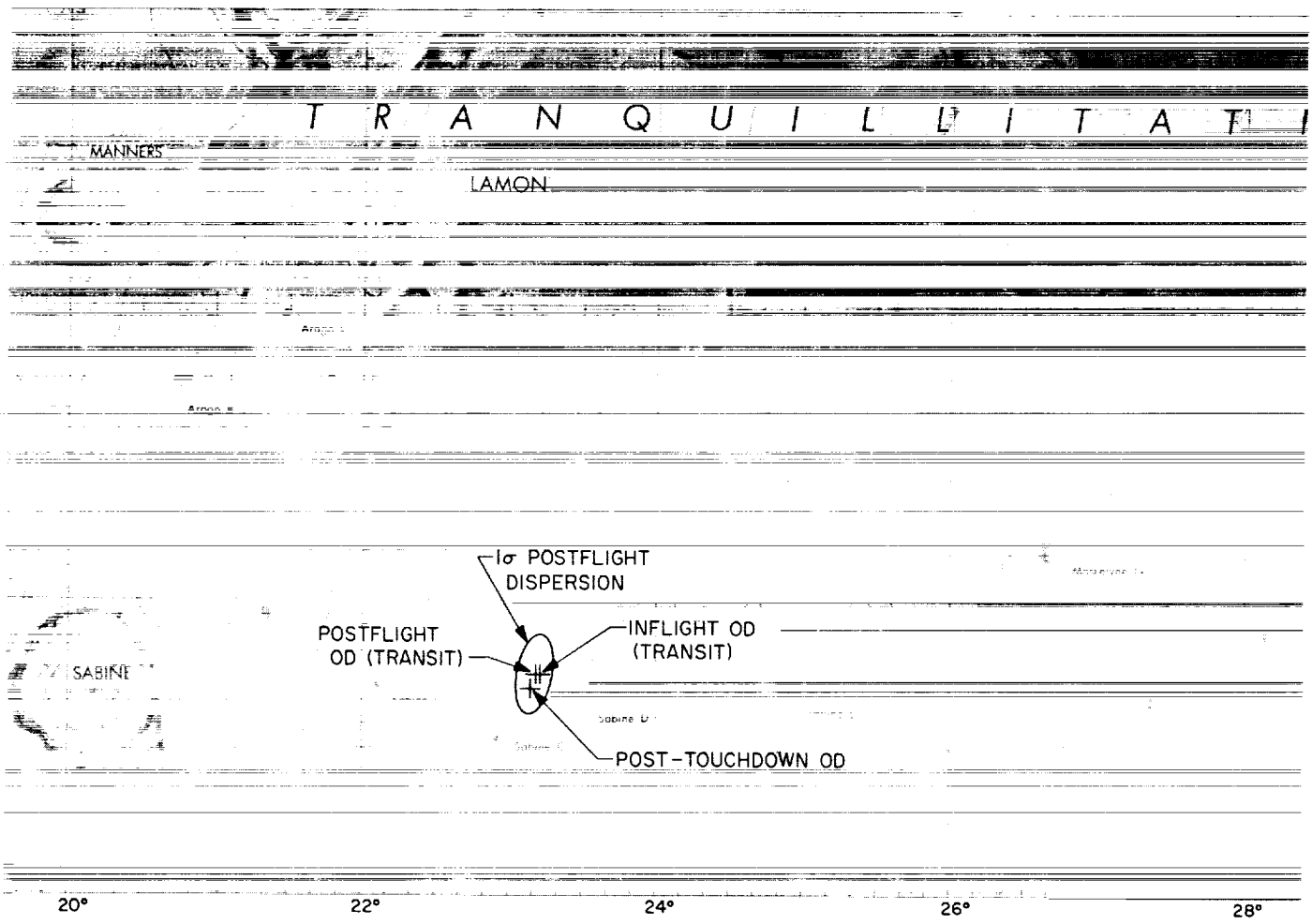

Fig. 28. Estimated *Surveyor V* landed location on lunar surface

Table 24. AFETR station locations used for JPL orbit solutions, *Surveyor V*

Station	Radar type	Geocentric radius, km	Geocentric latitude, deg (negative S)	Longitude, deg
Grand Canary	MPS-26	6373.7272	27.604886	344.365169
Pretoria	MPS-25	6375.7617	−25.7960	28.35670
Carnarvon	TPQ-18	6374.464	−24.7508	113.71608
Bermuda	FPS-16	6372.099	32.1744	295.34620

transfer orbit and the *Centaur* post-retromaneuver orbit to the SFOF. The transfer orbit data was used to compute an early JPL transfer orbit based solely on the C-band data. This early JPL orbit was used as a backup for possible unusual circumstances that could cause a failure of the AFETR orbit computation system. Under normal conditions, the early JPL orbit is used as a quick check on the AFETR transfer orbit. The *Centaur* post-retromaneuver orbit was made available to verify proper execution of the *Centaur* retromaneuver, which ensured (1) that the *Centaur* did not impact the moon and (2) that the spacecraft was separated from the booster sufficiently to prevent the Canopus seeker on board the spacecraft from locking up on the *Centaur*.

The AFETR tracking coverage for *Surveyor V* is shown in Fig. 29.

A. Analysis of Transfer Orbit Data

Because there was incomplete tracking coverage, no C-band tracking data were taken from 5 min before MECO 2 until almost 3 min after separation (Fig. 29). Since the high-thrust acceleration of the *Centaur* would perturb any transfer orbit solution, data acquired before MECO 2 could not be used. The C-band data taken after spacecraft/*Centaur* separation was questionable for use in the spacecraft transfer orbit solution because the C-band radars actually tracked the C-band transponder on the *Centaur*, not the spacecraft. After separation, the *Centaur* executed turnaround and lateral-thrust maneuvers preparatory to the retromaneuver. No inlock C-band data were taken until the *Centaur* was 2 min into its retrothrust maneuver.

There was also a delay in receiving the C-band data at Pasadena. Because of this delay, any computations on the C-band data would have delayed the scheduled start of DSS data orbit computations by several minutes. Because of the incomplete coverage and the delay in receiving data, it was decided not to compute an inflight AFETR solution at JPL.

For purposes of the postflight analysis, *Centaur* C-band data from Grand Canary was used to compute a transfer orbit solution. Two minutes of low-elevation data at a rate of 1 point/6 s were taken, starting 2 min after start of *Centaur* retrothrust. Figure 30 shows the elevation angles at Grand Canary during the time these data were taken.

The AFETR inflight transfer orbit solution was based on 11 points of Grand Canary data. One of the postflight solutions at JPL used the same 11 points of data. In Table 25, these AFETR and JPL solutions are compared to the best inflight solution based on pre-midcourse DSS data. Table 26 shows the data span used by JPL to compute this transfer orbit, which was based on C-band data and the associated statistics for the tracking data residuals. Figure 31 shows a time history of the residuals.

The three solutions agree fairly well in position but not in velocity. This result is to be expected, since the two solutions based on AFETR data include *Centaur* retrothrust data. By using *Centaur* retrothrust data, the solution yields too low a value for the total velocity of the

Table 25. Transfer orbit solutions, *Surveyor V*: Epoch on September 8, 1967 at 08:16:11.2 GMT

Parameter	Solutions with AFETR data		Best inflight solution from pre-midcourse DSS data
	Inflight solution by AFETR	Postflight solution by JPL	
Geocentric inertial position and velocity			
x, km	−404.19438	−398.20487	−399.85471
y, km	6134.6702	6132.3694	6131.1262
z, km	2373.0176	2373.3943	2376.6744
Dx, km/s	−10.261781	−10.261195	−10.263941
Dy, km/s	1.5632593	1.5563007	1.5994043
Dz, km/s	−3.440545	−3.4433698	−3.4193662
Total velocity, km/s	10.935505	10.934851	10.936116
Unbraked impact quantities			
B, km	841.59	2750.08	2903.6
B • TT, km	384.25	1643.1	2895.3
B • RT, km	−748.75	−2205.3	−219.60
Latitude, deg	11.19	41.06	2.32
Longitude, deg	327.06	1.41	23.64
Semimajor axis of impact dispersion ellipse (1σ value), km	—	7038.31	—
GMT of unbraked impact	23:26:32.2	00:16:48.740	23:25:15.379

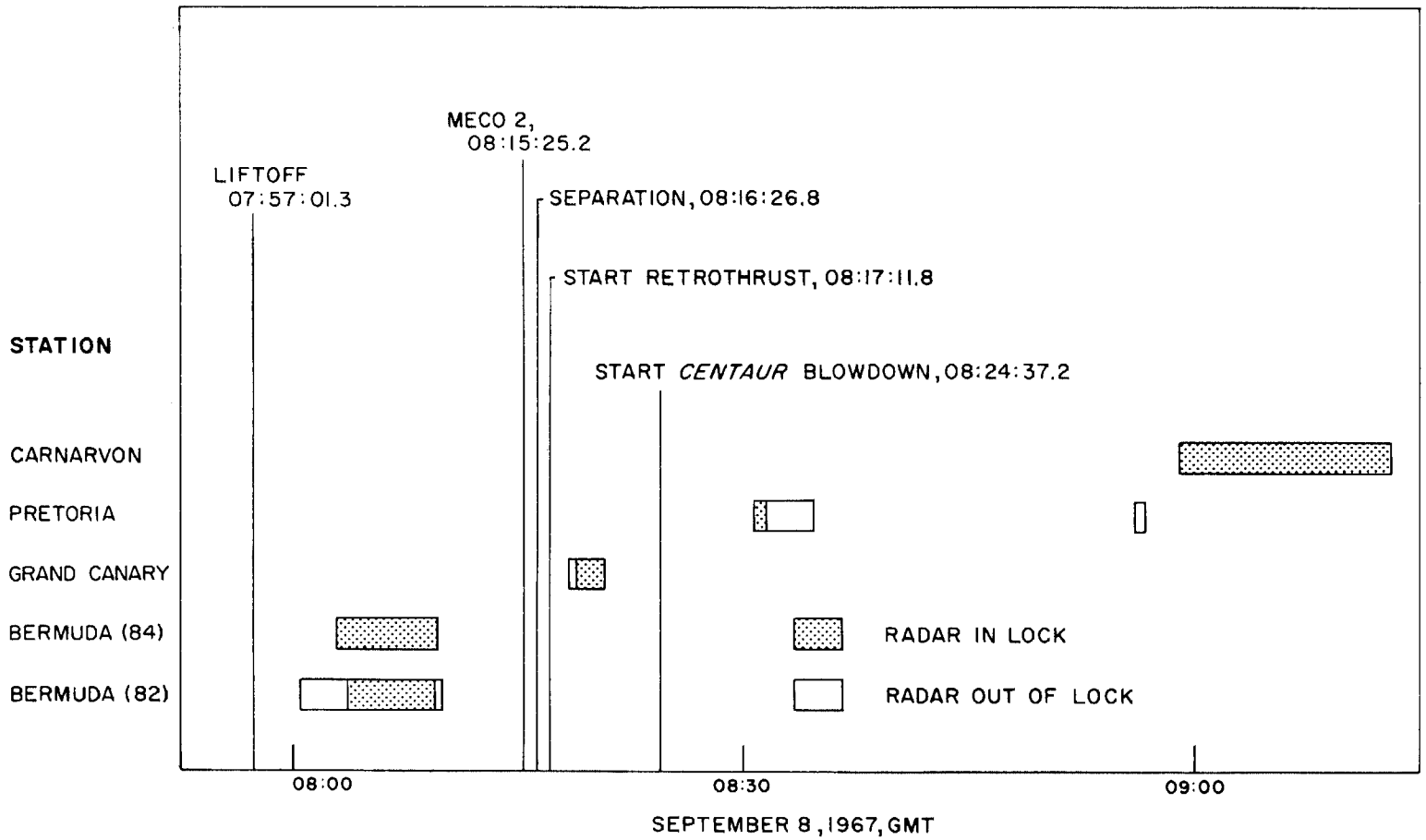

Fig. 29. AFETR tracking coverage, *Surveyor V*

spacecraft. In the AFETR solution, the total velocity is too low by about 0.62 m/s. For the postflight JPL solution based on AFETR data, the total velocity is about 1.27 m/s too low.

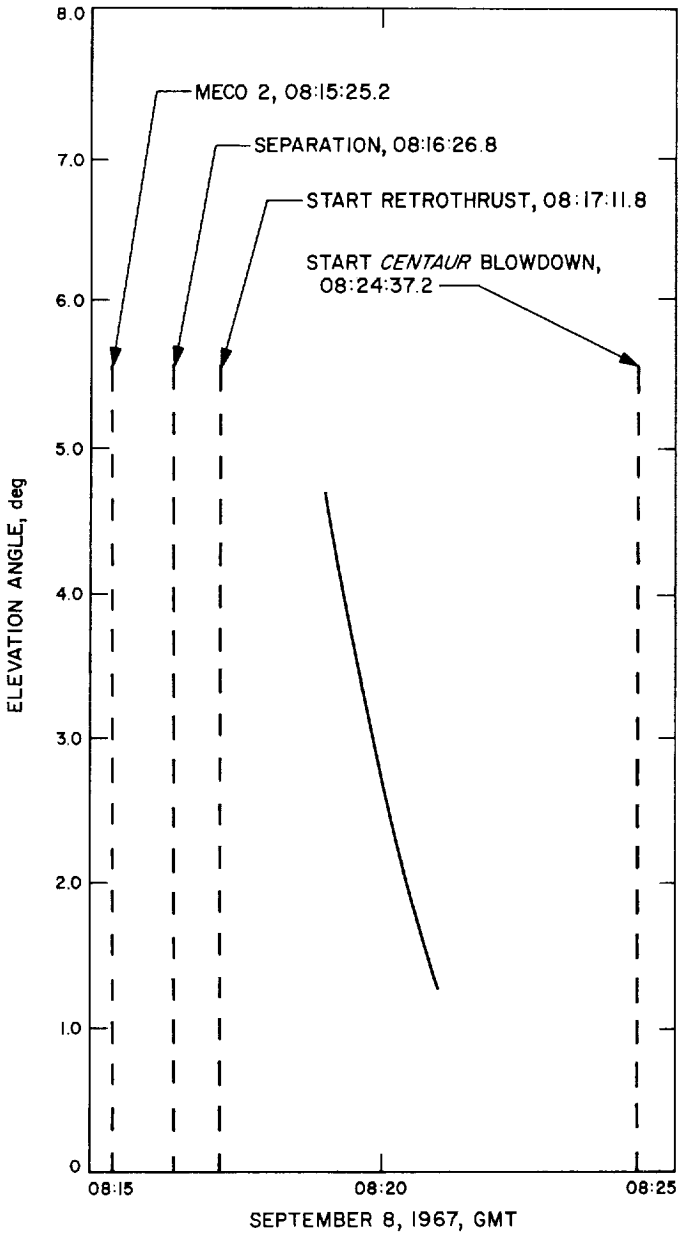

Fig. 30. Grand Canary elevation angles, *Surveyor V*

Even though both the AFETR inflight solution and the JPL postflight solution based on AFETR data used the same data span, they vary in the **B**-plane quantities. There is a difference of almost 1900 km in the **B** vector and 1 h in time of moon encounter. Possible causes for this difference in the C-band data transfer orbit solutions are:

(1) Modifications made to the *raw data* by the AFETR to compute the transfer orbit.

(2) Difference in the C-band tracking station locations used by AFETR and JPL.

(3) Different constants—such as for mass of earth and mass of moon—used by AFETR and JPL.

(4) The difference in the orbit determination programs used by JPL and AFETR.

The above causes are more fully discussed in the section on analysis of AFETR data in Ref. 4.

B. Analysis of Post-Retromaneuver Orbit Data

Centaur C-band tracking data from Carnarvon and Pretoria were available for post-retromaneuver orbit computations. Carnarvon provided almost 15 min of the post-retromaneuver data; Pretoria provided only about 2 min of the data. The range data from Pretoria was bad, so it was impossible to obtain a solution using the data from this source. Thus, only the Carnarvon data was used in both the JPL and AFETR post-retromaneuver computations. The elevation angles at the Carnarvon station are plotted in Fig. 32. Table 27 gives the AFETR and JPL

Table 27. Summary of post-retromaneuver orbit solutions, *Surveyor V*: epoch on September 8, 1967 at 08:59:17.900 GMT

Geocentric inertial position and velocity	Inflight orbit computed by AFETR	Postflight orbit computed by JPL
x, km	−17094.103	−17093.000
y, km	−1539.2672	−1539.0707
z, km	−7443.3714	−7443.4118
Dx, km/s	−3.8173601	−3.8180210
Dy, km/s	−3.9750524	−3.9754584
Dz, km/s	−3.1656423	−3.1639442

Table 26. Statistics of JPL postflight transfer orbit tracking data residuals from Grand Canary for *Surveyor V*

Data type	Begin data, GMT	End data, GMT	Number of points used	Standard deviation	Mean error
Range, km	08:19:06	08:20:06	11	0.0208	−0.00150
Azimuth, deg	08:19:06	08:20:06	11	0.0126	0.00000
Elevation, deg	08:19:06	08:20:06	11	0.0271	−0.00476

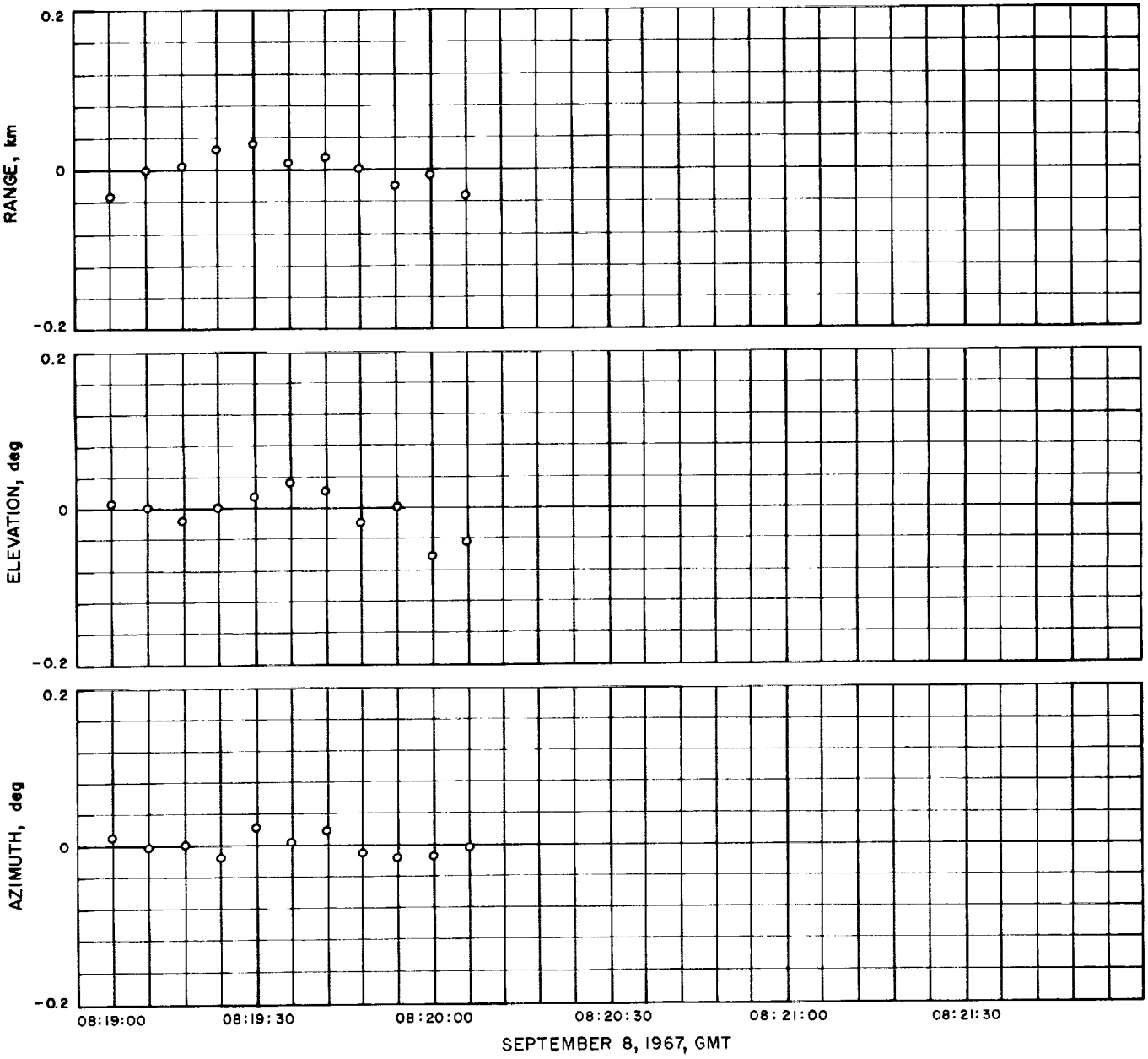

Fig. 31. Grand Canary tracking data residuals for postflight transfer orbit, *Surveyor V*

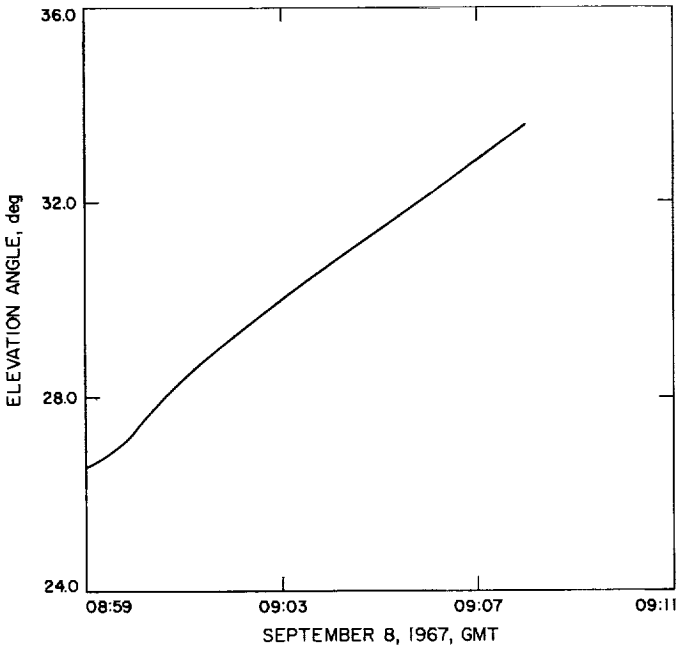

Fig. 32. Carnarvon elevation angles, *Surveyor V*

post-retromaneuver orbit solutions. The data used for the JPL solution and the statistics of the tracking data residuals for this flight phase are given in Table 28; and Fig. 33 shows the time history of the residuals of the JPL post-retromaneuver solution.

C. Conclusions

Only one source of C-band data was available for the computation of a spacecraft transfer orbit; this was low-elevation data taken during *Centaur* retrothrust. Processing these data in postflight analysis showed that it would yield a solution consistent with the AFETR inflight solution. The unbraked impact point of the best DSS solution fell within the impact dispersion ellipse of the JPL transfer orbit computed from the C-band data. For this reason, the rough solutions based on the C-band data may be considered consistent with the best inflight DSS solution.

The Pretoria data were of no value in determining the *Centaur* post-retromaneuver orbit. On the other hand, the Carnarvon data were acquired at high-elevation angles and yielded a reliable post-retromaneuver solution. The JPL and AFETR solutions agree closely.

Table 28. Statistics of JPL post-retromaneuver orbit tracking data residuals from Carnarvon for *Surveyor V*

Data type	Begin data, GMT	End data, GMT	Number of points used	Standard deviation	Mean error
Range, km	08:59:00	09:13:18	97	0.00857	−0.000181
Azimuth, deg	08:59:00	09:13:18	97	0.0153	−0.000005
Elevation, deg	08:59:00	09:13:18	96	0.0138	0.000009

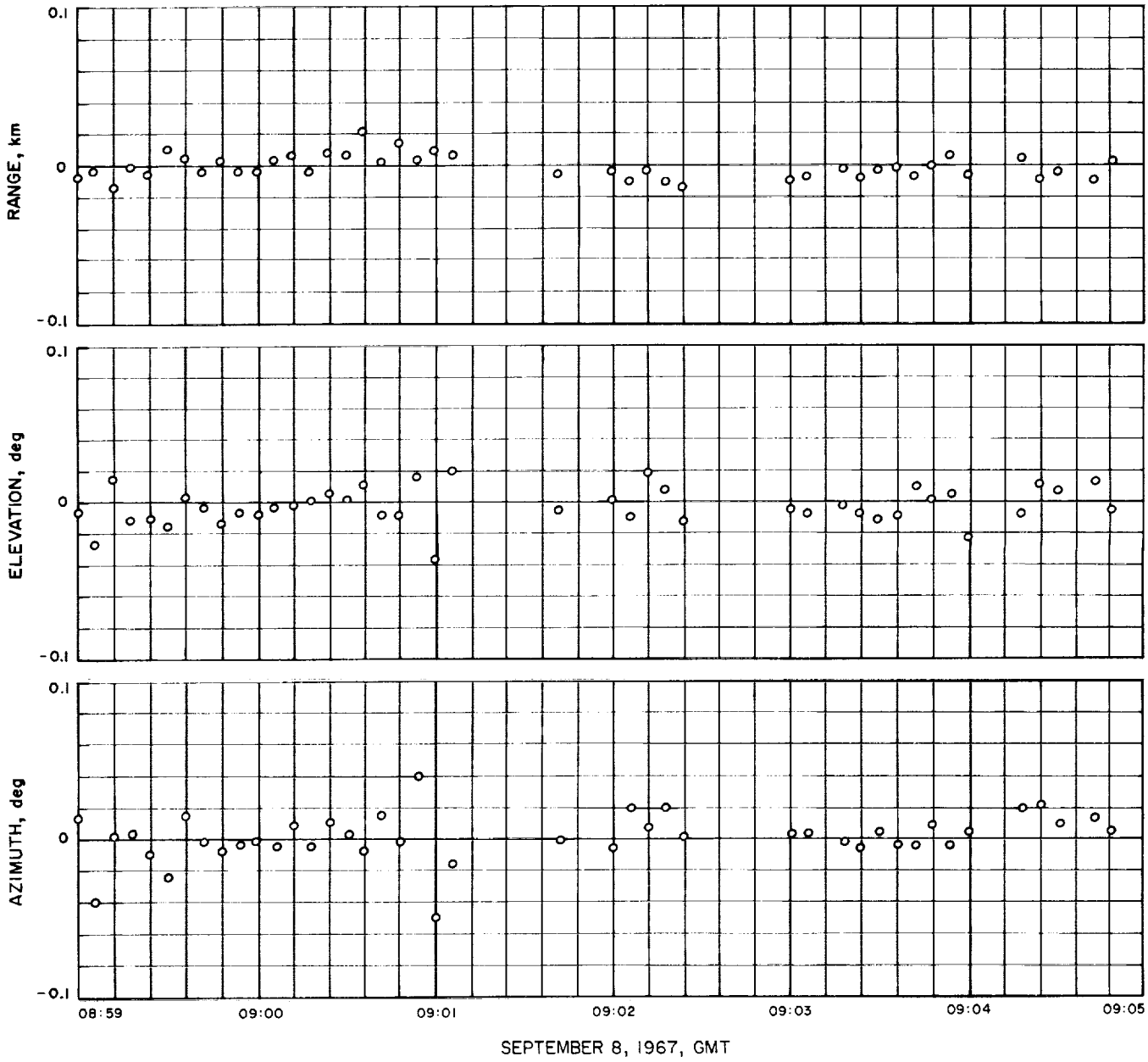

Fig. 33. Carnarvon tracking data residuals for post-retromaneuver orbit, *Surveyor V*

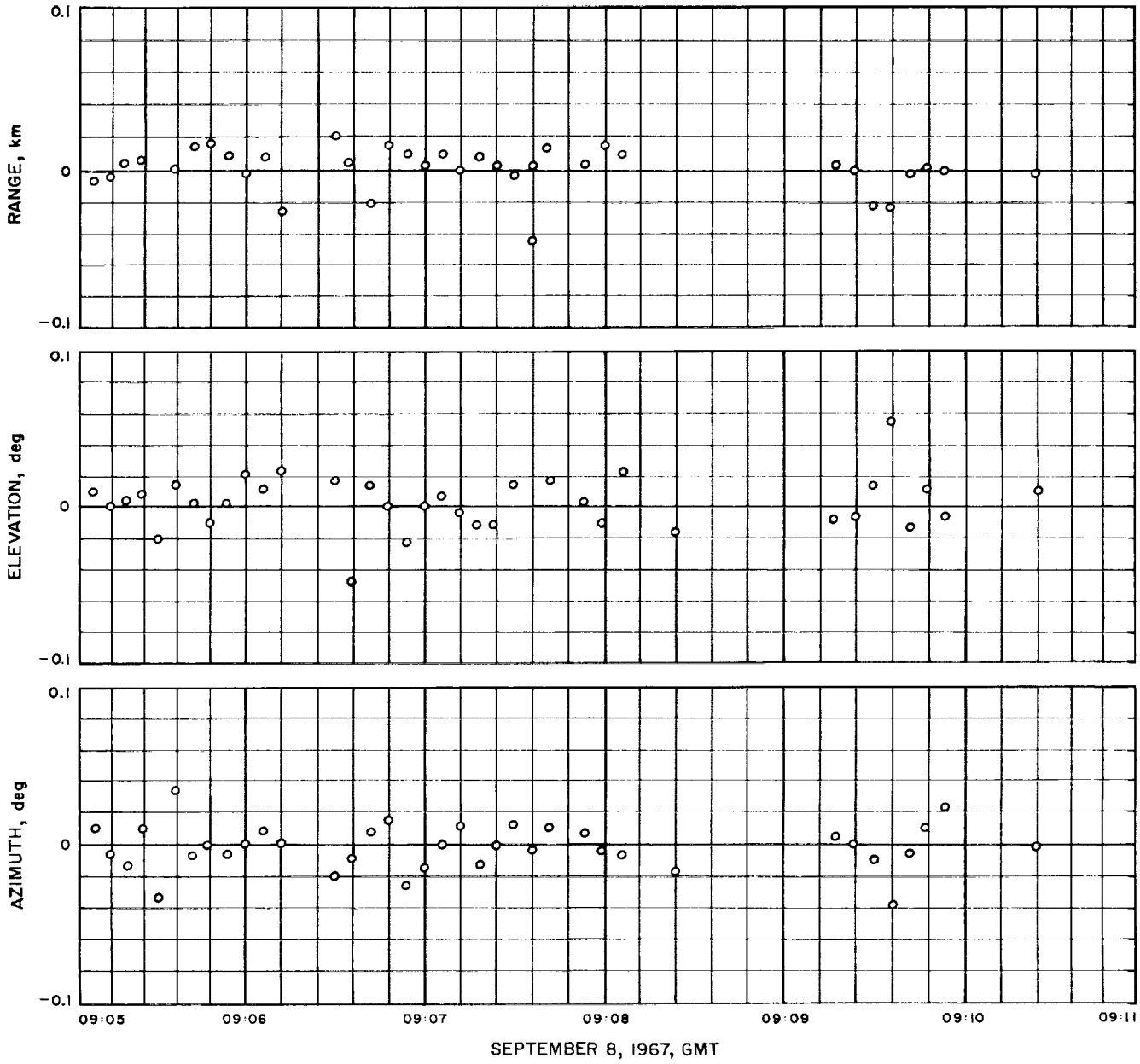
RANGE, km
0.1
0
−0.1
ELEVATION, deg
0.1
0
−0.1
AZIMUTH, deg
0.1
0
−0.1
09:05
09:06
09:07
09:08
09:09
09:10
09:11
SEPTEMBER 8, 1967, GMT

Fig. 33 (contd)

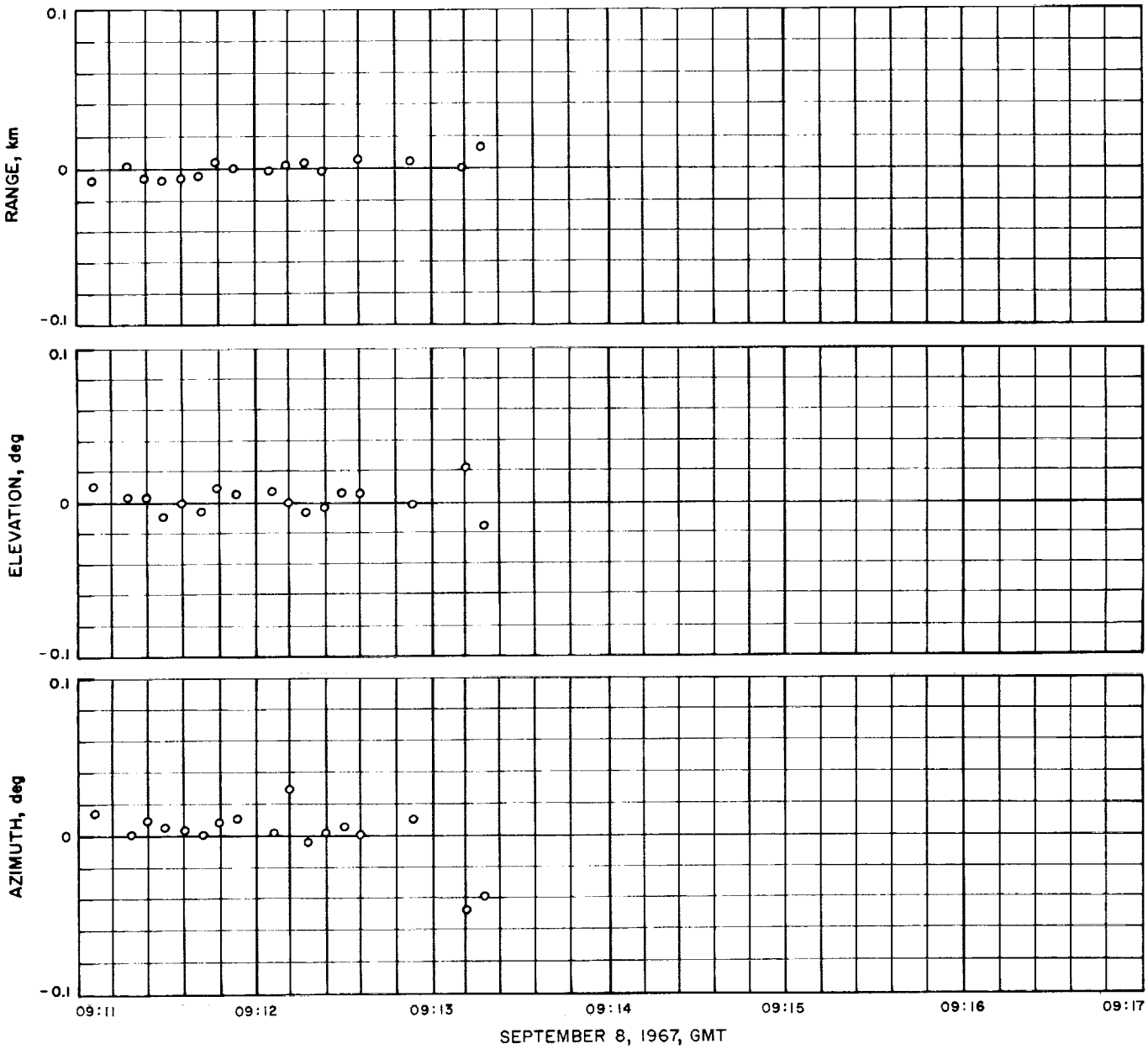
RANGE, km
0.1
0
-0.1
ELEVATION, deg
0.1
0
-0.1
AZIMUTH, deg
0.1
0
-0.1
09:11
09:12
09:13
09:14
09:15
09:16
09:17
SEPTEMBER 8, 1967, GMT

Fig. 33 (contd)

IX. *Surveyor VI* Inflight Orbit Determination Analysis

A. View Periods and Tracking Patterns

Information for Deep Space Station view periods and the tracking patterns is clearly summarized in the following figures and tables: Figure 34 summarizes the tracking station view periods and their data coverage for the period from launch to lunar touchdown. Figures 35–38 are tracking station stereographic projections for the prime tracking stations, which show the trace of the spacecraft trajectory for the view periods in Fig. 34. Table 29 summarizes the tracking data used for both inflight and postflight orbital calculations and analyses. This table provides a general picture of the performance of the data recording and handling systems.

B. Premaneuver Orbit Estimates

The customary initial orbit estimate based on AFETR data was not computed for the *Surveyor VI* mission because no data were available on which to base the transfer orbit computation. Data were garbled in transmission from the *Twin Falls* (Victory Ship) to the AFETR-Real Time Computer Center (RTCC), and no other station was tracking during the transfer orbit period (See Section XII).

The first estimate of the spacecraft orbit (PROR XA), based on DSS data only, was computed at $L + 1$ h, 59 min; computations were based on approximately 22 min of two-way doppler and angle (HA and dec) data from DSS 51 and 2 min of angle (HA and dec) data from DSS 42. Mapping this orbit solution forward to lunar encounter indicated that the correction required to achieve encounter at the prelaunch aim point was well within the nominal midcourse correction capability. These results were further verified by the second (ICEV) and third (PREL) orbit computations completed at $L + 3$ h, 3 min and $L + 4$ h, 21 min, respectively.

When sufficient two-way doppler data had been received to compute a *doppler only* orbit solution, the angle data were deleted. This was first accomplished in the PREL XA orbit computation, which utilized approximately 2½ h of two-way doppler data from DSS 42 and DSS 51. Removal of the angle data from the solution resulted in a change of approximately -1 km in $\mathbf{B} \cdot \mathbf{T}T$ and $+7$ km in $\mathbf{B} \cdot \mathbf{R}T$ when the solution was mapped to the moon.

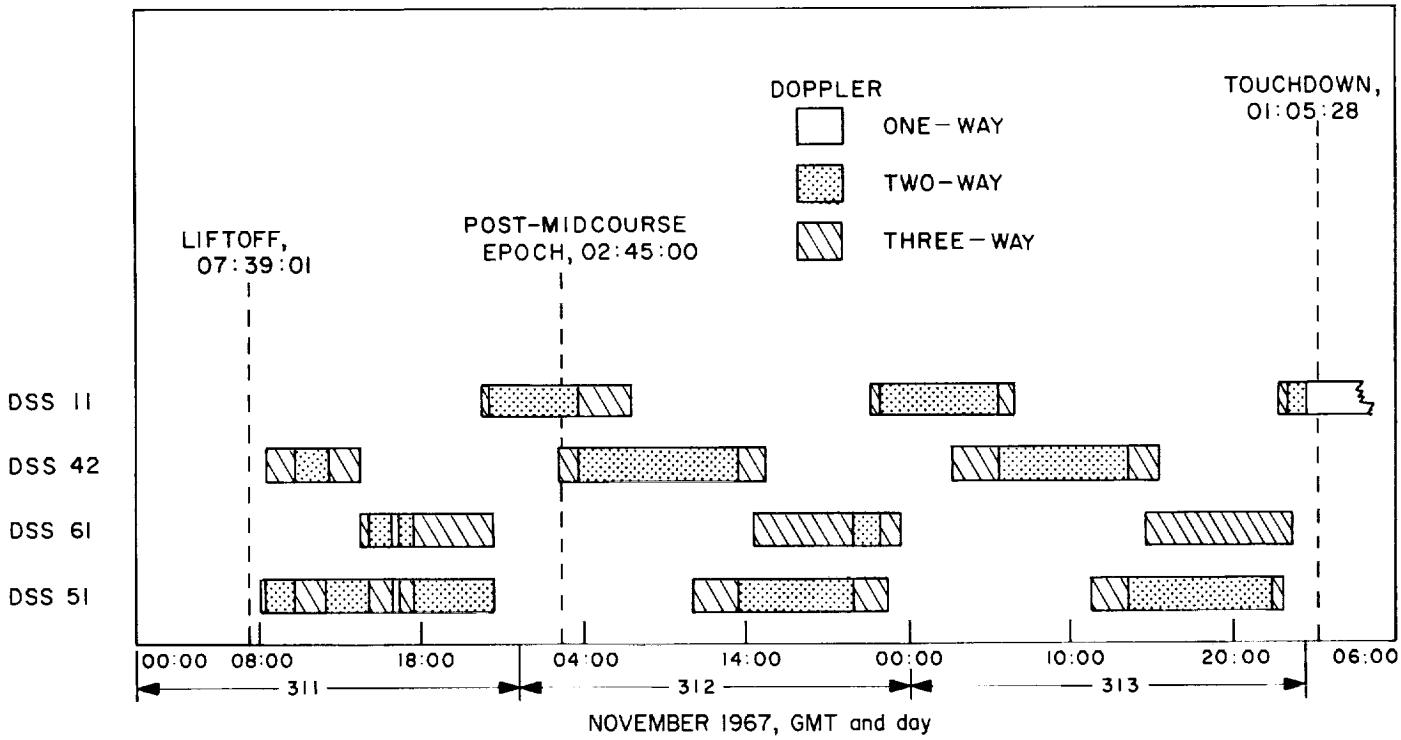

Fig. 34. DSS tracking coverage for *Surveyor VI*

Table 29. Summaries of data used in orbit determination, *Surveyor VI*

Station	Data type	Points received	Number of points used in real time		Bad format		Bad data condition code		Blunder points		Rejection limits on blunder points	Points used in postflight analysis best estimate
			Number	% of recd	Number	% of recd	Number	% of recd	Number	% of recd		
Premaneuver												
DSS 11	CC3	430	162	37.67	7	1.63	2	0.47	2	0.47	CC3	211
DSS 42	CC3	121	108	89.26	1	0.83	7	5.79	0	0.0	0.10 for 10-s	108
DSS 42	HA	442	85	19.23	11	2.49	59	13.35	46[a]	10.41	sample rate.	0
DSS 42	Dec	442	85	19.23	11	2.49	59	13.35	46	10.41	0.02 for 60-s	0
DSS 51	CC3	707	520	73.55	0	0.0	35	4.95	5	0.71	sample rate.	566
DSS 51	HA	1049	235	22.40	2	0.19	35	3.33	5	0.48		0
DSS 51	Dec	1049	235	22.40	2	0.19	35	3.33	3	0.29		0
DSS 61	CC3	141	43	30.50	1	0.71	28	19.86	4	2.84		99
											Angles 0.1 deg	
Postmaneuver												
DSS 11	CC3	614	504	82.08	0	0.0	23	3.75	6	0.98	(Same	512
DSS 42	CC3	1050	995	94.76	1	0.10	23	2.25	0	0.0	as	995
DSS 51	CC3	958	844	88.10	8	0.84	33	3.44	0	0.0	above)	845
DSS 61	CC3	96	0	0.0	0	0.0	4	4.17	11	11.46		0

[a]The high number of DSS 42 angle blunder points was due to a bug in the ODG in applying the angle corrections.

During the data consistency orbit computation period, nine orbit solutions were computed. These solutions included various combinations of two-way doppler data from DSS 42, DSS 51 and DSS 61. During this period, the first data from DSS 61 were received and found to be consistent[12] with data from DSS 42 and DSS 51. Angle data were not included in any of the DACO orbit solutions. As the computers became available, additional orbit solutions were computed to update and evaluate the data file as new data were added.

[12]Postflight analysis of early DSS 61 data indicates a small bias that could be removed by solving for station location parameters.

At the beginning of the last pre-midcourse (LAPM) orbit computation period, the following amount of usable two-way doppler was available: 1 h, 11 min from DSS 11, 1 h, 50 min from DSS 42, 11 h, 30 min from DSS 51 and 2 h, 32 min from DSS 61.

The LAPM orbit solutions were the first computations to utilize data from DSS 11, verifying its consistency with the other DSS data. After updating the ODP data file, the pre-midcourse orbit solution (LAPM XC) on which the midcourse maneuver was based was computed. This solution utilized all the two-way doppler data to MC − 3 h, 2 min. When this solution was mapped to the moon, it

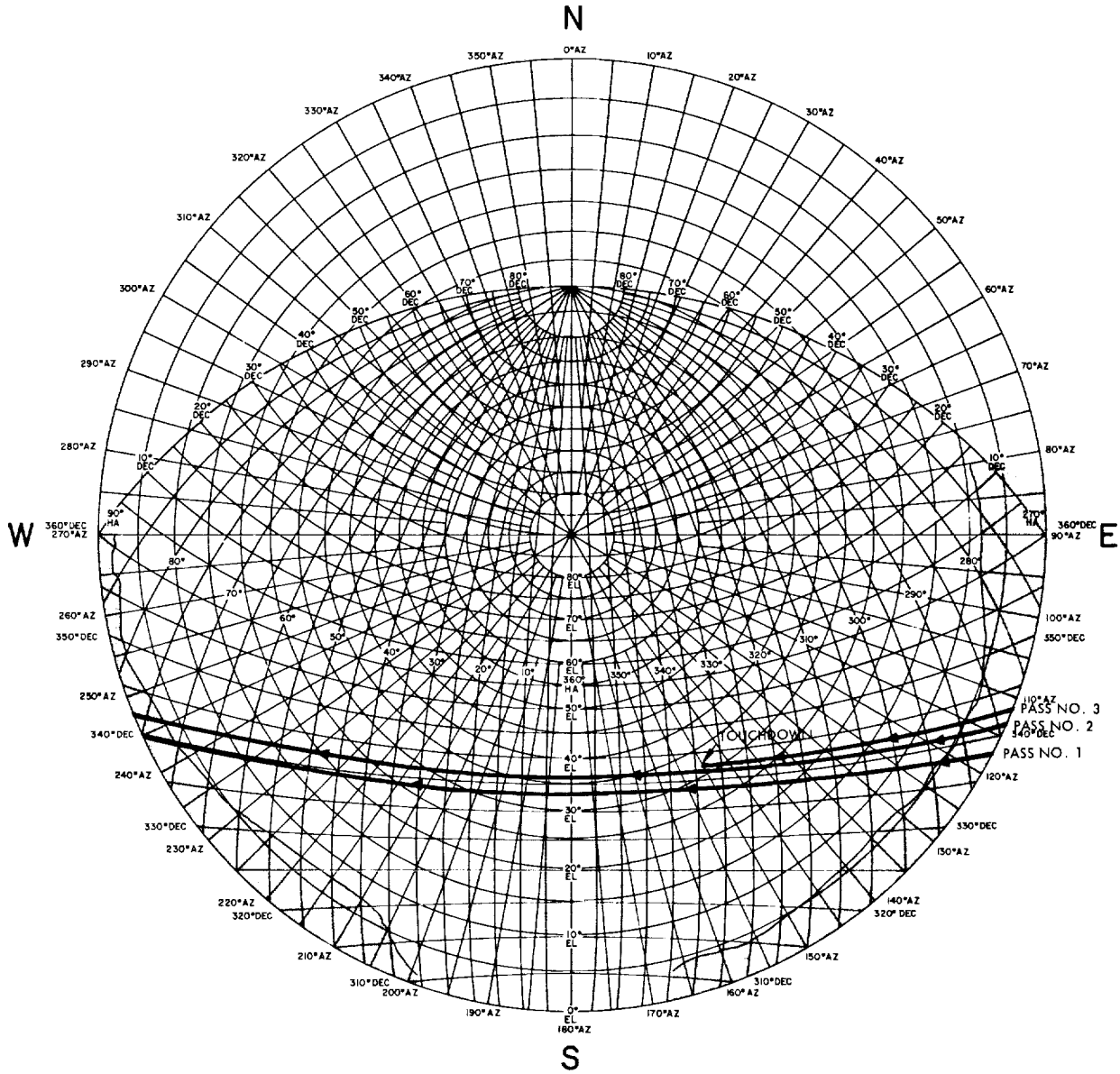

Fig. 35. DSS 11 stereographic projection, *Surveyor VI*

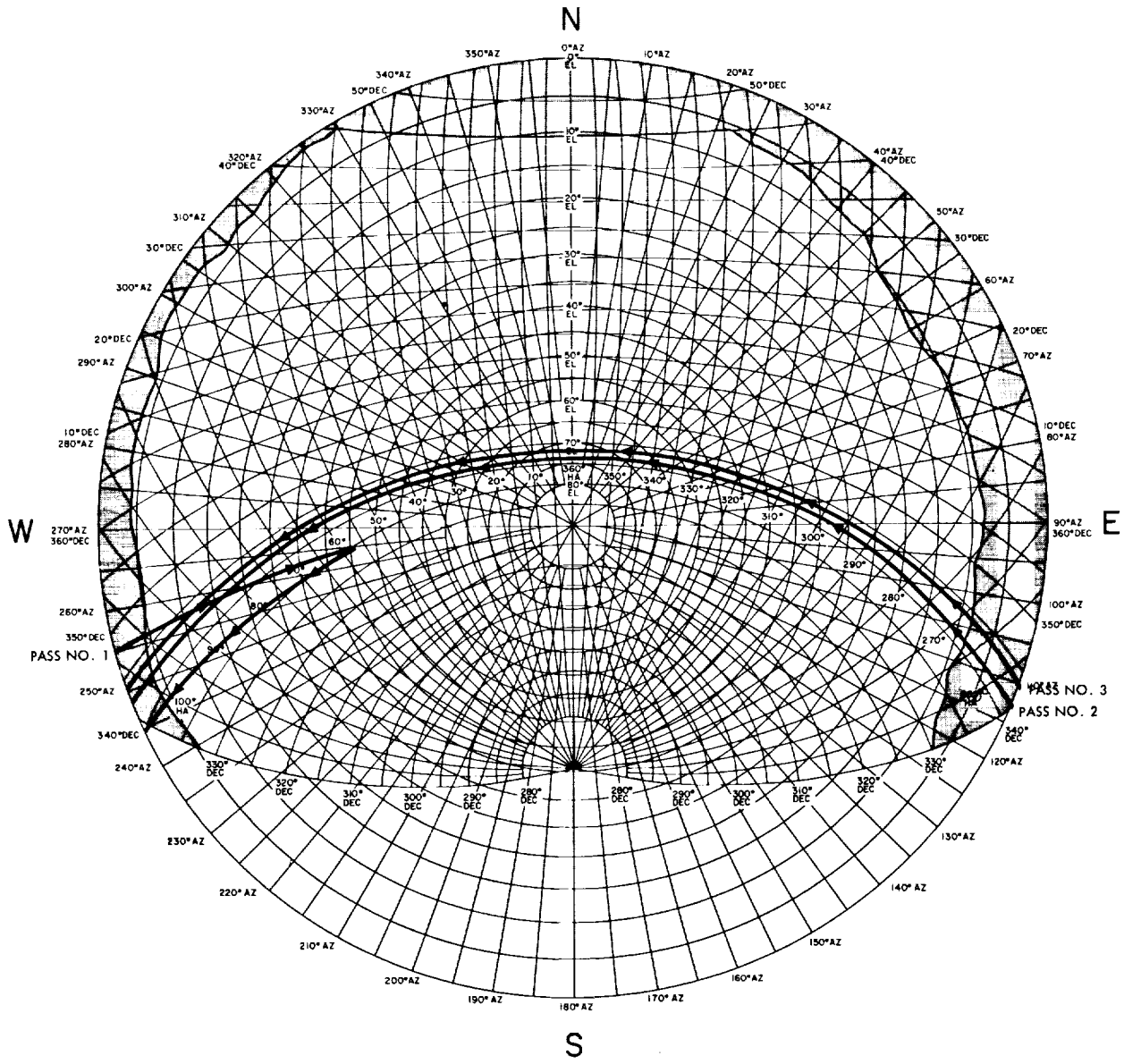

Fig. 36. DSS 42 stereographic projection, *Surveyor VI*

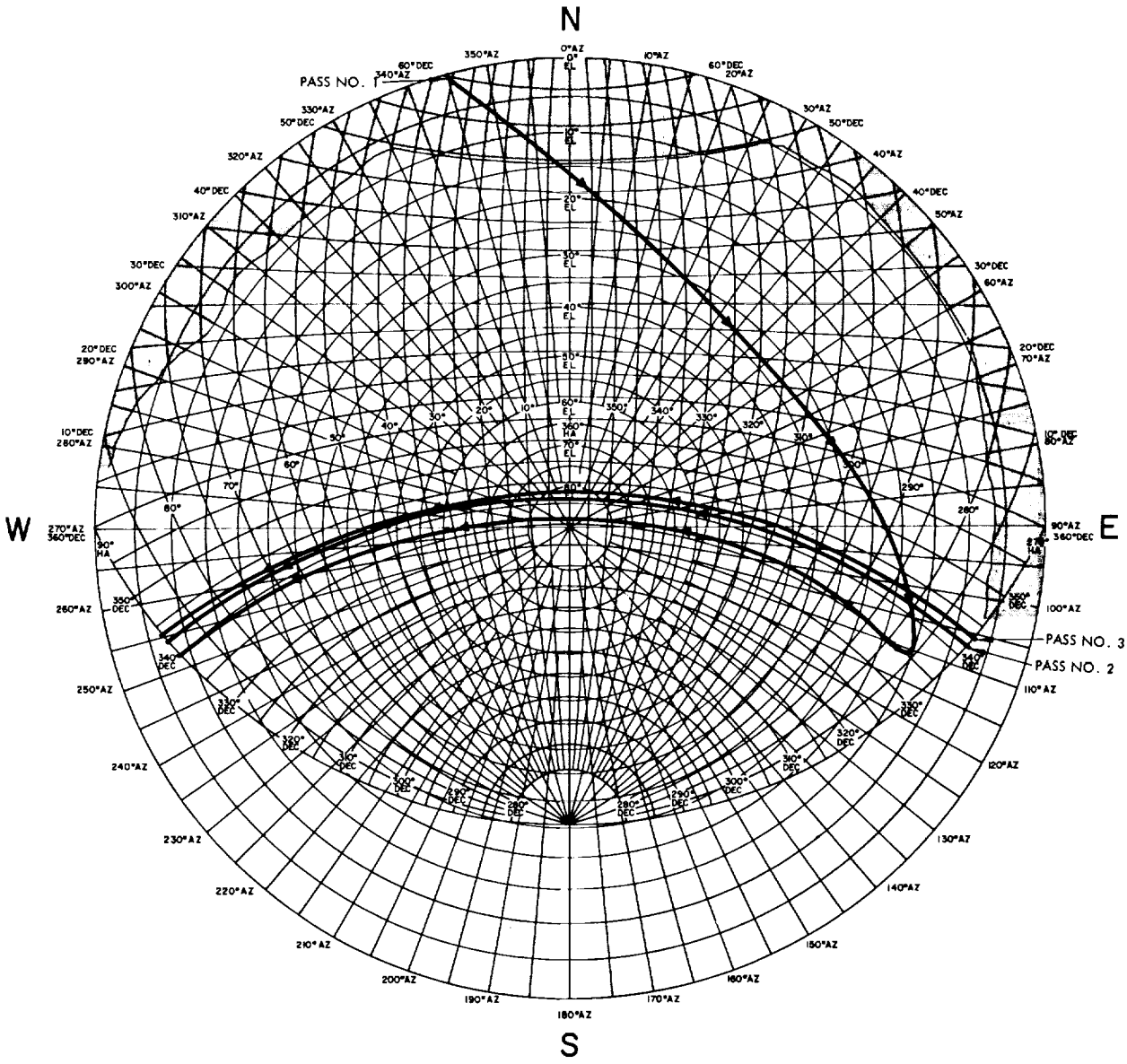

Fig. 37. DSS 51 stereographic projection, *Surveyor VI*

Table 30. *Surveyor VI* premaneuver computations

Orbit ID	Time computed, GMT		Target parameters and statistics[a]							
	Start	Stop	B, km	B • TT, km	B • RT, km	TL, h	SMAA, km (1σ)	SMIA, km (1σ)	THETA, deg (1σ)	$\sigma_{T,\,impact}$, s (1σ)
PROR XA	08:56	09:35	1740.71	1709.72	326.99	64.63	117.73	20.85	105.9	95.41
PROR YA	08:59	09:38	1720.54	1696.00	289.54	64.63	85.23	16.29	103.0	54.93
ICEV YA	09:55	10:22	1805.80	1753.65	430.84	64.60	65.92	6.36	99.56	19.69
ICEV XA	10:04	10:42	1807.70	1755.72	430.38	64.61	59.84	5.82	100.01	15.93
PREL XA	10:54	11:13	1808.22	1754.53	437.39	64.60	22.18	6.54	99.18	3.749
PREL YA	11:08	11:53	1807.95	1754.38	436.81	64.60	27.52	6.91	98.50	4.300
PREL XC	11:49	12:00	1808.34	1754.53	437.86	64.60	13.13	6.75	103.8	3.536
DACO XA	13:28	13:38	1807.72	1753.96	437.62	64.60	9.624	3.05	92.09	1.2204
DACO XB	14:14	15:00	1807.74	1753.98	437.57	64.60	9.253	2.62	94.87	0.8957
DACO YB	15:30	15:55	1808.42	1753.82	441.06	64.60	16.43	4.81	113.97	0.96069
DACO XC	15:30	16:05	1808.55	1754.25	439.87	64.60	7.399	2.48	96.39	0.79778
DACO YC	16:00	16:40	1807.89	1754.11	437.69	64.60	13.96	6.73	95.46	2.2378
DACO XE	17:27	17:44	1807.58	1753.99	436.88	64.60	5.246	3.17	101.03	0.7766
DACO YD	16:40	16:52	1807.62	1754.06	436.78	64.60	5.050	3.31	101.34	0.8168
LAPM XA	22:37	23:02	1806.42	1753.03	435.92	64.60	3.906	1.87	88.47	0.6965
LAPM YA	22:38	23:11	1808.43	1753.81	441.07	64.60	9.340	4.25	92.79	1.9272
LAPM XC[b]	23:30	23:41	1807.42	1753.30	438.99	64.60	11.07	4.09	95.28	1.8401
LAPM YC	23:46	23:59	1808.40	1753.75	441.20	64.60	11.19	4.91	96.12	2.2212
PRCL XA	03:22	03:49	1806.16	1752.57	436.70	64.60	3.234	1.66	80.21	0.62488
PRCL XB[c]	03:50	04:17	1807.17	1753.15	438.55	64.60	11.76	3.99	98.07	1.7711
PRCL XC	05:22	05:27	1807.42	1753.28	439.08	64.60	11.76	3.99	98.07	1.7709

[a]B-plane parameters defined in Appendix B. Statistics are defined as follows:

SMAA = Semimajor axis of dispersion ellipse.

SMIA = Semiminor axis of dispersion ellipse.

THETA = Orientation angle of SMAA measured counterclockwise from B • TT axis.

$\sigma_{T,\,impact}$ = Uncertainty in predicted unbraked impact time.

PHI_{99} = 99% lunar approach velocity vector point error.

SVFIXR = Uncertainty in magnitude of approach velocity vector at unbraked impact.

[b]Orbit solution used for midcourse maneuver computations.

[c]Current best estimate, premaneuver as of November 11, 1967.

Table 30 (contd)

Orbit ID	Target statistics[a] (contd)		Selenocentric conditions at unbraked impact				Data type and source
	PHI_{PP}, deg	SVFIXR, m/s (1σ)	Latitude, deg (Negative S)	Longitude, deg (East)	GMT	Solution type	
PROR XA	4.513	0.6700	−0.9879	359.65	00:36:57.370	6 × 6	DSS 51, CC3; DSS 42, DSS 51, angles
PROR YA	2.476	0.6341	−0.2448	359.35	00:36:46.050	6 × 6	
ICEV YA	0.9785	0.6184	−3.059	0.6650	00:35:53.985	6 × 6	
ICEV XA	0.8569	0.6178	−3.052	0.7128	00:35:49.512	6 × 6	
PREL XA	0.3484	0.6169	−3.187	0.6913	00:35:42.703	6 × 6	DSS 42, DSS 51, CC3
PREL YA	0.4118	0.6169	−3.175	0.6879	00:35:42.684	6 × 6	
PREL XC	0.2855	0.6169	−3.196	0.6916	00:35:42.777	6 × 6	DSS 42, DSS 51, CC3
DACO XA	0.1464	0.6169	−3.190	0.6786	00:35:43.075	6 × 6	
DACO XB	0.1401	0.6169	−3.189	0.6792	00:35:43.056	6 × 6	DSS 42, DSS 51, CC3
DACO YB	0.2656	0.6169	−3.256	0.6768	00:35:43.082	6 × 6	DSS 51, DSS 61, CC3
DACO XC	0.1133	0.6169	−3.234	0.6860	00:35:43.006	6 × 6	DSS 42, DSS 51, DSS 61, CC3
DACO YC	0.2420	0.6169	−3.192	0.6820	00:35:42.951	12 × 12	DSS 42, DSS 51, DSS 61, Est. Sta. loc.
DACO XE	0.0954	0.6169	−3.176	0.6791	00:35:42.948	6 × 6	DSS 42, DSS 51, DSS 61, CC3
DACO YD	0.0963	0.6169	−3.174	0.6806	00:35:42.886	6 × 6	
LAPM XA	0.6645	0.6169	−3.156	0.6573	00:35:43.071	6 × 6	DSS 11, DSS 42, DSS 51, DSS 61, CC3
LAPM YA	0.1693	0.6169	−3.257	0.6769	00:35:42.885	14 × 14	
LAPM XC[b]	0.1860	0.6169	−3.216	0.6646	00:35:42.987	14 × 14	
LAPM YC	0.2040	0.6169	−3.259	0.6755	00:35:42.917	14 × 14	DSS 11, DSS 42, DSS 51, CC3
PRCL XA	0.0549	0.6169	−3.171	0.6473	00:35:43.138	6 × 6	DSS 11, DSS 42, DSS 51, DSS 61, CC3
PRCL XB[c]	0.1992	0.6169	−3.207	0.6610	00:35:43.051	14 × 14	
PRCL XC	0.1992	0.6169	−3.218	0.6640	00:35:43.013	14 × 14	

indicated that unbraked impact would occur at 3.216 °S lat and 0.6646 °E lon, approximately 108 km south and 49 km east of the prelaunch aim point.

The numerical results of the premaneuver orbit computations are presented in Tables 30 and 31. Amounts and types of tracking data used in the various pre-midcourse orbit computations, together with the associated noise statistics, are given in Table 32. For the inflight best estimate of the spacecraft premaneuver orbit (PRCL XB), all usable data from DSS 11, DSS 42, DSS 51 and DSS 61 taken between the time of the initial DSS acquisition and the start of the midcourse maneuver—excluding data when the elevation angles were below 17 deg—were used. Figure 39 plots the pre-midcourse estimated unbraked impact point. Table 33 records the epochs used.

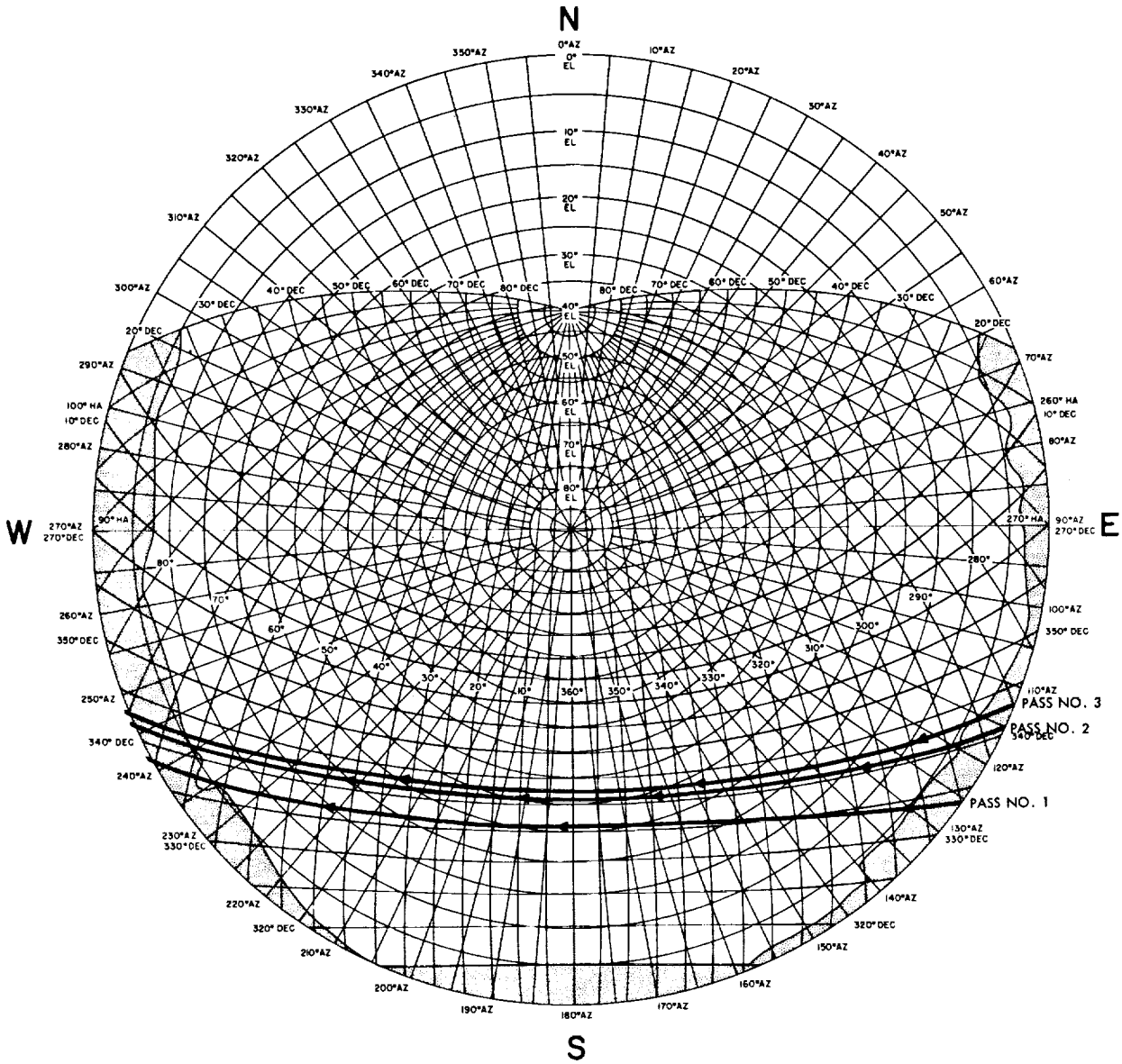

Fig. 38. DSS 61 stereographic projection, *Surveyor VI*

Table 31. *Surveyor VI* premaneuver position and velocity at injection epoch[a]

Orbit ID	Geocentric space-fixed position, km			Geocentric space-fixed velocity, km/s			Uncertainties, 1σ					
							Position, km			Velocity, m/s		
	x	y	z	Dx	Dy	Dz	σ_x	σ_y	σ_z	σ_{Dx}	σ_{Dy}	σ_{Dz}
PROR XA	−6259.1438	1587.9959	1134.8484	−3.6147849	−9.1311312	−4.8993231	1.4315	0.99944	1.4411	2.0564	0.74665	1.5496
PROR YA	−6259.4262	1588.3154	1134.4012	−3.6145318	−9.1312451	−4.8988113	0.88513	0.80559	0.99109	1.2358	0.61451	1.3376
ICEV YA	−6257.6108	1587.3184	1136.3150	−3.6168053	−9.1314916	−4.8998326	0.45952	0.64873	0.75425	0.35452	0.40390	0.94663
ICEV XA	−6257.5144	1587.3511	1136.3475	−3.6169431	−9.1315982	−4.8996857	0.43942	0.57852	0.69848	0.31835	0.35509	0.80310
PREL YA	−6257.0710	1587.3316	1136.6205	−3.6172565	−9.1323426	−4.8988002	0.38853	0.24969	0.42024	0.30649	0.38213	0.24589
PREL YB	−6257.0857	1587.3571	1136.5909	−3.6172486	−9.1323510	−4.8987627	0.75765	1.1190	1.3324	0.42112	0.46295	1.4346
PREL XC	−6257.0571	1587.3222	1136.6362	−3.6172651	−9.1323546	−4.8987954	0.21027	0.12151	0.20687	0.23372	0.23338	0.19865
DACO XA	−6257.0629	1587.3206	1136.6331	−3.6172491	−9.1323621	−4.8987845	0.15550	0.09676	0.15722	0.12173	0.18327	0.14647
DACO XB	−6257.0633	1587.3213	1136.6325	−3.6172496	−9.1323608	−4.8987857	0.15271	0.08933	0.15132	0.11963	0.17126	0.13691
DACO YB	−6256.9937	1587.2887	1136.6978	−3.6172841	−9.1324592	−4.8986968	0.21909	0.11695	0.22171	0.22967	0.25112	0.30346
DACO XC	−6257.0269	1587.3006	1136.6697	−3.6172730	−9.1323992	−4.8987603	0.12715	0.71565	0.12196	0.10875	0.14109	0.11981
DACO YC	−6257.0629	1587.3212	1136.6338	−3.6172530	−9.1323579	−4.8987892	0.18791	0.18775	0.19429	0.24108	0.19927	0.16619
DACO XE	−6257.0729	1587.3281	1136.6214	−3.6172459	−9.1323495	−4.8987928	0.11101	0.05618	0.08956	0.12263	0.11985	0.12285
DACO YD	−6257.0764	1587.3298	1136.6192	−3.6172459	−9.1323426	−4.8987994	0.10934	0.055787	0.086272	0.12520	0.11750	0.12289
LAPM XA	−6257.1025	1587.3283	1136.6008	−3.6172087	−9.1323303	−4.8988097	0.07288	0.04586	0.06486	0.06917	0.09521	0.09709
LAPM YA	−6257.0434	1587.2716	1136.6722	−3.6172434	−9.1323869	−4.8987881	0.11076	0.13211	0.12349	0.13453	0.16024	0.14801
LAPM XC[b]	−6257.0671	1587.2946	1136.6444	−3.6172267	−9.1323680	−4.8987915	0.13554	0.14742	0.14856	0.13661	0.18100	0.16029
LAPM YC	−6257.0468	1587.2685	1136.6715	−3.6172387	−9.1323819	−4.8987965	0.14014	0.15171	0.15145	0.16518	0.18311	0.16165
PRCL XA	−6257.1055	1587.3167	1136.6075	−3.6171959	−9.1323277	−4.8988220	0.06541	0.04038	0.05454	0.06376	0.09413	0.10401
PRCL XB[c]	−6257.0725	1587.3009	1136.6406	−3.6172232	−9.1323665	−4.8987853	0.14198	0.13950	0.18035	0.14805	0.18707	0.21861
PRCL XC	−6257.0660	1587.2949	1136.6476	−3.6172276	−9.1323718	−4.8987845	0.14198	0.13950	0.18035	0.14805	0.18707	0.21861

[a]See Table 33.

[b]Orbit used for midcourse computations.

[c]Current best estimate, November 11, 1967.

Table 32. Summary of premaneuver DSIF tracking data used in *Surveyor VI* orbit computations

Orbit ID	Station	Data type	Begin data, time		End data, time		Number of points	Standard deviation	Root mean square	Mean error	Data sample rate, s
			Date 1967	GMT	Date 1967	GMT					
PROR XA	DSS 42	HA	11/7	08:38:42	11/7	08:40:22	6	0.00550	0.0133	−0.0121	10
		Dec	11/7	08:38:42	11/7	08:40:22	9	0.0156	0.0352	−0.0316	10
	DSS 51	CC3	11/7	08:14:20	11/7	08:36:50	128	0.0710	0.0711	−0.00388	10
		HA	11/7	08:10:05	11/7	08:36:55	136	0.0138	0.0486	0.0467	10
		Dec	11/7	08:10:05	11/7	08:36:55	137	0.0130	0.0209	−0.0163	10
PROR YA	DSS 42	HA	11/7	08:38:42	11/7	08:40:22	10	0.0507	0.0527	0.0142	10
		Dec	11/7	08:38:42	11/7	08:40:22	10	0.0426	0.0654	−0.0496	10
	DSS 51	CC3	11/7	08:14:20	11/7	08:44:20	166	0.120	0.120	−0.00824	10
		HA	11/7	08:10:15	11/7	08:44:25	176	0.0771	0.0936	0.0532	10
		Dec	11/7	08:10:15	11/7	08:44:25	176	0.0510	0.0577	−0.0270	10
ICEV YA	DSS 42	HA	11/7	08:39:22	11/7	09:36:02	64	0.00537	0.0138	−0.0128	60
		Dec	11/7	08:39:22	11/7	09:36:02	64	0.00515	0.0234	−0.0229	60
	DSS 51	CC3	11/7	08:15:00	11/7	08:44:50	164	0.0844	0.0848	0.00789	10
		HA	11/7	08:14:15	11/7	08:44:55	172	0.0102	0.0511	0.0501	10
		Dec	11/7	08:14:15	11/7	08:44:55	172	0.0102	0.0200	−0.0172	10
	02311	CC3	11/7	08:47:32	11/7	09:36:32	40	0.0316	0.0336	−0.0115	60
		HA	11/7	08:47:02	11/7	09:37:02	44	0.00416	0.0506	0.0504	60
		Dec	11/7	08:47:02	11/7	09:37:02	44	0.00236	0.0119	−0.0117	60
ICEX XA	DSS 42	HA	11/7	08:39:22	11/7	09:51:02	84	0.00387	0.0140	−0.0135	60
		Dec	11/7	08 39:22	11/7	09:51:02	85	0.00472	0.0234	−0.0229	60
	DSS 51 pass 1	CC3	11/7	08:15:00	11/7	08:44:50	164	0.0920	0.0942	0.0201	10
		HA	11/7	08:14:15	11/7	08:44:55	172	0.0101	0.0505	0.0495	10
		Dec	11/7	08:14:15	11/7	08:44:55	172	0.0102	0.0206	−0.0179	10
	02311	CC3	11/7	08:47:32	11/7	09:51:32	59	0.0240	0.0253	−0.00794	60
		HA	11/7	08:47:02	11/7	09:52:02	63	0.00426	0.0498	0.0496	60
		Dec	11/7	08:47:02	11/7	09:52 02	63	0.00247	0.0117	−0.0114	60
PREL YA	DSS 42	CC3	11/7	10:13:32	11/7	10:32:32	18	0.00148	0.00152	−0.000434	60
	DSS 51	CC3	11/7	08:15:20	11/7	08:44:50	148	0.0399	0.0399	−0.000416	10
		CC3	11/7	08:47:32	11/7	10:03:32	62	0.00763	0.00764	−0.000465	60
PREL YB	DSS 51	CC3	11/7	08:15:20	11/7	08:44:50	148	0.0400	0.0400	−0.000403	10
		CC3	11/7	08:47:32	11/7	10:03:32	62	0.00773	0.00773	0.00244	60
PREL XC	DSS 42	CC3	11/7	10:13:32	11/7	11:29:32	74	0.00154	0.00154	−0.0000198	60
	DSS 51	CC3	11/7	08:15:20	11/7	08:44:50	148	0.0399	0.0399	−0.0000330	10
		CC3	11/7	08:47:32	11/7	10:03:32	68	0.00769	0.00769	−0.000108	60
DACO XA	DSS 42	CC3	11/7	10:13:32	11/7	12:03:32	108	0.00148	0.00159	0.000556	60
	DSS 51	CC3	11/7	08:15:20	11/7	08:44:50	148	0.0400	0.0400	−0.00146	10
		CC3	11/7	08:47:32	11/7	10:03:32	68	0.00786	0.00788	0.00632	60
		CC3	11/7	12:13:32	11/7	13:19:32	63	0.00735	0.00731	−0.000411	60

Table 32 (contd)

Orbit ID	Station	Data type	Begin data, time		End data, time		Number of points	Standard deviation	Root mean square	Mean error	Data sample rate, s
			Date 1967	GMT	Date 1967	GMT					
DACO XB	DSS 42	CC3	11/7	10:13:32	11/7	12:03:32	108	0.00151	0.00151	0.0000904	60
	DSS 51	CC3	11/7	08:15:20	11/7	08:44:50	148	0.0399	0.0399	−0.00129	60
		CC3	11/7	08:47:32	11/7	10:03:32	68	0.00784	0.00787	0.000675	60
		CC3	11/7	12:13:32	11/7	14:13:32	112	0.00707	0.00709	−0.000562	60
DACO YB	DSS 51	CC3	11/7	08:15:20	11/7	08:44:50	148	0.0416	0.0417	−0.00252	10
		CC3	11/7	08:47:32	11/7	10:03:32	62	0.00783	0.00797	0.00144	60
		CC3	11/7	12:13:32	11/7	14:37:32	113	0.00794	0.00810	−0.00161	60
	DSS 61	CC3	11/7	14:47:32	11/7	15:17:32	27	0.00828	0.0166	0.0144	60
DACO XC	DSS 42	CC3	11/7	10:13:32	11/7	12:03:32	108	0.00399	0.00401	−0.000402	60
	DSS 51	CC3	11/7	08:15:20	11/7	08:44:50	148	0.0403	0.0403	−0.000290	10
		CC3	11/7	08:47:32	11/7	10:03:32	68	0.00788	0.00789	−0.000452	60
		CC3	11/7	12:13:32	11/7	14:37:32	136	0.00771	0.00810	−0.00247	60
	DSS 61	CC3	11/7	14:47:32	11/7	15:33:32	35	0.00367	0.0145	0.0141	60
DACO YC	DSS 42	CC3	11/7	10:13:32	11/7	12:03:32	108	0.00159	0.00165	0.000457	60
	DSS 51	CC3	11/7	08:15:20	11/7	08:44:50	148	0.0399	0.0399	−0.00126	10
		CC3	11/7	08:47:32	11/7	10:03:32	18	0.00520	0.00565	0.00220	60
		CC3	11/7	12:13:32	11/7	14:37:32	113	0.00739	0.00739	−0.000151	60
	DSS 61	CC3	11/7	14:50:32	11/7	16:52:32	13	0.00247	0.00284	0.00139	60
DACO XE	DSS 42	CC3	11/7	10:13:32	11/7	12:03:32	108	0.00214	0.00234	−0.000958	60
	DSS 51	CC3	11/7	08:15:20	11/7	08:44:50	148	0.0399	0.0399	−0.000442	10
		CC3	11/7	08:47:32	11/7	10:03:32	20	0.00503	0.00589	0.00385	60
		CC3	11/7	12:13:32	11/7	17:33:32	137	0.00731	0.00765	−0.00222	60
		CC3	11/7	17:34.32	11/7	18:39:32	51	0.00719	0.00739	0.00170	60
	DSS 61	CC3	11/7	14:51:32	11/7	17:23:32	43	0.00244	0.00607	0.00555	60
DACO YD	DSS 42	CC3	11/7	10:13:32	11/7	12:03:32	108	0.00244	0.00247	−0.000371	60
	DSS 51	CC3	11/7	08:15:20	11/7	08:44:50	148	0.0398	0.0398	−0.000528	10
		CC3	11/7	08:47:32	11/7	10:03:32	18	0.00527	0.00636	0.00355	60
		CC3	11/7	12:13:32	11/7	17:35:32	114	0.00746	0.00753	−0.000968	60
		CC3	11/7	17:36:32	11/7	18:44:32	60	0.00810	0.00830	0.00181	60
	DSS 61	CC3	11/7	14:50:32	11/7	17:23:32	41	0.00252	0.00366	0.00266	60
LAPM XA	DSS 11	CC3	11/7	21:13:32	11/7	22:24:32	12	0.00446	0.0257	0.0253	60
	DSS 42	CC3	11/7	10:13:32	11/7	12:03:32	108	0.00441	0.00576	−0.00370	60
	DSS 51	CC3	11/7	08:15:32	11/7	08:44:50	148	0.0404	0.0405	0.00177	10
		CC3	11/7	08:47:32	11/7	10:03:32	68	0.00782	0.00889	−0.00423	60
	DSS 51	CC3	11/7	12:13:32	11/7	17:33:32	137	0.00730	0.00731	−0.000410	60
		CC3	11/7	17:34:32	11/7	12:55:32	176	0.00817	0.00900	0.00378	60
	DSS 61	CC3	11/7	14:51:32	11/7	17:23:32	7	0.000725	0.00363	0.00356	60
LAPM YA	DSS 11	CC3	11/7	22:13:32	11/7	22:30:32	18	0.00372	0.00375	−0.000488	60
	DSS 42	CC3	11/7	10:13:32	11/7	12:03:32	108	0.00154	0.00154	0.0000678	60

Table 32 (contd)

Orbit ID	Station	Data type	Begin data, time		End data, time		Number of points	Standard deviation	Root mean square	Mean error	Data sample rate, s
			Date 1967	GMT	Date 1967	GMT					
LAPM YA (contd)	DSS 51	CC3	11/7	08:15:20	11/7	08:44:50	148	0.0402	0.0402	−0.0000059	10
		CC3	11/7	08:47:32	11/7	10:03:32	62	0.00784	0.00790	−0.000764	60
		CC3	11/7	12:13:32	11/7	17:35:32	114	0.00741	0.00741	0.000206	60
		CC3	11/7	17:36:32	11/7	21:55:32	193	0.00727	0.00727	−0.000650	60
	DSS 61	CC3	11/7	14:50:32	11/7	17:23:32	90	0.00452	0.00452	−0.0000326	60
LAPM XC	DSS 11	CC3	11/7	22:13:32	11/7	23:18:32	59	0.00459	0.00459	0.000137	60
	DSS 42	CC3	11/7	10:13:32	11/7	12:03:32	108	0.00164	0.00171	−0.000461	60
	DSS 51	CC3	11/7	08:15:20	11/7	09:41:32	149	0.0403	0.0404	−0.00233	10
		CC3	11/7	09:42:32	11/7	10:03:32	19	0.00477	0.00506	−0.00167	60
		CC3	11/7	12:13:32	11/7	17:33:32	137	0.00736	0.00736	−0.000114	60
		CC3	11/7	17:34:32	11/7	22:02:32	237	0.00711	0.00713	−0.000525	60
	DSS 61	CC3	11/7	16:36:32	11/7	17:23:32	43	0.00296	0.00296	−0.000148	60
LAPM YC	DSS 11	CC3	11/7	22:13:32	11/7	23:36:32	69	0.00356	0.00366	0.000853	60
	DSS 42	CC3	11/7	10:13:32	11/7	12:03:32	108	0.00138	0.00162	0.000850	60
	DSS 51	CC3	11/7	08:15:20	11/7	09:41:32	149	0.0401	0.0401	−0.00127	10
		CC3	11/7	09:42:32	11/7	10:03:32	17	0.00553	0.00553	−0.0000574	60
		CC3	11/7	12:13:32	11/7	17:35:32	114	0.00740	0.00747	0.000955	60
		CC3	11/7	17:36:32	11/7	21:55:32	193	0.00728	0.00731	0.000600	60
PRCL XA	DSS 11	CC3	11/7	22:13:32	11/8	02:01:53	207	0.00648	0.00662	0.00134	60
	DSS 42	CC3	11/7	10:13:32	11/7	12:03:32	108	0.00507	0.00709	−0.00496	60
	DSS 51	CC3	11/7	08:15:20	11/7	09:41:32	149	0.0412	0.0412	−0.00190	10
		CC3	11/7	09:42:32	11/7	10:03:32	19	0.00499	0.0121	−0.0110	60
		CC3	11/7	12:13:32	11/7	17:33:32	137	0.00742	0.00811	0.00329	60
		CC3	11/7	17:34:32	11/7	22:02:32	237	0.00720	0.00732	0.00132	60
	DSS 61	CC3	11/7	16:36:32	11/7	17:23:32	43	0.00257	0.00533	0.00467	60
PRCL XB	DSS 11	CC3	11/7	22:13:32	11/8	02:01:53	162	0.0037	0.00349	0.000912	60
	DSS 42	CC3	11/7	10:13:32	11/7	12:03:32	108	0.00158	0.00160	0.000235	60
	DSS 51	CC3	11/7	08:15:20	11/7	09:41:32	149	0.0405	0.0405	−0.00213	10
		CC3	11/7	09:42:32	11/7	10:03:32	19	0.00512	0.00520	−0.000925	60
		CC3	11/7	12:13:32	11/7	17:33:32	137	0.00731	0.00738	0.000984	60
		CC3	11/7	17:34:32	11/7	22:02:32	215	0.00702	0.00705	0.000606	60
	DSS 61	CC3	11/7	16:36:32	11/7	17:23:32	43	0.00293	0.00305	0.000818	60
PRCL XC	DSS 11	CC3	11/7	22:13:32	11/8	02:01:53	162	0.00341	0.00342	−0.000363	60
	DSS 42	CC3	11/7	10:13:32	11/7	12:03:32	108	0.00163	0.00166	−0.000312	60
	DSS 51	CC3	11/7	08:15:20	11/7	09:41:32	149	0.0402	0.0403	−0.00268	10
		CC3	11/7	09:42:32	11/7	10:03:32	19	0.00492	0.00505	−0.00113	60
		CC3	11/7	12:13:32	11/7	17:33:32	137	0.00735	0.00737	0.000453	60
		CC3	11/7	17:34:32	11/7	22:02:32	215	0.00698	0.00698	−0.000218	60
	DSS 61	CC3	11/7	16:36:32	11/7	17:23:32	43	0.00288	0.00288	−0.0000227	60

Table 33. Epochs used in orbit solutions, *Surveyor VI*

Epoch		Orbits using[a] given epoch	Remarks
Date, 1967	GMT		
November 7	03:19:09.9	PROR, ICEV, PREL, DACO, LAPM, PRCL, PTD-PRE	Nominal transfer orbit injection (MECO 2)
November 8	15:00:00.0	1 POM, 2 POM, 3 POM 4 POM, 5 POM, POST, PTD-POST	Post-midcourse
November 9	18:00:00.0	FINAL	R — 5h, 40min

[a]PROR predict orbit
ICEV initial condition evaluation orbit
PREL preliminary midcourse orbit
DACO data consistency orbit
LAPM last pre-midcourse orbit
PRCL pre-midcourse cleanup orbit
PTD-PRE postflight pre-midcourse orbit
IPOM ith post-midcourse orbit
PTD-POST postflight post-midcourse orbit
FINAL AMR backup computation orbit

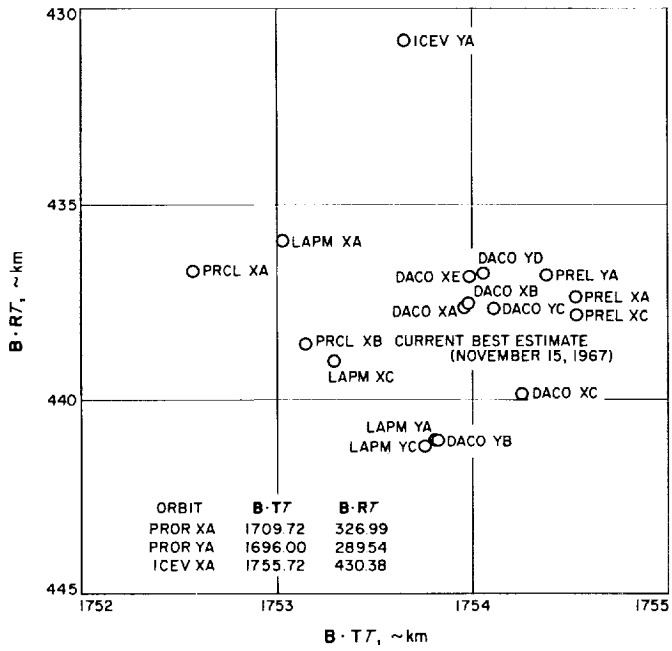

Fig. 39. Inflight estimated pre-midcourse unbraked impact point, *Surveyor VI*

C. Postmaneuver Orbit Estimates

The first post-midcourse (1 POM) orbit computations were completed approximately 10 h after maneuver execution. For the final (1 POM XG) orbit computation during this orbit period, approximately 48 min of DSS 11 data and 8 h of DSS 42 two-way doppler data were used. When the 1 POM XG solution was mapped to target, it indicated the unbraked impact point to be 0.08287 °N lat and 358.98 °E lon.

The necessity of having data from at least three tracking stations was further emphasized during the 2 POM orbit period when DSS 51 data were first used in the post-midcourse orbit solution. The final (second) post-midcourse orbit (2 POM YB) solution indicated the unbraked impact point to be 0.3736 °N lat and 358.93 °E lon (or 1.07°W lon). The DSS 51 data were consistent with DSS 11 and DSS 42 data. With the third station in the solution, the impact parameters settled down and never varied more than ±0.05 deg during the remaining orbit computations.

During the 3 POM orbit computation period, a problem was encountered with the data transmission lines from DSS 51. As a result of this, DSS 61 began tracking in a two-way mode. The data from DSS 61 seemed to be excessively noisy and erratic, so as soon as the lines were back up, DSS 51 took over the tracking task from DSS 61. The cause of the erratic data from DSS 61 has since been determined to be a bad rubidium crystal.

Because of the problems encountered with the data transmission lines from DSS 51, the possibility was considered of using DSS 61 during the time just prior to DSS 11 rise during the terminal phase. However, in view of the poor quality of DSS 61 data, it was decided to continue with DSS 51 tracking in a two-way mode and assume that any data lost could be replayed in time for the final orbit computations. This decision proved to be a good one, and DSS 11 and DSS 51 were used for the final orbit computations during the last 3 h of flight. The final terminal computations were based on the 5 POM WD orbit solution.

Numerical results of the inflight post-midcourse orbit solutions are presented in Tables 34 and 35. Figure 40 is a plot of the post-midcourse estimated unbraked impact point in **B**-space. The inflight best estimate of the landed *Surveyor VI* spacecraft is 0.60 km north and 7.1 km west of the final aim point. The amounts of tracking data used in the various post-midcourse orbit computations, together with the associated noise statistics, are given in Table 36. (See Table 33 for epochs used.)

Table 34. *Surveyor VI* postmaneuver computations

Orbit ID	Time computed, GMT		Target statistics[a]							
	Start	Stop	B, km	B • TT, km	B • RT, km	TL, h	SMAA, km (1σ)	SMIA, km (1σ)	THETA, deg (1σ)	$\sigma_{T,\ impact}$, s (1σ)
1 POM XA	06:53	06:59	1733.31	1712.51	267.75	46.29	521.3	246.6	85.87	137.712
1 POM XD	10:06	10:18	1731.71	1708.03	285.41	46.29	584.3	130.2	121.1	235.95
1 POM XG	13:40	14:08	1721.95	1700.10	273.47	46.29	383.96	33.02	108.7	136.29
2 POM XB	15:57	16:09	1714.71	1695.02	259.13	46.30	17.27	8.87	2.342	10.189
2 POM YB	18:33	18:39	1717.44	1697.88	258.46	46.30	9.366	7.657	22.03	4.9679
3 POM XB	03:05	03:40	1715.66	1696.06	258.59	46.30	7.621	3.811	172.8	4.294
3 POM XE	06:47	07:10	1713.77	1694.26	257.85	46.36	5.535	3.872	19.56	2.662
3 POM XF	08:40	08:56	1713.73	1694.21	257.96	46.30	4.45	3.75	35.86	2.066
3 POM WD	09:50	10:05	1713.40	1693.68	259.21	46.30	8.602	7.509	25.79	4.6370
4 POM XA	10:41	11:06	1713.26	1693.70	258.19	46.30	3.815	3.101	100.2	1.5286
4 POM XD	15:04	15:21	1712.76	1693.20	258.09	46.30	3.337	2.029	78.30	1.0016
4 POM WG	18:54,	19:48	1711.64	1692.13	257.70	46.30	14.61	8.569	116.41	3.4048
5 POM XA	19:29	19:53	1712.38	1692.81	258.19	46.30	3.192	0.7434	88.43	0.57937
5 POM XD	21:09	21:30	1712.17	1692.61	258.07	46.30	3.179	0.6026	87.95	0.54060
5 POM WD[a]	21:07	21:24	1711.70	1692.20	257.59	46.30	14.58	8.235	116.46	2.8789
FINAL WA	22:55	23:06	1711.72	1692.10	258.42	54.48	2.647	0.7687	84.07	0.53972
FINAL XA	23:04	23:19	1711.72	1692.08	258.62	5.747	2.559	0.7683	84.22	0.53766
FINAL WC	23:36	23:42	1711.73	1692.09	258.56	5.748	2.460	0.7539	83.72	0.52219
FINAL XC	23:44	00:55	1711.55	1691.89	258.68	5.748	2.462	0.7355	83.80	0.51227
FINAL WE[b]	00:10	00:21	1711.52	1691.85	258.71	5.748	2.446	0.7096	84.35	0.50256
FINAL WF	00:24	00:36	1711.32	1961.62	258.95	5.748	2.333	0.3981	88.93	0.43380
POST 2[c]	Postflight		1711.04	1691.62	257.11	46.30	9.059	3.637	93.20	1.130

[a]Orbit used for terminal maneuver computations.

[b]Orbit used for AMR backup calculations.

[c]Current best estimate, postmaneuver, as of November 14, 1967.

Table 34 (contd)

Orbit ID	Target statistics[a] (contd)		Selenocentric conditions at unbraked impact			Solution type	Data type and source
	PHI_{99}, deg	SVFIXR, m/s (1σ)	Latitude, deg (Negative S)	Longitude, deg (East)	GMT		
1 POM XA	10.375	0.7930	0.17579	359.25	00:58:20.519	6 × 6	DSS 11 and DSS 42
1 POM XD	16.81	1.053	−0.1568	359.15	00:58:20.250	6 × 6	
1 POM G	9.602	0.7838	0.08287	358.98	00:58:25.977	6 × 6	
2 POM XB	0.6694	0.6193	0.3647	358.87	00:58:31.459	6 × 6	CC3, DSS 11, DSS 42, and DSS 51
2 POM YB	0.3370	0.6184	0.3736	358.93	00:58:29.823	6 × 6	
3 POM XB	0.2874	0.6183	0.3736	358.89	00:58:30.487	6 × 6	
3 POM XE	0.1864	0.6181	0.3901	358.85	00:58:31.596	6 × 6	
3 POM XF	0.1453	0.6181	0.3881	358.85	00:58:31.614	6 × 6	
3 POM WD	0.3127	0.6183	0.3650	358.84	00:58:31.631	6 × 6	
4 POM XA	0.1087	0.6181	0.3843	358.84	00:58:31.866	6 × 6	
4 POM XD	0.0699	0.6180	0.3869	358.83	00:58:32.116	6 × 6	
4 POM WG	0.1901	0.6218	0.3947	358.81	00:58:32.785	12 × 12	
5 POM XA	0.0484	0.6182	0.3843	358.83	00:58:32.450	6 × 6	
5 POM XD	0.0476	0.6182	0.3869	358.82	00:58:32.549	6 × 6	
5 POM WD[a]	0.1869	0.6216	0.3967	358.82	00:58:32.883	15 × 15	
FINAL WA	0.0388	0.6183	0.3810	358.81	00:58:33.083	6 × 6	CC3, DSS 51 and DSS 11
FINAL XA	0.0375	0.6183	0.3772	358.81	00:58:33.098	6 × 6	
FINAL WC	0.0362	0.6183	0.3783	358.81	00:58:33.098	6 × 6	
FINAL XC	0.0362	0.6183	0.3761	358.80	00:58:32.994	6 × 6	
FINAL WE[b]	0.0360	0.6183	0.3757	358.81	00:58:32.972	6 × 6	
FINAL WF	0.0341	0.6182	0.3714	358.80	00:58:32.884	6 × 6	
POST 2[c]	0.1320	0.6189	0.4071	358.80	00:58:32.923	15 × 15	EST STD. 6 + RI, LO, and JETS

Table 35. *Surveyor VI* postmaneuver position and velocity at injection epoch[a]

Orbit ID	Geocentric space-fixed position			Geocentric space-fixed velocity			Uncertainties, 1σ					
							Position			Velocity		
	x, km	y, km	z, km	Dx, km/s	Dy, km/s	Dz, km/s	σ_x, km	σ_y, km	σ_z, km	σ_{Dx}, m/s	σ_{Dy}, m/s	σ_{Dz}, m/s
1 POM XA	139650.64	−99992.529	−60992.425	1.5840236	−0.67774031	−0.43841891	58.467	7.3496	94.094	1.2496	2.0041	2.7378
1 POM XD	139652.70	−99992.336	−60992.897	1.5840291	−0.67767581	−0.43850411	73.149	11.424	155.99	2.0338	1.1429	3.2851
1 POM XG	139651.26	−99992.578	−60988.985	1.5840789	−0.67765196	−0.43842509	60.969	7.4207	80.526	1.0509	0.24033	2.2244
2 POM XB	139648.84	−99992.868	−60985.758	1.5841211	−0.67764691	−0.43833698	3.2818	2.2300	5.2297	0.09804	0.12158	0.06153
2 POM YB	139649.25	−99992.578	−60986.556	1.5841053	−0.67766816	−0.43833990	2.4444	1.7674	2.7154	0.05135	0.06750	0.04677
3 POM XB	139649.29	−99992.723	−60986.129	1.5841136	−0.67765721	−0.43833695	1.9426	1.6457	2.4026	0.04430	0.05222	0.03130
3 POM XE	139648.81	−99993.006	−60985.698	1.5841248	−0.66764632	−0.43832841	1.3437	1.3089	1.8519	0.02887	0.03961	0.02467
3 POM XF	139648.82	−99993.011	−60985.697	1.5841250	−0.67764571	−0.43832885	1.2851	1.1807	1.5141	0.02292	0.03130	0.02437
3 POM WD	139649.35	−99993.176	−60984.772	1.5841245	−0.67763937	−0.43833790	2.1922	1.7076	2.5482	0.04784	0.06215	0.04612
4 POM XA	139648.75	−99993.100	−60985.553	1.5841277	−0.67764162	−0.43832904	1.2476	1.0827	1.2843	0.01752	0.02171	0.02432
4 POM XD	139648.66	−99993.187	−60985.455	1.5841305	−0.67763854	−0.43832729	1.1561	0.99927	1.1994	0.01144	0.01679	0.01947
4 POM WG	139648.80	−99993.157	−60984.705	1.5841295	−0.67763676	−0.43833169	5.5502	2.2529	6.8073	0.07193	0.10291	0.05930
5 POM XA	139648.61	−99993.233	−60985.433	1.5841326	−0.67763579	−0.43832674	1.1385	0.97936	1.1859	0.00565	0.00976	0.01911
5 POM XD	139648.52	−99993.289	−60985.471	1.5841340	−0.67763471	−0.43832528	1.1221	0.97273	1.1823	0.00485	0.00943	0.01886
5 POM WD	139648.71	−99993.119	−60984.586	1.5841304	−0.67763647	−0.43833010	5.2968	2.1393	6.3863	0.06952	0.10237	0.05228
FINAL WA	313357.20	−164287.61	−103427.61	0.95437454	−0.36196404	−0.23583125	0.77628	1.0347	1.8815	0.00685	0.01145	0.01584
FINAL XA	313357.20	−164287.52	−103427.74	0.95437498	−0.36196342	−0.23593190	0.77604	0.98715	1.8296	0.00671	0.01129	0.01568
FINAL WC	313357.19	−164287.55	−103427.70	0.95437492	−0.36196353	−0.23593165	0.75331	0.93549	1.7699	0.00621	0.01070	0.01555
FINAL XC	313357.42	−164287.49	−103427.79	0.95437353	−0.36196526	−0.23593321	0.72489	0.93702	1.7714	0.00605	0.01055	0.01552
FINAL WE	313357.47	−164287.48	−103427.81	0.95437327	−0.36196560	−0.23593351	0.68497	0.92914	1.7626	0.00593	0.01046	0.01538
FINAL WF	313357.68	−164287.37	−103427.97	0.95437296	−0.36196582	−0.23593492	0.28435	0.87546	1.6988	0.00559	0.01022	0.01466
POST 2	139648.61	−99993.395	−60984.705	1.5841255	−0.67765082	−0.43832036	2.2892	2.0473	3.6614	0.03236	0.06046	0.04566

[a]See Table 33 for epochs used.

Table 36. Summary of postmaneuver DSIF tracking data used in *Surveyor VI* orbit computations

Orbit ID	Station	Data type	Begin data, time		End data, time		Number of points	Standard deviation	Root mean square	Mean error	Data sample rate, s
			Date 1967	GMT	Date 1967	GMT					
1 POM XA	DSS 11	CC3	11/8	02:45:32	11/8	03:33:32	45	0.00142	0.00142	−0.0000163	60
	DSS 42	CC3	11/8	03:42:32	11/8	05:36:32	110	0.00163	0.00163	−0.0000111	60
1 POM XD	DSS 11	CC3	11/8	02:45:32	11/8	03:33:32	45	0.00144	0.00145	0.0000380	60
	DSS 42	CC3	11/8	03:42:32	11/8	08:36:32	283	0.00159	0.00159	0.00000518	60
1 POM XG	DSS 11	CC3	11/8	02:45:32	11/8	03:33:32	45	0.00145	0.00145	0.000114	60
	DSS 42	CC3	11/8	03:42:32	11/8	11:44:32	464	0.00163	0.00163	−0.00000105	60
2 POM XB	DSS 11	CC3	11/8	02:45:32	11/8	03:33:32	45	0.00189	0.00189	−0.000	60
	DSS 42	CC3	11/8	03:42:32	11/8	13:23:32	558	0.00160	0.00160	−0.0000131	60
	DSS 51	CC3	11/8	13:33:32	11/8	14:27:32	49	0.00706	0.00706	−0.0000199	60
2 POM YB	DSS 11	CC3	11/8	02:45:32	11/8	03:33:32	45	0.00160	0.00179	0.000803	60
	DSS 42	CC3	11/8	03:42:32	11/8	13:23:32	543	0.00205	0.00206	−0.000205	60
	DSS 51	CC3	11/8	13:33:32	11/8	18:10:32	269	0.00729	0.00729	0.000222	60
3 POM XB	DSS 11	CC3	11/8	02:45:32	11/8	03:33:32	45	0.00152	0.00500	0.00476	60
		CC3	11/8	22:18:32	11/9	01:04:32	112	0.00652	0.00655	0.000643	60
	DSS 42	CC3	11/8	03:42:32	11/8	13:23:32	558	0.00350	0.00376	−0.00138	60
	DSS 51	CC3	11/8	13:33:32	11/8	20:38:32	388	0.00908	0.00917	0.00129	60
3 POM XE	DSS 11	CC3	11/8	02:45:32	11/8	03:33:32	46	0.00193	0.00786	0.00762	60
		CC3	11/8	23:12:32	11/9	05:33:32	369	0.00412	0.00442	−0.00160	60
	DSS 42	CC3	11/8	03:42:32	11/8	13:23:32	557	0.00342	0.00403	−0.00214	60
		CC3	11/9	05:42:32	11/9	06:34:32	47	0.00188	0.00707	0.00682	60
	DSS 51	CC3	11/8	13:33:32	11/8	20:38:32	388	0.00890	0.00934	0.00283	60
3 POM XF	DSS 11	CC3	11/8	02:45:32	11/8	03:33:32	46	0.00201	0.00809	0.00783	60
		CC3	11/8	23:12:32	11/9	05:33:32	369	0.00402	0.00442	−0.00183	60
	DSS 42	CC3	11/8	03:42:32	11/8	13:23:32	558	0.00339	0.00400	−0.00211	60
		CC3	11/9	05:42:32	11/9	08:18:32	142	0.00396	0.00482	0.00274	60
	DSS 51	CC3	11/8	13:33:32	11/8	20:38:32	388	0.00896	0.00936	0.00273	60
3 POM WD	DSS 11	CC3	11/8	02:46:32	11/8	03:33:32	44	0.00146	0.00149	−0.000283	60
	DSS 42	CC3	11/8	03:42:32	11/8	13:23:32	558	0.00173	0.00173	0.0000823	60
	DSS 51	CC3	11/8	13:33:32	11/8	20:38:32	388	0.00712	0.00712	−0.0000793	60
4 POM XA	DSS 11	CC3	11/8	02:45:32	11/8	03:33:32	46	0.00217	0.00793	0.00763	60
		CC3	11/8	23:12:32	11/9	05:33:32	369	0.00371	0.00405	−0.00163	60
	DSS 42	CC3	11/8	03:42:32	11/8	13:23:32	558	0.00360	0.00416	−0.00209	60
		CC3	11/9	05:42:32	11/9	10:29:32	268	0.00403	0.00423	0.00127	60
	DSS 51	CC3	11/8	13:33:32	11/8	20:38:32	388	0.00913	0.00951	0.00267	60
4 POM XD	DSS 11	CC3	11/8	02:24:32	11/8	23:11:32	46	0.00238	0.00915	0.00883	60
		CC3	11/8	23:12:32	11/9	05:33:32	369	0.00345	0.00373	−0.00140	60
	DSS 41	CC3	11/8	03:42:32	11/8	13:23:32	558	0.00398	0.00459	−0.00229	60
		CC3	11/9	05:42:32	11/9	13:23:32	435	0.00344	0.00371	0.00138	60
	DSS 51	CC3	11/8	13:33:32	11/8	20:38:32	388	0.00909	0.00935	0.00223	60
		CC3	11/9	13:33:32	11/9	14:52:32	77	0.00780	0.00810	−0.00218	60
4 POM WG	DSS 11	CC3	11/8	02:45:32	11/8	23:11:32	46	0.00171	0.00172	0.000236	60
		CC3	11/8	23:12:32	11/9	05:33:32	361	0.00259	0.00259	0.000157	60

Table 36 (contd)

Orbit ID	Station	Data type	Begin data, time		End data, time		Number of points	Standard deviation	Root mean square	Mean error	Data sample rate, s
			Date 1967	GMT	Date 1967	GMT					
4 POM WG (contd)	DSS 42	CC3	11/8	03:42:32	11/8	13:23:32	558	0.00184	0.00184	−0.00000394	60
		CC3	11/9	05:42:32	11/9	13:23:32	437	0.00176	0.00176	0.000119	60
	DSS 51	CC3	11/8	13:33:32	11/8	20:38:32	388	0.00711	0.00711	0.0000862	60
		CC3	11/9	13:33:32	11/9	18:37:32	268	0.00708	0.00708	−0.0000875	60
5 POM XA	DSS 11	CC3	11/8	02:45:32	11/8	23:11:32	46	0.00278	0.0110	0.0107	60
		CC3	11/8	23:12:32	11/9	05:33:32	369	0.00335	0.00387	−0.00193	60
	DSS 42	CC3	11/8	03:42:32	11/8	13:23:32	558	0.00413	0.00471	−0.00227	60
		CC3	11/9	05:42:32	11/9	13:23:32	435	0.00300	0.00348	0.00175	60
	DSS 51	CC3	11/8	13:33:32	11/8	20:38:32	388	0.00921	0.00936	0.00168	60
		CC3	11/9	13:33:32	11/9	19:17:32	294	0.00738	0.00738	−0.000111	60
5 POM XD	DSS 11	CC3	11/8	02:45:32	11/8	03:33:32	46	0.00319	0.0135	0.0131	60
		CC3	11/8	23:12:32	11/9	05 33:32	369	0.00325	0.00404	0.00239	60
	DSS 42	CC3	11/8	03:42:32	11/8	13:23:32	558	0.00416	0.00469	−0.00217	60
		CC3	11/9	05:42:32	11/9	13:23:32	435	0.00295	0.00321	0.00128	60
	DSS 51	CC3	11/8	13:33:32	11/8	20:38:32	388	0.00931	0.00936	0.000978	60
		CC3	11/9	13:33:32	11/9	20:44:32	367	0.00866	0.00878	0.00145	60
5 POM WD	DSS 11	CC3	11/8	02:45:32	11/8	03:33:32	46	0.00177	0.00178	0.0000796	60
		CC3	11/8	23:12:32	11/9	05:33:32	361	0.00266	0.00267	0.000234	60
	DSS 42	CC3	11/8	03:42:32	11/8	13:23:32	558	0.00184	0.00184	0.00000263	60
		CC3	11/9	05:42:32	11/9	13:23:32	437	0.00174	0.00174	0.0000229	60
	DSS 51	CC3	11/8	13:33:32	11/8	20:38:32	388	0.00711	0.00711	−0.000138	60
		CC3	11/9	13:33:32	11/9	20:44:32	370	0.00735	0.00735	−0.000160	60
FINAL WA	DSS 11	CC3	11/9	22:18:32	11/9	22:47:32	26	0.00646	0.00652	0.000826	60
	DSS 51	CC3	11/9	19:19:32	11/9	22:08:32	158	0.00749	0.00749	0.0000448	60
FINAL XA	DSS 11	CC3	11/9	22:18:32	11/9	22:54:32	33	0.00601	0.00604	0.000577	60
	DSS 51	CC3	11/9	19:19:32	11/9	22:08:32	158	0.00745	0.00745	−0.000117	60
FINAL WC	DSS 11	CC3	11/9	22:18:32	11/9	23:26:32	54	0.00542	0.00543	0.000339	60
	DSS 51	CC3	11/9	19:19:32	11/9	22:08:32	158	0.00747	0.00747	−0.0000958	60
FINAL XC	DSS 11	CC3	11/9	22:18:32	11/9	23:36:32	56	0.00548	0.00549	0.000434	60
	DSS 51	CC3	11/9	19:19:32	11/9	22:08:32	158	0.00748	0.00748	−0.0000433	60
FINAL WE	DSS 11	CC3	11/9	22:18:32	11/9	23:39:32	71	0.00537	0.00538	0.000339	60
	DSS 51	CC3	11/9	19:19:32	11/9	22:08:32	158	0.00749	0.00749	−0.000144	60
FINAL WF	DSS 11	CC3	11/9	22:18:32	11/9	00:15:32	98	0.00471	0.00472	0.000247	60
	DSS 51	CC3	11/9	19:19:32	11/9	22:08:32	158	0.00748	0.00748	−0.0000278	60
POST 2	DSS 11	CC3	11/8	02:45:32	11/8	23:11:32	46	0.00185	0.00201	0.000785	60
	DSS 11	CC3	11/8	23:12:32	11/9	05:33:32	361	0.00302	0.00302	0.000143	60
	DSS 11	CC3	11/9	22:18:32	11/10	00:14:32	97	0.00650	0.00674	0.00177	60
	DSS 42	CC3	11/8	03:42:32	11/8	13:23:32	558	0.00166	0.00167	0.000191	60
	DSS 42	CC3	11/9	05:42:32	11/9	13:23:32	437	0.00191	0.00192	0.000148	60
	DSS 51	CC3	11/8	13:33:32	11/8	20:35:32	387	0.00711	0.00714	0.000610	60
	DSS 51	CC3	11/9	13:33:32	11/9	22:08:32	457	0.00759	0.00759	−0.000236	60

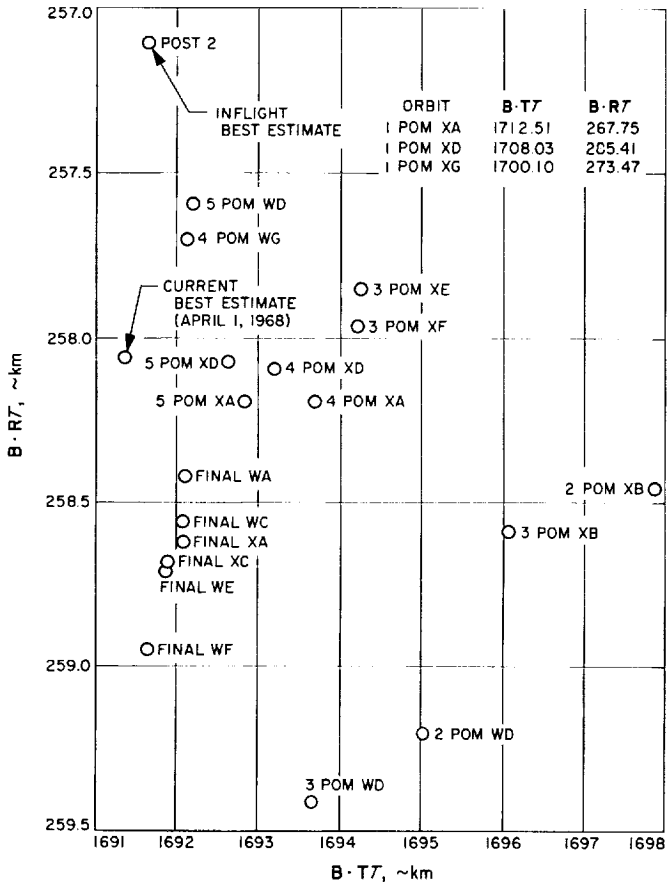

Fig. 40. Estimated post-midcourse unbraked impact point, *Surveyor VI*

D. AMR Backup Computations

After the 5 POM WD computation, primary OD emphasis was placed on obtaining the best estimate of unbraked impact time to be used for sending a ground command to back up the onboard AMR. All subsequent computations used *a priori* information from all post-maneuver tracking data up to 5 h, 40 min before the retrograde phase (R). This information was in the form of a covariance matrix mapped to $R - 5$ h, 40 min. The covariance matrix was degraded and expanded as discussed in Section II-A. In addition to being able to account for the SPODP model errors by use of this method, a considerable saving in program running time is achieved by working from the updated epoch. This fact is very important since the basic philosophy is that the near-moon data will yield the best estimate of unbraked impact time; in other words, as much near-moon data as possible should be included in the orbit solution while still being able to provide the results at $R - 40$ min (which is the lead time required to implement the backup command transmission).

For the AMR backup computations, a lunar elevation of 1736.0 km at the predicted unbraked impact point was used. This lunar elevation was obtained from NASA Langley Research Center and it was in close agreement with the elevation based on the appropriate ACIC lunar chart less 2.4 km. The 2.4 km is the amount by which the elevation based on the appropriate ACIC lunar chart exceeds the elevation obtained from the Ranger VI, VII and VIII tracking data. An *a priori* 1σ uncertainty of ± 1 km (roughly equivalent to ± 0.4 s) was assigned to the elevation.

The estimated unbraked impact time that was used for the AMR backup calculations was 00:58:32.972 GMT, which was obtained from the FINAL WE orbit solution. This solution contained data from DSS 51 (2 h, 29 min) and DSS 11 (1 h, 21 min) taken up to touchdown minus 1 h, 22 min (which was $R - 1$ h, 19 min). With this unbraked impact time, the nominal AMR mark time was computed to be 00:57:56:06 GMT, November 10, 1967. This time was used as the basic reference point from which the desired time of backup command transmission from the ground station (DSS 11) was calculated. The backup command was transmitted from DSS 11 at a time such that it was predicted to arrive at the spacecraft 1.28 s after the nominal AMR mark time. The time at which the AMR provided a mark pulse on board the spacecraft was 00:57:55.74 GMT ± 0.05 s. This observed time was 0.32 s earlier than the nominal AMR mark time used for backup calculations. The AMR backup command arrived at the spacecraft at 00:57:57.78 GMT ± 0.1 s, about 2.04 s after the AMR mark. The inflight results of AMR backup computations are given in Table 37. The difference between the estimated unbraked impact

Table 37. Inflight results of orbit determination terminal computations, *Surveyor VI*

Orbit solution data span[a]		Predicted selenocentric conditions at unbraked impact, November 10, 1967		
From	To	Latitude (South)	Longitude (East)	Time, GMT
MC[b]	E — 5h, 40min	0.3810	358.803	00:58:33.083
E — 5h, 40min	E — 1h, 56min	0.3787	358.813	00:58:33.085
E — 5h, 40min	E — 1h, 35min	0.3783	358.813	00:58:33.098
E — 5h, 40min	E — 1h, 28min	0.3773	358.810	00:58:33.025
E — 5h, 40min	E — 1h, 22min	0.3757	358.808	00:58:32.972
E — 5h, 40min	E — 46min	0.3714	358.803	00:58:32.884
Best estimate of unbraked impact time				00:58:32.885

[a]Solution used for initial estimate of AMR mark time.
[b]MC refers to initial post-midcourse epoch.

time provided for the AMR backup and the current best estimate (0.23 s) is well within the 0.5 s desired (1σ) orbit determination accuracy.

X. *Surveyor VI* Postflight Orbit Determination Analysis

The purpose of this section is to present the best estimate of the *Surveyor VI* flight path and other significant results obtained from analysis of the DSS tracking data. The analysis verified that both the premaneuver and postmaneuver inflight orbit solutions were within the *Surveyor* Project orbit determination accuracy requirements. The inflight philosophy of estimating only a minimum parameter set (i.e., the six components of the spacecraft position and velocity vectors) for the orbital computations was again proven valid.

For the postflight orbital computations and analysis, only two-way doppler data were used. The right hand column in the upper half of Table 29 summarizes the data used for the final premaneuver orbit computation in the postflight analysis. A comparison of this information with the amount of data used inflight shows that, in general, more two-way doppler data points were used for the postflight computations. This increase was the result of adding the low-elevation data (below 17 deg), which had been ignored for inflight computations. The decision to add these data was based on the use of improved values of the index of refraction for DSS 11, DSS 42, DSS 51 and DSS 61. It was felt that, with the new indices of refraction incorporated, the low-elevation data would contribute to the solution, rather than degrade it as has been suspected in the past. Corresponding entries in the lower part of Table 29 summarize the data used for postmaneuver orbit computations in postflight analysis. In this case, a few additional points were added from DSS 11 that had been ignored during inflight computations. Otherwise, the postflight analysis used the same data package that had been used inflight for post-midcourse computations.

A. Premaneuver Orbit Estimates

All the known bad data points were removed in the orbit data generator program (ODG) before the start of the postflight analysis. Low-elevation data which had been ignored inflight were added to the data tape, and a 6×6 solution (estimating the six components of position and velocity) was computed. Data residuals from this computation may be seen in Fig. 41. As seen in the figures, three problems existed: (1) during the first hour at DSS 11, data were unusually noisy, (2) DSS 42 data had a slight bias and (3) the first hour's data at DSS 61 were noisy and biased. In addition to these three problems, the usual curvature seen for low-elevation data is apparent at the beginning of the DSS 11, DSS 51, and DSS 61 passes.

To determine the data consistency between stations, numerous orbit solutions were computed by use of various combinations of data from DSS 11, DSS 42, DSS 51, and DSS 61. These data consistency computations indicated that, with the exception of the slight biases mentioned above, the stations were all consistent.

New values of indices of refraction for all four of the principal tracking stations were obtained from A. S. Liu (navigational accuracy group, JPL) and utilized in a 6×6 orbit solution. As a result, much of the curvature in the residual plots was removed, as can be seen in Fig. 42. Although the 6×6 fit with new indices of refraction was an improvement over the uncorrected solution, it was still not satisfactory. In an attempt to remove the remaining irregularities from the data fit, the estimate list was expanded to 18 to include the station-location parameters—radius, latitude and longitude—for DSS 11, DSS 42, DSS 51, and DSS 61. The resulting solution was good, but still had excessive noise on DSS 11 and DSS 61 data; residual plots can be seen in Fig. 43.

To isolate the problem causing the noisy data from DSS 11 and DSS 61, station logs were examined, and discussions were held with tracking data analysts. It was decided that the probable cause for the excessive noise on the data from DSS 61 was a faulty rubidium standard, which was later replaced (during post-midcourse tracking). No hypothesis was advanced to explain the noise for DSS 11 data. However, another data file was compiled using data from all stations without incorporating the resolver correction. A 6×6 solution, which used the data without resolver correction, was computed and resulted in the data residuals shown in Fig. 44. As seen in these residual plots, the DSS 11 data were not excessively noisy when compared to that of the other stations. From these results, one of two conclusions can be drawn: (1) either the resolver was not working properly or, (2) the data has some other problem which is masked by the noise removed by the resolver correction.

Numerous computer runs were made to estimate various combinations of physical constants and station-location parameters. The impact parameters that resulted

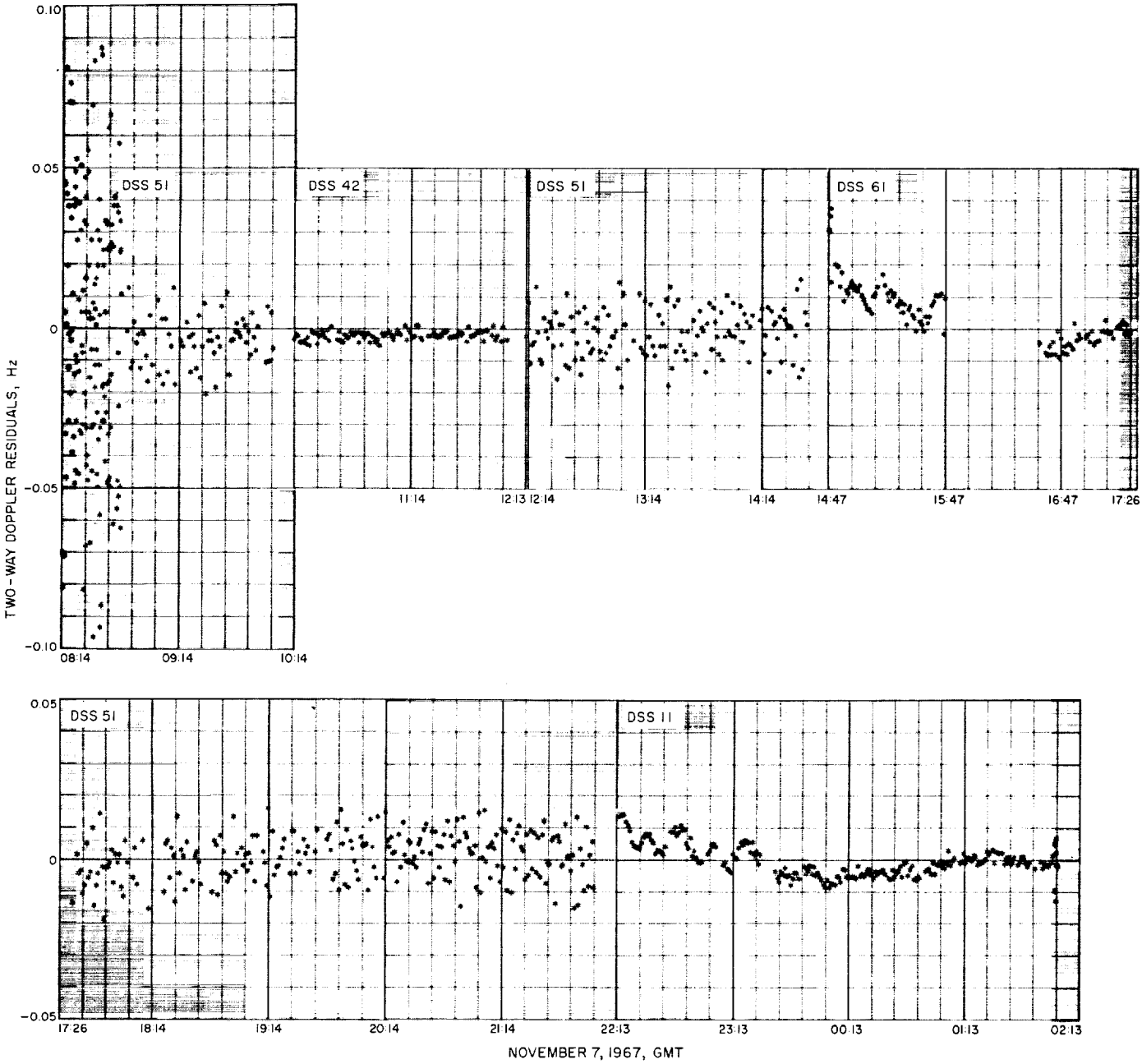

Fig. 41. Premaneuver two-way doppler residuals, *Surveyor VI* (6 × 6 solution, with resolver, old indices of refraction)

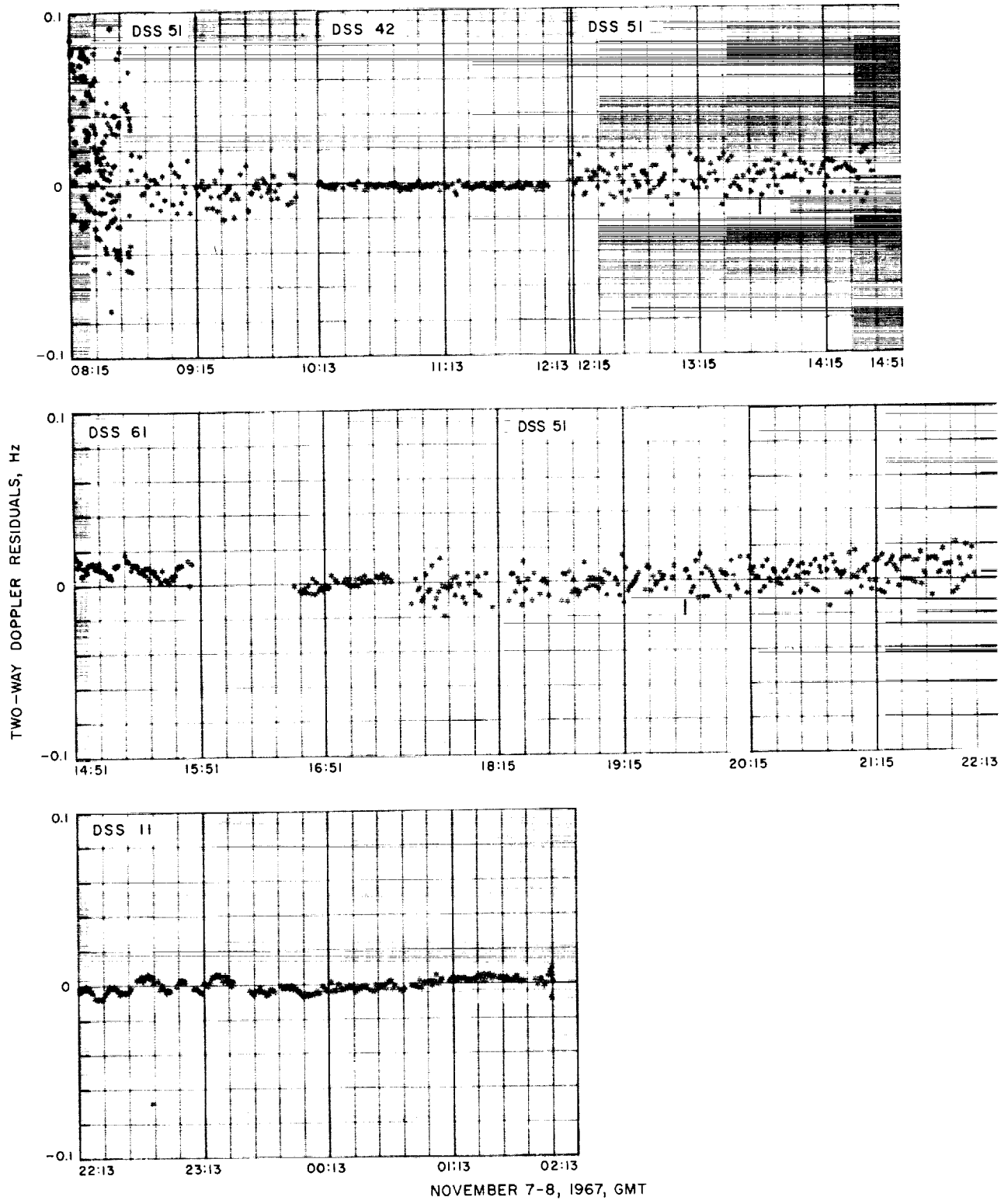

Fig. 42. Premaneuver two-way doppler residuals, *Surveyor VI* (6 × 6 solution, with resolver, new indices of refraction)

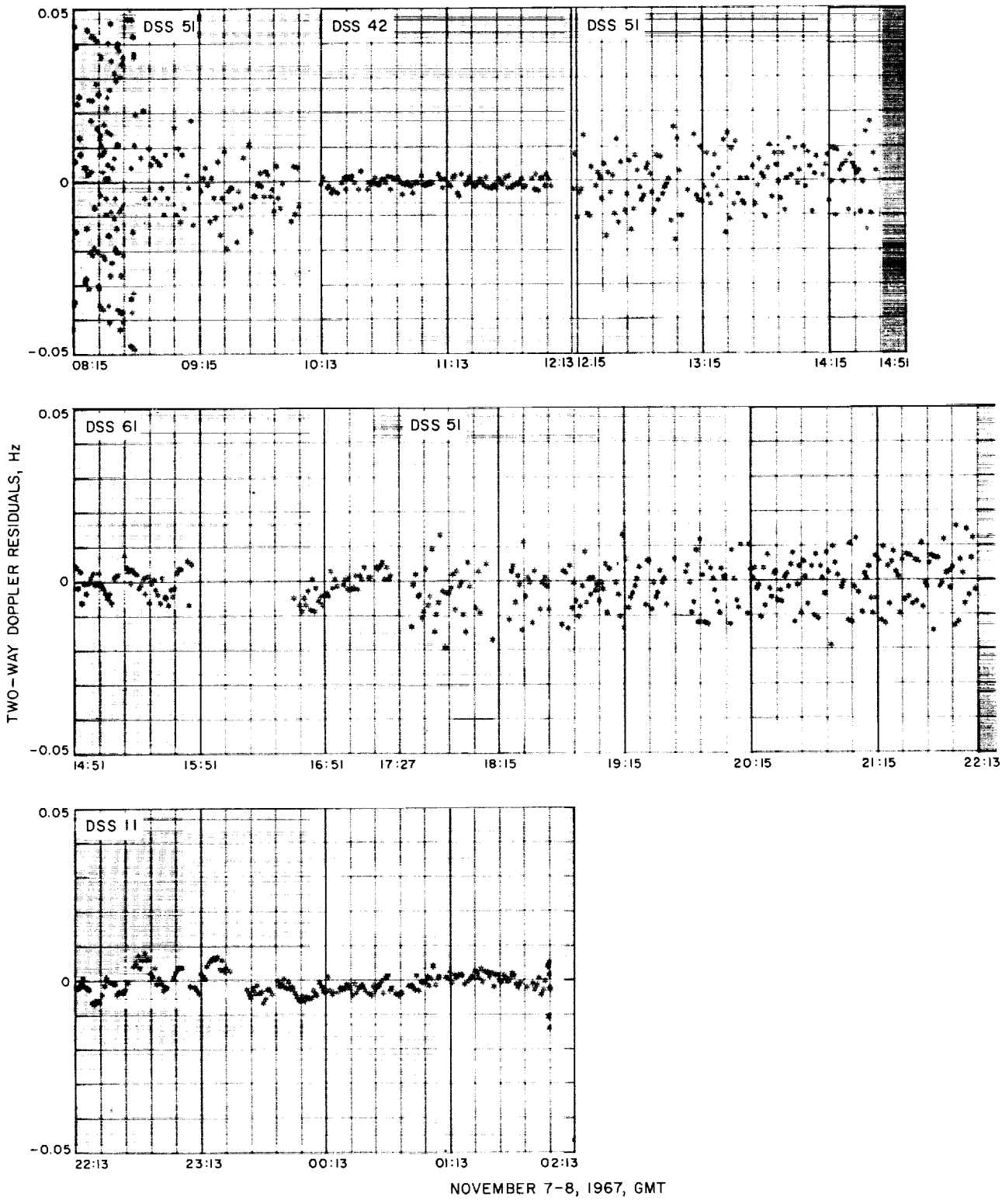

Fig. 43. Premaneuver two-way doppler residuals, *Surveyor VI* (18 × 18 solution, with resolver, new indices of refraction)

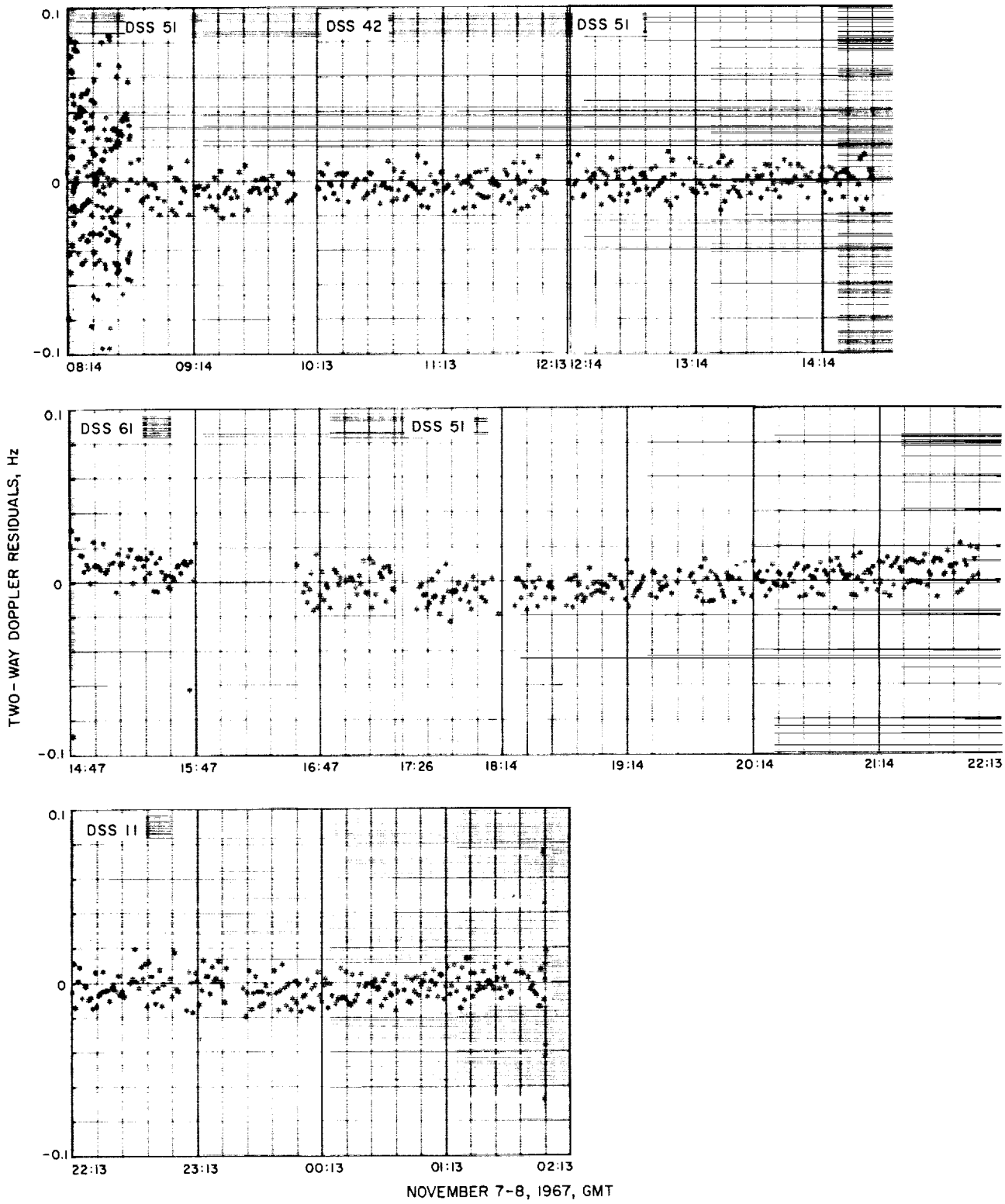

Fig. 44. Premaneuver two-way doppler residuals, *Surveyor VI* (6 × 6 solution, without resolver, new indices of refraction)

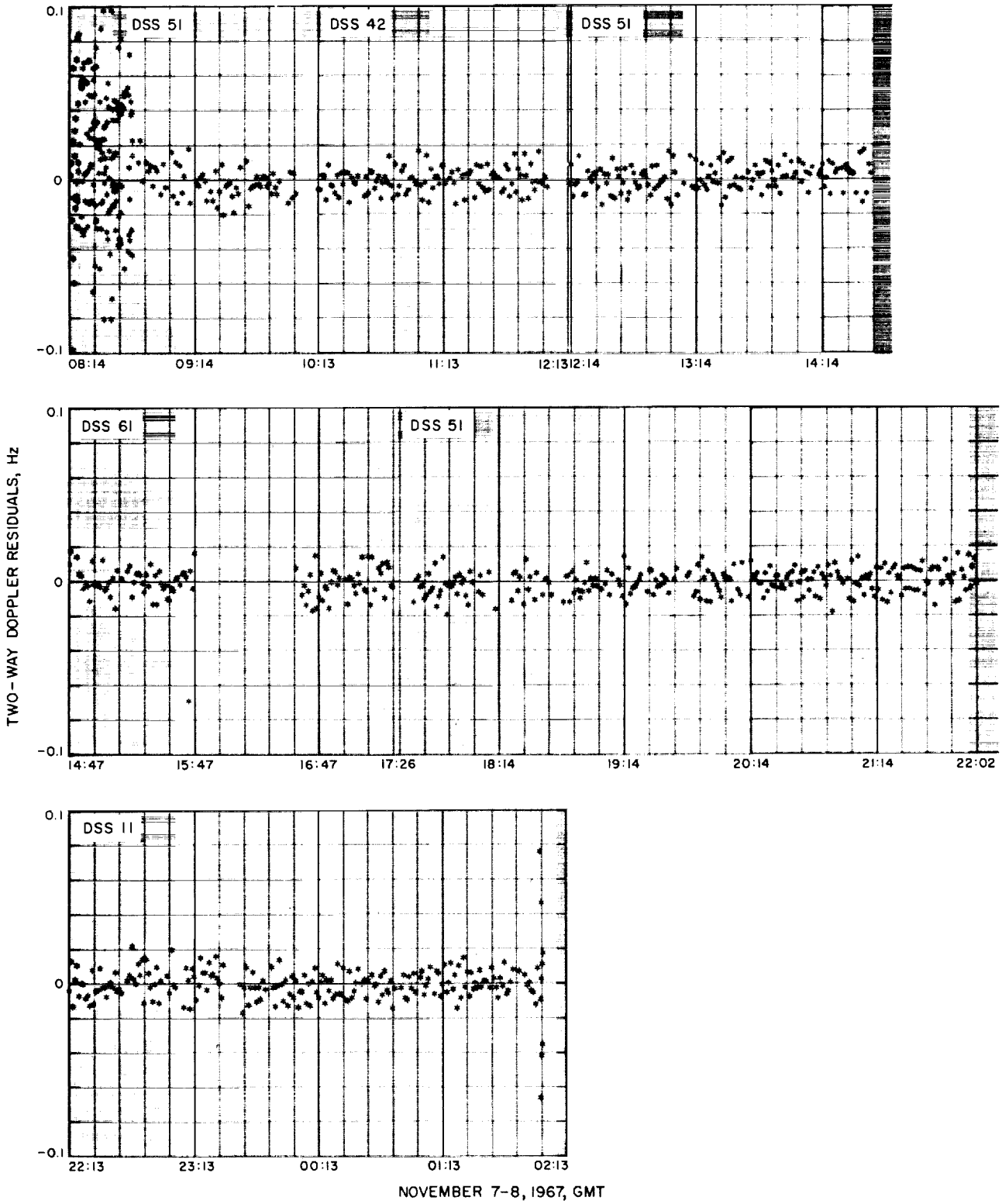

Fig. 45. Premaneuver two-way doppler residuals, *Surveyor VI* (14 × 14 solution, current best estimate, no resolver, new indices)

Table 38. Summary of postflight orbit parameters[a], *Surveyor VI*

Parameter	Pre-midcourse November 7, 1967, 08:03:19.099 GMT		Post-midcourse November 8, 1967, 02:45:00.000 GMT	
Geocentric position and velocity at epoch				
x, km ($\pm 1\sigma$)	−6257.0527	±0.2098	139648.95	±2.39
y, km	1587.2655	±0.3499	−99992.872	±1.788
z, km	1136.6727	±0.2563	−60985.485	±6.114
Dx, km/s	−3.6172085	±0.0004782	1.5841276	±0.0000347
Dy, km/s	−9.1324103	±0.0002703	−0.67764533	±0.00007039
Dz, km/s	−4.8987566	±0.0002388	−0.43832135	±0.00008929
Target statistics				
B, km	1806.98		1710.91	
B • **TT**, km	1752.37		1691.340	
B • **RT**, km	440.91		258.067	
1σ SMAA, km	10.00		2.50	
1σ SMIA, km	4.00		1.00	
THETA, deg	100.04		95.04	
$\sigma_{T\ impact}$, s	1.500		0.500	
PHI_{90}, deg	0.554911		0.128038	
1σ SVFIXR, m/s	0.617339		0.631401	
Latitude, deg	−3.2541		0.3889	
Longitude, deg	0.6507		358.7966	
Impact time, GMT	November 10, 1967, 00:35:43.638		November 10, 1967, 00:58:32.855	

[a]Current best estimate.

Table 39. Summary of data used in postflight (current best estimate) orbit solutions, *Surveyor VI*

Station	Begin data, time		End data, time		Number of points	Standard deviation	Root mean square	Mean error
	Date 1967	GMT	Date 1967	GMT				
Pre-midcourse								
DSS 11	11/7	22:13:32	11/8	02:02:03	211	0.00900	0.00901	−0.000474
DSS 42	11/7	10:13:32	11/7	12:03:32	108	0.00695	0.00697	−0.000515
DSS 51	11/7	08:14:20	11/7	08:44:50	124	0.0273	0.0278	0.00500
DSS 51	11/7	08:47:32	11/7	10:03:32	68	0.00860	0.00877	−0.00172
DSS 51	11/7	12:13:32	11/7	17:33:32	137	0.00739	0.00744	0.000820
DSS 51	11/7	17:34:32	11/7	22:02:32	237	0.00703	0.00706	−0.000641
DSS 61	11/7	14:47:32	11/7	17:23:32	99	0.00796	0.00796	−0.000271
Post-midcourse								
DSS 11	11/8	22:18:32	11/9	05:33:32	414	0.00337	0.00337	−0.0000805
DSS 11	11/9	22:18:32	11/10	00:15:32	98	0.00457	0.00458	0.000345
DSS 42	11/8	03:42:32	11/8	13:23:32	558	0.00160	0.00160	−0.0000298
DSS 42	11/9	05:42:32	11/9	13:23:32	437	0.00177	0.00177	−0.0000282
DSS 51	11/8	13:33:32	11/8	20:38:32	388	0.00711	0.00711	0.000154
DSS 51	11/9	13:33:32	11/9	22:08:32	457	0.00729	0.00729	−0.0000609

All data were two-way doppler.

from mapping the various solutions forward to target were consistently very close to each other. The philosophy used in determining the current best estimate of the pre-midcourse orbit for *Surveyor VI* was to use the solution with the minimum number of parameters estimated that still gives acceptable results. Based on this philosophy, the current best estimate of the pre-midcourse orbit for *Surveyor VI* is a 14×14 solution wherein the six position and velocity vectors of the spacecraft, plus the radius and longitude of the tracking stations, are the estimated parameters. This solution *does not* use the resolver correction. In terms of removing biases, the data fit is better than the similar solution (14×14) utilizing the resolver correction. The uncorrected, unbraked impact point predicted by this solution (latitude $= -3.254$ deg, longitude $= 0.651$ deg) is approximately 120 km southeast of the prelaunch aim point.

The residual plots from the current best estimate pre-midcourse orbit can be seen in Fig. 45. Numerical values from this solution are presented in Table 38 and the number of data points, together with associated statistics are given in Table 39. A graphical comparison between the predicted unbraked impact points (in the B-plane) of this solution and the inflight solutions may be seen in Fig. 46.

B. Postmaneuver Orbit Estimates

Prior to analyzing the *Surveyor VI* postmaneuver tracking data, all known or suspected bad data points were removed. The analysis was made to obtain an orbit solution by processing all postmaneuver tracking data in one block. This method differed from the inflight computations that, to meet the AMR backup requirements, required that the data be processed in two blocks. The lunar radius was changed from the pre-midcourse estimate of 1736.4 km to 1736.0 km for post-midcourse computations. This radius was based on the unbraked impact point predicted by the first post-midcourse orbit solutions. This value was obtained by subtracting 2.4 km from the elevation, the amount indicated by the difference between the elevation based on the ACIC charts and elevations obtained from *Ranger VI, VII,* and *VIII* tracking data (ACIC higher).

A 6×6 orbit solution that used all data from Canopus reacquisition after the maneuver to the last two-way doppler point received (approximately $E - 46$ min) was obtained and mapped forward to target. Examination of residual plots indicated a relatively good fit, considering the fact that there was approximately 40 h of post-

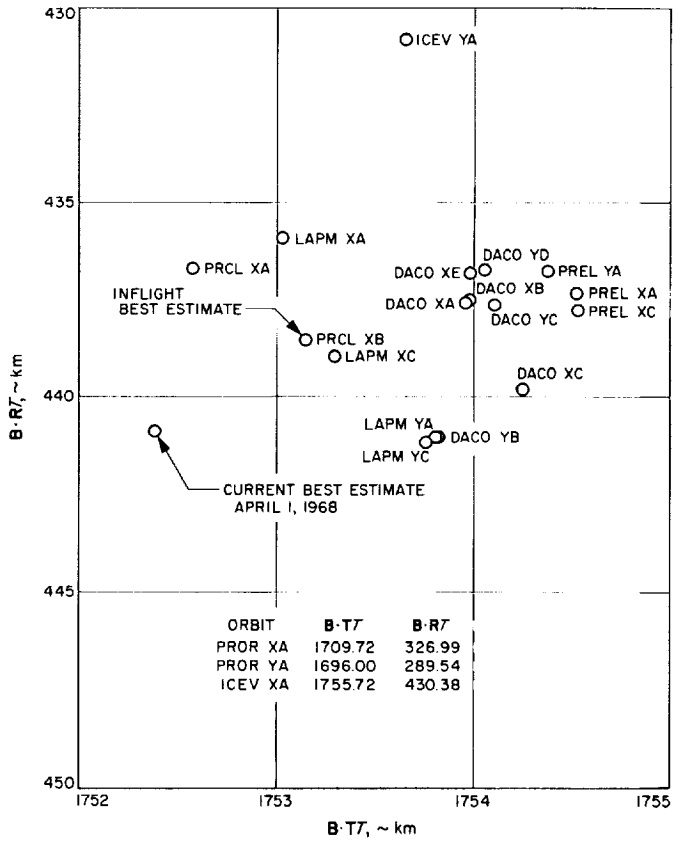

Fig. 46. Estimated pre-midcourse unbraked impact points, *Surveyor VI*

midcourse data. The residual plots for the 6×6 solution may be seen in Fig. 47. In this figure, data during the first hour at DSS 11 seems to be biased with respect to the other data. Also, the figure shows the data from DSS 61 to be excessively noisy. As expected, data from DSS 11 during the final 2 h did not fit well in the 6×6 solution. This fact is evident in the same figure in which, also, some systematic errors are apparent. Since the doppler resolver was incorporated, DSS 11 data exhibits this systematic error for the first hour or two of tracking. Similar problems were observed in the pre-midcourse data (Fig. 41). This problem is unique neither to *Surveyor* nor to DSS 11. Similar systematic errors were observed (Ref. 10) in *Lunar Orbiter* data from DSS 41 when the doppler resolver was incorporated on *Lunar Orbiter V*. Possible causes—such as transmitter oscillator instability, ionospheric and atmospheric effects, and station-peculiar transients—were advanced but not studied. Therefore, the actual cause of these phenomena remains to be solved by future studies.

The 6×6 solution on the post-midcourse data was consistent with the inflight results, but the data residuals indicated the fit was not as good as might be desired. After discussing the apparent problems in the data with tracking data analysts, it was decided that the DSS 61 data was bad because of a faulty rubidium crystal, which was replaced during post-midcourse tracking; subsequent analysis of three-way data indicated that the problem had been corrected. To improve the fit on the data, the estimated parameter list was expanded to 15 to include the station location parameters—geocentric radius, latitude and longitude—for DSS 11, DSS 42 and DSS 51; and the data from DSS 61 was deleted from the solution. The residuals from this solution are shown in Fig. 48. Comparison of this fit with the 6×6 solution shows it to be an improvement; but the final near-moon data from DSS 11 was not fitting well because of the large quantity (approximately 40 h) of data being fit. Numerous solutions were computed to check for data consistency and to solve for physical constants and nongravitational acceleration perturbations; the model used in solving for these perturbations is discussed in Section II-A. To fit the near-moon data well and still obtain a solution consistent with inflight and observed events, it was necessary to estimate the moon gravitational constant, $GM_{\mathfrak{C}}$. When the station location parameters, radius and longitude, $GM_{\mathfrak{C}}$, and acceleration perturbations f_1, f_2, and f_3 were estimated together (a 16×16 solution), a good solution resulted. The predicted unbraked impact time was within 0.233 s of the *observed* time, based on telemetry records. This 16×16 solution is considered to be the current best estimate of the *Surveyor VI* postmaneuver orbit. The maximum change from the nominal station locations observed in the best estimate solution was 11 m in the radius for DSS 51. The $GM_{\mathfrak{C}}$ estimate changed from a nominal of 4902.6309 to 4902.7283 km^3/s^2. The acceleration perturbations estimated are as follows:

$$f_1 = 0.197 \times 10^{-9}\ km/s^2$$

$$f_2 = 0.663 \times 10^{-10}\ km/s^2$$

$$f_3 = -0.494 \times 10^{-10}\ km/s^2$$

$$\Delta\ddot{\mathbf{r}} = 0.213 \times 10^{-9}\ km/s^2$$

These results indicate that some perturbations did exist in the postmaneuver trajectory and that their effect can be accounted for by solving for nongravitational acceleration perturbations. The cause of these perturbations has not been determined. However, solar radiation pressure, uncancelled velocity increments from normal operations of the attitude control system, possible gas and/or propellant leaks could be some of the causes for the perturbations. Although these perturbations were not accounted for in flight, orbit determination requirements were met. Residual plots from the 16×16 best estimate solution are shown in Fig. 49. Numerical values from the solution are presented in Table 38. The amount of data used in this solution, together with the associated data statistics, is shown in Table 39. Based on this current best estimate solution, the *Surveyor VI* spacecraft is estimated to be at 0.419 °N lat and 358.624 °E lon. This location is 0.002 deg ($\approx$0.1 km) north and 0.230 deg ($\approx$7 km) west of the final soft-landing aim point.

A graphical presentation comparing the current best estimate impact point with inflight solutions in the B-plane is presented in Fig. 40 (page 73).

C. Evaluation of Midcourse Maneuver Based on DSIF Tracking Data

The *Surveyor VI* midcourse maneuver can be evaluated by examining the velocity change at the midcourse epoch and by comparing the maneuver aim point with the target parameters from the best estimate post-midcourse orbit solution.

The *observed* velocity changes resulting from midcourse thrust (applied by igniting the vernier engines) are determined by differencing the velocity components of best estimate orbit solutions based on postmaneuver data, only, and on premaneuver data only. These solutions are independent, i.e., *a priori* information from premaneuver data is not used during the processing of postmaneuver data. The estimated maneuver execution errors at mid-

Table 40. *Surveyor VI* midcourse maneuver evaluated at midcourse epoch

Velocity[a] component	Current best estimate of premaneuver velocity, m/s (mapped to MC epoch[b])	Inflight[c] estimate of premaneuver velocity, m/s (mapped to MC epoch)	Current best estimate of postmaneuver velocity, m/s	Observed velocity change due to maneuver (best post minus best pre), m/s	Commanded[c] maneuver velocity change, m/s	Total maneuver errors	
						Execution errors[d] (observed change minus commanded change), m/s	OD errors (best pre minus inflight), m/s
Dx	1585.180	1585.178	1584.128	−1.050	−1.088	+0.038	−0.002
Dy	−685.927	−685.935	−677.645	+8.290	+8.235	+0.055	−0.008
Dz	−444.046	−444.040	−438.321	+5.719	+5.681	+0.038	+0.006

[a]All velocity components are given in geocentric space-fixed cartesian coordinates.

[b]Midcourse epoch is end of reorientation after midcourse maneuver on November 8, 1967, 02:45:00 GMT.

[c]Based on inflight premaneuver orbit solution (LAPM XC) used for final midcourse maneuver computations.

[d]Based on difference of best pre-midcourse and post-midcourse orbit estimates. The 1σ uncertainties associated with these determinations of midcourse velocity errors are of the same order as the errors, themselves. However, these determinations have particular merit because of their independence of the spacecraft system.

course epoch are determined by differencing the observed velocity changes and the commanded maneuver velocity increments. The remaining major contribution to the total maneuver error is made by the orbit determination process. This error source includes ODP computational and model errors, and errors in tracking data. These errors may be obtained by differencing the velocity components, at midcourse epoch, of the best estimate premaneuver orbit and the inflight orbit solution used for the maneuver computations. Numerical results of this part of the evaluation are presented in Table 40. In the table, it can be seen that the execution errors in *Dx, Dy* and *Dz* were only 0.038, 0.055, and 0.038 m/s, respectively. The OD errors are also very small. Total maneuver errors for *Surveyor VI* were well within specifications.

Table 41. Impact points, *Surveyor VI*

a. Unbraked impact points

Source	Latitude, deg	Longitude, deg
Best estimate of pre-midcourse	−3.254	0.651
Inflight orbit (LAPM XC)	−3.216	0.617
Best estimate of post-midcourse	0.389	358.797
Maneuver unbraked aim point	0.387	359.027

b. Estimated midcourse errors mapped to unbraked impact point

Source	Δ Latitude		Δ Longitude	
	deg	km	deg	km
OD errors[a]	−0.038	−1.140	+0.034	+1.020
Maneuver error[b]	+0.040	+1.200	−0.264	−7.920
Overall errors[c]	+0.002	+0.060	−0.230	−6.900

[a]OD errors = current best premaneuver estimate *minus* orbit used for maneuver computations (LAPM XC).

[b]Maneuver errors = overall errors *minus* OD errors.

[c]Overall errors = current best postmaneuver estimate *minus* aiming point.

A more meaningful evaluation can be made by examining certain critical target parameters. Since the primary objective of the midcourse maneuver is to achieve lunar encounter at a selected landing site, the maneuver unbraked aim point is used as the basic reference for this evaluation. The unbraked aim point for *Surveyor VI* was 0.387-deg latitude and 359.027-deg longitude. Based on the predicted unbraked impact point from the best estimate inflight orbit solution (LAPM XC), trajectory corrections were computed to achieve landing at the desired site. To evaluate the total maneuver error at the target the maneuver aim point is compared with the predicted, unbraked impact point from the current best estimate postmaneuver orbit solution. Orbit determination errors can be obtained by differencing the unbraked target parameters of the current best estimate premaneuver orbit solution and the inflight orbit solution used for maneuver computations. Execution errors, consisting of both attitude maneuver errors and engine system errors, are then determined by differencing the total and OD errors. Numerical results of these computations are presented in Table 41. In the table, it can be seen that encounter was achieved within +0.002-deg latitude and −0.230-deg longitude of the desired aiming point. These differences in latitude and longitude are roughly equivalent to +0.06 km and −6.90 km, respectively, on the lunar surface; OD position errors are well within the expected accuracy. In general, the accuracy of the *Surveyor VI* midcourse maneuver was well within *Surveyor* Project specifications. It should be noted that these results cannot be used for an accurate evaluation of the *Centaur* injection accuracy, because the inflight aim point was not the same as the prelaunch aim point.

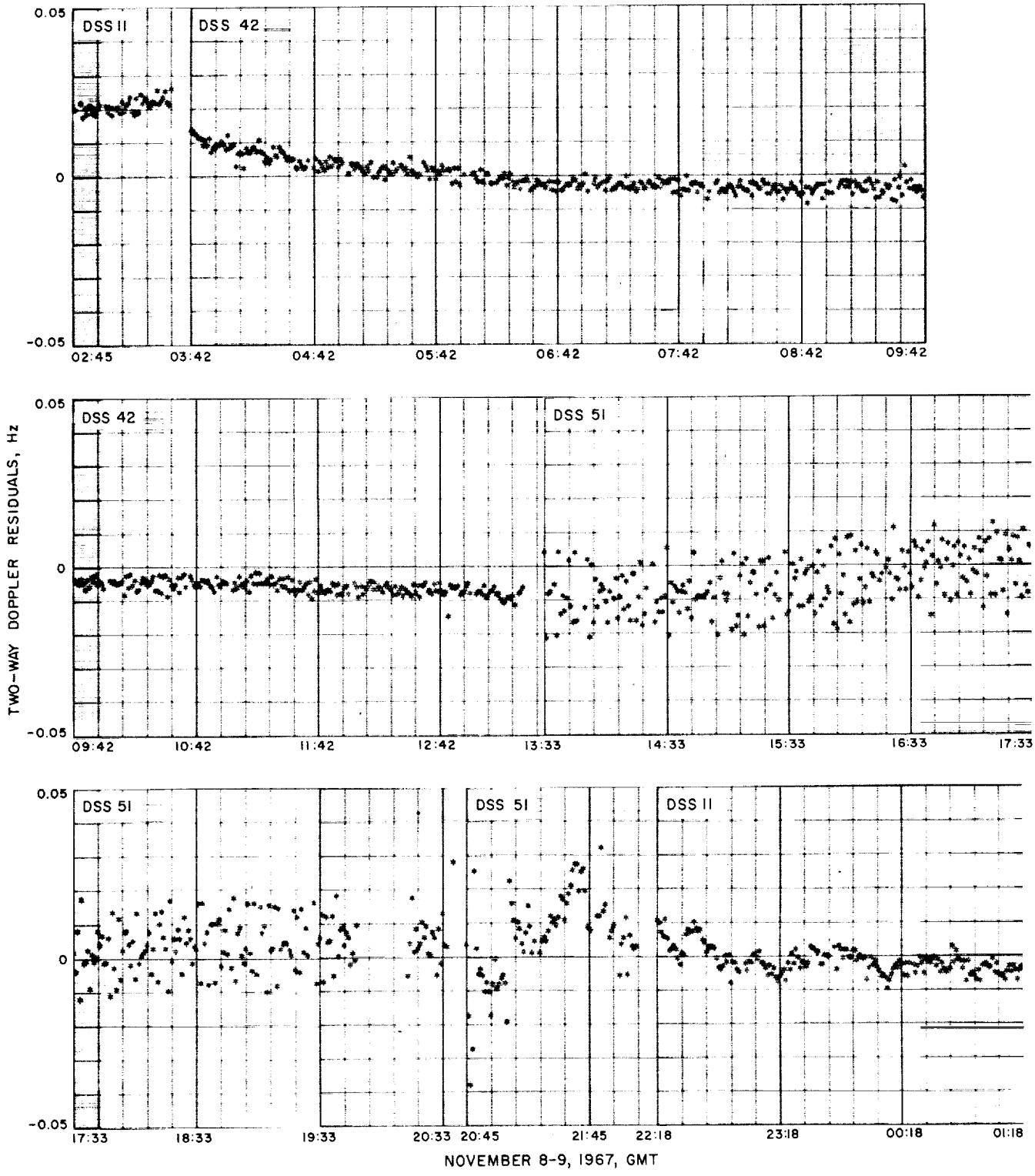

Fig. 47. Postmaneuver two-way doppler residuals, *Surveyor VI*
(6 × 6 solution, trajectory *not* corrected for perturbations)

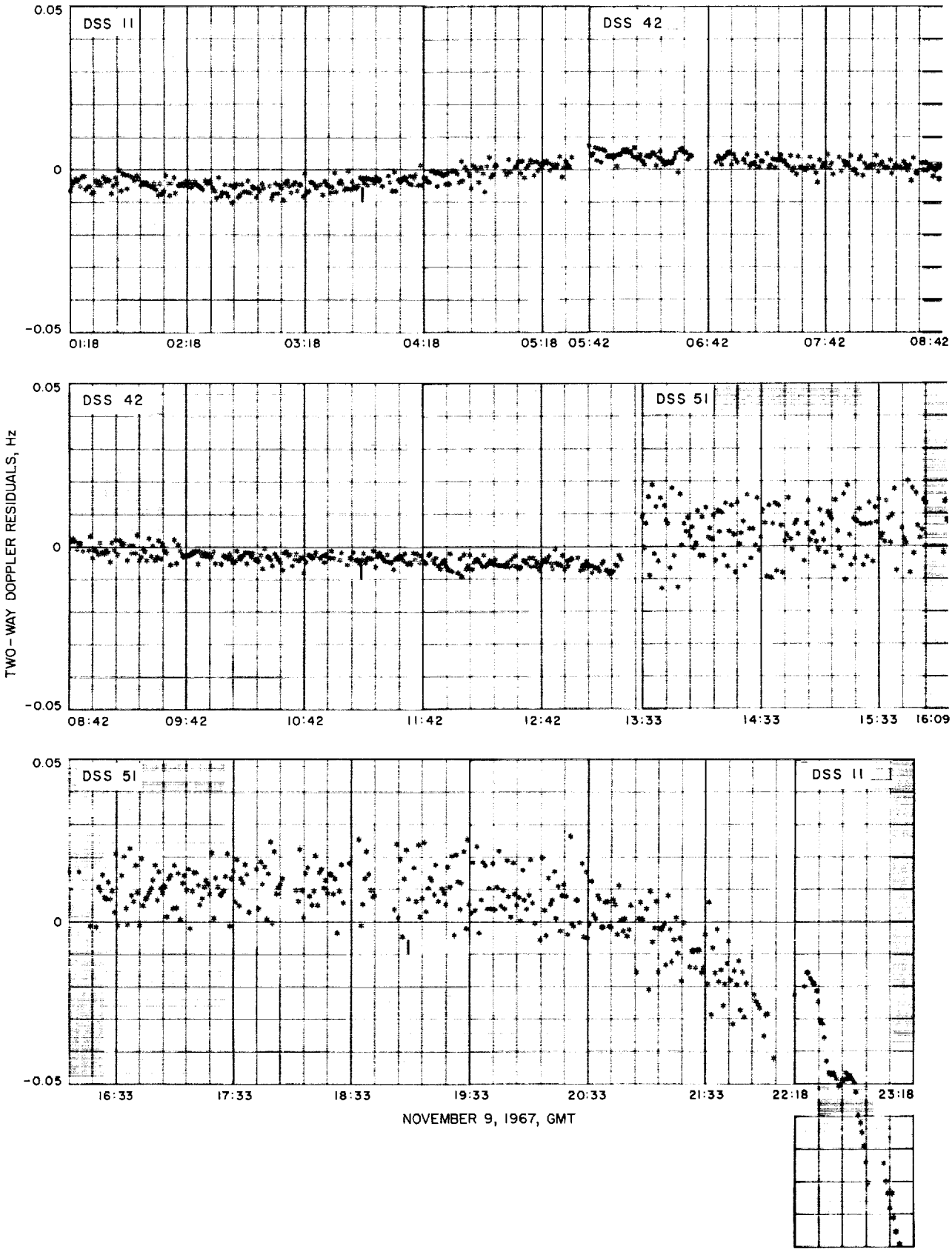
0.05
0
-0.05
DSS 11
DSS 42
01:18
02:18
03:18
04:18
05:18
05:42
06:42
07:42
08:42
DSS 42
DSS 51
08:42
09:42
10:42
11:42
12:42
13:33
14:33
15:33
16:09
DSS 51
DSS 11
16:33
17:33
18:33
19:33
20:33
21:33
22:18
23:18
TWO-WAY DOPPLER RESIDUALS, Hz
NOVEMBER 9, 1967, GMT

Fig. 47 (contd)

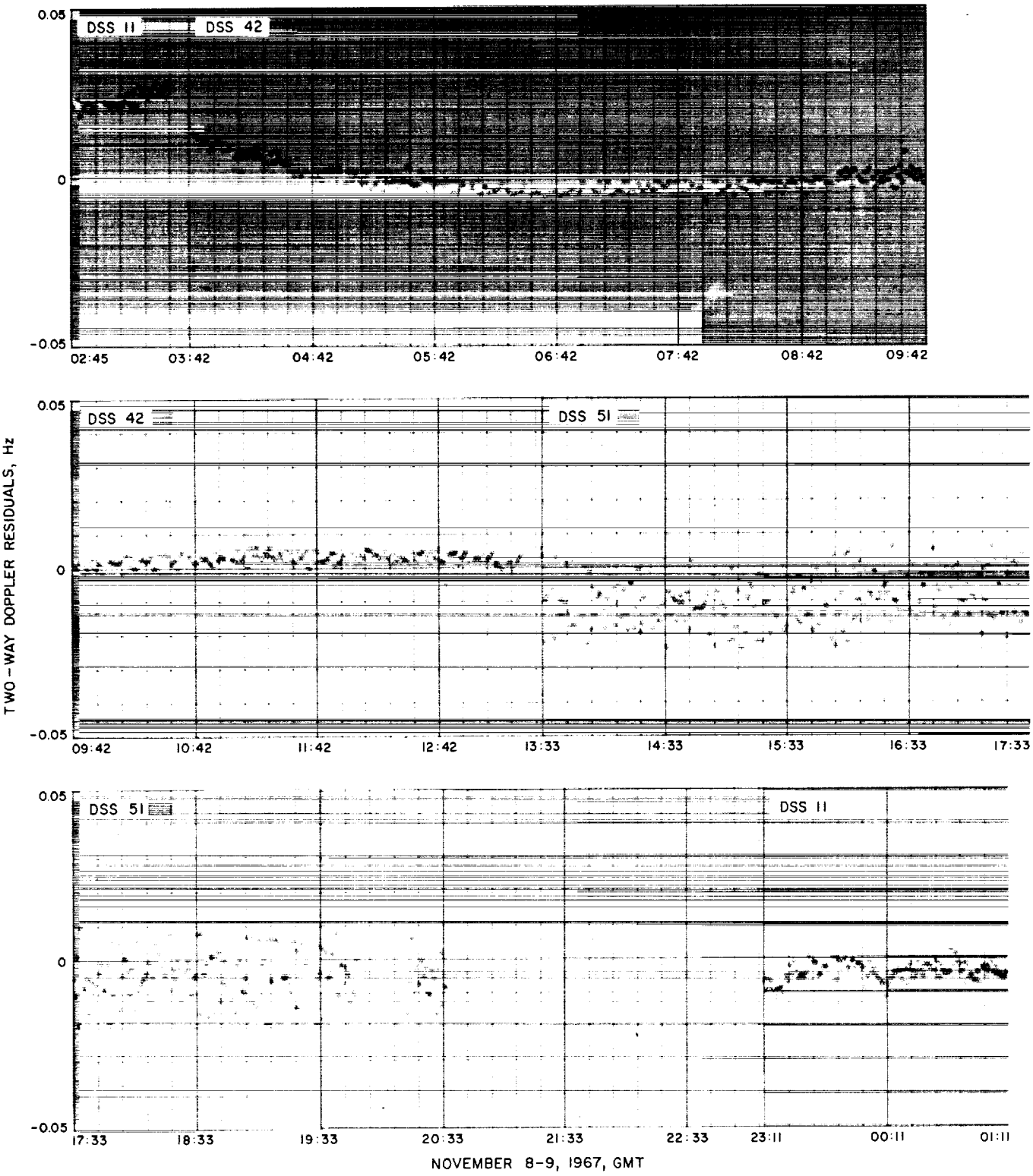

Fig. 48. Post-midcourse two-way doppler residuals, *Surveyor VI* (15 × 15 solution, trajectory not corrected for perturbations)

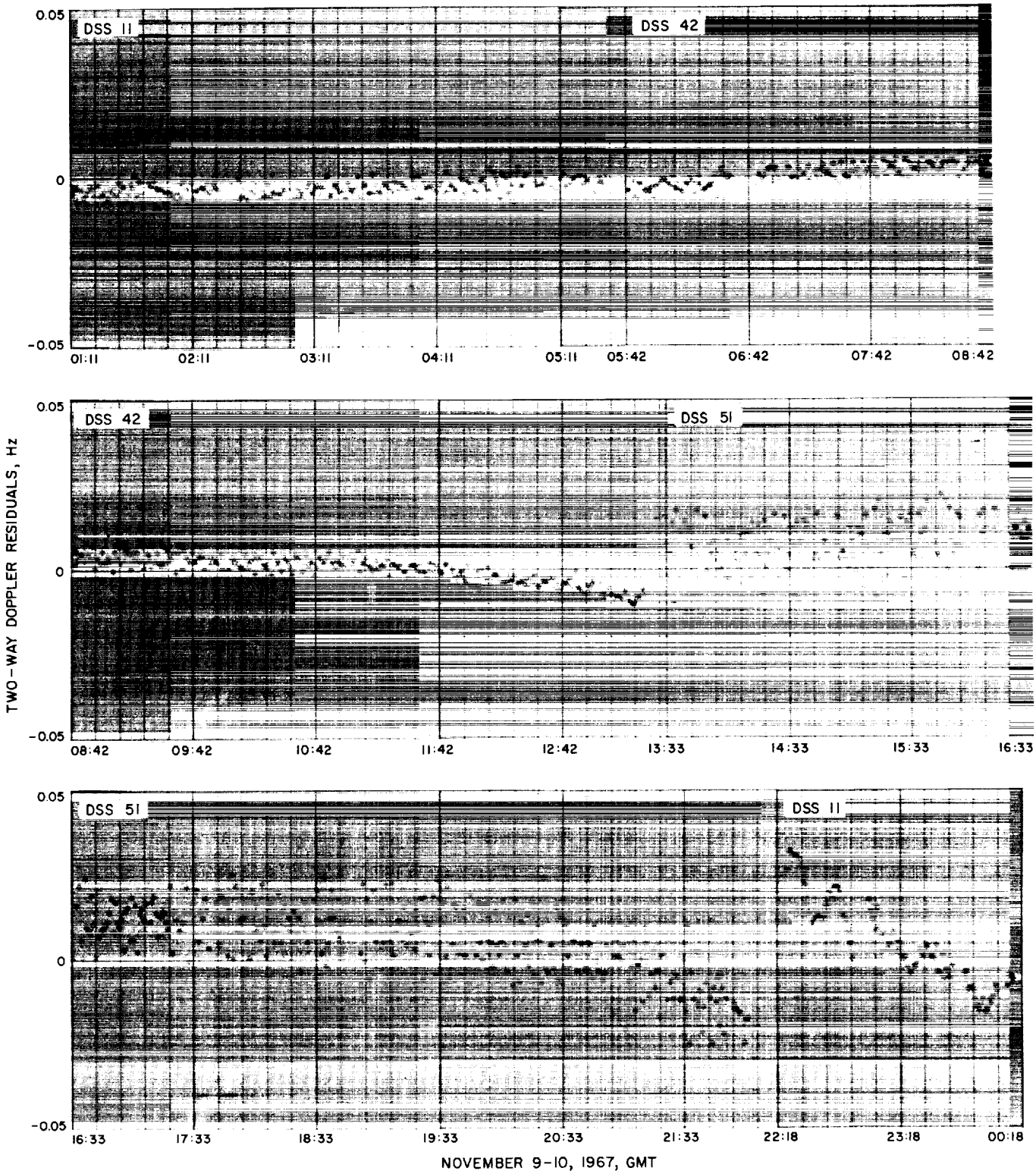
0.05
0
-0.05
DSS 11
DSS 42
01:11
02:11
03:11
04:11
05:11
05:42
06:42
07:42
08:42
DSS 42
DSS 51
08:42
09:42
10:42
11:42
12:42
13:33
14:33
15:33
16:33
DSS 51
DSS 11
16:33
17:33
18:33
19:33
20:33
21:33
22:18
23:18
00:18
TWO-WAY DOPPLER RESIDUALS, Hz
NOVEMBER 9-10, 1967, GMT

Fig. 48 (contd)

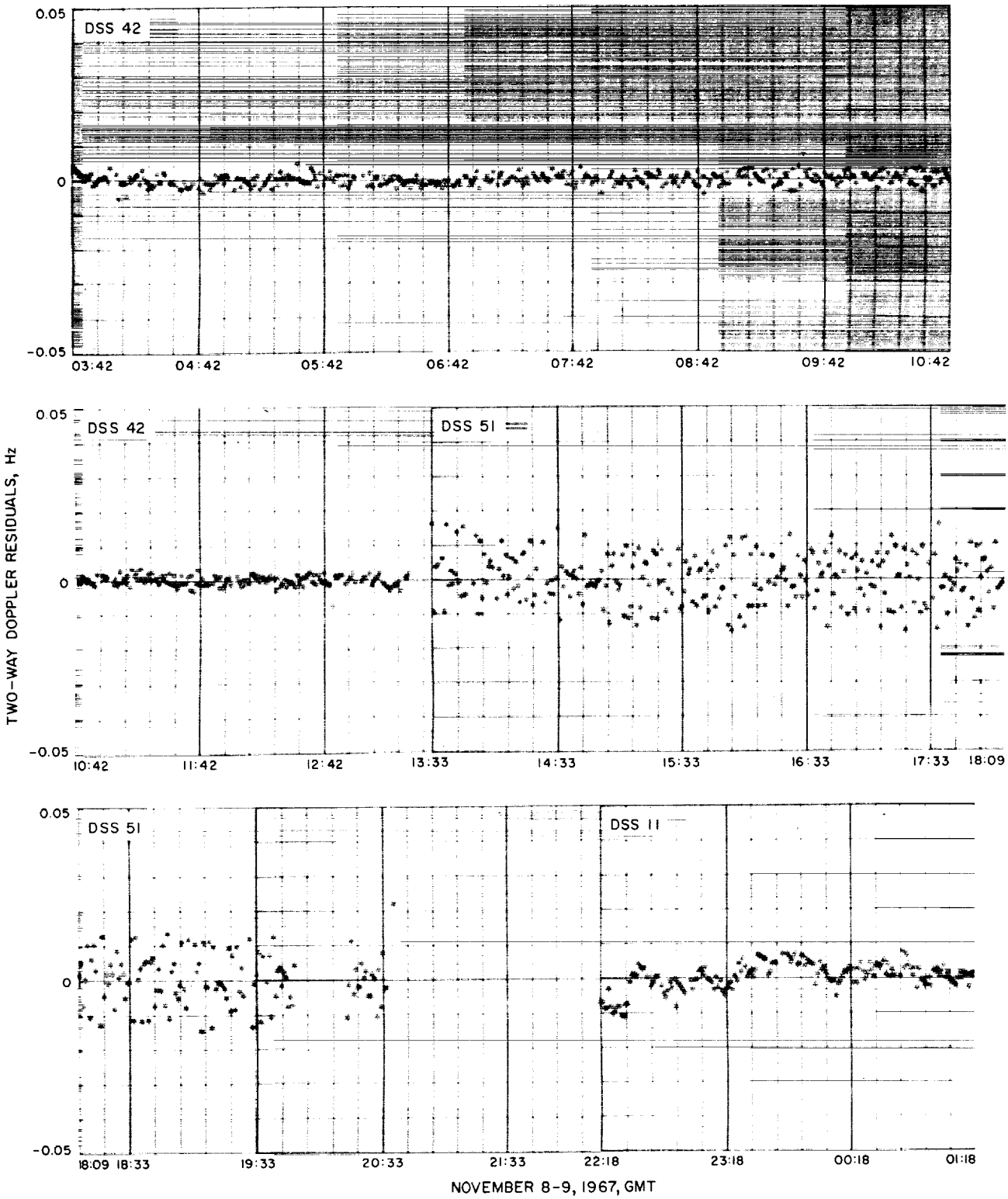

Fig. 49. Post-midcourse two-way doppler residuals, *Surveyor VI* (16 × 16 solution, trajectory corrected for perturbations)

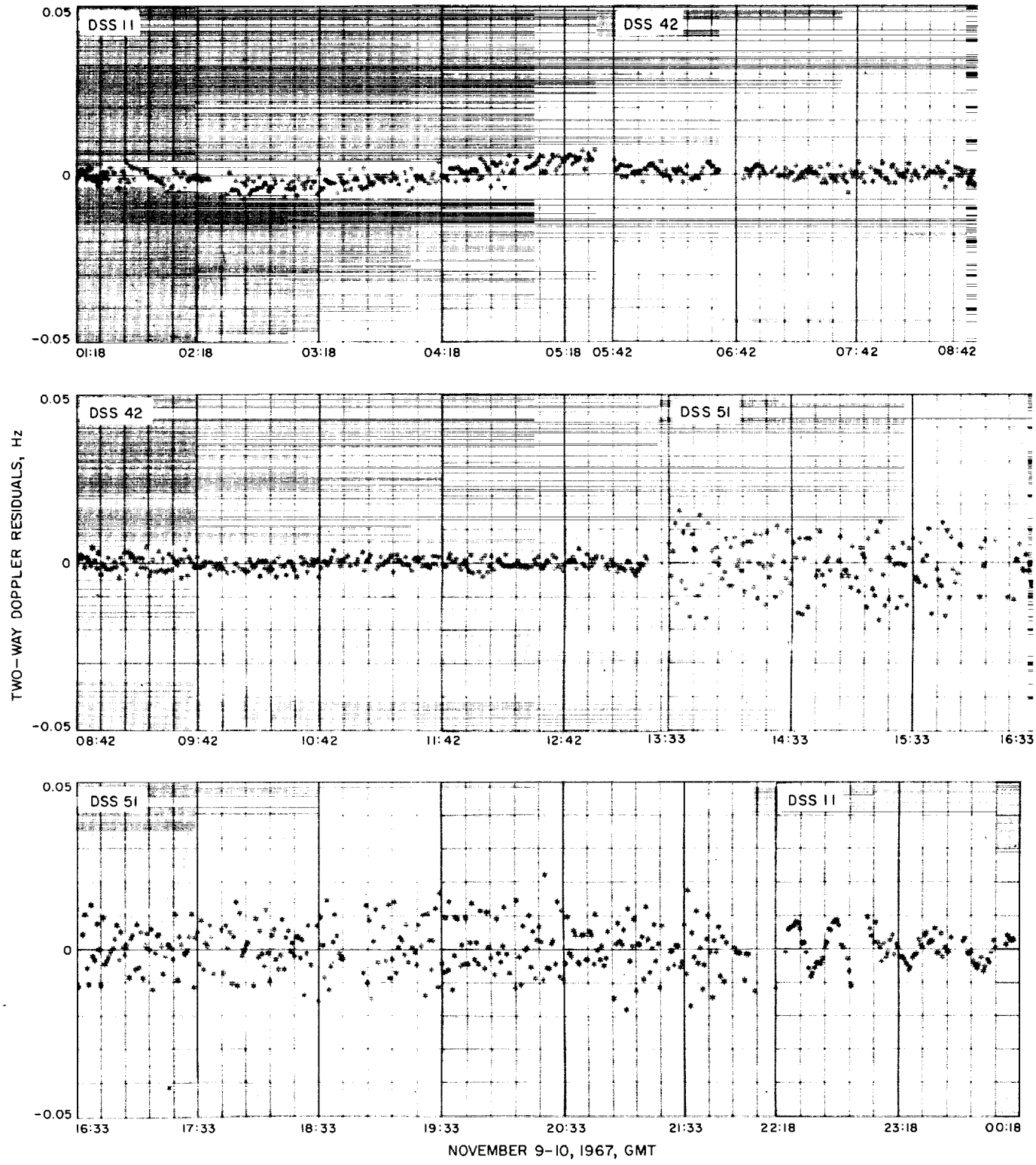
DSS 11
DSS 42
DSS 42
DSS 51
DSS 51
DSS 11
0.05
0
-0.05
TWO-WAY DOPPLER RESIDUALS, Hz
01:18
02:18
03:18
04:18
05:18
05:42
06:42
07:42
08:42
09:42
10:42
11:42
12:42
13:33
14:33
15:33
16:33
17:33
18:33
19:33
20:33
21:33
22:18
23:18
00:18
NOVEMBER 9-10, 1967, GMT

Fig. 49 (contd)

Table 42. Station locations and statistics, *Surveyor VI* (referenced to 1903.0 pole)

Station	Data source	Distance off spin axis r_s, km	1σ r_s, standard deviation, m	Geocentric longitude, deg	1σ longitude standard deviation, m	Geocentric radius, deg	Geocentric latitude,[b] deg
DSS 11	*Mariner II*	5206.3357	3.9	243.15058	8.8	6372.0044	35.208035
	Mariner IV, cruise	404	10.0	67	20.0	2.0188	08144
	Mariner IV, post-encounter	378	37.0	72	40.0	2.0161	08151
	Pioneer VI, Dec. 1965–June 1966	359	9.6	92	10.3	2.0286	08030
	Goddard Land Survey, Aug. 1966	718	29.0	94	35.0	2.0640	08230
	Surveyor I, post-touchdown	276	2.9	85	23.8	2.6446	16317
	Surveyor I, inflight, post-midcourse, only	200	50.8	98	59.4	1.9975	08192
	Surveyor III, inflight	408	29.7	00	49.0	2.0230	08192
	Surveyor IV, inflight	326	41.1	97	49.0	2.0129	08192
	Surveyor V, inflight	256	47.0	92	39.0	2.0043	08192
	Surveyor VI, inflight	337	30.3	91	43.0	2.0141	08192
DSS 42	*Mariner IV*, cruise	5205.3478	10.0	148.98136	20.0	6371.6882	−35.219410
	Mariner IV, post-encounter	.3480	28.0	134	29.0	.6824	19333
	Pioneer VI, Dec. 1965–June 1966	.3384	5.0	151	8.1	.6932	19620
	Goddard Land Survey, Aug. 1966	.2740	52.0	000	61.0	.7030	20750
	Surveyor I, post-touchdown	.3474	3.5	130	22.1	.6651	19123
	Surveyor I, inflight, post-midcourse, only	.3465	32.7	166	41.1	.6834	19372
	Surveyor III, inflight	.3522	26.5	146	45.0	.6905	19372
	Surveyor IV, inflight	.3487	34.8	161	49.0	.6861	19372
	Surveyor V, inflight, post-midcourse, only	.3448	33.9	156	35.0	.6814	19372
	Surveyor VI, inflight	.3501	24.6	153	45.0	.6879	19372
DSS 51	Combined *Rangers*, LE-3[a]	5742.9315	8.5	27.68572	22.2	6375.5072	−25.739169
	Ranger VI, LE-3	203	19.7	72	69.3	.4972	9215
	Ranger VII, LE-3	211	25.5	83	61.3	.4950	9157
	Ranger VIII, LE-3	372	22.3	48	85.0	.5130	9159
	Ranger IX, LE-3	626	56.6	80	49.5	.5322	8993
	Mariner IV, cruise	363	10.0	40	20.0	.5120	9148
	Mariner IV, post-encounter	365	40.0	57	38.0	.5143	9198
	Pioneer VI, Dec. 1965–June 1966	332	11.6	69	12.0	.5094	9176
	Goddard Land Survey, Aug. 1966	706	39.0	86	43.0	.5410	8990
	Surveyor I, inflight	380	38.3	78	41.0	.5144	9169
	Surveyor III, inflight	312	35.0	74	46.2	.5069	9169
	Surveyor IV, inflight	337	39.3	75	46.8	.5096	9169
	Surveyor V, inflight	355	44.1	74	31.5	.5116	9169
	Surveyor VI, inflight	413	25.6	70	43.0	.5180	9169
DSS 61	*Lunar Orbiter II*, doppler	4862.6067	9.6	355.75115	44.4	6369.9932	40.238566
	Lunar Orbiter II, doppler and ranging	.6118	3.4	138	4.0	69.9999	8566
	Mariner IV, post-encounter	.6063	14.0	099	24.0	70.0009	8655
	Pioneer VI, Dec. 65–June 66	.6059	8.8	103	10.4	70.0060	8715
	Surveyor III, inflight	.6054	24.5	126	47.0	70.0046	8701
	Surveyor V, inflight, pre-midcourse, only	.5962	72.2	125	75.0	69.9921	8701

[a]Lunar ephemeris 3 (DE-15); all *Surveyor* inflight solutions used LE-4 (DE-19).

[b]Latitude was not estimated for *Surveyor* inflight solutions.

D. Estimated Tracking Station Locations and Physical Constants

1. Computations. The best estimates of $GM_\oplus$, $GM_\mathbb{C}$ and station location parameters for the *Surveyor VI* mission were determined by computations which estimate the following parameters: the spacecraft position and velocity at an epoch; $GM_\oplus$; $GM_\mathbb{C}$; spacecraft acceleration perturbations f_1, f_2 and f_3; the solar radiation constant G; and two components (geocentric radius and longitude) of station locations for each of four Deep Space Stations—DSS 11, DSS 42, DSS 51, and DSS 61. These solutions were computed using only the two-way doppler data from DSS 11, DSS 42, and DSS 51 for both the pre-midcourse and post-midcourse phases. Data from DSS 61 were available from pre-midcourse only. To obtain the best estimate of the solved-for parameters, the pre-midcourse data block was combined with the post-midcourse data block. The procedure of combining the two data blocks is to fit only the pre-midcourse data, accumulate the normal equations at the injection epoch, and map the converged estimate to the midcourse epoch with a linear mapping of the inverted normal equation matrix (i.e., covariance matrix). The estimate is then incremented with the best estimate of the maneuver, and the mapped covariance matrix is corrupted in the velocity increment and used as *a priori* for the post-midcourse data fit. The ephemerides used in the reduction was one of the latest JPL ephemerides (DE-19) with the updated mass ratios and Eckert's corrections.

2. Results. The results of these computations are presented in Table 42 in an unnatural station coordinate system (geocentric radius, latitude, and longitude) and in a natural coordinate system (r_s, λ, Z) where r_s is the distance off the spin axis (in the station meridian), λ is the longitude and Z is along the earth spin axis. (See Fig. 21, page 43.)

The numerical results presented in Table 42 indicate that the solution for r_s and longitude of DSS 42 are several meters higher and lower, respectively, than most of the previous *Surveyor* solutions. The value for r_s is only 2 m higher than the solution for *Surveyor IV* and is only 5.3 m larger than the smallest solution (for *Surveyor V*); therefore, it is not considered to be outside a reasonable deviation from the other solutions. Although the value of DSS 42 longitude is 3 m less than the *Surveyor V* solution, it is still within the range of previous solutions listed. The DSS 51 and DSS 61 solutions for r_s are a few meters higher and lower, respectively, than most of the previous solutions listed. However, all of the *Surveyor VI* station location solutions are reasonably close to previous solutions, with the possible exception of DSS 61 r_s. However, this number was based on a small amount of pre-midcourse data, only, and can not be compared to the other solutions.

Table 43. Physical constants and statistics, *Surveyor VI*

Data source	$GM_\oplus$, km³/s²	1σ standard deviation, km³/s²	$GM_\mathbb{C}$, km³/s²	1σ standard deviation, km³/s²
Lunar Orbiter II (doppler)	398600.88	2.14	4902.6605	0.29
Lunar Orbiter II (doppler and ranging)	398600.37	0.68	4902.7562	0.13
Combined *Rangers*	398601.22	0.37	4902.6309	0.074
Ranger VI	398600.69	1.13	4902.6576	0.185
Ranger VII	398601.34	1.55	4902.5371	0.167
Ranger VII	398601.14	0.72	4902.6304	0.119
Ranger IX	398601.42	0.60	4902.7073	0.299
Surveyor I	398601.27	0.78	4902.6492	0.237
Surveyor III	398601.11	0.84	4902.6420	0.246
Surveyor IV	398601.19	0.99	4902.6297	0.247
Surveyor V	398601.10	0.60	4902.6298	0.236
Surveyor VI	398601.11	0.54	4902.6425	0.235

The solved-for $GM_\oplus$ and $GM_\mathbb{C}$ for *Surveyor VI* are given in Table 43, along with previous solutions. The value for $GM_\oplus$ is very consistent with all previous solutions and is within 1σ of all previous solutions listed. It is only 0.01 larger than the *Surveyor V* solution listed directly above it. The value for $GM_\mathbb{C}$ is very consistent with previous solutions, being slightly higher than solutions for *Surveyors III*, *IV*, and *V* and slightly lower than for *Surveyor I*. It is also within 1σ of all the other solutions listed.

3. Conclusion. Although station location solutions differed slightly from previous *Surveyor* solutions, they are well within 1σ of the previous solutions and there is no reason to suspect that they are not good; they should be considered in arriving at a best estimate of station locations based on all *Surveyor* data. As with the other *Surveyor* solutions listed in Table 42 and 43, these solutions used the most current estimate[13] of indices of refraction for the Deep Space Stations. The correlation matrix on postmaneuver data with premaneuver data as *a priori* is given in Table 44.

The solution for $GM_\oplus$ and $GM_\mathbb{C}$ are very near the previous *Surveyor* solutions, thus adding to their confidence as *good* solutions.

[13]Indices of refraction obtained from A. S. Liu, Navigational Accuracy Group, JPL: DSS 11 = 240, DSS 42 = 310, DSS 51 = 240, DSS 61 = 300.

Table 44. Correlation matrix of estimated parameters, *Surveyor VI* (postmaneuver data with premaneuver data as *a priori*)

Standard deviation		x	y	z	Dx	Dy	Dz	$GM_\oplus$	G	GM_ζ	f_1	f_2	f_3	R_{11}	Lon_{11}	R_{42}	Lon_{42}	R_{51}	Lon_{51}
x	0.80	1.000	0.589	0.097	−0.168	0.136	−0.174	−0.138	0.001	0.299	−0.153	−0.146	0.089	−0.038	0.550	−0.018	0.530	−0.100	0.569
y	1.57		1.000	−0.743	−0.141	0.281	−0.341	−0.135	0.000	−0.031	−0.177	0.107	−0.176	0.587	0.774	0.635	0.823	0.646	0.862
z	2.33			1.000	0.040	−0.195	0.239	0.056	0.001	0.289	0.072	−0.291	0.324	−0.753	−0.457	−0.776	−0.539	−0.863	−0.558
Dx	0.014				1.000	0.436	0.295	0.062	0.000	0.711	−0.893	−0.005	−0.152	−0.080	−0.122	−0.243	0.017	−0.087	−0.033
Dy	0.032					1.000	−0.723	0.082	0.001	0.286	−.0708	−0.678	0.538	0.372	0.517	0.394	0.527	0.333	0.517
Dz	0.048						1.000	−0.050	−0.001	0.272	0.038	0.727	−0.711	−0.465	−0.567	−0.612	−0.460	−0.421	−0.492
$GM_\oplus$	0.54							1.000	0.005	−0.071	−0.053	−0.128	0.089	−0.119	0.074	−0.023	0.005	0.153	−0.002
G	0.10								1.000	0.000	−0.008	0.000	0.000	0.001	0.000	0.000	0.000	0.000	0.000
GM_ζ	0.24									1.000	−0.676	−0.055	−0.044	−0.216	0.077	−0.365	0.132	−0.374	0.089
f_1	0.26×10^{-9}										1.000	0.228	−0.030	−0.076	−0.266	0.028	−0.394	−0.086	−0.355
f_2	0.26×10^{-9}											1.000	−0.976	0.080	−0.290	−0.063	−0.131	0.114	−0.150
f_3	0.50×10^{-9}												1.000	−0.110	0.209	0.051	0.014	−0.164	0.043
R_{11}	0.037													1.000	0.469	0.737	0.485	0.705	0.489
Lon_{11}	0.00043														1.000	0.560	0.911	0.518	0.928
R_{42}	0.030															1.000	0.554	0.793	0.591
Lon_{42}	0.00045																1.000	0.570	0.961
R_{51}	0.028																	1.000	0.582
Lon_{51}	0.00043																		1.000

XI. Observations and Conclusions From *Surveyor VI*

A. Tracking Data Evaluation

In general, DSIF station operations during the *Surveyor VI* mission were effectively implemented. From the time of first two-way acquisition of the spacecraft over DSS 51 until shortly before retroignition, the spacecraft was almost continuously in two-way lock, and station transfers were rapid and effectively executed. The only major losses of good two-way doppler data occurred during the second passes over DSS 51 and DSS 61. Johannesburg lost ground communications at 19:38:02 GMT on November 8, and at 20:45:02, an unscheduled transfer of the spacecraft was made to DSS 61, which stayed in two-way lock until the spacecraft was transferred to DSS 11 at 22:19:02. The two-way doppler data taken at DSS 61 during this time (approximately 1½ h) was unusable because of excessively high noise; the problem was traced to the rubidium crystal; and when a rubidium crystal change was made during the third pass, an immediate improvement to reasonable levels was observed in the three-way data at DSS 61. The only other appreciable loss of two-way data occurred during Canopus acquisition over this station when an unexpected loss of two-way lock occurred and reacquisition of two-way was not attempted until completion of Canopus acquisition, approximately 50 min later.

1. Pre-midcourse angular tracking. In general, doppler data yields far greater accuracy in the determination of a spacecraft orbit than does angular data and is, therefore, used almost exclusively in the orbit determination process during most of the mission. The one exception is for the launch phase, when little doppler data are available and a quick determination of the orbit necessitates the use of both doppler and angle data. During the *Surveyor VI* mission, angle data from DSS 51 and DSS 42 were used in the orbit determination program during the first passes of these two stations. To improve the quality of the angular data to be used in the ODP, it is first corrected for antenna optical pointing error as discussed in Section II-B.

Experience gained in past missions has shown that the correction coefficients do not remove all systematic pointing errors. Since DSS 51 was the initial acquisition station, the angular data taken by it was the most important angular data for use in the early orbits. These data, when fit through the final postflight orbit, show a bias of +0.040 deg HA and −0.025 deg dec. These values are slightly higher than DSS 51 first-pass angle biases averaged over previous *Surveyor* missions (+0.030 deg HA and −0.020 deg dec) but can still be regarded as being reasonably consistent with past DSS 51 experience in tracking *Surveyor*. The DSS 42 first-pass angular data were also used in various inflight orbit iterations. When passed through the final postflight orbit, these data show biases of −0.020 deg HA and −0.035 deg dec. These biases agree reasonably with past DSS 42 experience in tracking *Surveyor*. It is indicated that the angle correction coefficients for DSS 42 are more effective in hour angle than in declination; for instance, the averaged DSS 42 biases for *Surveyor III* and *V* missions are −0.005 deg HA and −0.045 deg dec.

2. Pre-midcourse phase doppler tracking. The *Surveyor VI* doppler data is noteworthy since it was this mission that marked the first wide-scale use of the doppler resolver at the Deep Space Stations and the corresponding use of the data produced in the orbit determination process during an actual flight. In measuring doppler frequencies, the tracking data handling (TDH) system counts the number of signal *zero* crossings during a given time interval; this differs from the actual doppler frequency by fractions of a cycle which are alternately lost from one time interval and erroneously added to the next. This error, commonly referred to as truncation error, depends on the data sample rate—clearly, the longer the sample interval, the smaller the relative error. For 60-s count data, such a truncation error produces a standard deviation of approximately 0.008 Hz in two-way doppler data. The doppler resolver effectively measures the fraction of a cycle from the start of a time interval to the first *zero* crossing, and correctly adds it to, or subtracts it from, the basic frequency measurement. The net result of the use of the doppler resolver for good two-way data is a reduction, by approximately a factor of four, of the standard deviation which is about 0.002 Hz for 60-s count data. During *Surveyor VI*, three tracking stations—DSS 11, DSS 42, and DSS 61—had doppler resolvers, whereas DSS 51 did not. The difference is immediately evident by comparison of the first-pass, two-way doppler data from DSS 51, without resolver, in Fig. 50 to the first-pass, two-way doppler data of DSS 42, with resolver, in Fig. 51.

The Johannesburg station, the first to view the spacecraft after injection, began taking good two-way, 10-s count doppler data at 08:14:15 GMT on November 7, 1967. The sample rate was changed to 60-s at 08:46:02, and the spacecraft was transferred to DSS 42 at 10:05:02. The early data from DSS 51 was quite acceptable; it showed a standard deviation of 0.040 Hz for 10-s count data and of 0.007 Hz for 60-s count data—both figures are

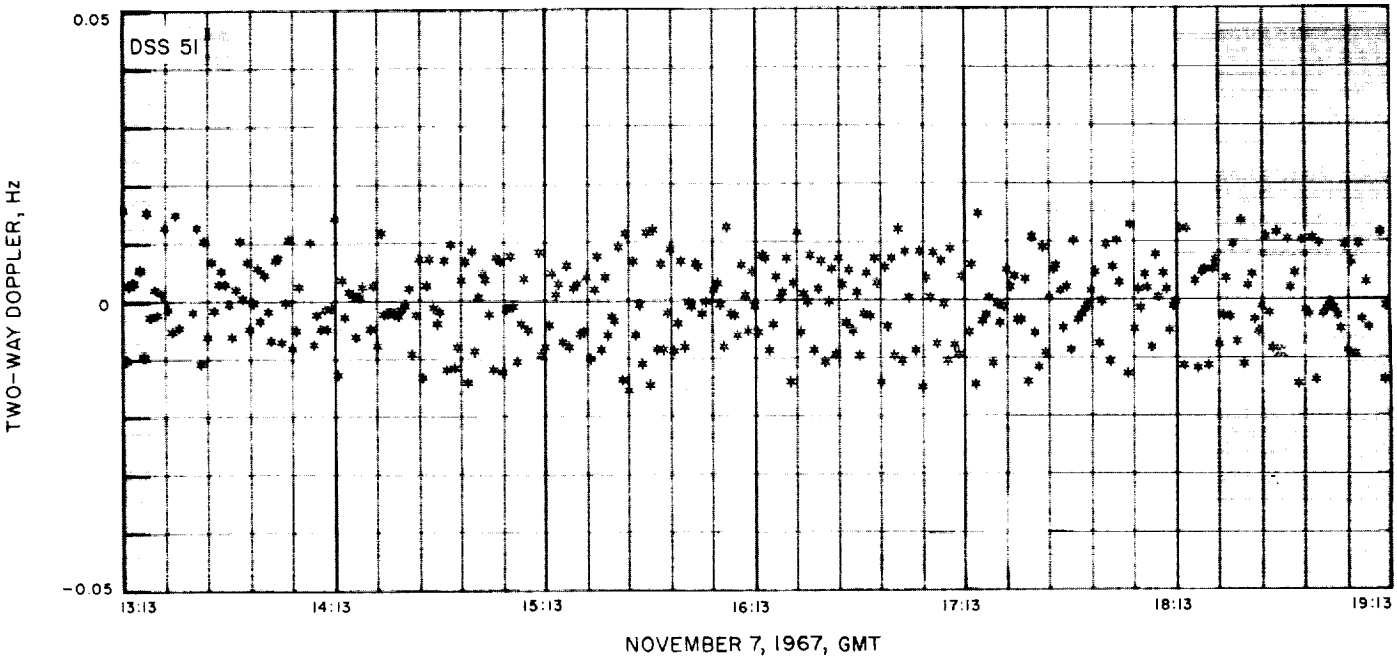

Fig. 50. Two-way doppler residuals without resolver, *Surveyor VI*

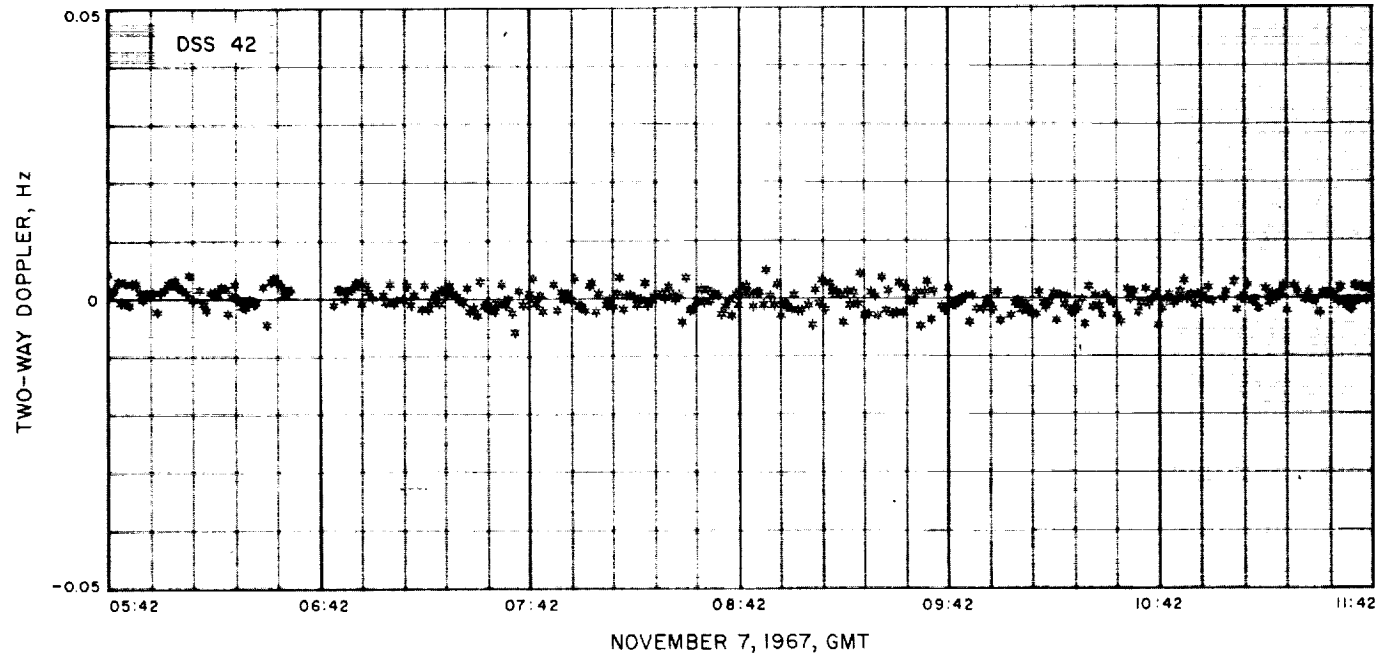

Fig. 51. Two-way doppler residuals with resolver, *Surveyor VI*

nominal for nonresolver data. The Tidbinbilla station, which was in the two-way mode from 10:05:02 to 12:10:02, took excellent data with a standard deviation of 0.0015 Hz. The spacecraft was transferred to the Robledo Deep Space Station at 12:10:02, which remained in two-way lock until 14:45:02 when a transfer was made back to DSS 51. The data from DSS 61 was quite noisy, showing a standard deviation of 0.011 Hz, which is 6 or 7 times higher than nominal. Data from this station continued to deteriorate in subsequent passes until the rubidium unit was changed; it is probable that this excessively noisy first-pass data can also be attributed to the problem with the faulty crystal. The Pioneer Deep Space Station acquired the spacecraft in the two-way mode at 22:10:02 and continued thusly until the time of the midcourse maneuver at 02:20:00 on November 8, 1967. The doppler data from DSS 11 during this period is only fair; it shows a standard deviation of 0.005 Hz, which is not quite as good as would be expected for resolver data. This above described two-way data from all three stations can be seen in Fig. 43.

Early analysis of the *Surveyor VI* trajectory indicated that a midcourse maneuver during the first pass over DSS 11 would be most advantageous; therefore, the maneuver was executed during this pass. Engine ignition was programmed for November 8 at 02:20:00, with a total burn time of 10.28 s that provided acceleration of 10 m/s. Results of the maneuver, shown in the two-way doppler data over DSS 11, are presented in Fig. 52. As can be seen from the data, the midcourse maneuver resulted in a doppler shift over DSS 11 of approximately −113.5 Hz.

3. Post-midcourse phase doppler tracking. All post-midcourse orbit computations used only two-way doppler from the prime stations, DSS 51, DSS 42, DSS 61 and DSS 11. Very good to excellent two-way doppler data was returned during this period, with one significant exception. As previously mentioned, DSS 61 took noisy two-way doppler data during their first pass; during their second pass, the spacecraft was tracked in the two-way mode for approximately 1½ hours and the noise on the

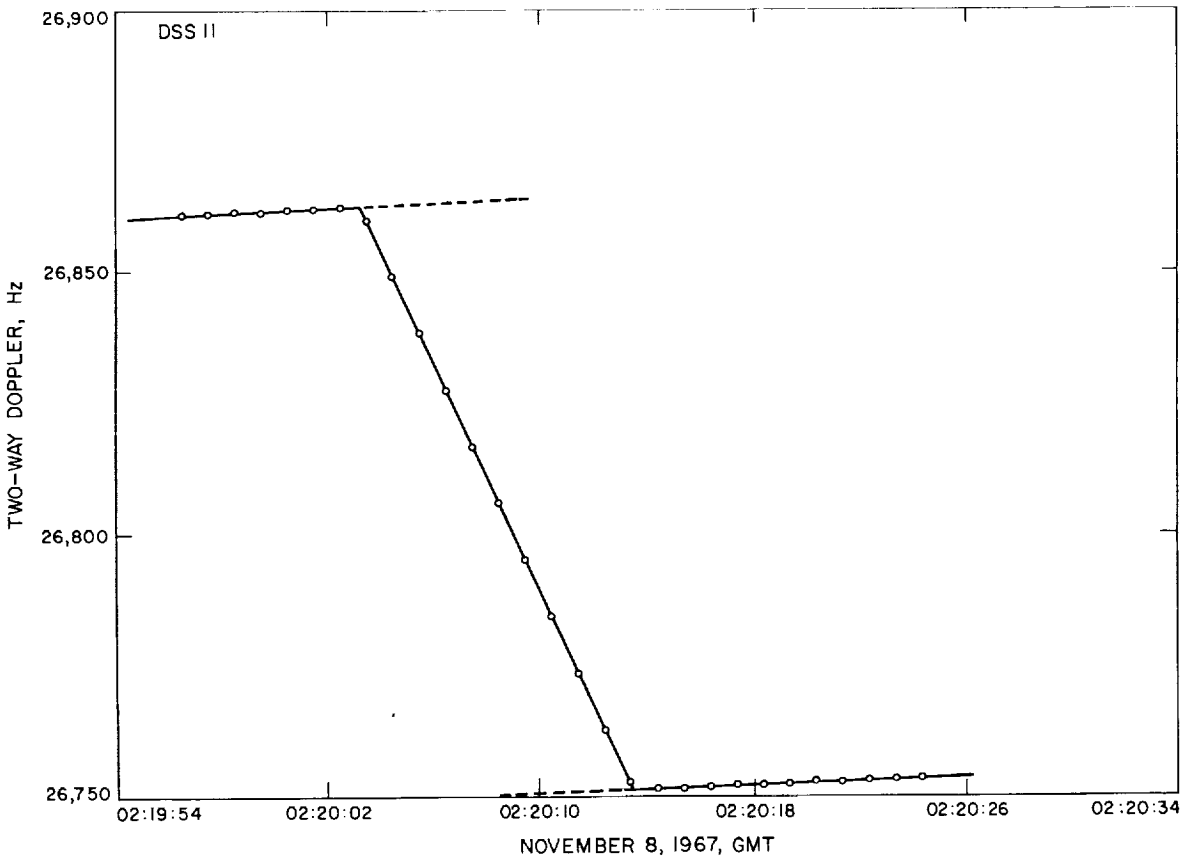

Fig. 52. Midcourse maneuver doppler data, *Surveyor VI*

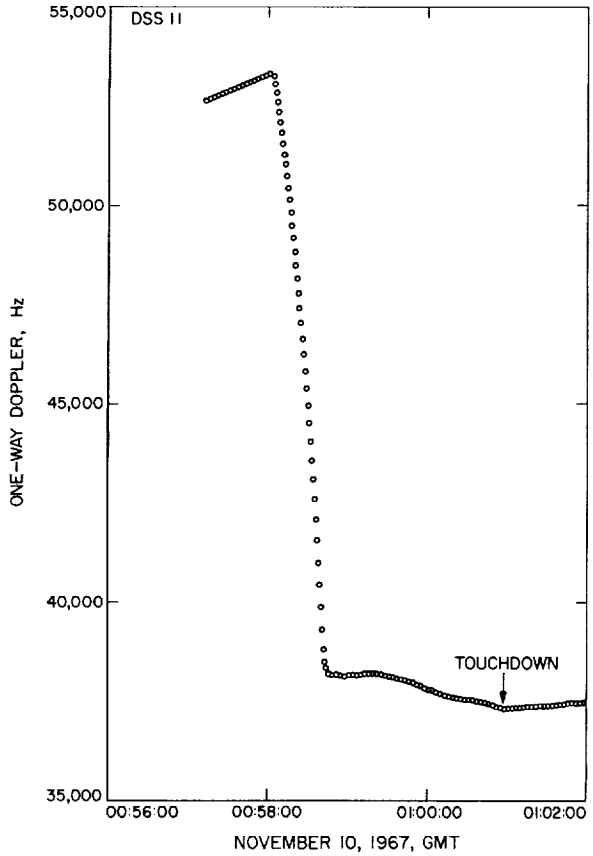

Fig. 53. Retrograde phase doppler data, *Surveyor VI*

data was 0.013 Hz higher (Fig. 47). It was felt that, perhaps, the high noise was due to a marginal rubidium unit, and when this unit was changed during the third pass of DSS 61, an immediate reduction of the noise in the three-way doppler residuals was noted. Excellent data were acquired by DSS 42 during the post-midcourse phase; the two-way doppler residuals show a standard deviation of 0.0017 Hz, which is by far the least noisy data taken by any station during *Surveyor VI*. The DSS 42 two-way doppler residuals during this period can be seen in Fig. 49. With the exception of the time for 1 h following the maneuver, DSS 11 took very good two-way doppler data during the post-midcourse phase; two-way doppler residuals from this station indicated a standard deviation of 0.003 Hz during this period. Residuals from DSS 11 for the post-midcourse phase are shown in Figs. 47 and 49. As seen in Fig. 47, the first hour of DSS 11 post-midcourse data is biased. Finally, DSS 51 took uniformly good data during the post-midcourse phase; two-way doppler residuals from this station produced a standard deviation of 0.0075 Hz, which is just about as good as is possible with a nonresolver station. These residuals are displayed in Fig. 49.

4. Touchdown phase doppler. Final inflight orbit calculations indicated a retroignition time of 00:58:01.5 on November 10, 1967. A soft landing occurred at 01:01:06.3 GMT, after a flight of 65 h, 22 min, 5 s. The results of the retroengine burn, as seen in the one-way doppler data at DSS 11, are presented in Fig. 53.

B. Comparison of Inflight and Postflight Results

The orbit determination inflight results can be evaluated by comparing them to the results obtained from the postflight computations. The degree to which these results agree is primarily influenced by the success attained in detecting and eliminating bad, or questionable, tracking data from the inflight computations and accounting for all trajectory perturbations. Of these, the largest variations are usually caused by bad or questionable data resulting from equipment malfunction, incorrect time information, or incorrect frequency information. Other than gross blunder points, these data are not easily detected unless two-way doppler data are available from more than one station. That is, the least squares method used to fit data in the ODP gives no information on constant data biases when data are available from only one station. Therefore, a comparison can be made only when data from more than one station are available. Furthermore, data must be available from three or more stations to isolate bad blocks of data.

The most meaningful comparison between inflight and postflight orbit determination results can be made by examining the critical target parameters—namely, the unbraked impact time and impact location. These results are summarized in Table 45. In the table, it can be seen that *the inflight premaneuver impact point was in error by 0.038 deg in latitude and 0.034 deg in longitude.* This is well within the uncertainty associated with the inflight estimate. The inflight postmaneuver impact point associated with the orbit solution (5 POM WD) used for the terminal attitude maneuver computations was in error by 0.008 deg in latitude and 0.019 deg in longitude. It should be noted that these errors are also within the stated uncertainties associated with the inflight estimates. The inflight predicted unbraked impact time used to provide the AMR backup was in error by 0.320 s, which was within the 1σ uncertainty of 0.500 s.

The best estimate of the landing point determined by transit tracking data (i.e., current best postmaneuver orbit), and the landing points determined by independent observations are presented in Table 45. One of the independent observations was obtained by processing track-

ing data from the landed spacecraft. The other one was obtained via optical methods, i.e., correlating *Surveyor VI* television photos of surrounding lunar horizon features with the *Lunar Orbiter* photos of the same lunar region. In Fig. 54 it can be seen that the estimated location based on the preliminary analysis of the landed spacecraft tracking data falls within the 1σ dispersion ellipse associated with the transit location. The estimate based on the *Lunar Orbiter* photos is just within the 1σ uncertainty of the transit estimate. The inflight unbraked impact time and impact time predicted by the current best postmaneuver orbit solution differ by only 0.002 s.

Based on the results of the comparison between inflight and postflight results, it may be concluded that all OD requirements were met.

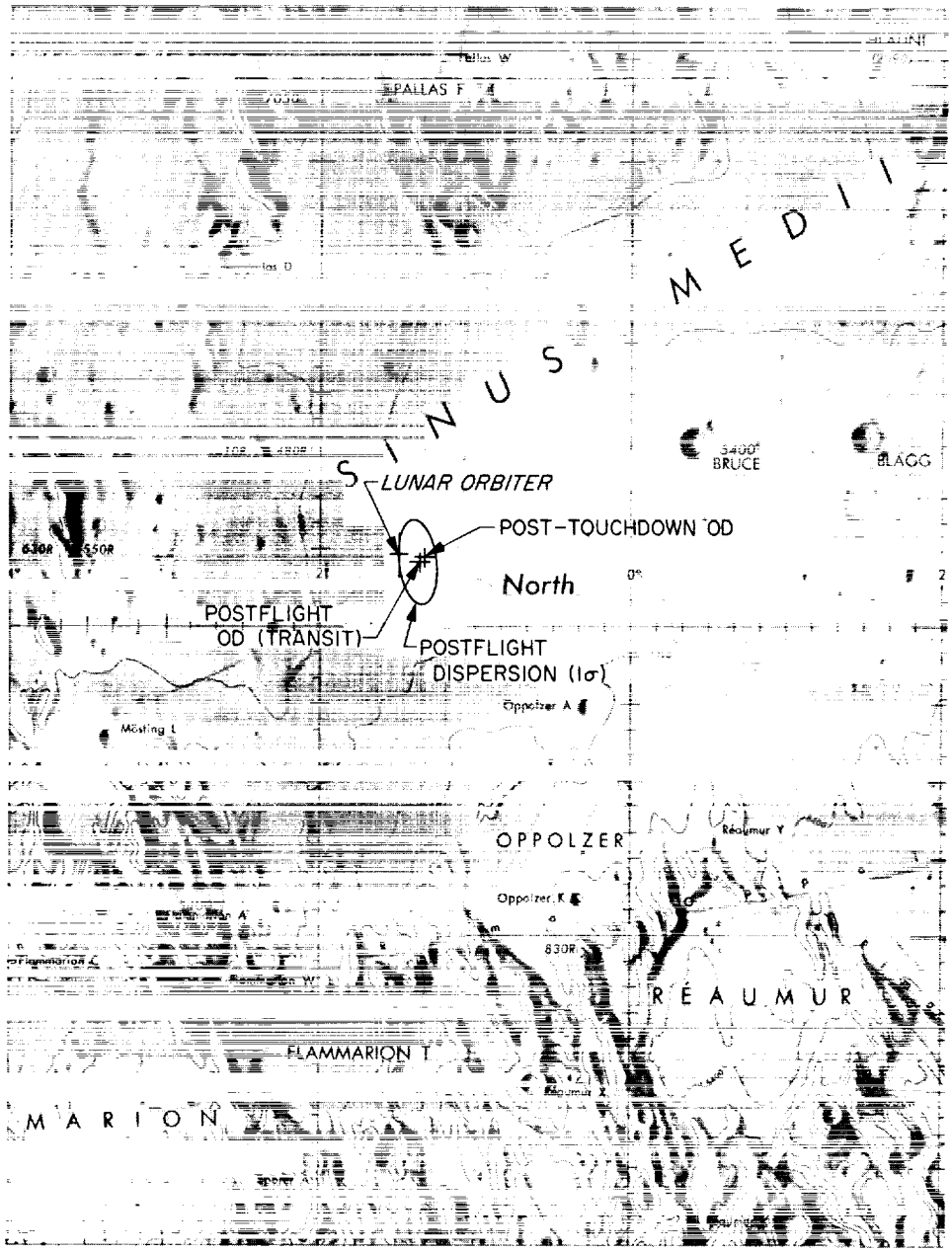

Fig. 54. *Surveyor VI* landing location

Table 45. Summary of target impact parameters, *Surveyor VI*

Source	Estimated impact or landed location		Uncertainty about estimated impact point (1σ dispersion ellipse)			Estimated unbraked impact time, GMT (Nov. 10, 1967)	Uncertainty in estimated unbraked impact time (1σ), s
	Latitude, deg (Negative S)	Longitude, deg	SMAA, km	SMIA, km	THETA, deg		
PREMANEUVER UNCORRECTED							
Inflight OD	−3.216	0.6646	11.07	4.09	95.28	00:35:42.987	1.840
Postflight OD	−3.254	0.6507	10.00	4.00	100.04	00:35:43.638	1.500
POSTMANEUVER TRANSIT							
Inflight OD	0.3967	358.816	14.58	8.235	116.46	00:58:32.883	2.879
Postflight OD	0.3889	358.797	2.50	1.00	95.04	00:58:32.885	0.500
Observed unbraked impact time						00:58:32.652	0.050
POST LANDING							
Postflight OD (adjusted)	0.419	358.624					
Lunar Orbiter correlation	0.470	358.520					
Post touchdown OD	0.456	358.632					

XII. Analysis of Air Force Eastern Test Range (AFETR) Tracking Data, *Surveyor VI*

The AFETR supported the *Surveyor* Missions by computing injection conditions and classical orbital elements for the parking orbit, the spacecraft transfer orbit, and the *Centaur* post-retromaneuver orbit. The injection conditions were computed by the AFETR and relayed to the SFOF in Pasadena where they were used as the initial values for early JPL orbit computations. The AFETR also transmitted initial acquisition information to the SFOF, for possible relay to the DSIF stations. The input for the AFETR calculations was the *Centaur* C-band tracking data obtained from various AFETR and MSFN tracking stations; the locations of these stations are given in Table 46.

In addition to fulfilling these requirements, the AFETR transmitted the C-band tracking data taken during the transfer orbit and the *Centaur* post-retromaneuver orbit to the SFOF. The transfer orbit data was used to compute an early JPL transfer orbit based solely on the C-band data. This early JPL orbit was used as a backup, for any unusual circumstances cause a failure of the AFETR orbit computation system. Under normal conditions, the early JPL orbit was used as a quick check on the AFETR transfer orbit. The *Centaur* post-retromaneuver orbit was made available to verify that the retromaneuver was performed properly to ensure (1) that the *Centaur* would not impact the moon and (2) that the spacecraft would be separated from this booster stage sufficiently to prevent its being locked onto by the Canopus sensor on board the spacecraft. The AFETR tracking coverage for *Surveyor VI* is shown in Fig. 55.

Table 46. AFETR station locations used for JPL inflight transfer orbit, *Surveyor VI*

Station	Radar type	Geocentric radius, km	Geocentric latitude, deg (Negative S)	Geocentric longitude, deg
Pretoria	MPS-25	6375.7617	−25.7960	28.35670
Carnarvon	FPQ-6	6374.464	−24.7508	113.71608
Twin Falls[a]	FPS-16	6378.14	1.986	−1.000
Grand Canary	MPS-26	6373.7272	27.604886	344.365169

[a]All *Twin Falls* ship data referenced to these coordinates.

A. Analysis of Transfer Orbit Data

The launch azimuth for *Surveyor VI* was 82.995 deg. At this launch azimuth the *Twin Falls* tracking ship was the only C-band data source for the transfer orbit data (Fig. 55). Unfortunately, the data transmitted from the *Twin Falls* was garbled, and only three usable data points were received at the SFOF.

Because of the data transmission problem with *Twin Falls* and because no other C-band data was available, neither JPL nor AFETR personnel computed a transfer orbit from C-band data. There is no C-band data available for postflight analysis of the transfer orbit, so no further analysis was made.

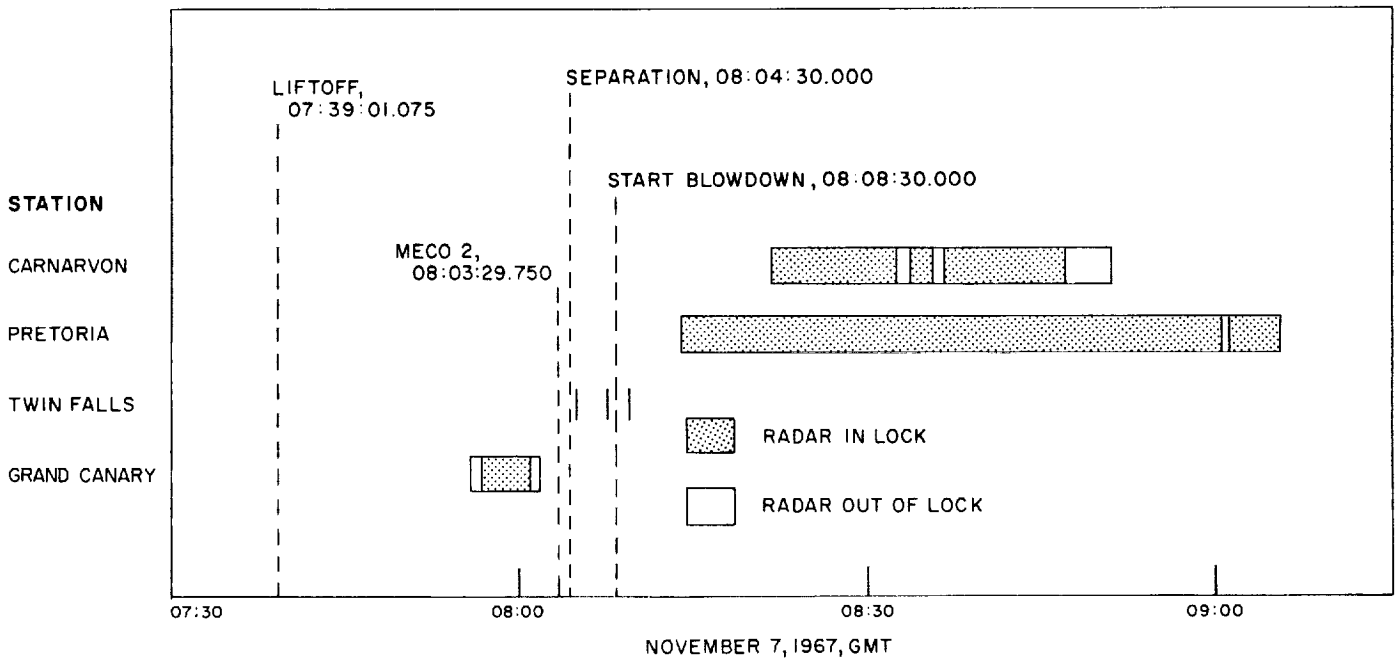

Fig. 55. AFETR tracking coverage for *Surveyor VI*

B. Analysis of Post-Retromaneuver Orbit Data

Centaur C-band tracking data from Carnarvon and Pretoria was available for post-retromaneuver orbit computations. Carnarvon provided almost 54 min of the data and Pretoria about 30 min. In postflight analysis, three different solutions were made: One solution used all postretro orbit data from both stations; one solution used Carnarvon data, only; and one solution used Pretoria data only. These solutions are labeled Postflight Orbit 1, 2, and 3, respectively. In Table 47 the AFETR and JPL post-retromaneuver orbit solutions are given. The data used for the JPL solutions and the statistics of the post-retromaneuver orbit tracking data residuals are given in Table 48. The data used for the AFETR solution was Carnarvon data, only, from 08:22:06 to 08:32:48 GMT.

C. Conclusions of the Postflight Analysis of the Post-Retromaneuver Orbit Data

Both the Carnarvon and Pretoria data were very noisy and had many blunder points. The two data

Table 47. Summary of *Centaur* post-retromaneuver orbit solutions, *Surveyor VI* (Epoch November 7, 1967 at 08:23:05.900 GMT)

Geocentric inertial position and velocity	Inflight orbit computed by AFETR	Postflight orbit 1 computed by JPL	Postflight orbit 2 computed by JPL	Postflight orbit 3 computed by JPL
x, km	−5743.9053	−5748.2889	−5748.3352	−5748.6560
y, km	−8368.9096	−8356.6866	−8357.1218	−8356.0636
z, km	−4387.0713	−4381.3314	−4379.7687	−4382.4042
Dx, km/s	2.7777096	2.7780003	2.7757232	2.7704347
Dy, km/s	−6.8691546	−6.8739285	−6.8723790	−6.8699934
Dz, km/s	−3.9076953	−3.9103623	−3.9120008	−3.9155811
Encounter Quantities				
B, km	33784.12	31742.23	33403.26	35848.37
B • TT, km	33735.23	31697.08	33362.88	35809.74
B • RT, km	−1816.87	−1692.37	−1641.92	−1663.65
Closest approach on 11/10/67, GMT	15:03:07.600	14:32:16.863	14:58:11.614	15:30:26.138

Table 48. Statistics of JPL *Centaur* post-retromaneuver orbit tracking, *Surveyor VI*. Data Residuals

Solution	Station	Data type	Data span, GMT		Number of points used	Standard deviation	Mean error
			Start	End			
Postflight 1	Pretoria	Azimuth, deg	08:14:30	09:05:42	79	0.132	0.0154
		Elevation, deg	08:14:30	08:20:48	51	0.0216	−0.0344
		Range, km	08:14:30	08:20:48	52	0.835	−0.000502
	Carnarvon	Azimuth, deg	08:22:12	08:41:06	129	0.0143	0.00320
		Elevation, deg	08:22:12	08:41:06	128	0.00745	−0.0126
		Range, km	08:22:12	08:41:06	130	2.48	−0.00472
Postflight 2	Carnarvon	Azimuth, deg	08:22:12	08:41:06	126	0.00607	0.0000769
		Elevation, deg	08:22:12	08:41:06	126	0.00531	−0.00517
		Range, km	08:22:12	08:41:06	89	0.182	−0.00186
Postflight 3	Pretoria	Azimuth, deg	08:14:30	09:05:42	79	0.133	−0.000269
		Elevation, deg	08:14:30	08:20:48	51	0.0265	−0.00197
		Range, km	08:14:30	08:20:48	52	0.832	0.000354

sources seemed to have range values that were inconsistent. However, it was possible to obtain fairly reliable post-retromaneuver solutions from the *Centaur* post-retromaneuver orbit data. The related AFETR and JPL solutions based only on Carnarvon data agree very well in encounter parameters.

XIII. *Surveyor VII* Inflight Orbit Determination Analysis

A. View Periods and Tracking Patterns

Figure 56 summarizes the tracking station view periods and their data coverage for the period from launch to lunar touchdown. Figures 57 through 60 are tracking station stereographic projections for the prime tracking stations which show the trace of the spacecraft trajectory for the view periods in Fig. 56. Table 49 summarizes the tracking data used for both inflight and postflight orbital calculations and analyses. This table provides a general picture of the performance of the data recording and handling systems.

B. Premaneuver Orbit Estimates

The initial transfer orbit estimate based on AFETR data was computed for the *Surveyor VII* mission by use of 7 points of range and angle data from Pretoria. This estimate indicated a very nominal launch that would result in a lunar encounter without a midcourse correction. (See Section XVI for analysis of AFETR data.)

The first estimate of the spacecraft orbit (PROR YA), based on DSS data only, was computed at launch plus 1 h, 50 min, based on approximately 17 min of two-way doppler and angle (HA–dec) data from DSS 42. When mapped to the moon, this orbit solution indicated a lunar encounter would be achieved without a midcourse correction. Further, it indicated that the correction required to achieve encounter at the desired aim point near Tycho was well within the nominal midcourse correction capability. These results were further verified by the second (ICEV) and third (PREL) orbit computations completed at launch plus 2 h, 49 min and 4 h, 32 min, respectively.

When sufficient two-way doppler data had been received to compute a *doppler only* orbit solution, the angle data were deleted. This was first accomplished in the PREL YA orbit computation, which utilized approximately 2 h 8 min of two-way doppler data from DSS 42. Removing the angle data from the solution resulted in a change of approximately 45 km in $\mathbf{B}\cdot\mathbf{T}T$ and 174 km in $\mathbf{B}\cdot\mathbf{R}T$ when the solution was mapped to lunar encounter, showing that the early angle data were biased with respect to the doppler data.

During the data consistency (DACO) and nominal maneuver (NOMA) orbit computation periods, 11 orbit solutions were computed with various combinations of two-way doppler data from DSS 42, DSS 51, and DSS 61. During this period, the first data from DSS 61 were received. It was felt, at first, that either DSS 61 or DSS 51 data were biased. However, deletion of either station from the orbit solution did not change the orbital estimate significantly. There was some problem with the pre-midcourse data, which made it difficult to fit all together. However, isolation of this problem remained for postflight analysis (see Section XIV).

To minimize the OD uncertainties for an expected second maneuver, it was decided to perform the first maneuver at $L + 17$ h. This forced the LAPM orbit solution back in time such that no DSS 11 data were in the solution (LAPM YB) used for the midcourse computations. At the beginning of the last pre-midcourse (LAPM) orbit computation period, the following amount of usable two-way doppler data were available: 4 h, 26 min from DSS 42; 3 h, 09 min from DSS 51; and 2 h, 57 min from DSS 61. The last orbit solution computed (LAPM YC) during the LAPM orbit computation period was the first solution to utilize data from DSS 11 that seemed to be consistent with the other data. The pre-midcourse orbit solution (LAPM YB) on which the midcourse maneuver was based was computed using all the two-way doppler data midcourse minus 3 h, 49 min. When mapped to the moon, this solution indicated an unbraked impact point at 5.936° S lat and 5.392° E lon, approximately 17 km south and 55 km east of the prelaunch aim point.

The numerical results of the premaneuver orbit computations are presented in Tables 50 and 51. Amounts and types of tracking data used in the various pre-midcourse orbit computations, together with the associated data statistics are given in Table 52. For the inflight best estimate of the spacecraft premaneuver orbit (PRCL YE), all usable data from DSS 11, DSS 42, DSS 51, and DSS 61 taken from initial Deep Space Station acquisition to start of midcourse maneuver were used. See Fig. 61 for B-plane[14] impact points. Residual plots resulting from the inflight best estimate, PRCL YE, orbit solution are presented in Fig. 62. The effect of the midcourse maneuver as evidenced by the doppler shift is shown in Fig. 63. Epochs used are in Table 53.

C. Postmaneuver Orbit Estimates

The first post-midcourse (1 POM) orbit computations were completed approximately 10 h after maneuver execution. For the final (1 POM WF) orbit computation during this orbit period, approximately 5 h, 38 min of DSS 11 data and 2 h, 50 min of DSS 42 two-way doppler data were used. When the 1 POM WF solution was mapped to target, it indicated an unbraked impact point of 41.079°S lat and 348.697°E lon, approximately 3.2 km from the maneuver aim point. The final terminal computations were based on the 5 POM YD orbit solution.

Numerical results of the inflight post-midcourse orbit solutions are presented in Tables 54 and 55. Figure 64 is a plot of the post-midcourse estimated, unbraked impact point in B-space. The inflight best estimate[15] of the landed *Surveyor VII* spacecraft is 4.6 km south and 1.3 km east of the final aim point. The amounts of tracking data used in the various post-midcourse orbit computations, together with the associated noise statistics, are given in Table 56. Figure 65 presents the residual plots from the inflight best estimate post-midcourse orbit solution, PTD-1. Figure 66 shows the effect of the retromaneuver as seen in the one-way doppler data from DSS 11.

D. AMR Backup Computations

After the 5 POM YD computations, primary emphasis was placed on obtaining the best estimate of unbraked impact time to be used for sending a ground command to back up the onboard altitude marking radar. All subsequent computations used *a priori* information from all postmaneuver tracking data up to retrothrust minus 5 h, 40 min. This information was in the form of a covariance matrix mapped to $R - 5$ h, 40 min. The covariance matrix was degraded and expanded, as discussed in Section II-A. In addition to being able to account for the SPODP model errors by using this method, a considerable saving in program running time was achieved by working with the updated epoch. This was very important, since the basic philosophy was that the near-moon data would yield the best estimate of unbraked impact time. This would require that as much near-moon data as possible be included in the orbit solution; at the same time, it was necessary to provide the results at retrothrust minus 40 min—the lead time required to implement the backup command transmission.

For the AMR backup computations, a lunar elevation of 1736.6 km at the predicted unbraked impact point was used. This lunar elevation, obtained from NASA Langley Research Center, was consistent with the elevation based on the appropriate ACIC lunar chart, less 2.4 km. The 2.4 km is the amount by which the elevation based on the ACIC chart exceeds the elevation obtained from *Ranger VI*, *VII*, and *VIII* tracking data. An *a priori* 1σ uncertainty of ± 1 km (roughly equivalent to ± 0.4 s) was assigned to this elevation.

The estimated unbraked impact time that was used for the AMR backup calculations was 01:02:47.7 GMT on January 10, 1968. This time was an extrapolation from the "FINAL" orbit solutions, which indicated a trend that would make this value reasonable. FINAL orbit solutions had yielded estimated unbraked impact times

[14]See Appendix B for definition of B-plane.

[15]Based on the PTD-1 solution.

from 01:02:49.365 to 01:02:47.844 GMT, and the estimated time was progressively earlier as more near-moon data were used in the solutions. Hence, 01:02:47.7 GMT was presented by the OD group as the best estimate of unbraked impact time. With this unbraked impact time (01:02:47.7 GMT), the nominal AMR mark time was computed to be 01:02:11.28 GMT on January 10, 1968. This time was used as the basic reference point from which the desired time of backup command transmission from the ground station (DSS 11) was calculated. The backup command was computed to be transmitted from DSS 11 at such a time that it was predicted to arrive at the spacecraft 3.09 s after the nominal AMR mark time. According to postflight analysis of telemetry tape records, the AMR backup actually arrived 3.92 s after the actual AMR mark occurred. The time at which the AMR provided a mark pulse on board the spacecraft was 01:02:10.60 $\pm$0.05 s (1σ) GMT. This observed time was 0.68 s earlier than the nominal AMR mark time used for backup calculations. The AMR backup command arrived at the spacecraft at 01:02:14.52 $\pm$0.1 s (1σ) GMT. The inflight results of the AMR backup (FINAL) orbit computations are given in Table 57. The difference between the estimated unbraked impact time provided for the AMR backup computations and the current best estimate (0.21 s) is well within the 0.7-s 1σ uncertainty given inflight.

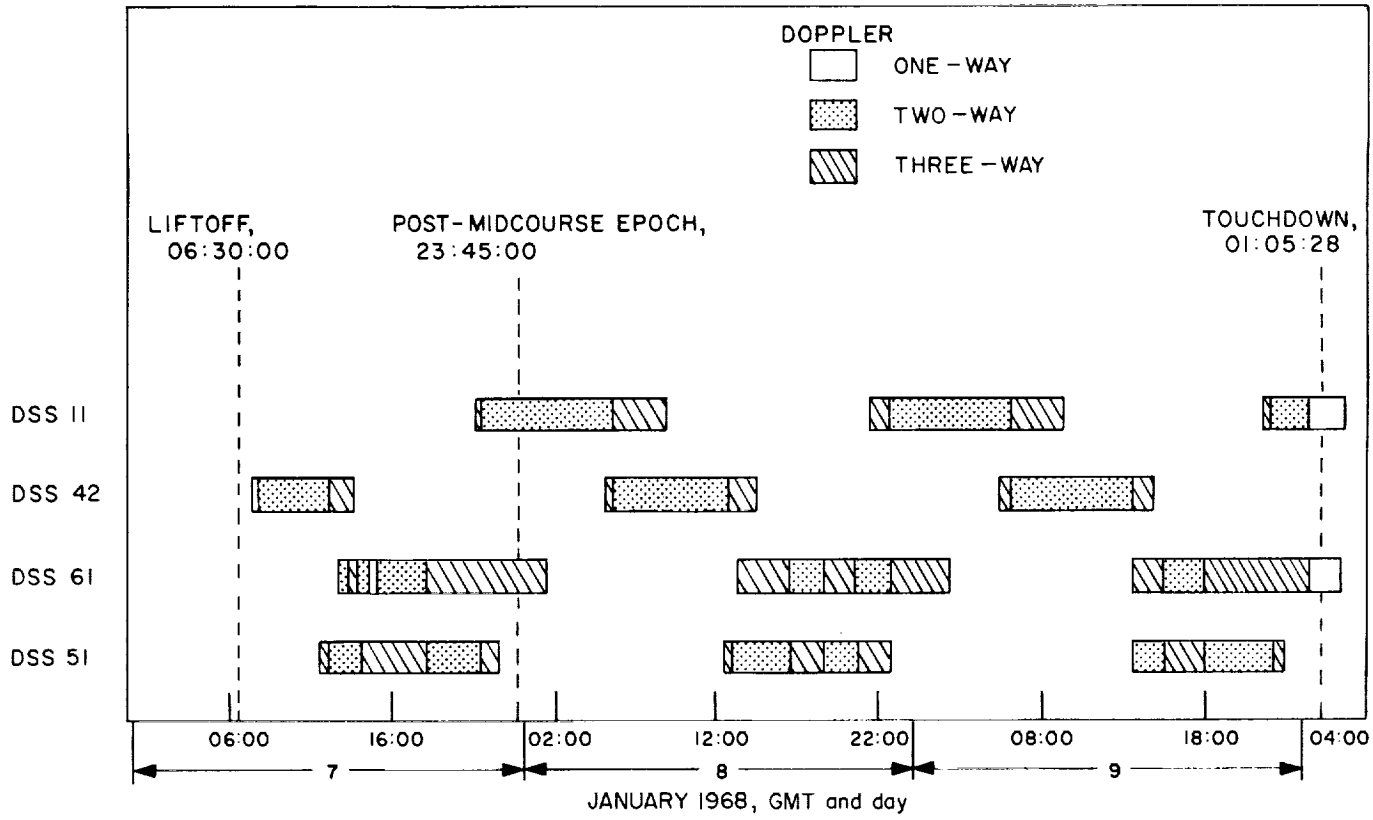

Fig. 56. *Surveyor VII* DSS tracking coverage

Table 49. Summaries of data used in orbit determination, *Surveyor VII*

Station	Data type	Points recd	Points used in real time		Bad format		Bad data condition code		Blunder points		Rejection limits on blunder points	Points used in postflight analysis, best estimate
			Number	% of recd	Number	% of recd	Number	% of recd	Number	% of recd		
Premaneuver data												
DSS 11	CC3	294	98	33.3	1	0.3	0	0.0	3	1.0	CC3	98
DSS 42	CC3	431	399	92.6	0	0.0	7	1.6	2	0.5	0.10 for 10-s sample rate;	399
	HA	573	233	40.7	0	0.0	29	5.1	5	0.9	0.03 for 60-s sample rate	0
	Dec	573	233	40.7	0	0.0	29	5.1	4	0.7		0
DSS 51	CC3	323	199	61.6	2	0.6	12	3.7	21	6.5		
DSS 61	CC3	224	172	76.8	1	0.4	20	8.9	1	0.4	Angles 0.1	199 172
Postmaneuver data												
DSS 11	CC3	995	890	89.4	15	1.5	16	1.6	4	0.4	CC3	886
DSS 42	CC3	883	811	91.8	0	0.0	6	0.7	4	0.5	0.10 for 10-s sample rate;	851
DSS 51	CC3	683	524	76.7	10	1.5	28	4.1	6	0.9	0.03 for 60-s sample rate	576
DSS 61	CC3	388	333	85.8	3	0.8	21	5.4	0	0.0		333
											Angles 0.1	

Table 50. *Surveyor VII* premaneuver computations

Orbit ID	Time computed, GMT		Target statistics							
	Start	Stop	B, km	B • TT, km	B • RT, km	TL, h	SMAA, km (1σ)	SMIA, km (1σ)	THETA, deg	$\sigma_{T,\ impact}$, s (1σ)
ETR	07:14	07:49	2040.01	1993.36	433.77	65.94	1625.89	125.54	178.00	3397.35
PROR YA	07:59	08:20	2077.98	2009.10	530.61	65.61	619.91	117.40	93.01	234.58
PROR WA	08:30	08:48	1990.70	1979.69	209.07	65.65	129.45	78.15	99.03	35.93
ICEV YA	08:45	09:10	2013.60	2003.80	198.47	65.65	94.39	71.91	115.53	22.591
ICEV WA	09:03	09:19	2008.73	1999.05	196.91	65.65	84.33	63.17	133.19	16.862
PREL YA	09:44	10:25	2081.80	2048.16	372.79	65.64	1628.2	117.6	127.73	103.90
PREL WA	09:45	10:11	2089.39	2054.35	381.07	65.64	1742.5	124.8	128.23	107.53
PREL WB	10:39	11:02	2078.98	2045.70	370.50	65.64	661.32	47.50	120.04	55.682
DACO YB	13:40	14:06	2091.93	2054.78	392.50	65.64	229.93	5.245	113.90	20.296
DACO WC	16:39	17:05	2067.48	2037.30	352.00	65.64	21.954	4.516	120.68	2.1188
NOMA YA	17:42	18:02	2091.90	2056.14	385.14	65.64	56.120	4.241	119.32	4.6736
NOMA WA	18:10	18:30	2073.18	2041.87	358.98	65.64	17.007	4.140	120.00	1.6152
NOMA WB	18:34	18:59	2084.52	2049.50	380.52	65.64	27.897	5.262	113.34	2.4889
NOMA YC	18:57	19:16	2078.19	2045.94	364.73	65.64	34.684	16.420	115.65	5.4599
LAPM WA	19:14	19:34	2084.03	2049.14	379.72	65.64	22.029	5.233	114.18	1.8893
LAPM YA	19:29	19:50	2075.02	2043.89	358.06	65.64	40.26	16.70	112.48	5.6610
LAPM YB[a]	19:59	20:25	2075.45	2044.16	359.04	65.64	39.97	16.66	112.71	5.6303
LAPM YC	22:25	22:55	2076.01	2043.70	364.88	65.64	7.2959	2.239	104.44	0.76516
PRCL YC	01:31	01:50	2076.08	2043.70	365.25	65.64	6.958	2.063	99.965	0.74373
PRCL YD	02:00	02:25	2076.05	2043.77	364.71	65.64	7.980	2.345	101.03	0.84583
PRCL YE[b]	02:34	02:56	2076.17	2043.84	364.94	65.64	8.258	2.414	101.72	0.86785

[a]Orbit used for midcourse computations.

SMAA = semimajor axis of dispersion ellipse.
SMIA = semiminor axis of dispersion ellipse.
THETA = orientation angle of dispersion ellipse measured counter clockwise from B • TT axis.
$\sigma_{T,\ impact}$ = uncertainty in predicted unbraked impact time.
PHI_{99} = 99% velocity vector pointing error.
SVFIXR = uncertainty in magnitude of velocity vector at unbraked impact.

[b]Inflight best estimate, premaneuver as of January 10, 1968.

Table 50 (contd)

Orbit ID	Target statistics (contd)		Selenocentric conditions at unbraked impact			Type solution	Data used and source
	PHI_{90}, deg	SVFIXR, m/s (1σ)	Latitude, deg (South)	Longitude, deg	Jan. 10, 1968, GMT		
ETR	134.82	0.0101	−7.414	4.389	00:58:08.146	6 × 6	AFETR
PROR YA	17.355	1.0245	−9.316	4.910	01:01:01.189	6 × 6	
PROR WA	2.914	0.6213	−2.988	3.650	01:03:12.910	6 × 6	
ICEV YA	2.084	0.6151	−2.786	4.225	01:03:16.407	6 × 6	
ICEV WA	1.783	0.6134	−2.755	4.109	01:03:16.218	6 × 6	
PREL YA	31.65	0.8495	−6.206	5.511	01:02:52.683	6 × 6	Doppler only
PREL WA	33.87	0.8797	−6.369	5.678	01:02:52.018	6 × 6	
PREL WB	12.97	0.6702	−6.161	5.447	01:02:52.831	6 × 6	
DACO YB	4.457	0.6196	−6.593	5.708	01:02:50.619	6 × 6	CC3, DSS 42, DSS 51
DACO WC	0.43761	0.6112	−5.798	5.212	01:02:54.784	6 × 6	CC3, DSS 42, DSS 51, DSS 61
NOMA YA	1.0999	0.6116	−6.449	5.729	01:02:51.466	6 × 6	CC3, DSS 42, DSS 61
NOMA WA	0.01558	0.6112	−5.935	5.335	01:02:53.999	6 × 6	CC3, DSS 42, DSS 51, DSS 61
NOMA WB	0.53421	0.6112	−6.358	5.557	01:02:51.834	6 × 6	CC3, DSS 42, DSS 51
NOMA YC	0.74416	0.6114	−6.048	5.444	01:02:53.124	12 × 12	CC3, DSS 42, DSS 51, DSS 61 Estimated station location (radius and longitude)
LAPM WA	0.41979	0.6112	−6.342	5.547	01:02:51.904	6 × 6	
LAPM YA	0.81803	0.6115	−5.917	5.383	01:02:53.640	12 × 12	CC3, DSS 42, DSS 51, DSS 61 Station location (radius and longitude)
LAPM YB[a]	0.81352	0.6115	−5.936	5.392	01:02:53.534	12 × 12	CC3, DSS 42, DSS 51, DSS 61 Station location (radius and longitude)
LAPM YC	0.13188	0.6111	−6.051	5.389	01:02:53.098	6 × 6	CC3, DSS 11, DSS 42, DSS 51, DSS 61
PRCL YC	0.12270	0.6111	−6.058	5.390	01:02:53.073	6 × 6	All CC3
PRCL YD	0.1426	0.6111	−6.048	5.391	01:02:53.115	14 × 14	All CC3; estimated R and Ion
PRCL YE[b]	0.1482	0.6111	−6.052	5.393	01:02:53.103	18 × 18	All CC3; estimated R and Ion

Table 51. *Surveyor VII* premaneuver position and velocity at injection epoch[a]

Orbit ID	Geocentric space-fixed position			Geocentric space-fixed velocity			Uncertainties 1σ					
							Position			Velocity		
	x, km	y, km	z, km	Dx, km/s	Dy, km/s	Dz, km/s	σ_x, km	σ_y, km	σ_z, km	σ_{Dx}, m/s	σ_{Dy}, m/s	σ_{Dz}, m/s
ETR	−3237.8706	−5041.9248	−2658.4687	9.2785905	−4.6451746	−3.5874319	0.35857	0.27709	0.52420	5.0395	4.2471	7.4663
PROR YA	9449.5600	−6125.0614	−4462.3471	7.9192694	1.4103732	0.098358311	1.5724	1.7640	4.6701	0.57297	2.1600	7.4413
PROR WA	9449.5991	−6123.8733	−4465.6658	7.9189073	1.4102455	0.10182494	1.0169	1.1026	2.4234	0.35737	1.2301	1.3435
ICEV YA	9449.2484	−6124.2201	−4465.6556	7.9190123	1.4097051	0.10186046	0.96900	1.0721	2.2503	0.34546	1.1580	0.95872
ICEV WA	9449.3123	−6124.1285	−4465.7593	7.9189843	1.4098720	0.10186558	0.92766	1.0475	2.1577	0.33682	1.1023	0.83043
PREL YA	9448.6145	−6127.1986	−4457.4061	7.9199260	1.4085489	0.10229014	12.754	25.169	47.879	7.9506	17.440	5.0597
PREL WA	9448.5358	−6127.2097	−4457.1005	7.9199762	1.4084405	0.10226007	13.807	26.907	50.613	8.5019	18.816	5.5477
PREL WB	9448.6456	−6127.1504	−4457.4768	7.9199106	1.4085885	0.10230692	4.3174	10.555	23.273	3.3069	6.3102	1.3177
DACO YB	9448.5178	−6127.5866	−4456.3861	7.9200442	1.4083678	0.10236350	1.2512	3.8220	9.3062	1.1885	2.0045	0.15312
DACO WC	9448.7529	−6126.8585	−4458.1739	7.9198174	1.4087448	0.10234402	0.15744	0.38526	0.81758	0.11712	0.24432	0.11603
NOMA YA	9448.5173	−6127.3913	−4457.0277	7.9199883	1.4084216	0.10222245	0.34749	0.77303	1.6606	0.24883	0.47388	0.23010
NOMA WA	9448.6935	−6127.0085	−4457.8603	7.9198626	1.4086518	0.10234234	0.12445	0.29734	0.62906	0.09067	0.19177	0.11544
NOMA WB	9448.5885	−6127.3703	−4456.9136	7.9199769	1.4084809	0.10235877	0.16846	0.49839	1.2120	0.15378	0.27447	0.12060
NOMA YC	9448.6367	−6127.0848	−4457.7735	7.9198857	1.4085963	0.10227540	0.36248	0.74950	1.4623	0.19630	0.51209	0.16584
LAPM WA	9448.5933	−6127.3552	−4456.9505	7.9199722	1.4084888	0.10235785	0.14514	0.41985	1.0084	0.12851	0.23886	0.12055
LAPM YA	9448.6614	−6126.9782	−4458.0859	7.9198501	1.4086436	0.10226138	0.36811	0.81464	1.7527	0.22346	0.52994	0.17434
LAPM YB[b]	9448.6578	−6126.9896	−4458.0533	7.9198541	1.4086390	0.10225866	0.36790	0.81360	1.7474	0.22240	0.52979	0.17291
LAPM YC	9448.6818	−6127.0168	−4457.8364	7.9198684	1.4086526	0.10226155	0.04235	0.11737	0.30629	0.03679	0.06730	0.06842
PRCL YC	9448.6811	−6127.0219	−4457.8175	7.9198702	1.4086515	0.10226341	0.03656	0.10871	0.30085	0.03424	0.05989	0.06922
PRCL YD	9448.6739	−6127.0282	−4457.8199	7.9198717	1.4086455	0.10226905	0.043738	0.12481	0.348044	0.038869	0.068785	0.082394
PRCL YE[c]	9448.6722	−6127.0320	−4457.8125	7.9198727	1.4086439	0.10226823	0.04590	0.13037	0.36234	0.04054	0.07177	0.08608

[a]See Table 54 for epochs used.
[b]Orbit used for midcourse computations.
[c]Current best estimate, January 10, 1968.

Table 52. Summary of premaneuver DSS tracking data used in *Surveyor VII* orbit computations

Orbit ID	Station	Data type	Begin data		End data		Number of points	Standard deviation	Root mean square	Mean error	Data sample rate, s
			Date 1968	GMT	Date 1968	GMT					
ETR	DSS 71	Az	1/7	07:05:06	1/7	07:05:42	7	0.0121	0.0121	−0.000264	
		El	1/7	07:05:06	1/7	07:05:42	7	0.00358	0.00359	−0.000149	
		R	1/7	07:05:06	1/7	07:05:42	7	0.00337	0.00337	0.0000207	
PROR YA	DSS 42	CC3	1/7	07:28:07	1/7	07:45:17	99	0.0129	0.0129	0.000326	10,[a] 60
		HA	1/7	07:28:02	1/7	07:45:22	96	0.00559	0.00559	−0.0000383	10,[a] 60
		Dec	1/7	07:28:02	1/7	07:45:22	96	0.00456	0.00457	−0.000219	10,[a] 60
PROR WA	DSS 42	CC3	1/7	07:28:07	1/7	08:23:32	202	0.0901	0.123	0.0844	10,[a] 60
		HA	1/7	07:28:02	1/7	08:24:02	204	0.0609	0.0609	−0.000306	10,[a] 60
		Dec	1/7	07:28:02	1/7	08:24:02	204	0.0311	0.0311	−0.0000360	10,[a] 60
ICEV YA	DSS 42	CC3	1/7	07:28:07	1/7	08:41:32	212	0.0173	0.0175	0.00210	10,[a] 60
		HA	1/7	07:28:02	1/7	08:42:02	219	0.00703	0.00744	−0.00245	10,[a] 60
		Dec	1/7	07:28:02	1/7	08:42:02	219	0.0132	0.0140	−0.00465	10,[a] 60
ICEV WA	DSS 42	CC3	1/7	07:28:07	1/7	08:55:32	226	0.0181	0.0182	0.00145	10,[a] 60
		HA	1/7	07:28:02	1/7	08:56:02	233	0.00896	0.00951	−0.00317	10,[a] 60
		Dec	1/7	07:28:02	1/7	08:56:02	233	0.0143	0.0154	−0.00572	10,[a] 60
PREL YA	DSS 42	CC3	1/7	07:28:07	1/7	09:36:32	265	0.00490	0.00490	−0.0000313	10,[a] 60
PREL WA	DSS 42	CC3	1/7	07:28:07	1/7	09:33:32	262	0.00499	0.00499	−0.000171	10,[a] 60
PREL WB	DSS 42	CC3	1/7	07:28:07	1/7	10:32:32	321	0.00456	0.00456	−0.0002	10,[a] 60
DACO YB	DSS 42	CC3	1/7	07:28:07	1/7	11:54:32	399	0.00480	0.00480	−0.0000355	10,[a] 60
		CC3	1/7	12:22:32	1/7	13:54:32	80	0.00210	0.00214	0.000421	60
DACO WC	DSS 42	CC3	1/7	07:28:17	1/7	11:54:32	398	0.00503	0.00504	0.000290	
	DSS 51	CC3	1/7	12:22:32	1/7	13:53:32	76	0.00396	0.00421	0.00143	60
	DSS 61	CC3	1/7	14:56:32	1/7	16:30:32	91	0.00646	0.00646	−0.000335	60
NOMA YA	DSS 42	CC3	1/7	07:28:07	1/7	11:54:32	399	0.00431	0.00432	−0.000222	10,[a] 60
	DSS 61	CC3	1/7	12:22:32	1/7	17:32:32	167	0.00321	0.00321	−0.0000672	60
NOMA WA	DSS 42	CC3	1/7	07:28:07	1/7	11:54:32	399	0.00724	0.00724	0.000122	10,[a] 60
	DSS 51	CC3	1/7	12:22:32	1/7	13:53:32	76	0.00238	0.00616	0.00568	60
	DSS 61	CC3	1/7	14:03:32	1/7	17:53:32	188	0.00907	0.00908	−0.000234	60
NOMA WB	DSS 42	CC3	1/7	07:28:07	1/7	11:54:32	399	0.00463	0.00463	0.0000612	10,[a] 60
	DSS 51	CC3	1/7	12:22:32	1/7	13:53:32	76	0.00269	0.00276	0.000630	60
	DSS 51	CC3	1/7	18:03:32	1/7	18:31:32	19	0.00251	0.00269	0.000977	60
NOMA YC	DSS 42	CC3	1/7	07:28:07	1/7	11:54:32	399	0.00418	0.00419	−0.000296	10,[a] 60
	DSS 51	CC3	1/7	12:22:32	1/7	13:53:32	80	0.00324	0.00325	0.000177	60
	DSS 51	CC3	1/7	18:03:32	1/7	18:50:32	28	0.00235	0.00255	−0.000994	60
	DSS 61	CC3	1/7	14:03:32	1/7	17:53:32	188	0.00447	0.00451	−0.000599	60
LAPM WA	DSS 42	CC3	1/7	07:28:07	1/7	11:54:32	399	0.00476	0.00476	0.000114	10,[a] 60
	DSS 51	CC3	1/7	12:22:32	1/7	13:53:32	76	0.00252	0.00255	0.000392	60
	DSS 51	CC3	1/7	18:03:32	1/7	19.06:32	35	0.00512	0.00513	−0.0000832	60
LAPM YA	DSS 42	CC3	1/7	07:28:17	1/7	11:54:32	398	0.00419	0.00419	−0.000148	10,[a] 60
	DSS 51	CC3	1/7	12:22:32	1/7	13:53:32	80	0.00428	0.00428	−0.000110	60

[a]Between 07:28 and 07:29.

Table 52 (contd)

Orbit ID	Station	Data type	Begin data		End data		Number of points	Standard deviation	Root mean square	Mean error	Data sample rate, s
			Date 1968	GMT	Date 1968	GMT					
LAPM YA (contd)	DSS 51	CC3	1/7	18:03:32	1/7	19:05:32	34	0.00567	0.00568	0.000187	60
	DSS 61	CC3	1/7	14:56:32	1/7	17:53:32	172	0.00210	0.00219	−0.000632	60
LAPM YB	DSS 42	CC3	1/7	07:28:17	1/7	11:54:32	398	0.00429	0.00430	−0.000294	10,[a] 60
	DSS 51	CC3	1/7	12:22:32	1/7	13:53:32	79	0.00397	0.00399	0.000389	60
	DSS 51	CC3	1/7	18:03:32	1/7	19:41:32	53	0.00468	0.00474	0.000755	60
	DSS 61	CC3	1/7	14:56:32	1/7	17:53:32	172	0.00227	0.00227	0.000123	60
LAPM YC	DSS 11	CC3	1/7	21:24:32	1/7	22:16:32	51	0.00312	0.00386	0.00240	60
	DSS 42	CC3	1/7	07:28:07	1/7	11:54:32	399	0.00920	0.00965	−0.00291	10,[a] 60
	DSS 51	CC3	1/7	12:22:32	1/7	13:53:32	80	0.00200	0.0123	0.0121	60
	DSS 51	CC3	1/7	18:03:32	1/7	21:12:32	119	0.00759	0.0122	0.09956	60
	DSS 61	CC3	1/7	14:03:32	1/7	17:53:32	188	0.00733	0.00921	−0.00558	60
PRCL YC	DSS 11	CC3	1/7	21:24:32	1/7	23:07:32	98	0.00276	0.00317	0.00156	60
	DSS 42	CC3	1/7	07:28:07	1/7	11:54:32	399	0.00871	0.00915	−0.00278	10, 60
	DSS 51	CC3	1/7	12:22:32	1/7	13:53:32	80	0.00201	0.0123	0.0121	60
	DSS 51	CC3	1/7	18:03:32	1/7	21:12:32	119	0.00774	0.0124	0.00974	60
	DSS 61	CC3	1/7	14:56:32	1/7	17:53:32	172	0.00781	0.00979	−0.00591	60
PRCL YD	DSS 11	CC3	1/7	21:24:32	1/7	23:07:32	98	0.00286	0.00330	0.00165	60
	DSS 42	CC3	1/7	07:28:07	1/7	11:54:32	399	0.00688	0.00721	−0.00216	10,[a] 60
	DSS 51	CC3	1/7	12:22:32	1/7	13:53:32	80	0.00178	0.00745	0.00723	60
	DSS 51	CC3	1/7	18:03:32	1/7	21:12:32	119	0.00606	0.00894	0.00658	60
	DSS 61	CC3	1/7	14:56:32	1/7	17:53:32	172	0.00744	0.00823	−0.00352	60
PRCL YE	DSS 11	CC3	1/7	21:24:32	1/7	23:07:32	98	0.00280	0.00319	0.00153	60
	DSS 42	CC3	1/7	07:28:07	1/7	11:54:32	399	0.00679	0.00706	−0.00192	10,[a] 60
	DSS 51	CC3	1/7	12:22:32	1/7	13:53:32	80	0.00178	0.00710	0.00687	60
	DSS 51	CC3	1/7	18:03:32	1/7	21:12:32	119	0.00604	0.00873	0.00629	60
	DSS 61	CC3	1/7	14:56:32	1/7	17:53:32	172	0.00719	0.00790	−0.00327	60

[a]Between 07:28 and 07:29.

Table 53. Epochs used in orbit solutions

Epoch		Orbits using given epoch	Remarks
Date 1968	GMT		
January 7	27:00:00.0	ETR, PROR, ICEV, PREL, DACO, LAPM, PRCL	$t + 1$h
January 7	45:00:00.0	1 POM, 2 POM, 3 POM, 4 POM, 5 POM, PTD	Post-midcourse
January 9	21:00:00.0	FINAL	$R - 5$ h, 40 min

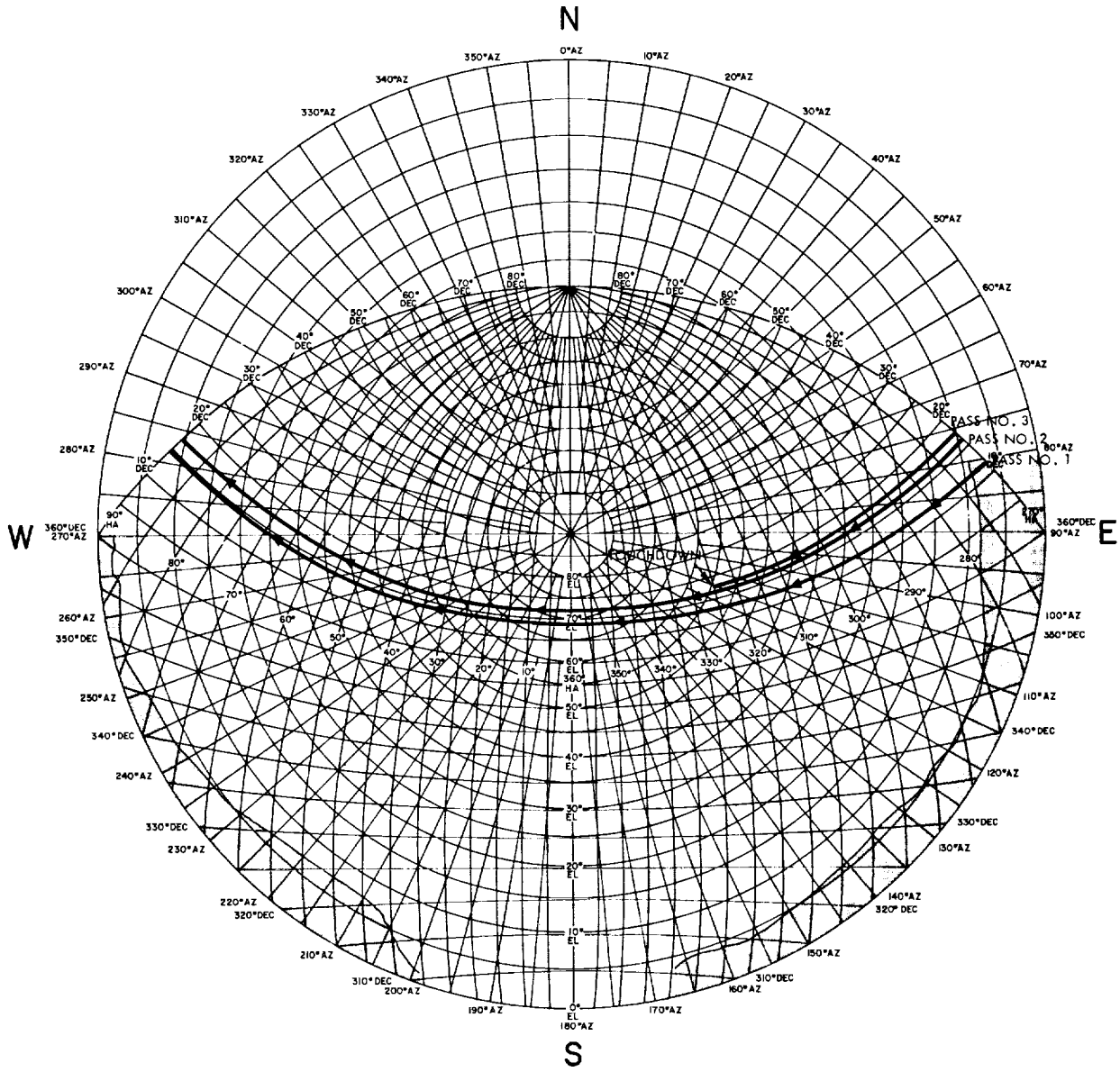

Fig. 57. DSS 11 stereographic projection, *Surveyor VII*

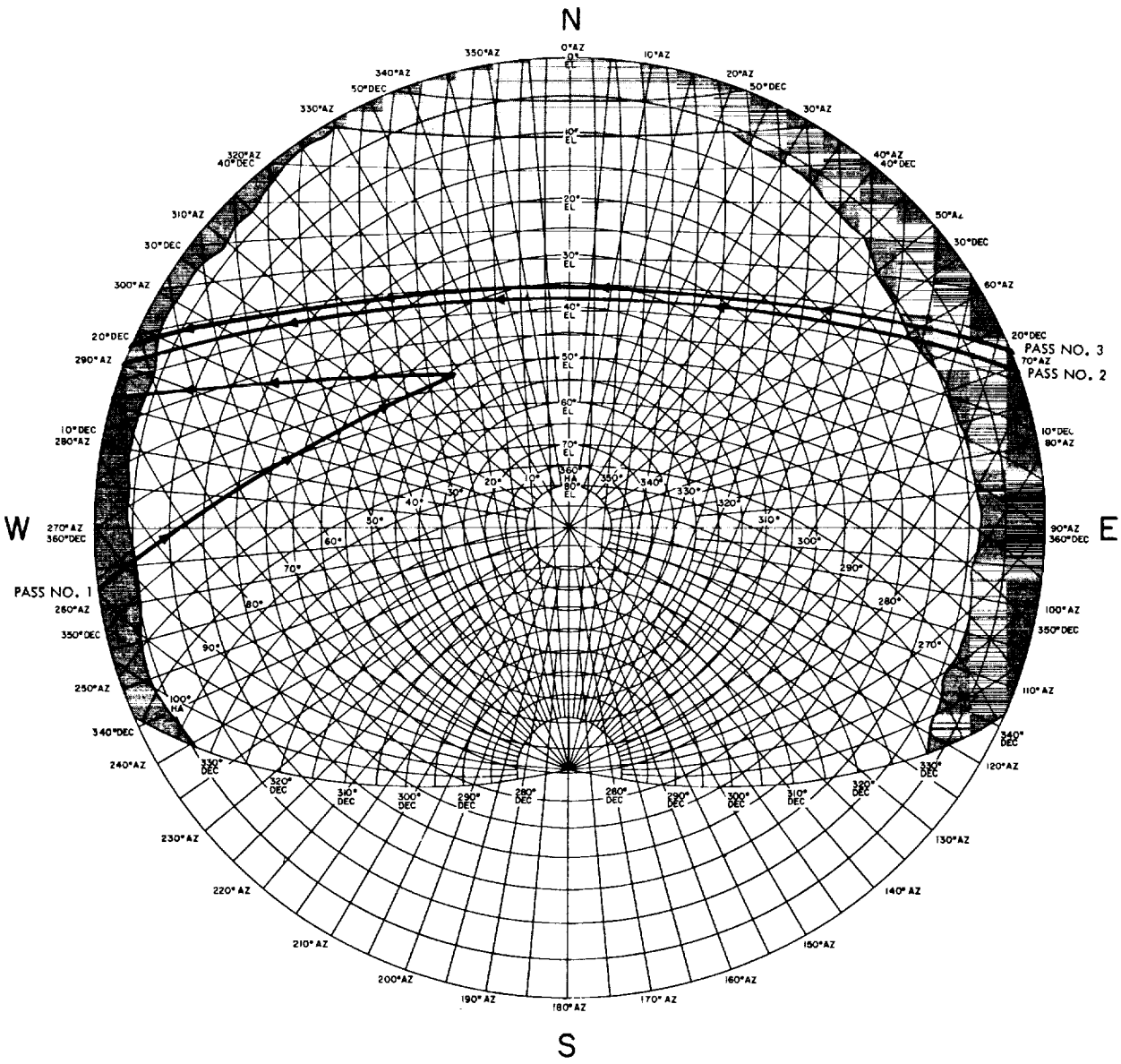

Fig. 58. DSS 42 stereographic projection, *Surveyor VII*

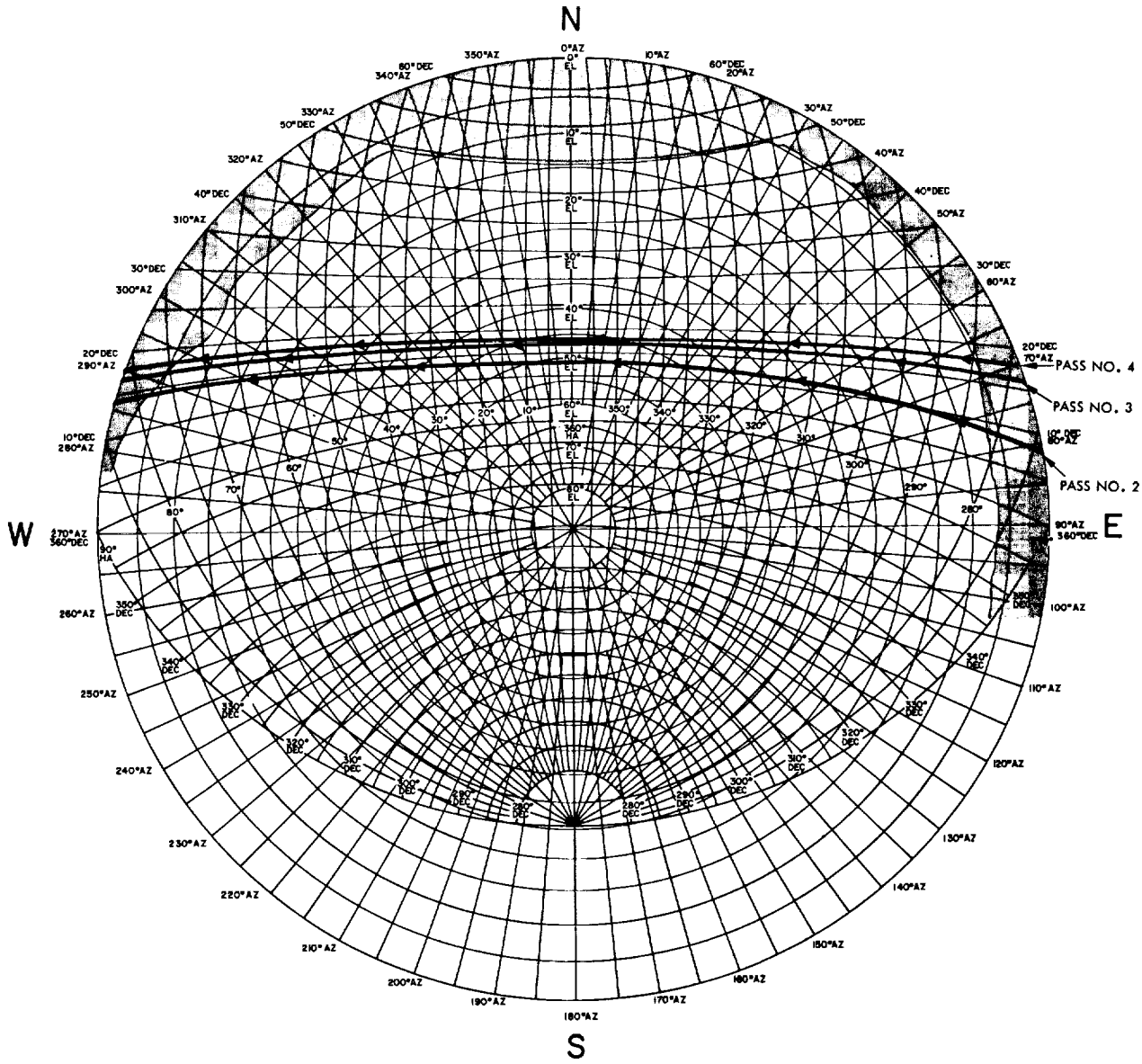

Fig. 59. DSS 51 stereographic projection, *Surveyor VII*

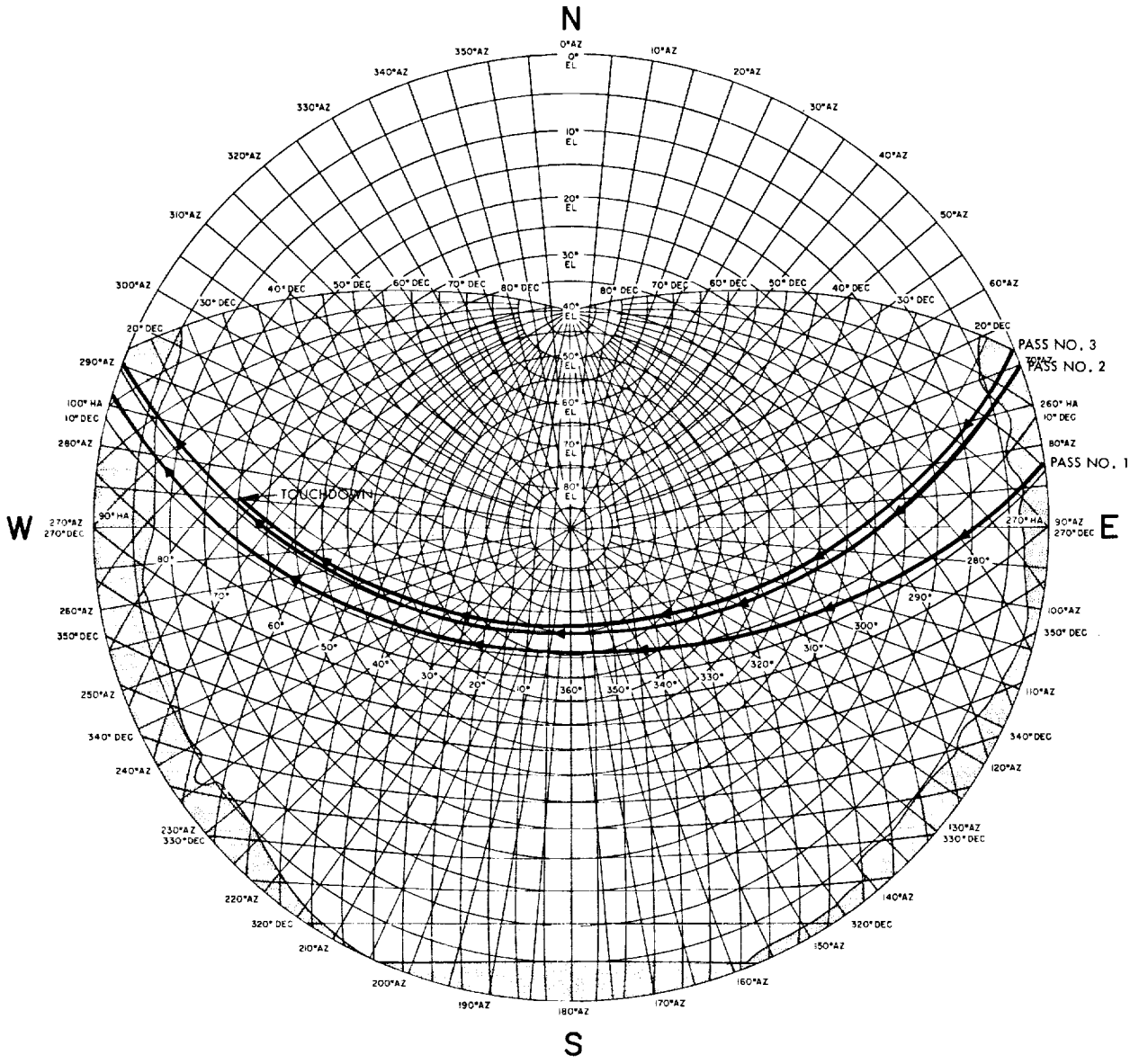

Fig. 60. DSS 61 stereographic projection, *Surveyor VII*

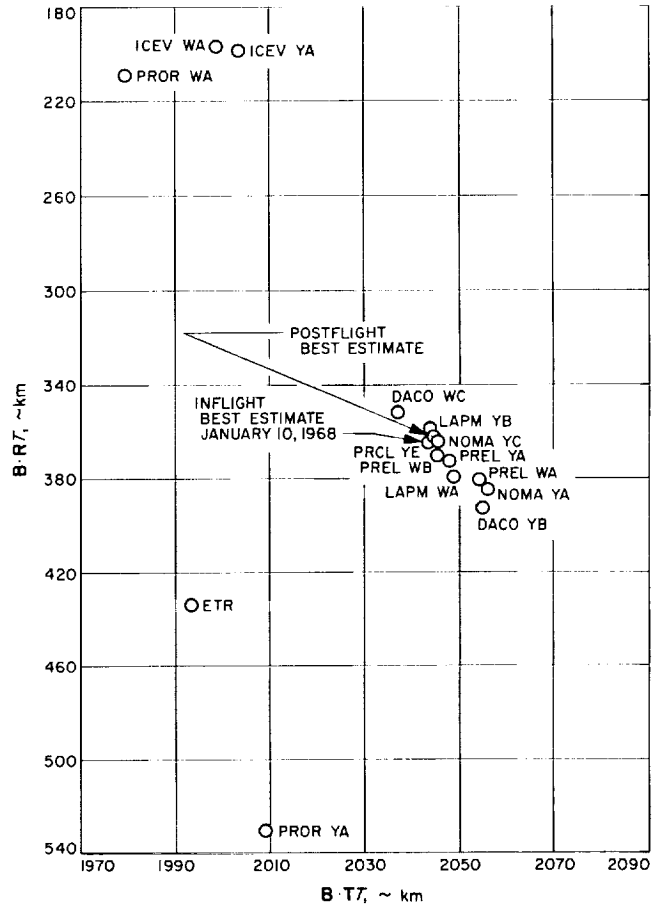

Fig. 61. Estimated pre-midcourse unbraked impact point, *Surveyor VII*

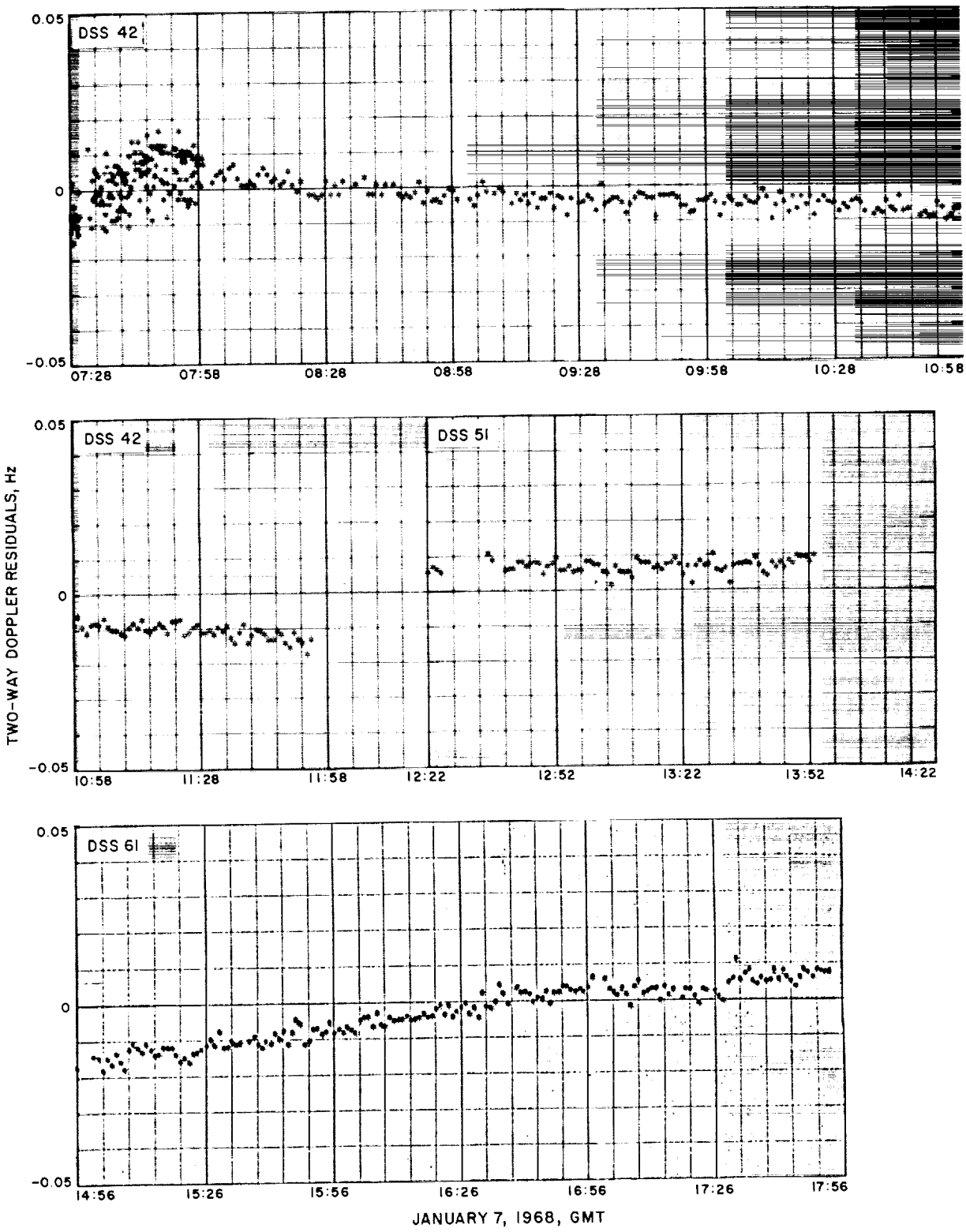

Fig. 62. Pre-midcourse two-way doppler residuals, *Surveyor VII* (inflight best estimate, PRCL YE, solution)

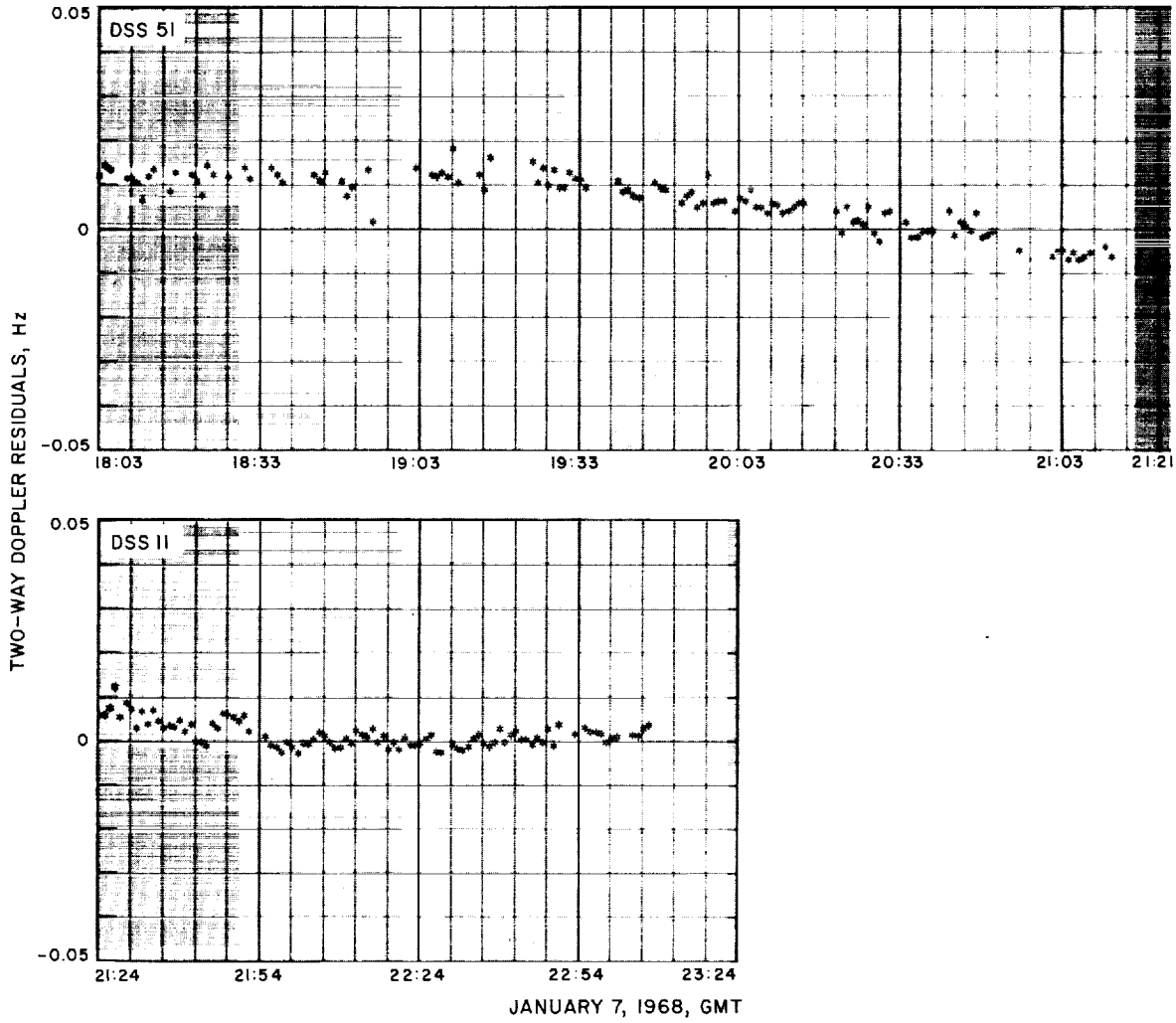
DSS 51
0.05
0
-0.05
18:03
18:33
19:03
19:33
20:03
20:33
21:03
21:21
DSS 11
0.05
0
-0.05
21:24
21:54
22:24
22:54
23:24
TWO-WAY DOPPLER RESIDUALS, Hz
JANUARY 7, 1968, GMT

Fig. 62 (contd)

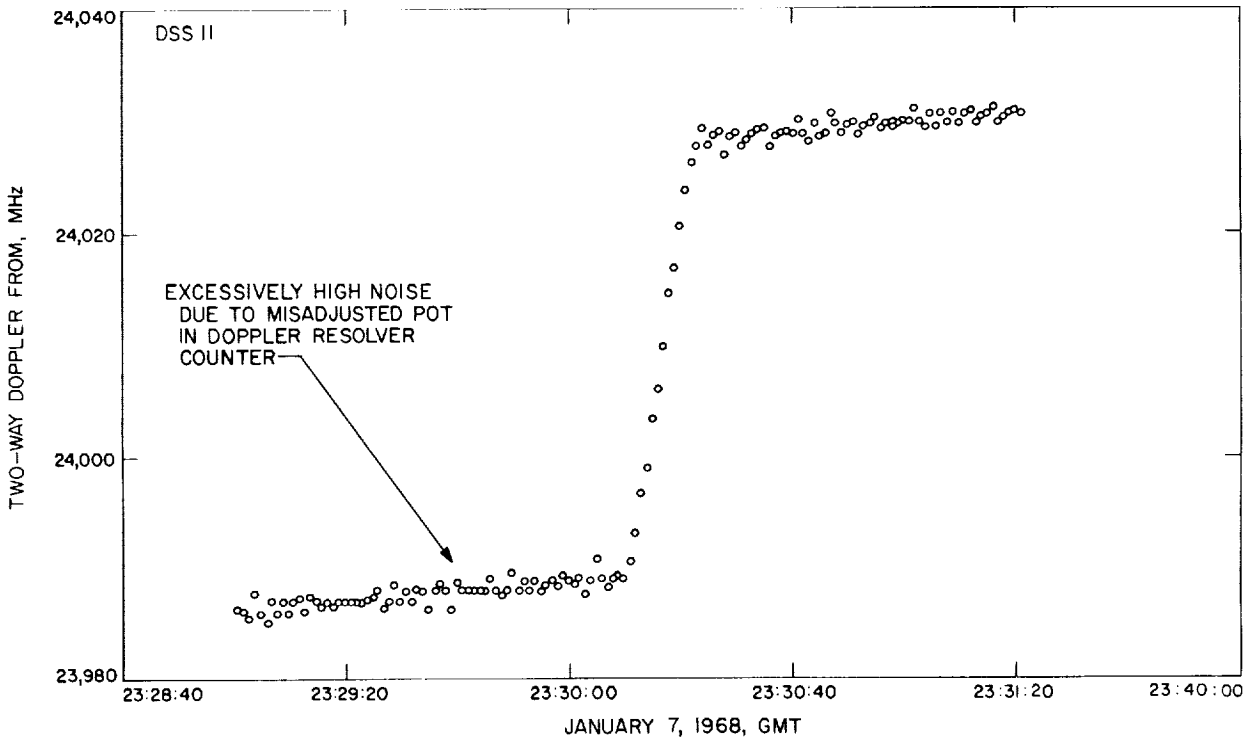

Fig. 63. Midcourse maneuver doppler data, *Surveyor VII*

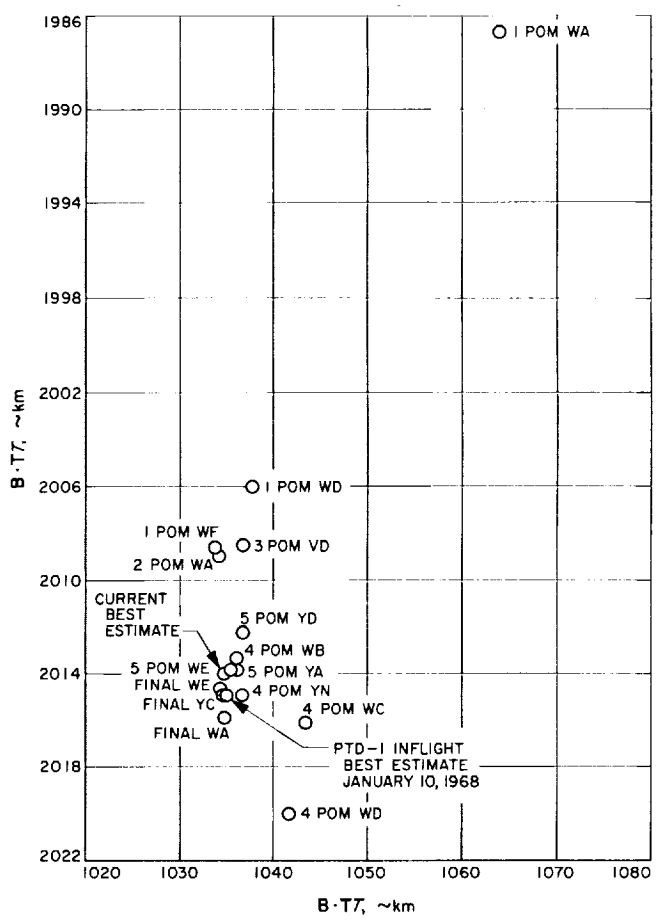

Fig. 64. Post-midcourse unbraked impact point, *Surveyor VII*

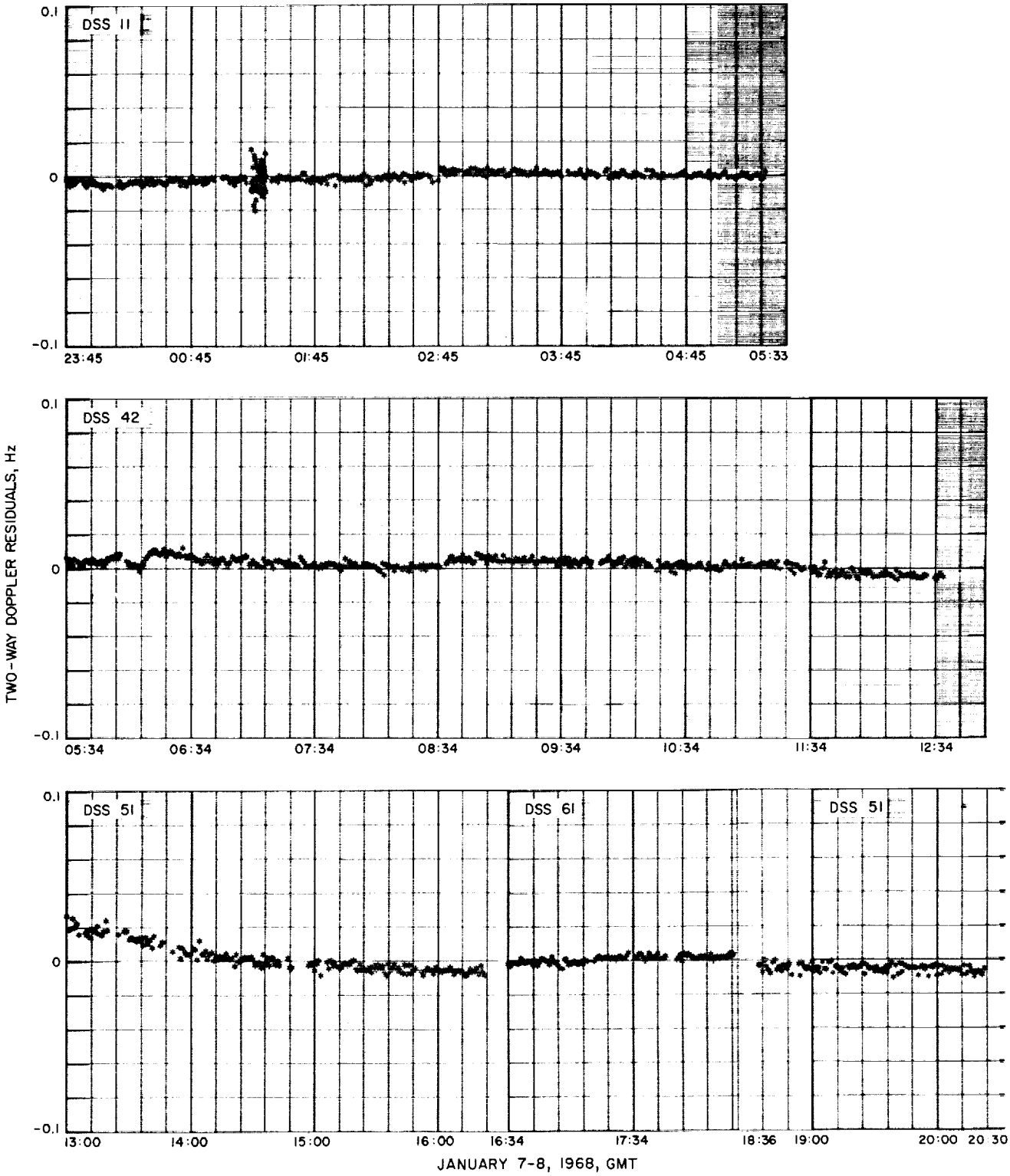

Fig. 65. Postmaneuver doppler residuals, *Surveyor VII* (inflight best estimate, PTD-1 solution)

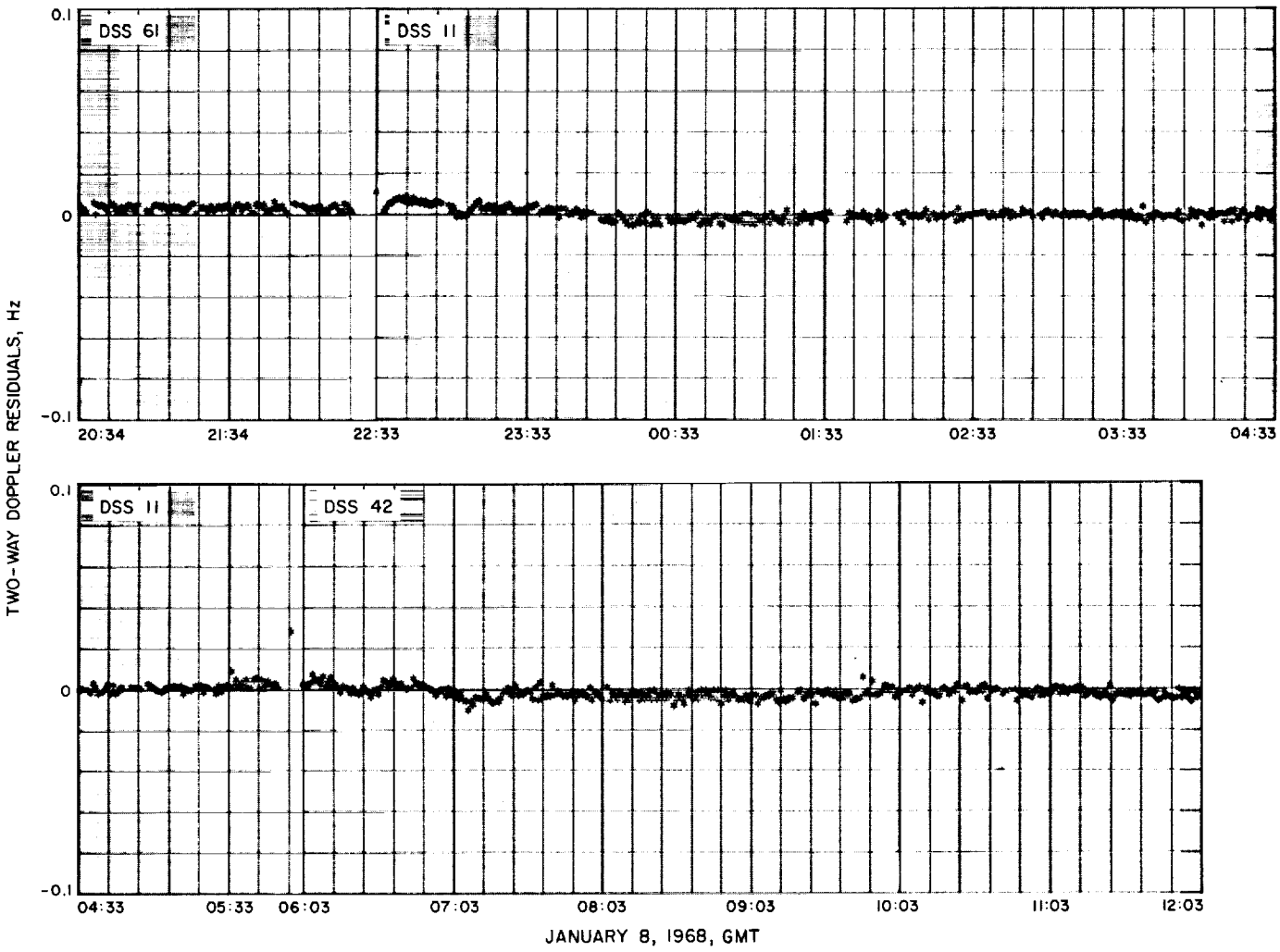
DSS 61
DSS 11
0.1
0
-0.1
20:34
21:34
22:33
23:33
00:33
01:33
02:33
03:33
04:33
DSS 11
DSS 42
0.1
0
-0.1
04:33
05:33
06:03
07:03
08:03
09:03
10:03
11:03
12:03
TWO-WAY DOPPLER RESIDUALS, Hz
JANUARY 8, 1968, GMT

Fig. 65 (contd)

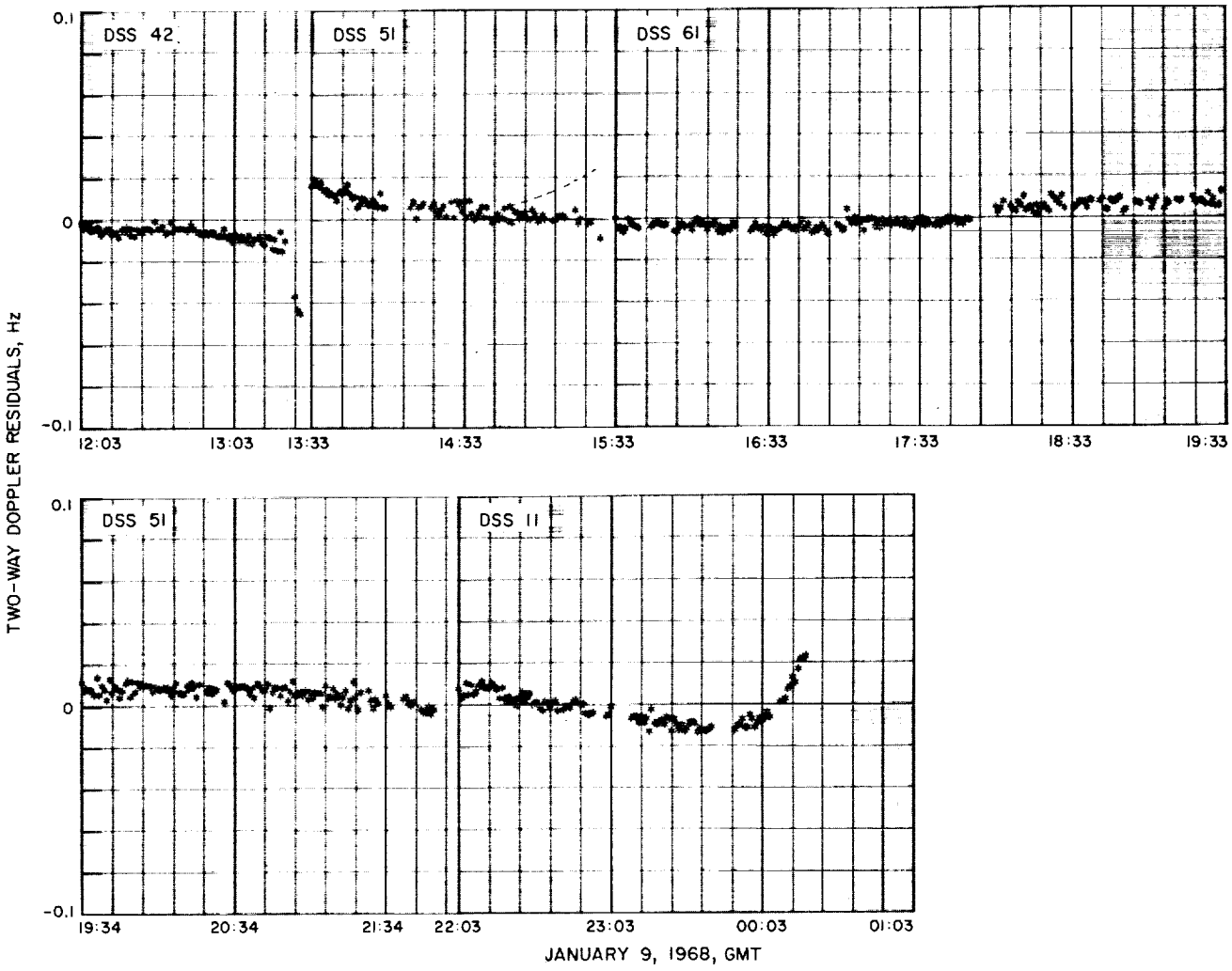
DSS 42
DSS 51
DSS 61
DSS 51
DSS 11
0.1
0
-0.1
12:03
13:03
13:33
14:33
15:33
16:33
17:33
18:33
19:33
19:34
20:34
21:34
22:03
23:03
00:03
01:03
TWO-WAY DOPPLER RESIDUALS, Hz
JANUARY 9, 1968, GMT

Fig. 65 (contd)

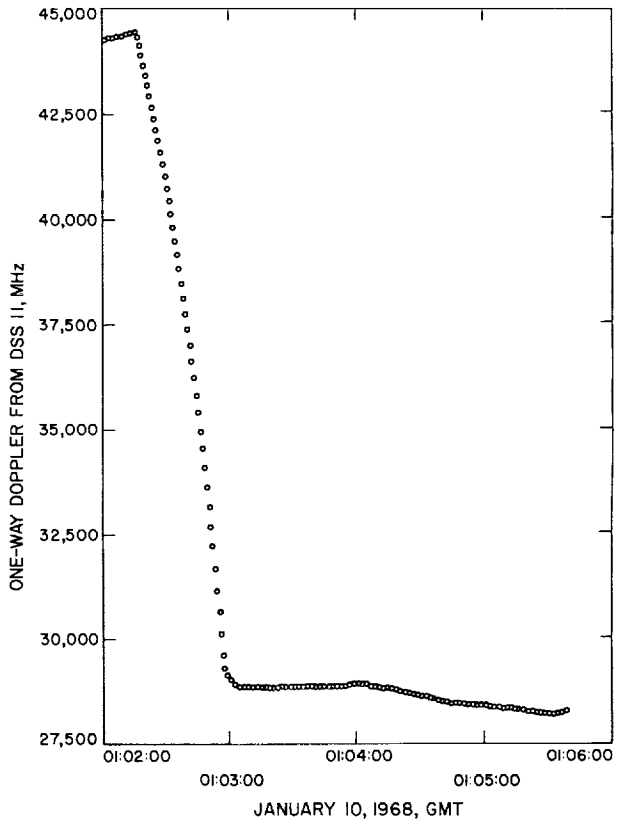

Fig. 66. Retromaneuver phase doppler data, *Surveyor VII*

Table 54. *Surveyor VII* postmaneuver computations

Orbit ID	Time computed, GMT		Target statistics							
	Start	Stop	B, km	B • TT, km	B • RT, km	TL, h	SMAA, km (1σ)	SMIA, km (1σ)	THETA, deg	$\sigma_{T,\ impact}$, s (1σ)
1 POM WA	02:55	03:11	2253.88	1064.32	1986.76	49.32	122.28	24.83	14.75	38.887
1 POM WD	06:32	06:40	2258.53	1037.95	2005.89	49.32	196.49	62.31	47.99	262.56
1 POM WF	08:38	08:47	2259.11	1033.92	2008.63	49.32	139.33	16.70	66.68	41.342
2 POM WA	09:21	09:40	2259.53	1034.42	2008.85	49.32	138.73	14.17	66.73	35.792
3 POM YA	13:01	13:30	2256.07	1036.43	2003.91	49.32	33.302	11.49	56.27	30.901
3 POM YB	14:34	14:47	2260.73	1036.68	2009.03	49.32	29.656	5.039	57.99	14.530
3 POM WB	16:38	17:00	2261.36	1035.49	2010.35	49.32	21.938	3.983	62.73	9.2499
3 POM WC	17:12	17:34	2260.18	1036.54	2008.48	49.32	19.976	3.926	61.04	8.9475
3 POM YD	15:50	16:25	2260.33	1036.92	2008.46	49.32	21.188	3.537	59.72	9.6952
4 POM WA	21:17	21:41	2261.91	1037.22	2010.08	49.32	18.285	3.027	60.11	8.3373
4 POM WB	23:01	23:21	2264.23	1036.02	2013.31	49.32	15.706	2.731	59.20	7.4480
4 POM WC	23:46	00:30	2270.17	1043.50	2016.13	49.32	23.063	15.86	77.48	9.2005
4 POM WD	01:18	01:39	2272.78	1041.74	2019.98	49.32	30.714	19.716	91.74	11.716
4 POM WG	06:40	07:05	2266.44	1035.23	2016.19	49.32	10.65	2.484	69.33	4.3418
4 POM WH	07:09	07:28	2264.08	1036.05	2013.12	49.32	12.27	2.245	68.35	4.8841
4 POM WI	08:03	08:24	2263.76	1036.35	2012.61	49.32	12.56	2.250	68.15	5.0370
4 POM WP	11:25	11:45	2262.11	1037.22	2010.31	49.32	7.987	1.956	70.69	3.0774
4 POM YK	12:22	12:47	2264.52	1033.82	2014.76	49.32	27.770	9.026	72.54	15.454
4 POM YN	18:30	19:03	2265.91	1036.67	2014.86	49.32	7.414	2.054	74.63	2.6573
5 POM YA	18:45	19:50	2264.75	1036.15	2013.82	49.32	15.622	6.133	63.152	5.8582
5 POM YD[a]	21:00	21:39	2263.62	1036.74	2012.25	49.32	11.68	5.474	68.22	3.3393
5 POM WE	21:30	22:03	2264.50	1035.67	2013.79	49.32	4.630	0.6770	82.15	1.5021
FINAL WA	23:04	23:18	2265.97	1034.72	2015.93	5.720	1.8401	0.8584	88.71	0.72792
FINAL YA	23:08	23:18	2266.09	1034.72	2016.06	5.720	1.8247	0.8584	88.71	0.72202
FINAL YB	23:27	23:37	2265.75	1034.68	2015.70	5.720	1.6906	0.8521	87.04	0.67536
FINAL WC	23:35	23:46	2265.48	1034.64	2015.42	5.720	1.5328	0.8283	82.71	0.62170
FINAL YC	23:39	23:50	2264.95	1034.49	2014.90	5.720	1.2657	0.6435	63.98	0.52028
FINAL WD	23:50	00:12	2264.93	1034.49	2014.88	5.720	1.2477	0.6134	62.02	0.51233
FINAL WE	00:13	00:28	2264.77	1034.44	2014.73	5.720	1.1963	0.4738	55.37	0.48781
FINAL YD	00:19	00:30	2264.73	1034.43	2014.68	5.720	1.1911	0.4517	54.58	0.48527
FINAL WF	00:33	00:45	2264.60	1034.40	2014.56	5.720	1.1753	0.3908	52.56	0.47988
FINAL YE	00:35	00:50	2264.60	1034.40	2014.56	5.720	1.1761	0.3920	52.60	0.47995
PTD−1[b]	POST	FLIGHT	2265.09	1034.81	2014.89	49.32	3.808	1.44	28.13	0.84805

[a]Orbit used for terminal maneuver computations.

[b]Current best estimate, postmaneuver, as of January 10, 1968.

Table 54 (contd)

Orbit ID	Target statistics (contd)		Selenocentric conditions at unbraked impact			Type solution	Data and source
	PHI_{BR}, deg	SVFIXR, m/s (1σ)	Latitude, deg (south)	Longitude, deg	Jan. 10, 1968, GMT		
1 POM WA	3.151	0.6252	−40.534	349.334	01:02:38.131	6 × 6	Premaneuver *a priori* DSS 11, only
1 POM WD	13.685	0.9926	−41.010	348.784	01:02:46.394	6 × 6	No *a priori* DSS 11, DSS 42
1 POM WF	2.513	0.6251	−41.079	348.697	01:02:53.240	6 × 6	No *a priori* DSS 11, DSS 42
2 POM WA	2.271	0.6215	−41.084	348.71	01:02:52.028	6 × 6	No *a priori* DSS 11, DSS 42
3 POM YA	1.656	0.6188	−40.967	348.72	01:02:51.660	6 × 6	CC3, DSS 11, DSS 42
3 POM YB	0.6425	0.6121	−41.085	348.78	01:02:45.581	6 × 6	CC3, DSS 11, DSS 42, DSS 51
3 POM WB	0.3885	0.6114	−41.117	348.76	01:02:46.601	6 × 6	CC3, DSS 11, DSS 42, DSS 51
3 POM WC	0.3838	0.6114	−41.072	348.77	01:02:45.841	6 × 6	CC3, DSS 11, DSS 42, DSS 51, DSS 61
3 POM YD	0.4145	0.6115	−41.071	348.78	01:02:45.525	6 × 6	CC3, DSS 11, DSS 42, DSS 51, DSS 61
4 POM WA	0.3532	0.6114	−41.109	348.80	01:02:45.462	6 × 6	CC3, DSS 11, DSS 42, DSS 51, DSS 61
4 POM WB	0.31843	0.6113	−41.186	348.80	01:02:46.584	6 × 6	CC3, DSS 11, DSS 42, DSS 51, DSS 61
4 POM WC	0.42626	0.6146	−41.244	349.03	01:02:47.004	17 × 17	CC3, (DSS 11, DSS 42, DSS 51, DSS 61) Station location and jets
4 POM WD	0.52075	0.6169	−41.34	349.02	01:02:48.422	17 × 17	CC3, (DSS 11, DSS 42, DSS 51, DSS 61) Station location and jets
4 POM WG	0.1657	0.6111	−41.25	348.80	01:02:47.974	6 × 6	CC3, DSS 11, DSS 42, DSS 61
4 POM WH	0.1835	0.6111	−41.18	348.80	01:02:46.927	6 × 6	CC3, DSS 11, DSS 42, DSS 51
4 POM WI	0.1889	0.6111	−41.17	348.80	01:02:46.627	6 × 6	CC3, DSS 11, DSS 42, DSS 51 (2nd pass)
4 POM WP	0.11550	0.6111	−41.114	348.80	01:02:45.516	6 × 6	CC3, DSS 11, DSS 42, DSS 51
4 POM YK	0.60492	0.6132	−41.222	348.75	01:02:51.446	17 × 17	CC3, DSS 11, DSS 42, DSS 51
4 POM YN	0.09508	0.6111	−41.222	348.83	01:02:46.578	14 × 14	CC3, DSS 11, DSS 42, DSS 51, DSS 61
5 POM YA	0.26075	0.6123	−41.198	348.81	01:02:48.673	17 × 17	CC3, DSS 11, DSS 42, DSS 51, DSS 61
5 POM YD[a]	0.14545	0.6118	−41.161	348.81	01:02:47.393	17 × 17	CC3, DSS 11, DSS 42, DSS 51, DSS 61
5 POM WE	4.1010	0.6110	−41.198	348.79	01:02:47.064	6 × 6	CC3, DSS 11, DSS 42, DSS 51, DSS 61
FINAL WA	2.1032	0.6110	−41.249	348.79	01:02:48.315	10 × 10	CC3, DSS 11, DSS 51
FINAL YA	0.02102	0.6110	−41.252	348.79	01:02:48.365	10 × 10	CC3, DSS 11, DSS 51
FINAL YB	0.02093	0.6110	−41.243	348.78	01:02:48.229	10 × 10	CC3, DSS 11, DSS 51
FINAL WC	0.02083	0.6110	−41.237	348.78	01:02:48.123	10 × 10	CC3, DSS 11, DSS 51
FINAL YC	0.02713	0.6110	−41.225	348.77	01:02:47.92	10 × 10	CC3, DSS 11, DSS 51
FINAL WD	0.02068	0.6110	−41.225	348.77	01:02:47.936	10 × 10	CC3, DSS 11, DSS 51
FINAL WE	0.02591	0.6110	−41.221	348.77	01:02:47.888	10 × 10	CC3, DSS 11, DSS 51
FINAL YD	0.02058	0.6110	−41.220	348.77	01:02:47.877	10 × 10	CC3, DSS 11, DSS 51
FINAL WF	0.02487	0.6110	−41.217	348.76	01:02:47.844	10 × 10	CC3, DSS 11, DSS 51
FINAL YE	0.02050	0.6110	−41.217	348.76	01:02:47.845	10 × 10	CC3, DSS 11, DSS 51
PTD−1[b]	0.06407	0.6112	−41.224	348.78	01:02:48.056	17 × 17	CC3, DSS 11, DSS 42, DSS 51, DSS 61 All post-midcourse data

Table 55. *Surveyor VII* postmaneuver position and velocity at injection epoch[a]

Orbit ID	Geocentric space-fixed position			Geocentric space-fixed velocity			Uncertainties, 1σ					
							Position			Velocity		
	x, km	y, km	z, km	Dx, km/s	Dy, km/s	Dz, km/s	σ_x, km	σ_y, km	σ_z, km	σ_{Dx}, m/s	σ_{Dy}, m/s	σ_{Dz}, m/s
1 POM YA	137531.32	91462.119	41092.872	1.2432098	1.2848534	0.62835553	0.68760	0.92051	2.2141	0.48119	0.65181	0.16169
1 POM WD	137529.88	91469.689	41085.346	1.2431299	1.2849978	0.62832630	64.373	63.214	357.61	0.84862	1.7219	1.5261
1 POM WF	137528.45	91468.092	41076.658	1.2431059	1.2850451	0.62835547	21.180	12.526	69.073	0.20945	0.49889	0.80994
2 POM WA	137528.82	91468.421	41078.486	1.2431097	1.2850385	0.62834565	20.298	11.156	61.986	0.19838	0.48328	0.79234
3 POM YA	137528.05	91468.245	41076.695	1.2431154	1.2850226	0.62837623	7.9531	9.6623	43.474	0.11715	0.22870	0.24021
3 POM YB	137530.51	91470.200	41088.956	1.2431279	1.2850029	0.62829723	2.7428	5.3847	8.6926	0.07764	0.16104	0.08675
3 POM WB	137530.54	91469.914	41088.396	1.2431222	1.2850138	0.62829484	2.6503	4.4500	4.4746	0.05145	0.11064	0.07815
3 POM WC	137530.36	91470.118	41088.488	1.2431267	1.2850038	0.62830254	2.3976	4.3538	4.4969	0.05012	0.10499	0.06600
3 POM YD	137530.40	91470.230	41088.755	1.2431287	1.2850009	0.62830070	2.3392	4.4809	4.7225	0.05380	0.11285	0.06381
4 POM WA	137530.59	91470.490	41088.766	1.2431312	1.2850013	0.62829070	2.2330	4.2007	4.1013	0.04651	0.09775	0.05578
4 POM WB	137530.92	91470.117	41088.403	1.2431262	1.2850154	0.62827679	2.0771	4.0098	3.8429	0.04187	0.08657	0.04573
4 POM WC	137529.17	91468.651	41087.089	1.2431145	1.2850195	0.62831412	4.9140	5.2127	5.7330	0.06194	0.12274	0.12208
4 POM WD	137529.88	91468.251	41086.598	1.2431055	1.2850416	0.62829654	5.4443	6.0084	7.7841	0.06369	0.11206	0.13839
4 POM WG	137531.38	91469.225	41087.465	1.2431210	1.2850301	0.62826648	1.9844	3.3033	2.4211	0.02314	0.05193	0.04152
4 POM WH	137531.02	91469.647	41087.841	1.2431248	1.2850176	0.62828016	2.1262	3.4498	2.4198	0.02572	0.05939	0.04722
4 POM WI	137530.96	91469.743	41088.178	1.2431262	1.2850143	0.62828108	2.1558	3.4898	2.6287	0.02627	0.06096	0.04735
4 POM WP	137530.51	91470.583	41088.616	1.2431316	1.2850014	0.62828992	1.7125	2.7490	2.1043	0.01676	0.03783	0.03264
4 POM YK	137529.12	91467.745	41084.025	1.2431178	1.2850282	0.62830776	9.0969	6.6884	14.900	0.07835	0.15692	0.26095
4 POM YN	137530.85	91470.423	41088.402	1.2431305	1.2850143	0.62826672	1.6511	2.6607	2.7307	0.01440	0.03258	0.03370
5 POM YA	137530.01	91468.629	41085.516	1.2431190	1.2850295	0.62828979	4.1646	5.2876	7.3957	0.05186	0.07679	0.10564

[a]See Table 53 for epochs used.

Table 55 (contd)

Orbit ID	Geocentric space-fixed position			Geocentric space-fixed velocity			Uncertainties, 1σ					
							Position			Velocity		
	x, km	y, km	z, km	Dx, km/s	Dy, km/s	Dz, km/s	σ_x, km	σ_y, km	σ_z, km	σ_{Dx}, m/s	σ_{Dy}, m/s	σ_{Dz}, m/s
5 POM YD	137530.41	91469.043	41086.542	1.2431183	1.2850328	0.62827703	2.9848	4.0519	4.6305	0.04115	0.06186	0.06951
5 POM WE	137531.04	91469.876	41087.565	1.2431239	1.2850200	0.62827803	1.4976	2.4098	1.5112	0.00665	0.01862	0.02302
FINAL WA	267038.74	242161.32	116113.79	0.65827227	0.76464719	0.38647574	0.23353	0.97187	1.3897	0.01190	0.01398	0.01472
FINAL YA	267038.73	242161.34	116113.68	0.65827160	0.76464829	0.38647531	0.23368	0.97171	1.3780	0.01184	0.01382	0.01470
FINAL YB	267038.73	242161.32	116113.97	0.65827363	0.76464535	0.38647649	0.23281	0.97111	1.2647	0.01120	0.01269	0.01454
FINAL WC	267038.72	242161.31	116114.20	0.65827518	0.7646431	0.38647745	0.22884	0.97063	1.1166	0.01047	0.011507	0.01433
FINAL YC	267038.67	242161.34	116114.64	0.65827756	0.76464009	0.38647939	0.21197	0.97029	0.76359	0.00942	0.00987	0.01388
FINAL WD	267038.67	242161.34	116114.66	0.65827760	0.76464003	0.38647947	0.21020	0.96973	0.72806	0.00937	0.00978	0.01383
FINAL WE	267038.65	242161.33	116114.78	0.65827783	0.76463956	0.38648018	0.20486	0.96944	0.59704	0.009311	0.009644	0.013626
FINAL YD	267038.65	242161.33	116114.82	0.65827775	0.76463956	0.38648044	0.20443	0.96973	0.58004	0.00931	0.00964	0.01359
FINAL WF	267038.64	242161.31	116114.92	0.65827741	0.76463866	0.38648121	0.20315	0.96786	0.53450	0.00926	0.00964	0.01347
FINAL YE	267038.64	242161.31	116114.91	0.65827738	0.76463967	0.38648120	0.20329	0.96835	0.53574	0.00926	0.00964	0.01348
PTD-1	137530.65	91469.543	41087.172	1.2431289	1.2850197	0.62826964	1.7995	2.5750	3.0459	0.02049	0.03747	0.04403

Table 56. Summary of postmaneuver DSS tracking data used in *Surveyor VII* orbit computations

Orbit ID	Station	Data type	Begin data		End data		Number of points	Standard deviation	Root mean square	Mean error	Sample data rate, s
			Date 1968	GMT	Date 1968	GMT					
1 POM WA	DSS 11	CC3	1/7	23:45:32	1/8	02:44:32	207	0.00591	0.00598	−0.000886	10[a], 60
1 POM WD	DSS 11	CC3	1/7	23:45:32	1/8	05:23:32	361	0.00318	0.00318	−0.0000534	10[a], 60
	DSS 42	CC3	1/8	05:34:32	1/8	06:09:32	36	0.00322	0.00325	0.000434	60
1 POM WF	DSS 11	CC3	1/7	23:45:32	1/8	05:23:32	361	0.00320	0.00320	0.0000210	10[a], 60
	DSS 42	CC3	1/8	05:34:32	1/8	08:24:32	170	0.00289	0.00289	−0.0000359	60
2 POM WA	DSS 11	CC3	1/7	23:45:32	1/8	05:23:32	361	0.00317	0.00317	0.0000568	10[a], 60
	DSS 42	CC3	1/8	05:34:32	1/8	09:14:32	218	0.00273	0.00273	0.0000706	60
3 POM YA	DSS 11	CC3	1/7	23:45:32	1/8	05:23:32	355	0.00322	0.00322	0.0000805	10[a], 60
	DSS 42	CC3	1/8	05:34:32	1/8	12:44:32	327	0.00245	0.00245	−0.0000149	60
3 POM YB	DSS 11	CC3	1/7	23:45:32	1/8	05:23:32	355	0.00460	0.00463	0.000496	10[a], 60
	DSS 42	CC3	1/8	05:34:32	1/8	12:38:32	326	0.00305	0.00318	−0.000915	60
	DSS 51	CC3	1/8	12:49:32	1/8	14:37:32	64	0.00730	0.00752	0.00183	60
3 POM WB	DSS 11	CC3	1/7	23:45:32	1/8	05:23:32	361	0.00496	0.00499	0.000517	10[a], 60
	DSS 42	CC3	1/8	05:34:32	1/8	12:38:32	409	0.00294	0.00310	−0.000992	60
	DSS 51	CC3	1/8	12:49:32	1/8	16:23:32	185	0.00499	0.00507	0.000858	60
3 POM WC	DSS 11	CC3	1/7	23:45:32	1/8	05:23:32	361	0.00475	0.00479	0.000671	10[a], 60
	DSS 42	CC3	1/8	05:34:32	1/8	12:38:32	409	0.00257	0.00280	−0.00113	60
	DSS 51	CC3	1/8	13:00:32	1/8	16:23:32	174	0.00463	0.00487	0.00151	60
	DSS 61	CC3	1/8	16:34:32	1/8	17:01:32	28	0.00173	0.00342	−0.00295	60
3 POM YD	DSS 51	CC3	1/8	13:00:32	1/8	15:58:32	149	0.00543	0.00551	0.000943	60
	DSS 61	CC3	1/8	16:34:32	1/8	18:23:32	104	0.00354	0.00370	−0.00106	60
	DSS 61	CC3	1/8	20:33:32	1/8	20:37:32	5	0.000826	0.0173	0.0172	60
	DSS 11	CC3	1/7	23:45:32	1/8	05:23:32	361	0.00460	0.00462	0.000479	10[a], 60
	DSS 42	CC3	1/8	05:34:32	1/8	12:38:32	409	0.00284	0.00296	−0.000833	60
4 POM WA	DSS 11	CC3	1/7	23:45:32	1/8	05:23:32	361	0.00375	0.00376	0.000171	10[a], 60
	DSS 42	CC3	1/8	05:34:32	1/8	12:38:32	409	0.00484	0.00492	−0.000883	60
	DSS 51	CC3	1/8	13:00:32	1/8	16:23:32	174	0.00597	0.00598	0.000276	60
	DSS 51	CC3	1/8	18:34:32	1/8	20:23:32	60	0.00261	0.0109	0.0106	60
	DSS 61	CC3	1/8	16:34:32	1/8	18:23:32	104	0.00309	0.00628	−0.00546	60
	DSS 61	CC3	1/8	20:33:32	1/8	20:55:32	21	0.00162	0.00968	0.00954	60
4 POM WB	DSS 11	CC3	1/7	23:45:32	1/8	05:23:32	361	0.00353	0.00354	−0.000288	60
	DSS 11	CC3	1/8	22:33:32	1/8	22:45:32	5	0.00159	0.00375	−0.00339	10[a], 60
	DSS 42	CC3	1/8	05:34:32	1/8	12:38:32	409	0.00645	0.00646	−0.000363	10[a], 60
	DSS 51	CC3	1/8	13:00:32	1/8	16:23:32	174	0.00524	0.00526	0.000502	60
	DSS 51	CC3	1/8	18:34:32	1/8	20:23:32	74	0.00215	0.00646	0.00609	60
	DSS 61	CC3	1/8	16:34:32	1/8	18:23:32	104	0.00337	0.00990	−0.00931	60
	DSS 61	CC3	1/8	20:33:32	1/8	22:23:32	104	0.00231	0.00703	0.00664	60
4 POM WC	DSS 11	CC3	1/7	23:45:32	1/8	05:23:32	361	0.00408	0.00411	0.000552	10[a], 60
	DSS 11	CC3	1/8	22:33:32	1/8	23:30:32	49	0.00377	0.00383	−0.000693	10[a], 60
	DSS 42	CC3	1/8	05:34:32	1/8	12:38:32	409	0.00360	0.00384	−0.00133	60

[a]Between 01:14 and 01:22 GMT.

Table 56 (contd)

Orbit ID	Station	Data type	Begin data		End data		Number of points	Standard deviation	Root mean square	Mean error	Sample data rate, s
			Date 1968	GMT	Date 1968	GMT					
4 POM WC (contd)	DSS 51	CC3	1/8	13:00:32	1/8	16:23:32	174	0.00579	0.00623	0.00230	60
	DSS 51	CC3	1/8	18:34:32	1/8	20:23:32	74	0.00213	0.00463	0.00411	60
	DSS 61	CC3	1/8	16:34:32	1/8	18:23:32	104	0.00238	0.00497	−0.00436	60
	DSS 61	CC3	1/8	20:33:32	1/8	22:23:32	104	0.00170	0.00248	0.00180	60
4 POM WD	DSS 11	CC3	1/7	23:45:32	1/8	05:23:32	361	0.00367	0.00367	0.0000991	10[a], 60
	DSS 11	CC3	1/8	22:33:32	1/9	00:45:32	125	0.00412	0.00414	−0.000432	10[a], 60
	DSS 42	CC3	1/8	05:34:32	1/8	12:38:32	409	0.00367	0.00374	−0.000734	60
	DSS 51	CC3	1/8	13:00:32	1/8	16:23:32	174	0.00465	0.00473	0.000874	60
	DSS 51	CC3	1/8	18:34:32	1/8	20:23:32	109	0.00251	0.00362	0.00260	60
	DSS 61	CC3	1/8	16:34:32	1/8	18:23:32	104	0.00313	0.00421	−0.00281	60
	DSS 61	CC3	1/8	20:33:32	1/8	22:23:32	104	0.00156	0.00208	0.00137	60
4 POM WG	DSS 11	CC3	1/7	23:47:32	1/8	05:22:02	75	0.00220	0.00257	−0.00132	10[a], 60
	DSS 11	CC3	1/8	22:33:32	1/9	04:21:02	69	0.00318	0.00356	−0.00160	10[a], 60
	DSS 42	CC3	1/8	05:36:32	1/8	12:36:32	81	0.00736	0.00739	0.000732	60
	DSS 61	CC3	1/8	13:02:32	1/8	18:22:02	22	0.00279	0.00434	−0.00333	60
	DSS 61	CC3	1/8	20:35:32	1/8	22:22:02	22	0.00132	0.00983	0.00974	60
4 POM WH	DSS 11	CC3	1/7	23:47:32	1/8	05:22:02	75	0.00195	0.00201	−0.000469	10[a], 60
	DSS 11	CC3	1/8	22:33:32	1/9	04:53:02	75	0.00458	0.00478	−0.00137	10[a], 60
	DSS 42	CC3	1/8	05:36:32	1/8	12:36:32	81	0.00597	0.00606	−0.00102	60
	DSS 51	CC3	1/8	13:02:32	1/8	16:23:02	33	0.00332	0.00389	0.00201	60
	DSS 51	CC3	1/8	18:36:32	1/8	20:21:32	18	0.00131	0.0103	0.0103	60
4 POM WI	DSS 11	CC3	1/7	23:47:32	1/8	05:22:02	75	0.00228	0.00236	−0.000625	10[a], 60
	DSS 11	CC3	1/8	22:33:32	1/9	05:32:32	83	0.00617	0.00617	−0.000141	10[a], 60
	DSS 42	CC3	1/8	05:36:32	1/8	12:36:32	81	0.00520	0.00521	0.000214	60
	DSS 51	CC3	1/8	13:02:32	1/8	16:23:02	30	0.00191	0.00228	0.00125	60
4 POM WP	DSS 11	CC3	1/7	23:47:32	1/8	05:22:02	75	0.00234	0.00243	0.00641	10[a], 60
	DSS 11	CC3	1/8	22:33:32	1/9	05:58:32	88	0.00919	0.00944	−0.00217	10[a], 60
	DSS 42	CC3	1/8	05:36:32	1/8	12:36:32	81	0.00527	0.00530	−0.000546	60
	DSS 42	CC3	1/9	06:05:32	1/9	09:46:02	44	0.00605	0.00812	0.00542	60
	DSS 51	CC3	1/8	13:02:32	1/8	16:23:02	33	0.00304	0.00304	−0.0000074	60
4 POM YK	DSS 11	CC3	1/7	23:45:32	1/8	05:23:32	359	0.00329	0.00329	0.000182	10[a], 60
	DSS 11	CC3	1/8	22:33:32	1/9	05:58:32	415	0.00321	0.00321	0.000107	10[a], 60
	DSS 42	CC3	1/8	05:34:32	1/8	12:38:32	396	0.00276	0.00278	−0.000324	60
	DSS 42	CC3	1/9	06:03:32	1/9	07:25:32	78	0.00376	0.00665	0.00549	60
	DSS 51	CC3	1/8	13:00:32	1/8	16:23:32	148	0.00288	0.00309	0.00113	60
4 POM YN	DSS 11	CC3	1/7	23:45:32	1/8	05:23:32	359	0.0158	0.0159	0.000790	10[a], 60
	DSS 11	CC3	1/8	22:33:32	1/9	05:58:32	415	0.00722	0.00725	−0.000687	10[a], 60
	DSS 42	CC3	1/8	05:34:32	1/8	12:38:32	396	0.00744	0.00744	−0.0000931	60
	DSS 42	CC3	1/9	06:03:32	1/9	13:29:32	415	0.00751	0.00751	−0.0000256	60
	DSS 51	CC3	1/8	13:00:32	1/8	16:23:32	148	0.00712	0.00764	−0.00279	60

[a]Between 01:14 and 01:22 GMT.

Table 56 (contd)

Orbit ID	Station	Data type	Begin data		End data		Number of points	Standard deviation	Root mean square	Mean error	Sample data rate, s
			Date 1968	GMT	Date 1968	GMT					
4 POM YN (contd)	DSS 51	CC3	1/8	18:34:32	1/8	20:23:32	108	0.00731	0.00739	0.00105	60
	DSS 51	CC3	1/9	13:33:32	1/9	14:41:32	44	0.00788	0.0144	0.0120	60
	DSS 61	CC3	1/8	16:34:32	1/8	18:23:32	102	0.00716	0.00740	−0.00188	60
	DSS 61	CC3	1/8	20:33:32	1/8	22:23:32	104	0.00598	0.00608	0.00112	60
5 POM YA	DSS 11	CC3	1/7	23:45:32	1/8	05:23:32	359	0.0157	0.0157	−0.000191	10[a], 60
	DSS 11	CC3	1/8	22:33:32	1/9	05:58:32	415	0.00688	0.00688	−0,000104	10[a], 60
	DSS 42	CC3	1/8	05:34:32	1/8	12:38:32	396	0.00759	0.00759	0.0000814	60
	DSS 42	CC3	1/9	06:03:32	1/9	13:29:32	415	0.00720	0.00722	−0.000571	60
	DSS 51	CC3	1/8	13:00:32	1/8	16:23:32	148	0.00720	0.00751	−0.00212	60
	DSS 51	CC3	1/8	18:34:32	1/8	20:23:32	108	0.00734	0.00747	0.00140	60
	DSS 51	CC3	1/8	13:33:32	1/9	15:27:32	81	0.00702	0.00804	0.00392	60
	DSS 61	CC3	1/8	16:34:32	1/8	18:23:32	102	0.00699	0.00700	0.000333	60
	DSS 61	CC3	1/8	20:33:32	1/8	22:23:32	104	0.00600	0.00623	0.00168	60
	DSS 61	CC3	1/9	15:38:32	1/9	17:03:32	64	0.00708	0.00727	−0.00163	60
5 POM YD	DSS 11	CC3	1/7	23:45:32	1/8	05:23:32	359	0.00361	0.00361	−0.0000666	10[a], 60
	DSS 11	CC3	1/8	22:33:32	1/8	05:58:32	415	0.00330	0.00333	−0.000494	10[a], 60
	DSS 42	CC3	1/8	05:34:32	1/8	12:38:32	396	0.00384	0.00385	0.000249	60
	DSS 42	CC2	1/9	06:03:32	1/9	13:29:32	415	0.00260	0.00274	−0.000864	60
	DSS 51	CC3	1/8	13:00:32	1/8	16:23:32	148	0.00343	0.00400	−0.00207	60
	DSS 51	CC3	1/8	18:34:32	1/8	20:23:32	108	0.00226	0.00235	0.000628	60
	DSS 51	CC3	1/9	13:33:32	1/9	15:27:32	81	0.00479	0.00726	0.00546	60
	DSS 51	CC3	1/9	18:03:32	1/9	20:31:32	116	0.00300	0.00333	0.00145	60
	DSS 61	CC3	1/8	16:34:32	1/8	18:23:32	102	0.00227	0.00235	−0.000582	60
	DSS 61	CC3	1/8	20:33:32	1/8	22:23:32	104	0.00142	0.00429	0.00405	60
	DSS 61	CC3	1/9	15:33:32	1/9	17:53:32	127	0.00310	0.00343	−0.00148	60
5 POM WE	DSS 11	CC3	1/7	23:55:32	1/8	05:23:32	351	0.00318	0.00373	0.00195	10[a], 60
	DSS 11	CC3	1/8	22:33:32	1/9	05:58:32	408	0.00617	0.00834	−0.00562	10[a], 60
	DSS 42	CC3	1/8	05:34:32	1/8	12:38:32	396	0.00775	0.00827	−0.00288	60
	DSS 42	CC3	1/9	06:03:32	1/9	12:59:32	391	0.00460	0.00708	0.00538	60
	DSS 51	CC3	1/8	13:00:32	1/8	16:23:32	148	0.00332	0.00338	−0.000632	60
	DSS 51	CC3	1/8	18:34:32	1/8	20:23:32	81	0.00218	0.0047	0.00427	60
	DSS 51	CC3	1/9	18:03:32	1/9	20:52:32	131	0.0115	0.0116	0.0116	60
	DSS 61	CC3	1/8	16:34:32	1/8	18:23:32	102	0.00306	0.00754	−0.00689	60
	DSS 61	CC3	1/8	20:33:32	1/8	22:23:32	104	0.00208	0.00762	0.00733	60
	DSS 61	CC3	1/9	16:00:32	1/9	17:53:32	109	0.00247	0.00254	0.000609	60
FINAL WA	DSS 11	CC3	1/9	22:03:32	1/9	22:54:32	52	0.00251	0.00251	0.000120	10[a], 60
	DSS 51	CC3	1/9	19:21:32	1/9	21:53:32	139	0.00279	0.00279	0.00000351	60
FINAL YA	DSS 11	CC3	1/9	22:03:32	1/9	22:59:32	55	0.00314	0.00314	0.0000599	10[a], 60
	DSS 51	CC3	1/9	19:21:32	1/9	21:53:32	137	0.00278	0.00278	0.00000535	60
FINAL YB	DSS 11	CC3	1/9	22:03:32	1/9	23:16:32	65	0.00331	0.00331	0.0000639	10[a], 60

[a]Between 01:14 and 01:22 GMT.

Table 56 (contd)

Orbit ID	Station	Data type	Begin data		End data		Number of points	Standard deviation	Root mean square	Mean error	Sample data rate, s
			Date 1968	GMT	Date 1968	GMT					
	DSS 51	CC3	1/9	19:21:32	1/9	21:53:32	137	0.00285	0.00285	−0.00000178	60
FINAL WC	DSS 11	CC3	1/9	22:03:32	1/9	23:29:32	76	0.00258	0.00258	0.0000112	10[a], 60
	DSS 51	CC3	1/9	19:21:32	1/9	21:53:32	139	0.00289	0.00289	0.0000457	60
FINAL YC	DSS 11	CC3	1/9	22:03:32	1/9	23:55:32	94	0.00233	0.00233	0.0000260	10[a], 60
	DSS 51	CC3	1/9	19:21:32	1/9	21:53:32	137	0.00286	0.00286	0.0000873	60
FINAL WD	DSS 11	CC3	1/9	22:03:32	1/9	23:59:32	97	0.00282	0.00285	0.000409	10[a], 60
	DSS 51	CC3	1/9	19:21:32	1/9	21:53:32	139	0.00282	0.00282	0.0000263	60
FINAL WE	DSS 11	CC3	1/9	22:03:32	1/9	00:15:32	109	0.00275	0.00279	0.000484	10[a], 60
	DSS 51	CC3	1/9	19:21:32	1/9	21:53:32	139	0.00281	0.00281	0.0000913	60
FINAL YD	DSS 11	CC3	1/9	22:03:32	1/10	00:14:32	110	0.00219	0.00219	−0.0000366	10[a], 60
	DSS 51	CC3	1/9	19:21:32	1/9	21:53:32	137	0.00282	0.00282	0.0000891	60
FINAL WF	DSS 11	CC3	1/9	22:03:32	1/10	00:20:32	117	0.00227	0.00227	−0.0000449	10[a], 60
	DSS 51	CC3	1/9	19:21:32	1/9	21:53:32	139	0.00280	0.00280	0.0000457	60
FINAL YE	DSS 11	CC3	1/9	22:03:32	1/10	00:20:32	116	0.00229	0.00229	−0.0000274	10[a], 60
	DSS 51	CC3	1/9	19:21:32	1/9	21:53:32	132	0.00282	0.00282	0.0000481	60
PTD-1	DSS 11	CC3	1/7	23:45:32	1/8	05:23:32	359	0.00355	0.00369	−0.00101	
	DSS 11	CC3	1/8	22:33:32	1/9	05:58:32	415	0.00297	0.00298	0.000182	
	DSS 11	CC3	1/9	22:03:32	1/10	00:20:32	116	0.00801	0.00816	−0.00157	
	DSS 42	CC3	1/8	05:34:32	1/8	12:38:32	396	0.00355	0.00420	0.00225	
	DSS 42	CC3	1/9	06:03:32	1/9	13:29:32	415	0.00267	0.00367	−0.00251	
	DSS 51	CC3	1/8	13:00:32	1/8	16:23:32	148	0.00541	0.00550	−0.000968	
	DSS 51	CC3	1/8	18:34:32	1/8	20:23:32	108	0.00231	0.00597	−0.00550	
	DSS 51	CC3	1/9	13:33:32	1/9	15:27:32	81	0.00427	0.00561	0.00365	
	DSS 51	CC3	1/9	18:03:32	1/9	21:53:32	185	0.00293	0.00719	0.00657	
	DSS 61	CC3	1/8	16:34:32	1/8	18:23:32	102	0.00194	0.00209	0.000761	
	DSS 61	CC3	1/8	20:33:32	1/8	22:23:32	104	0.00139	0.00350	0.00321	
	DSS 61	CC3	1/9	15:33:32	1/9	17:53:32	127	0.00206	0.00395	−0.00336	

[a]Between 01:14 and 01:22 GMT.

Table 57. Inflight results of orbit determination terminal computations

Orbit solution data span[a]		Predicted selenocentric conditions at unbraked impact (January 10, 1968)			Orbit solution data span[a]		Predicted selenocentric conditions at unbraked impact (January 10, 1968)		
From	To	Latitude, deg (South)	Longitude, deg (East)	GMT	From	To	Latitude, deg (South)	Longitude, deg (East)	GMT
Midcourse[b]	$E-5$ h, 40 min	−41.161	348.810	01:02:47.393	$E-5$ h, 40 min	$E-1$ h, 10 min	−41.225	348.770	01:02:47.942
$E-5$ h, 40 min	$E-2$ h, 06 min	−41.252	348.787	01:02:48.365	$E-5$ h, 40 min	$E-51$ min	−41.220	348.767	01:02:47.877
$E-5$ h, 40 min	$E-1$ h, 49 min	−41.243	348.783	01:02:48.229	$E-5$ h, 40 min	$E-45$ min	−41.217	348.765	01:02:47.845
Best estimate of unbraked impact time				01:02:47.914					

[a]Solution used for initial estimate of AMR mark time.

[b]Initial post-midcourse epoch.

XIV. *Surveyor VII* Postflight Orbit Determination Analysis

This section presents the best estimate of the *Surveyor VII* flight path and other significant results obtained from analysis of the DSS tracking data. The analysis verified that both the premaneuver and postmaneuver, inflight orbit solutions were within the orbit determination accuracy requirements of the *Surveyor* Project. The inflight philosophy of estimating only a minimum parameter set (i.e., the six components of the spacecraft position and velocity vectors) for the orbital computations was again proven valid.

For the postflight orbital computations and analysis, only two-way doppler data were used. The right most column of Table 49 summarizes the data used for final premaneuver orbit computation in the postflight analysis. A comparison between the amount of data used inflight and this column shows that, except for angle data, the same number of points were used in postflight analysis as inflight. This indicates that an efficient job was done inflight in removing bad data from the data file. Table 49 also summarizes the data used for postmaneuver orbit computations in postflight analysis. In this case, some low-elevation data were restored to the data file, resulting in more data used postflight than inflight for DSS 42 and DSS 51. The DSS 11 and DSS 61 data files were nearly the same postflight as inflight.

A. Premaneuver Orbit Estimates

All the *known* bad data points were removed in the orbit data generator program (ODG) before the start of the postflight analysis. However, it was known that something was wrong with some of the data that precluded fitting all premaneuver data together. As mentioned in Section XIII, inflight analysis had failed to isolate the problem. After the final data tape had been compiled, a 6×6 solution was computed. The data inconsistencies are evidenced by the *apparent* skews and biases as seen in the data residuals for the 6×6 solution in Fig. 67.

Data consistency runs were computed to isolate the bad data that was the disturbing force behind the bad 6×6 solution. When DSS 51 or DSS 61 data were weighted out of the orbit solution, data from the remaining three stations still failed to fit together well. Since the problem was apparent inflight before DSS 11 data were available, DSS 11 was discounted as being the bad data source. This left only DSS 42 as the culprit. Weighting out DSS 42 data resulted in the data fit shown in Fig. 68. As seen in the plots, data from DSS 11, DSS 51, and DSS 61 fit together fairly well without DSS 42 data to influence the solution.

Since DSS 42 had taken nearly 5 h of prime two-way doppler data, it was desirable to use these data if possible. Therefore, to compensate for the inconsistencies, a 9×9 solution was computed with the estimate list including the station location parameters for the Tidbinbilla Deep Space Station. This solution was a significant improvement over the 6×6 solution but, still, was not as good as desired. To further improve the fit, the estimate list was expanded to 18 to include the station location parameters from DSS 11, DSS 42, DSS 51, and DSS 61. To allow the DSS 42 station locations to move to compensate for the apparent perturbation in the data, an *a priori* 1σ uncertainty of 200 m was assigned to the radius, latitude, and longitude for this station. All other station locations were assigned an *a priori* of 100 m (1σ). The resulting 18×18 solution was a very good fit with orbit parameters consistent with expected values. The longitude of DSS 42 moved approximately 30 m, indicating the possibility of a time bias in the data from the station. A bias of approximately 75 m/sec could account for the 30 m change.

The 18×18 solution discussed above is considered to be the best estimate of the *Surveyor VII* premaneuver orbit. The uncorrected, unbraked impact point predicted by this solution (latitude $= -6.009$ deg, longitude $=$ 5.414 deg) is approximately 8.6 km southeast of the prelaunch aim point.

The residual plots from the best estimate pre-midcourse orbit can be seen in Fig. 69. Numerical values from this solution are presented in Table 58 and the number of data points, together with associated statistics are given in Table 59. A graphical comparison between the predicted unbraked impact points (in the **B**-plane) of this solution and the inflight solutions may be seen in Fig. 61.

B. Postmaneuver Orbit Estimates

Prior to starting the analysis of the *Surveyor VII* postmaneuver tracking data, all known or suspected bad data points were removed. The objective of the analysis in this section was to obtain an orbit solution based on processing all postmaneuver tracking data in one block. This differed from the inflight computations, which required that the data be processed in two blocks to meet the AMR backup requirements. The lunar radius of 1736.6 km is the same as used for inflight computations as discussed in Section XIII-D.

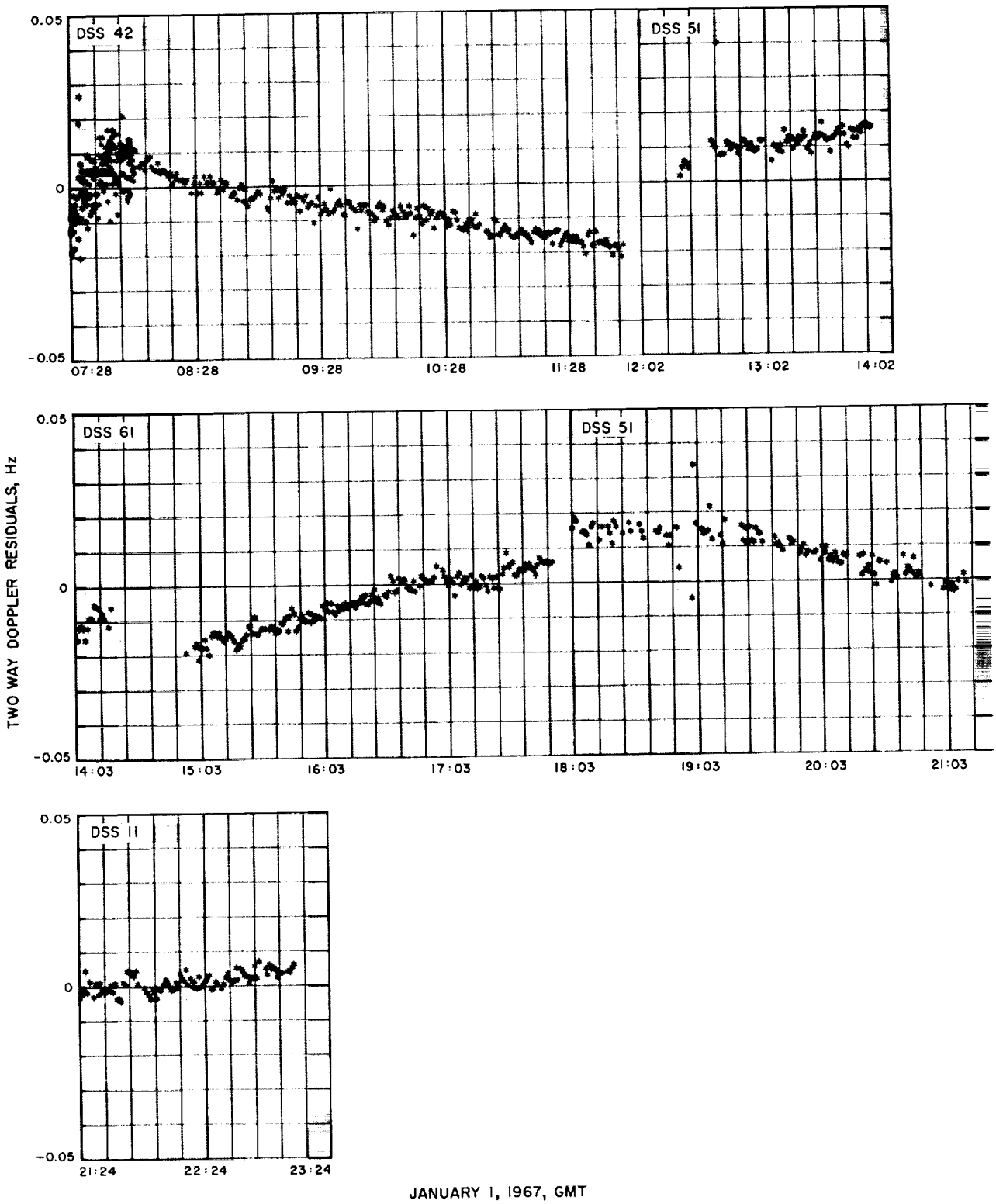

Fig. 67. Premaneuver two-way doppler residuals, *Surveyor VII* (6 × 6 solution, all two-way doppler data)

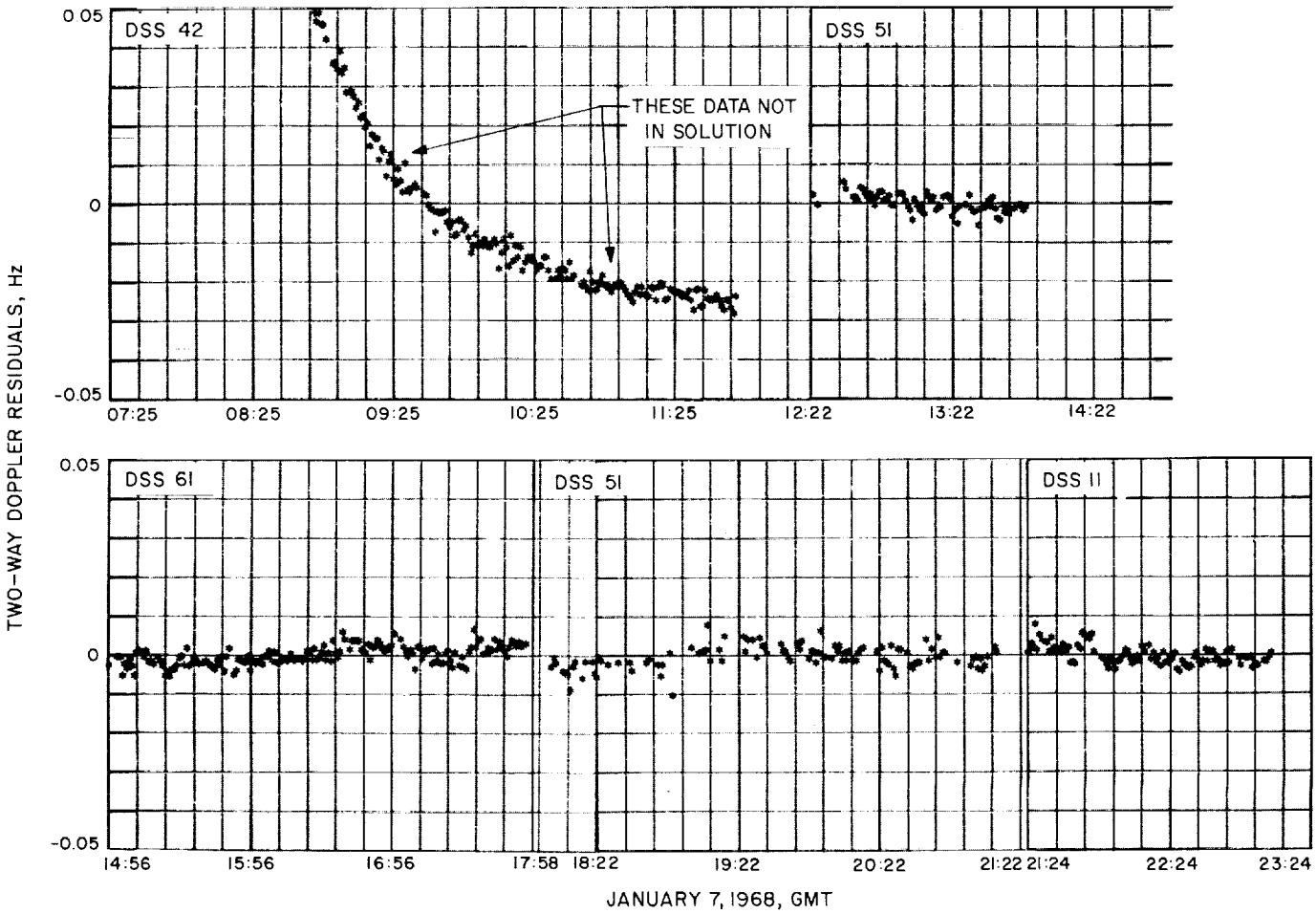

Fig. 68. Premaneuver doppler residuals, *Surveyor VII* (6 × 6 solution, DSS 42 weighted out)

A 6 × 6 orbit solution that used all the two-way doppler data from Canopus reacquisition after the maneuver to the last two-way doppler point received (approximately 45 min before encounter) was obtained and mapped to target. Results were consistent with inflight values, but the data residuals (observed minus computed) indicated a rather poor fit, as seen in Fig. 70. Also, indicated on the figures are several gyro drift checks, which account for several of the minor data perturbations. Systematic data perturbations are again apparent, similar to perturbations seen in data from DSS 11 and DSS 61 taken during the *Surveyor VII* mission. Although the 6 × 6 solution was not a good fit, it was as good as expected when fitting that much (≈40 h) data. Experience from analysis of past missions has indicated that it is difficult to fit more than 20 h with a 6 × 6 solution. Shown in the 4th frame of Fig. 70 are the last data taken before encounter. The significant effect of the near-moon data can be seen in the residuals as they get worse toward the end of the data block.

The DSS 42 tracking station was *suspected* to be causing a lot of the problems in fitting the *Surveyor VII* post-midcourse data. However, when weighted out of the solution, DSS 42 residuals did not reveal any significant biases. To further isolate any bad blocks of data, several additional data consistency runs were made with various combinations of data. These runs revealed no inconsistencies between stations.

To further refine the solution and improve the data fit, the estimate list was expanded to 18 to include the station location parameters (geocentric radius and longitude) for DSS 11, DSS 42, DSS 51, and DSS 61; GM_c, and nongravitational acceleration perturbations (discussed in Section II-A). Also added to improve the solution was an improved set of values of index of refraction as supplied by A. S. Liu.[16] The curvature noted in the residual signature for low-elevation data taken near DSS rise or

[16]Navigational Accuracy Group, JPL.

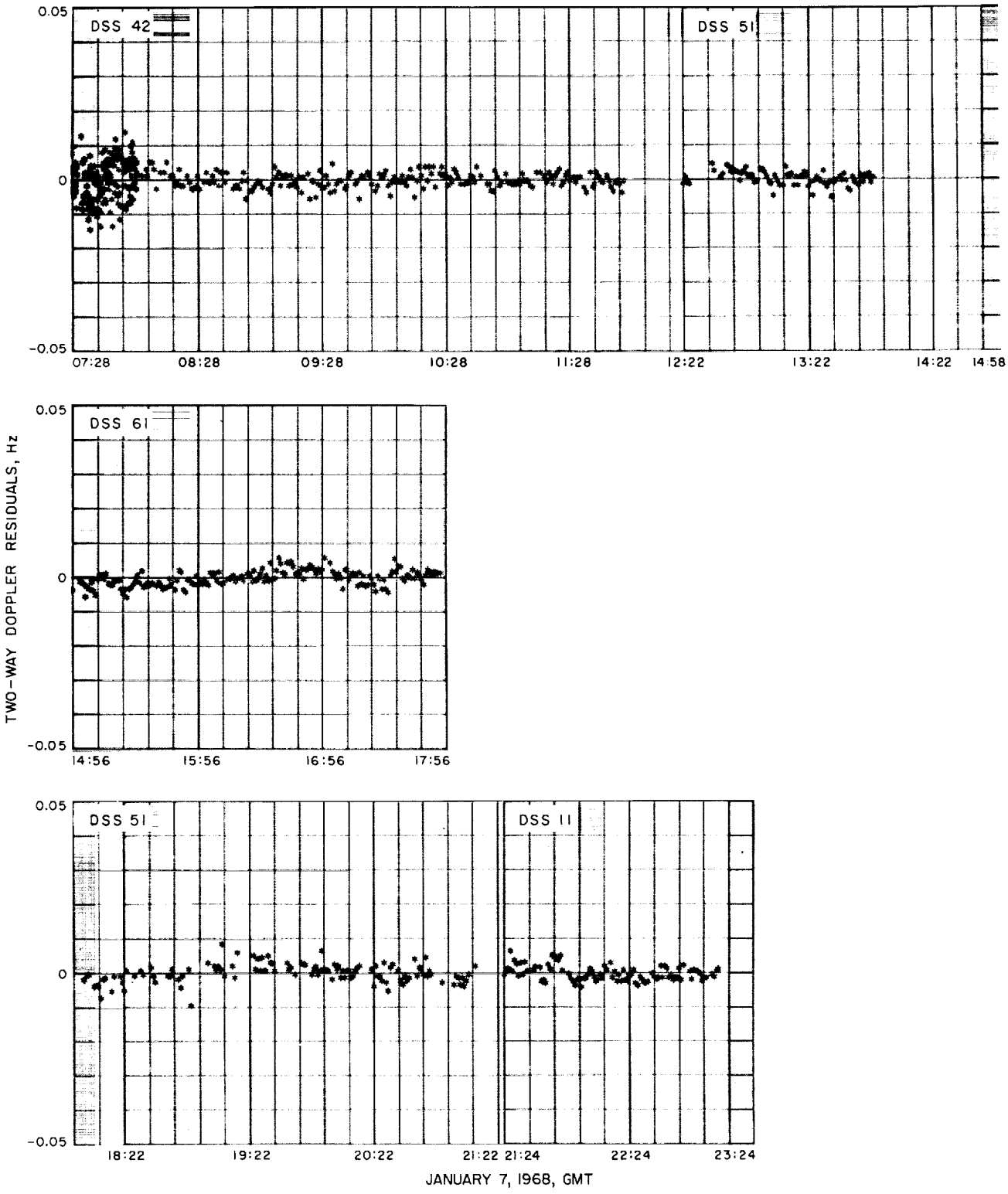

Fig. 69. Premaneuver two-way doppler residuals, *Surveyor VII* (18 × 18 solution, current best estimate)

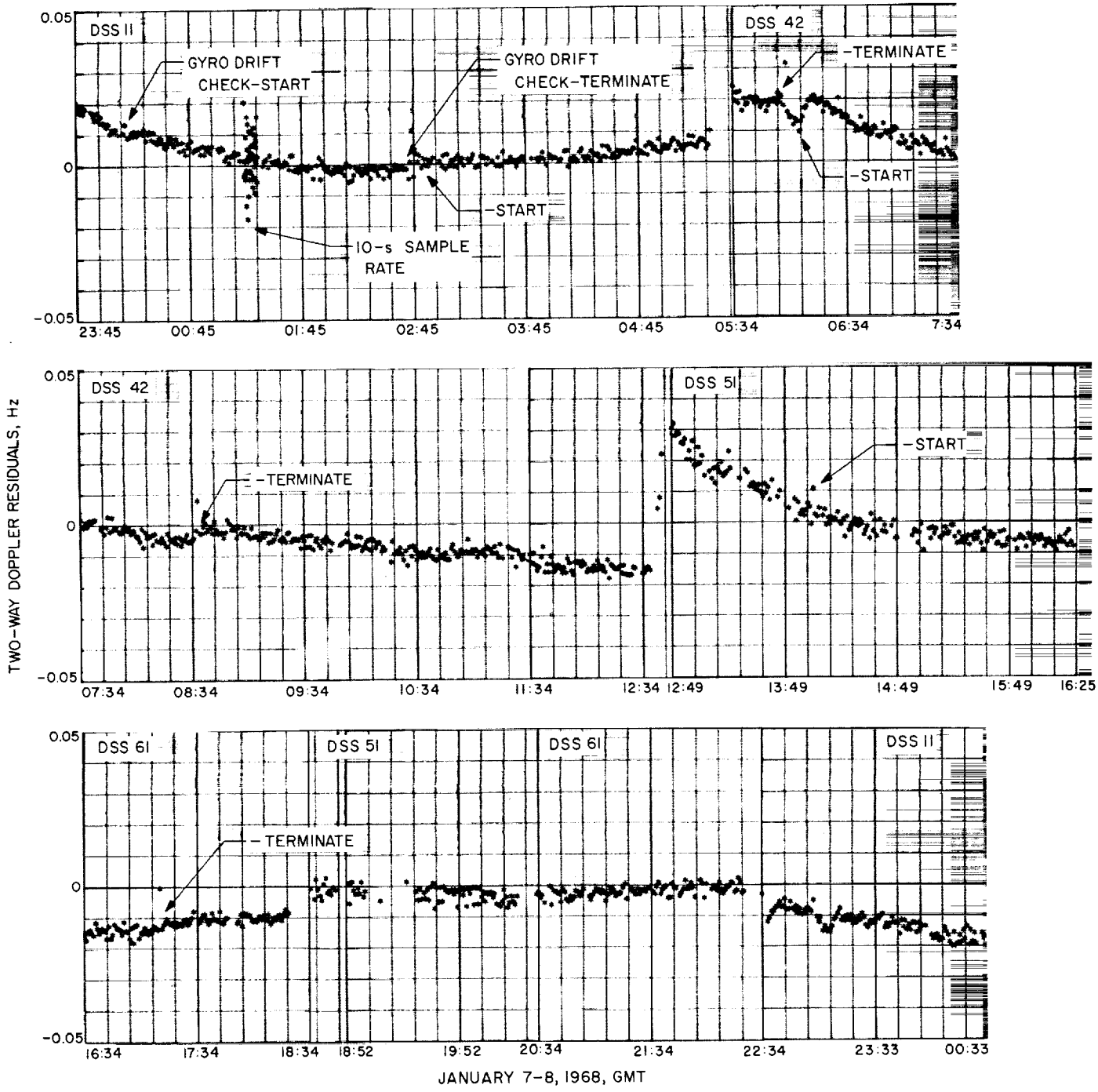

Fig. 70. Postmaneuver two-way doppler residuals, *Surveyor VII* (6 × 6 solution, trajectory *not* corrected for perturbations)

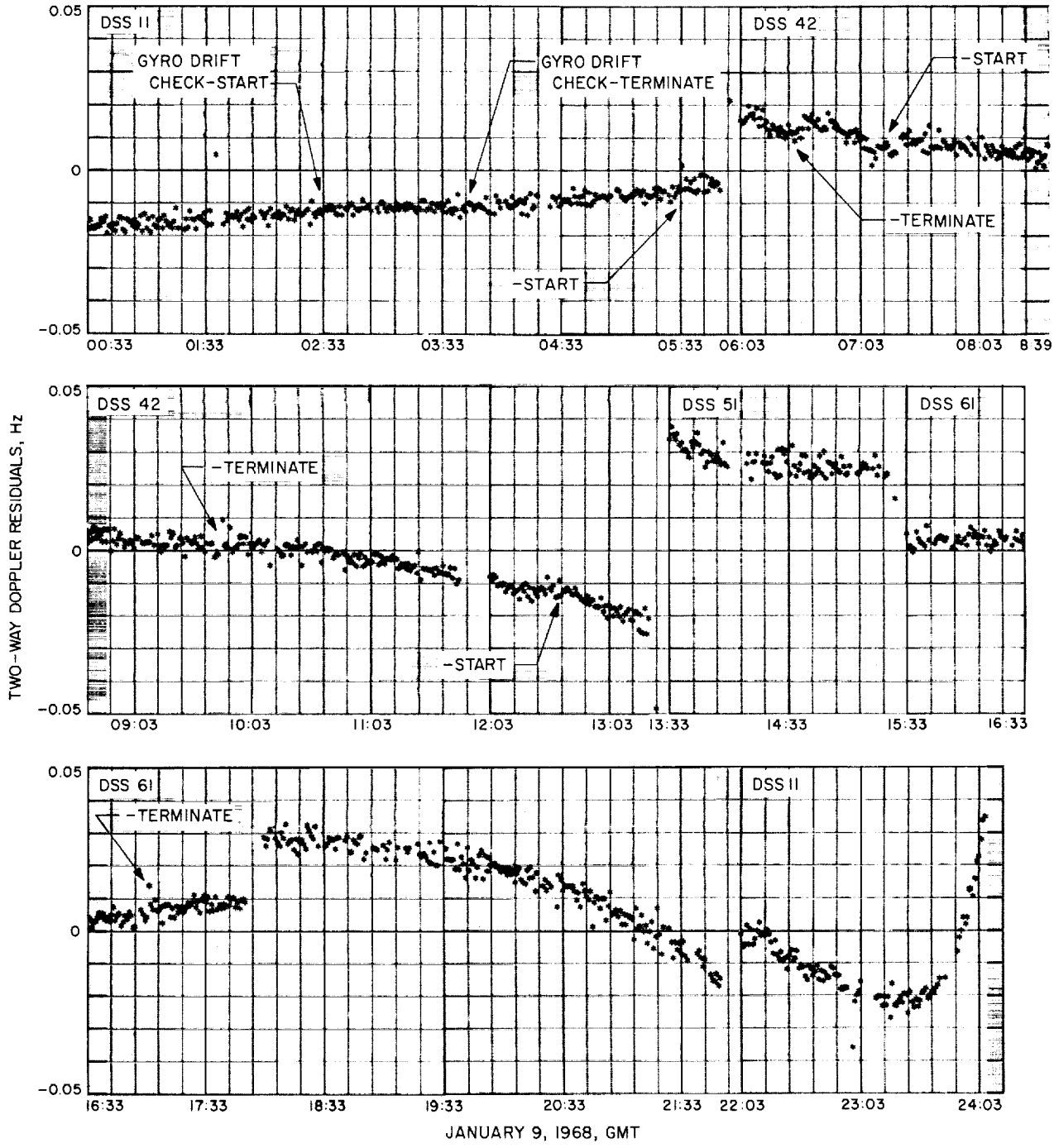
0.05
0
-0.05
DSS 11
GYRO DRIFT
CHECK-START
GYRO DRIFT
CHECK-TERMINATE
DSS 42
-START
-TERMINATE
-START
00:33
01:33
02:33
03:33
04:33
05:33
06:03
07:03
08:03
8 39
DSS 42
-TERMINATE
DSS 51
DSS 61
-START
09:03
10:03
11:03
12:03
13:03
13:33
14:33
15:33
16:33
DSS 61
-TERMINATE
DSS 11
16:33
17:33
18:33
19:33
20:33
21:33
22:03
23:03
24:03
TWO-WAY DOPPLER RESIDUALS, Hz
JANUARY 9, 1968, GMT

Fig. 70 (contd)

set was significantly reduced by using the new indices of refraction. The 18×18 solution, as discussed above, resulted in an acceptable data fit and is considered to be the best estimate of the *Surveyor VII* post-midcourse orbit.

The greatest change in the estimated station locations was a 24-m increase in the geocentric radius (RI) of DSS 61. The GM_ε changed from a nominal of 4902.6309 to 4902.7826 km^3/s^2. The acceleration perturbations estimated are as follows:

$$f_1 = 0.889 \times 10^{-10}\ km/s^2$$

$$f_2 = 0.308 \times 10^{-10}\ km/s^2$$

$$f_3 = -0.371 \times 10^{-10}\ km/s^2$$

$$\Delta\ddot{\mathbf{r}} = 1.0113 \times 10^{-10}\ km/s^2$$

These results indicate that some perturbations did exist in the postmaneuver data or trajectory and that their effect can be accounted for by solving for nongravitational perturbations. The cause of these perturbations has not been determined; however, solar radiation pressure, uncancelled velocity increments from normal operations of the attitude control system, possible gas and/or propellant leaks could be some of the causes for the perturbations. Although these perturbations were not accounted for in flight, orbit determination requirements were met. Residual plots from the best estimate 18×18 solution are given in Fig. 71. Numerical values from the solution are presented in Table 58. The amount of data used in this solution, along with the associated data statistics is shown in Table 59. Based on this *current best estimate* solution, the *Surveyor VII* spacecraft is estimated to be at 41.021 °S lat and 348.560 °E lon. This is 0.131 deg ($\approx$3.9 km) south and 0.07 deg ($\approx$1.6 km) west of the final soft-landing aim point. A graphical comparison of the current best estimate and inflight solutions in the **B**-plane is given in Fig. 64.

C. Evaluation of Midcourse Maneuver Based on DSIF Tracking Data

The *Surveyor VII* midcourse maneuver can be evaluated by examining the velocity change at the midcourse epoch and by comparing the maneuver aim point with the target parameters from the best estimate post-midcourse orbit solution.

The *observed* velocity changes due to midcourse thrust (applied by igniting the vernier engines) are determined by differencing the velocity components of best estimate orbit solutions based on postmaneuver data, only, and premaneuver data, only. These solutions are independent; *a priori* information from premaneuver data is not used during the processing of postmaneuver data. The estimated maneuver execution errors, at midcourse epoch, are determined by differencing the observed velocity changes and the commanded maneuver velocity increments. The remaining major contribution to the total maneuver error is made by the orbit determination process. This error source includes ODP computational and model errors, and errors in tracking data. These errors may be obtained by differencing the velocity components, at midcourse epoch, of the best estimate premaneuver orbit and the inflight orbit solution used for the maneuver computations. Numerical results of this part of the evaluation are presented in Table 60. In the table, it can be seen that the execution errors in *Dx*, *Dy* and *Dz* were only -0.001, $+0.024$, and -0.010 m/s, respectively. The OD errors are also very small. Total maneuver errors for *Surveyor VII* were well within specifications.

A more meaningful evaluation can be made by examining certain critical target parameters. Since the primary objective of the midcourse maneuver is to achieve lunar encounter at a selected landing site, the maneuver unbraked aim point is used as the basic reference for this evaluation. The unbraked aim point (Table 61) for *Surveyor VII* was -41.071 deg latitude and 348.837 deg longitude. Based on the predicted unbraked impact point from the best estimate inflight orbit solution (LAPM YB), trajectory corrections were computed to achieve landing at the desired site. To evaluate the total maneuver error at the target, the maneuver aim point is compared with the predicted unbraked impact point from the current best estimate postmaneuver orbit solution. Orbit determination errors can be obtained by differencing the unbraked target parameters of the current best estimate premaneuver orbit solution and the inflight orbit solution used for maneuver computations. Execution errors, consisting of both attitude maneuver errors and engine system errors, are then determined by differencing the total and OD errors. Numerical results of these computations are presented in Table 62. In the table, it can be seen that encounter was achieved within -0.131-deg latitude and -0.070-deg longitude of the desired aiming point. These differences in latitude and longitude are roughly equivalent to -3.93 and -1.58 km, respectively, on the lunar surface. The OD position errors are well within the expected accuracy. In general, the accuracy of the *Surveyor VII* midcourse maneuver was well within *Surveyor* Project specifications. It should be noted that these results cannot be used to accurately evaluate the *Centaur* injection accuracy since the inflight aim point was not the same as the prelaunch aim point.

Table 58. Summary of postflight orbit parameters,[a] *Surveyor VII*

Parameter	Pre-midcourse (January 7, 1968)		Post-midcourse (January 7, 1968)	
Geocentric position and velocity at epoch				
x, km ($\pm 1\sigma$)	9448.6336	±0.1575	137530.44	±2.83
y, km	−6127.0104	±0.5573	91469.333	±5.144
z, km	−4458.0034	±1.6203	41087.875	±7.095
Dx, km/s	7.9198646	±0.0001710	1.2431239	±0.0000434
Dy, km/s	1.4086357	±0.0002703	1.2850204	±0.0000910
Dz, km/s	0.10222106	±0.00035439	0.62828068	±0.00008481
Target statistics				
B, km	2076.7611		2264.2178	
B • TT, km	2044.8425		1034.7070	
B • RT, km	362.71657		2013.9689	
1σ SMAA, km	15.0		2.5	
1σ SMIA, km	5.0		1.0	
THETA, deg	107.08		32.91	
$\sigma_{T,impact}$, s	2.777		0.500	
PHI_{99}, deg	0.58088622		0.11169465	
1σ SVFIXR, m/s	0.61124483		0.61788562	
Latitude, deg	−6.0087265		−41.202011	
Longitude, deg	5.4141312		348.76701	
Impact time, GMT	January 10, 1968, 01:02:52.983		January 10, 1968, 01:02:47.914	

[a]Current best estimate.

Table 59. Summary of data used in postflight (current best estimate) orbit solutions, *Surveyor VII*

Station	Begin data		End data		Number of points	Standard deviation	Root mean square	Mean error
	Date 1968	GMT	Date 1968	GMT				
Pre-midcourse								
DSS 11	1/7	21:24:32	1/7	23:07:32	98	0.00211	0.00213	−0.000267
DSS 42	1/7	07:28:07	1/7	11:54:32	399	0.00407	0.00408	−0.000224
DSS 51	1/7	12:22:32	1/7	13:53:32	80	0.00194	0.00194	0.000140
DSS 51	1/7	18:03:32	1/7	21:12:32	119	0.00269	0.00269	−0.0000944
DSS 61	1/7	14:56:32	1/7	17:53:32	172	0.00228	0.00230	−0.000280
Post-midcourse								
DSS 11	1/7	23:46:32	1/8	05:23:32	358	0.00326	0.00327	−0.000312
DSS 11	1/8	22:33:32	1/9	05:58:32	415	0.00254	0.00263	0.000700
DSS 11	1/9	22:03:32	1/10	00:17:32	113	0.00386	0.00403	−0.00116
DSS 42	1/8	05:34:32	1/8	12:38:32	409	0.00280	0.00307	0.00127
DSS 42	1/9	06:03:32	1/9	13:29:32	442	0.00393	0.00428	−0.00169
DSS 51	1/8	13:00:32	1/8	16:23:32	174	0.00462	0.00497	−0.00184
DSS 51	1/8	18:34:32	1/8	20:23:32	108	0.00219	0.00425	−0.00365
DSS 51	1/9	13:33:32	1/9	15:27:32	95	0.00379	0.00494	0.00317
DSS 51	1/9	18:03:32	1/9	21:53:32	196	0.00258	0.00436	0.00351
DSS 61	1/8	16:34:32	1/8	18:23:32	102	0.00169	0.00316	0.00268
DSS 61	1/8	20:33:32	1/8	22:23:32	104	0.00169	0.00172	−0.000326
DSS 61	1/9	15:33:32	1/9	17:53:32	127	0.00194	0.00297	−0.00225

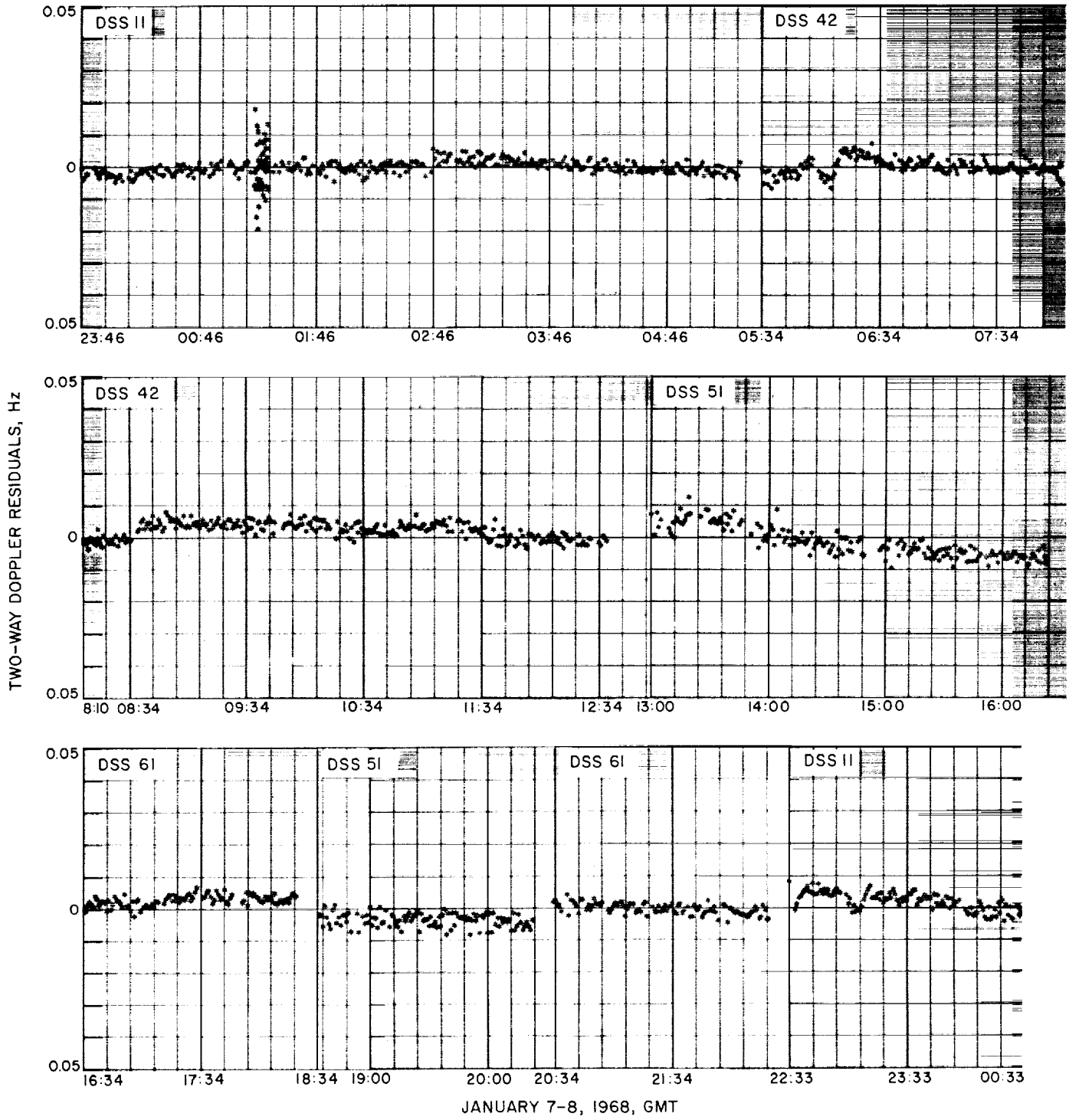

Fig. 71. Postmaneuver two-way doppler residuals, *Surveyor VII* (18 × 18 solution, current best estimate)

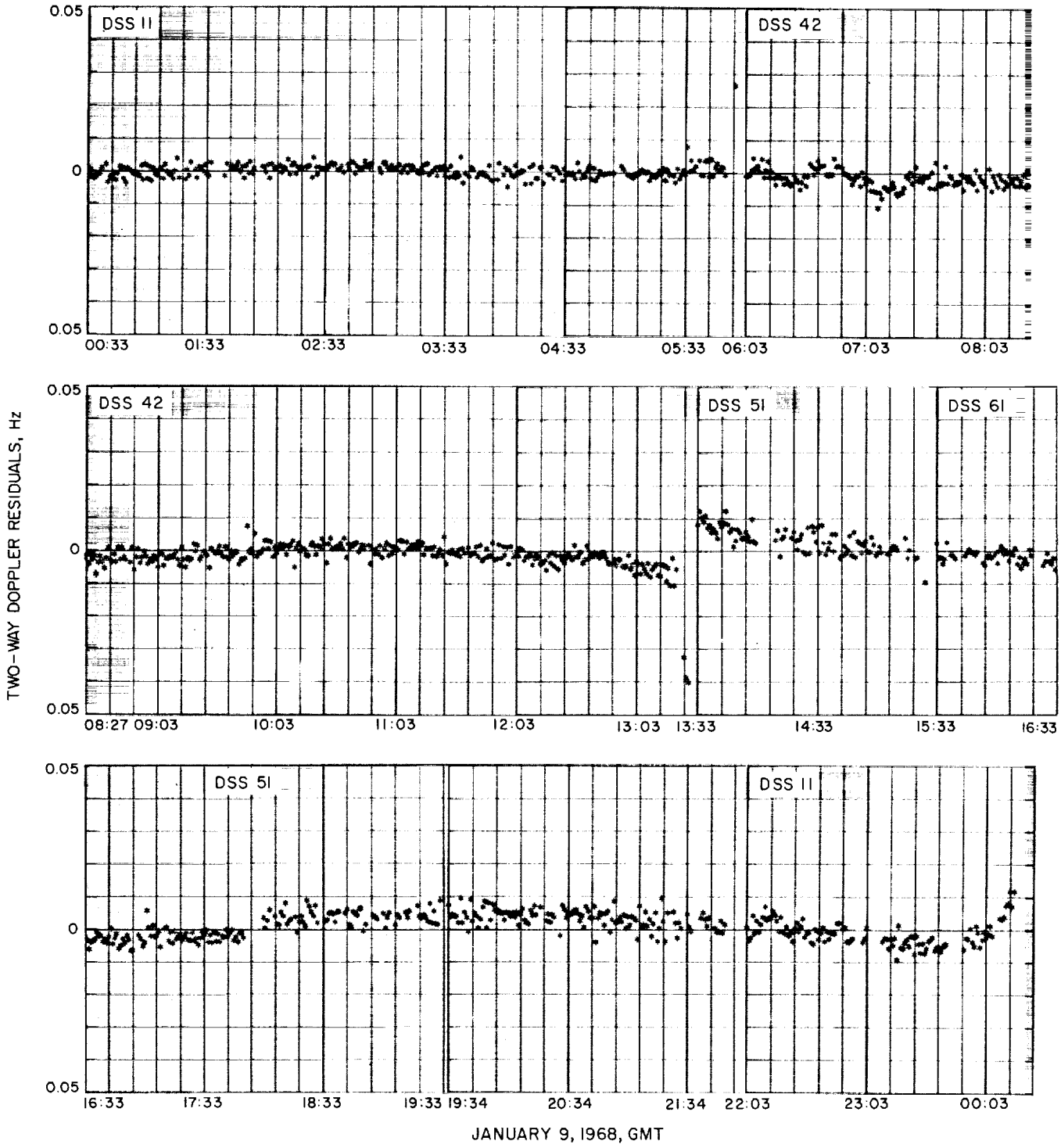
0.05
DSS 11
DSS 42
0
0.05
00:33
01:33
02:33
03:33
04:33
05:33
06:03
07:03
08:03
TWO-WAY DOPPLER RESIDUALS, Hz
0.05
DSS 42
DSS 51
DSS 61
0
0.05
08:27
09:03
10:03
11:03
12:03
13:03
13:33
14:33
15:33
16:33
0.05
DSS 51
DSS 11
0
0.05
16:33
17:33
18:33
19:33
19:34
20:34
21:34
22:03
23:03
00:03
JANUARY 9, 1968, GMT

Fig. 71 (contd)

Table 60. *Surveyor VII* midcourse maneuver evaluated at midcourse epoch[a]

Velocity components[b]	Current best estimate of premaneuver velocity,[c] m/s	Inflight estimate of premaneuver velocity,[c] m/s	Current best estimate of postmaneuver velocity, m/s	Observed velocity change due to maneuver (best post minus best pre), m/s	Commanded[d] maneuver velocity change, m/s	Total maneuver errors	
						Execution errors[e] (observed change minus commanded change), m/s	OD errors (best pre minus inflight), m/s
Dx	1243.9915	1243.9854	1243.1239	−0.8615	−0.8603	−0.0012	+0.0061
Dy	1276.4607	1276.4566	1285.0204	+8.5638	+8.5401	+0.0237	+0.0041
Dz	635.27574	635.29304	628.28068	−7.01236	−7.00281	−0.00955	−0.0173

[a]Midcourse epoch: end of reorientation after midcourse maneuver: January 7, 1968, 23:45:00 GMT.

[b]All velocity components are given in geocentric space-fixed cartesian coordinates.

[c]Mapped to midcourse epoch.

[d]Based on inflight premaneuver orbit solution (LAPM YB) used for final midcourse maneuver computations.

[e]Based on differences of best pre-midcourse and post-midcourse orbit estimates, the 1σ uncertainties associated with these determinations of midcourse velocity errors are of the same order as the errors, themselves. However, these determinations have particular merit because of their independence of the spacecraft system.

Table 61. Impact points, *Surveyor VII*

a. Unbraked impact points

Source	Latitude	Longitude
Best estimate of pre-midcourse	−6.009	5.414
Inflight orbit (LAPM YB)	−5.936	5.392
Best estimate of post-midcourse	−41.202	348.767
Maneuver unbraked aim point	−41.071	348.837

b. Estimated midcourse errors mapped to unbraked impact point

Source	Δ Latitude		Δ Longitude	
	deg	km	deg	km
OD errors[a]	−0.073	−2.19	+0.022	+0.50
Maneuver error[b]	−0.058	−1.74	−0.092	−2.08
Overall errors[c]	−0.131	−3.93	−0.070	−1.59

[a]OD errors = current best premaneuver estimate *minus* orbit used for maneuver computations (LAPM YB).

[b]Maneuver errors = overall errors *minus* OD errors.

[c]Overall errors = current best postmaneuver estimate *minus* aiming point.

D. Estimated Tracking Station Locations and Physical Constants

1. Method of analysis. Computations were made to determine the best estimate of $GM_{\oplus}$, $GM_{\mathfrak{C}}$, and station location parameters for the *Surveyor VII* mission. The total parameters estimated in these computations were: the spacecraft position and velocity at an epoch; $GM_{\oplus}$; $GM_{\mathfrak{C}}$; spacecraft acceleration perturbations f_1, f_2 and f_3; the solar radiation constant G; and two components (geocentric radius and longitude) of station locations for each of DSS 11, DSS 42, DSS 51, and DSS 61. These solutions were computed by using only the two-way doppler data from DSS 11, DSS 42, DSS 51, and DSS 61 for both the pre-midcourse and post-midcourse phases. To obtain the best estimate of the solved for parameters, the pre-midcourse data block was combined with the post-midcourse data block. The procedure of combining the two data blocks is to fit only the pre-midcourse data, accumulate the normal equations at the injection epoch, and map the converged estimate to the midcourse epoch with a linear mapping of the inverted normal equation matrix (i.e., covariance matrix). The estimate is then incremented with the best estimate of the maneuver, and the mapped covariance matrix is corrupted in the velocity increment and used as *a priori* for the post-midcourse data fit. The ephemeris used in the reduction was one of the latest JPL ephemerides (DE-19) with the updated mass ratios and Ekert's corrections.

2. Results and Conclusions. The results of these computations are presented in Table 62 in an unnatural station coordinate system (geocentric radius, latitude, and longitude) and in a natural coordinate system (r_s, λ, Z) where r_s is the distance off the spin axis (in the station meridian), λ is the longitude, and Z is along the earth spin axis (see Fig. 21, p. 43).

The numerical results of *Surveyor VII* DSS location estimates are, in general, consistent with the range of the previous *Surveyor* estimates. The exceptions, r_s (DSS 42),

Table 62. Station locations and statistics, *Surveyor VII* (referenced to 1903.0 pole)

Station	Data source	Distance off spin axis r_s, km	1σ r_s standard deviation, m	Geocentric longitude, deg	1σ longitude standard deviation, m	Geocentric radius, deg	Geocentric latitude,[c] deg
DSS 11	*Mariner II*	5206.3357	3.9	243.15058	8.8	6372.0044	35.208035
	Mariner IV, cruise	404	10.0	067	20.0	2.0188	08144
	Mariner IV, post-encounter	378	37.0	072	40.0	2.0161	08151
	Pioneer VI, Dec. 1965–June 1966	359	9.6	092	10.3	2.0286	08030
	Goddard Land Survey, Aug. 1966	718	29.0	094	35.0	2.0640	08230
	Surveyor I, post-touchdown	276	2.9	085	23.8	2.6446	16317
	Surveyor I, inflight, post-midcourse, only	200	50.8	098	59.4	1.9975	08192
	Surveyor III, inflight	408	29.7	100	49.0	2.0230	08192
	Surveyor IV, inflight	326	41.1	097	49.0	2.0129	08192
	Surveyor V, inflight	256[a]	47.0	092	39.0	2.0043	08192
	Surveyor VI, inflight	337	30.3	091	43.0	2.0141	08192
	Surveyor VII, inflight	359	26.1	086[a]	36.0	2.0164	08184
DSS 42	*Mariner IV*, cruise	5205.3478	10.0	148.98136	20.0	6371.6882	−35.219410
	Mariner IV, post-encounter	.3480	28.0	134	29.0	.6824	19333
	Pioneer VI, Dec. 1965–June 1966	.3384	5.0	151	8.1	.6932	19620
	Goddard Land Survey, Aug. 1966	.2740	52.0	000	61.0	.7030	20750
	Surveyor I, post-touchdown	.3474	3.5	130	22.1	.6651	19123
	Surveyor I, inflight, post-midcourse, only	.3465	32.7	166	41.1	.6834	19372
	Surveyor III, inflight	.3522	26.5	146[a]	45.0	.6905	19372
	Surveyor IV, inflight	.3487	34.8	161	49.0	.6861	19372
	Surveyor V, inflight, post-midcourse, only	.3448	33.9	156	35.0	.6814	19372
	Surveyor VI, inflight	.3501	24.6	153	45.0	.6879	19372
	Surveyor VII, inflight	.3445	27.1	156	35.0	.6807	19368
DSS 51	Combined *Rangers*, LE3[b]	5724.9315	8.5	27.68572	22.2	6375.5072	−25.739169
	Ranger VI, LE3	203	19.7	72	69.3	.4972	9215
	Ranger VII, LE3	211	25.5	83	61.3	.4950	9157
	Ranger VIII, LE3	372	22.3	48	85.0	.5130	9159
	Ranger IX, LE3	626	56.6	80	49.5	.5322	8993

[a]This number is questionable because of possible error in the station data.

[b]Lunar ephemeris 3 (DE 15); all *Surveyor* inflight solutions used LE4 (DE 19)

[c]Latitude was not estimated for *Surveyor* inflight solutions.

Table 62 (contd)

Station	Data source	Distance off spin axis r_s, km	1σ r_s standard deviation, m	Geocentric longitude, deg	1σ longitude standard deviation, m	Geocentric radius, deg	Geocentric latitude,[c] deg
DSS 51 (contd)	*Mariner IV*, cruise	363	10.0	40	20.0	.5120	9148
	Mariner IV, post-encounter	365	40.0	57	38.0	.5143	9198
	Pioneer VI, Dec. 1965–June 1966	332	11.6	69	12.0	.5094	9176
	Goddard Land Survey, Aug. 1966	706	39.0	86	43.0	.5410	8990
	Surveyor I, inflight	380	38.3	78	41.0	.5144	9169
	Surveyor III, inflight	312	35.0	74	46.2	.5069	9169
	Surveyor IV, inflight	337	39.3	75	46.8	.5096	9169
	Surveyor V, inflight	355	44.1	74	31.5	.5116	9169
	Surveyor VI, inflight	413	25.6	70	43.0	.5180	9169
	Surveyor VII, inflight	309	32.5	73	36.7	.5062	9165
DSS 61	*Lunar Orbiter II*, doppler	4862.6067	9.6	355.75115	44.4	6369.9932	40.238566
	Lunar Orbiter II, doppler and ranging	.6118	3.4	138	4.0	69.9999	8566
	Mariner IV, post-encounter	.6063	14.0	099	24.0	70.0009	8655
	Pioneer VI, Dec. 1965–June 1966	.6059	8.8	103	10.4	70.0060	8715
	Surveyor III, inflight	.6054	24.5	126	47.0	70.0046	8701
	Surveyor V, inflight, pre-midcourse, only	.5962	72.2	125	75.0	69.9921	8701
	Surveyor VII, inflight	.6062	27.3	129	39.0	70.0050	8701

r_s (DSS 61), and longitude (DSS 61), or only 1, 1, and 3 m, respectively, from the nearest previous *Surveyor* solutions. All of them are within the range of the other solutions listed, i.e., *Ranger*, *Mariner*, *Lunar Orbiter* and *Pioneer*.

Surveyor station location solutions yield associated statistics that are higher than the other missions listed. This is because of the larger effective data weights and smaller amounts of data for the *Surveyor* missions. The improved values[17] of DSS indices of refraction were incorporated in the *Surveyor* solutions. Previous to the availability of new indices, a value of 340 was used for all the DSS.

The solved-for $GM_\oplus$ and GM_ζ for *Surveyor VII* are given in Table 63, along with previous solutions. The value for $GM_\oplus$ is very near the mean value for all *Surveyor* solutions (398601.15) and is well within the combined *Ranger* solutions minus 1σ. The value for GM_ζ, which is +0.0035 from the *Surveyor* mean value (4902.6394), is also within the range of previous *Surveyor* solutions. It is slightly smaller than the *Lunar Orbiter II* value shown, but well within the combined *Ranger* value plus 1σ.

[17]Indices of refraction obtained from A. S. Liu, Navigational Accuracy Group, JPL: DSS 11 = 240, DSS 42 = 310, DSS 51 = 240, DSS 61 = 300.

Table 63. Physical constants and statistics, *Surveyor VII*

Data source	$GM_\oplus$, km^3/s^2	1σ standard deviation, km^3/s^2	GM_ζ, km^3/s^2	1σ standard deviation, km^3/s^2
Lunar Orbiter II[a] (doppler)	398600.88	2.14	4902.6605	0.29
Lunar Orbiter II[a] (doppler and ranging)	389600.37	0.68	4902.7562	0.13
Combined *Rangers*[b]	398601.22	0.37	4902.6309	0.074
Ranger VI	398600.69	1.13	4902.6576	0.185
Ranger VII	398601.34	1.55	4902.5371	0.167
Ranger VIII	398601.14	0.72	4902.6304	0.119
Ranger IX	398601.42	0.60	4902.7073	0.299
Surveyor I	398601.27	0.78	4902.6492	0.237
Surveyor III	398601.11	0.84	4902.6420	0.246
Surveyor IV	398601.19	0.99	4902.6297	0.247
Surveyor V	398601.10	0.60	4902.6298	0.236
Surveyor VI	398601.11	0.54	4902.6425	0.235
Surveyor VII	398601.11	0.80	4902.6429	0.235

The correlation matrix in postmaneuver data with premaneuver data as *a priori* is given in Table 64.

Standard deviation		x	y	z	
x	1.07	1.000	−0.502	−0.695	−0.
y	1.32		1.000	−0.268	0.
z	3.06			1.000	0.
Dx	0.017				1
Dy	0.042				
Dz	0.044				
$GM_{\oplus}$	0.79				
G	0.10				
GM_{ζ}	0.23				
f_1	0.26×10^{-9}				
f_2	0.40×10^{-9}				
f_3	0.49×10^{-9}				
R_{21}	0.029				
Lon_{21}	0.00034				
R_{42}	0.032				
Lon_{42}	0.00032				
R_{51}	0.029				
Lon_{51}	0.00031				
R_{61}	0.035				
Lon_{61}	0.00037				

Table 64. Correlation matrix of estimated parameters, *Surveyor VII* (postmaneuver data with premaneuver data as *a priori*)

	Dy	Dz	$GM_{\oplus}$	G	$GM_{\mathbb{C}}$	f_1	f_2	f_3	R_{11}	Lon_{11}	R_{42}	Lon_{42}	R_{51}	Lon_{51}	R_{61}	Lon_{61}
7	0.637	−0.659	0.032	0.003	−0.032	−0.333	−0.649	0.750	−0.548	−0.112	−0.519	−0.408	−0.487	−0.432	−0.323	−0.220
2	−0.055	−0.004	0.484	−0.004	0.080	−0.039	−0.006	−0.019	−0.197	0.575	−0.253	0.556	−0.284	0.597	−0.273	0.589
6	−0.690	0.760	−0.399	0.000	−0.042	0.440	0.754	−0.836	0.803	−0.404	0.805	−0.064	0.801	−0.071	0.619	−0.295
0	−0.874	0.632	0.033	−0.002	−0.509	0.977	0.789	−0.594	0.381	0.417	0.457	−0.268	0.448	−0.203	0.441	−0.236
—	1.000	−0.921	0.082	0.002	0.264	−0.901	−0.978	0.889	−0.620	0.347	−0.717	0.119	−0.705	0.067	−0.611	0.198
		1.000	−0.101	−0.001	0.007	0.706	0.957	−0.943	0.689	−0.295	0.790	−0.088	0.791	−0.045	0.655	−0.206
			1.000	0.005	−0.031	−0.020	−0.131	0.159	−0.305	0.152	−0.309	−0.022	−0.171	0.076	−0.164	0.150
				1.000	0.000	−0.009	−0.001	0.000	0.001	0.000	0.001	0.000	−0.001	0.001	0.000	0.000
					1.000	−0.378	−0.222	0.164	0.025	0.334	0.027	0.235	−0.002	0.177	0.068	0.234
						1.000	0.822	−0.620	0.443	−0.465	0.545	−0.328	0.544	−0.272	0.544	−0.298
							1.000	−0.953	0.688	−0.381	0.760	0.138	0.742	−0.096	0.628	−0.254
								1.000	−0.721	0.283	−0.762	0.002	−0.745	−0.028	−0.578	0.186
									1.000	−0.459	0.688	−0.251	0.680	−0.275	0.601	−0.420
										1.000	−0.419	0.858	−0.490	0.834	−0.445	0.848
											1.000	−0.186	0.777	−0.158	0.636	−0.327
												1.000	−0.274	0.913	−0.302	0.830
													1.000	−0.243	0.672	−0.403
														1.000	−0.304	0.827
															1.000	−0.253
																1.000

XV. Observations and Conclusions from *Surveyor VII*

A. Tracking Data Evaluation

In general, DSIF station tracking operations during the *Surveyor VII* mission were effectively implemented. This is judged by the fact that the DSN was able to provide very high-quality data to the orbit determination group such that they were able to meet all orbital accuracy requirements for such events as the midcourse maneuvers, retromotor ignition backup, etc. From the time of first two-way acquisition of the spacecraft over DSS 42 until shortly before retroignition, the spacecraft was almost continuously in two-way lock, and station transfers were rapid and effectively executed. The only major losses of good two-way doppler data occurred during the first passes over DSS 51 and DSS 11. Because of a faulty frequency shifter unit, DSS 51 lost approximately one-half hour of good two-way doppler at the start of the first pass. The problem was eliminated by replacing the unit. During the time of the midcourse maneuver, DSS 11 lost 30 min of doppler resolver data because of a misadjusted potentiometer in the resolver counter; however, the basic two-way doppler data was not affected. The problem was eliminated by correctly adjusting the potentiometer. The resultant effect from these data losses on the mission was negligible. Standard deviations quoted in this section include some data points that were rejected as being of questionable quality for the postflight orbit determination.

1. Pre-midcourse angular tracking. In general, doppler data yields far greater accuracy in the determination of a spacecraft orbit than does angular data and is, therefore, used almost exclusively in the orbit determination process during most of the mission. The one exception is for the launch phase, when little doppler data are available, and a quick determination of the orbit necessitates the use of both doppler and angle data. During the *Surveyor VII* mission, angle data from DSS 42 was used in the orbit determination program during the first pass of this station. To improve the quality of the angular data to be used in the ODP, it is first corrected for antenna optical pointing error as discussed in Section II-B.

Since DSS 42 was the initial acquisition station, the angular data taken by it were the most important angular data for use in the early orbits. These data, when fit through the final postflight orbit, show a bias of −0.030 deg HA and −0.035 deg dec. In previous *Surveyor* missions, the correction coefficients for DSS 42 have usually been more effective in hour angle than in declination. For instance, the hour angle and declination angle biases for DSS 42 averaged over *Surveyor III*, *V*, and *VI* missions are −0.010 deg and −0.040 deg, respectively. This small discrepancy (between previous *Surveyor* missions and that of *Surveyor VII*) is explained by the fact that the corrections are dependent on declination, and for the particular *Surveyor VII* first-pass declination (approximately 10 deg), the corrections produce about the same accuracy in declination as in hour angle. The DSS 51 first pass angular data indicated a bias of +0.035 deg HA and −0.025 deg dec when fit through the final postflight orbit. These values are quite consistent with previous *Surveyor*–DSS 51 experience; for instance, the hour angle and declination biases averaged over *Surveyor III*, *IV*, and *VI* missions are +0.035 deg and −0.020 deg, respectively. The DSS 61 angular data (uncorrected) showed biases of −0.020 deg HA and −0.015 deg dec.

2. Pre-midcourse phase doppler tracking. *Surveyor VI* marked the first use of doppler resolver data during the inflight portion of a *Surveyor* mission, and considerable operational confidence was gained in its use; for *Surveyor VII*, all participating stations were equipped with doppler resolvers and the data were, of course, used inflight. In measuring doppler frequencies, the TDH system counts the number of signal zero crossings during a given time interval; this signal differs from the actual doppler frequency by fractions of a cycle which are alternately lost from one time-interval and erroneously added to the next. This error, commonly referred to as truncation error, depends on the data sample rate (clearly, the longer the sample interval, the smaller the relative error); for 60-s count data, this truncation error produces a standard deviation of approximately 0.008 Hz in two-way doppler data. The doppler resolver effectively measures the fraction of a cycle from the start of a time-interval to the first zero crossing, and correctly adds it to, or subtracts it from, the basic frequency measurement. The net result of the use of the doppler resolver for good two-way data is a reduction of the standard deviation approximately by a factor of 4, or by about 0.002 Hz for 60-s count data.

Tidbinbilla Deep Space Station, the first station to view the spacecraft after injection, began taking good two-way, 10-s count doppler data at 07:28:02 GMT on January 7, 1968. The sample rate was changed to 60-s at 08:00:02, and the spacecraft was transferred to DSS 51 at 12:00:02. The early data from DSS 42 was acceptable, although postflight analysis revealed a probable time bias. It showed a standard deviation of 0.005 Hz—a quite nominal figure for a combination of 60-s count and 10-s count data. The Johannesburg Deep Space Station, which was in the

two-way mode from 12:00:02 to 14:00:02 and then, again, from 18:00:02 to 21:20:02, took somewhat noisy data, which showed a standard deviation of approximately 0.007 Hz for the combined period. This higher-than-expected standard deviation can probably be attributed to a slight degradation of the data during the first portion of this station's two-way track, when trouble was encountered with a frequency shifter unit. First pass two-way doppler data from Robledo Deep Space Station was quite nominal, showing a standard deviation of 0.005 Hz. The Pioneer Deep Space Station took quite noisy data during the first (pre-midcourse) pass; the two-way doppler residuals indicated a standard deviation of 0.025 Hz for a combination of 60-s and 10-s count data. This high noise was caused by the previously mentioned doppler resolver problem encountered by DSS 11 during their first pass. The noisy DSS 11 data were eliminated from postflight orbit computations. Residuals from DSS 42, DSS 51, DSS 61, and DSS 11 for *Surveyor VII* first-pass period are shown in Fig. 69.

Early analysis of the *Surveyor VII* trajectory indicated a midcourse maneuver during the first pass over DSS 11 would be most advantageous, and therefore, the midcourse maneuver was executed during this pass. Engine ignition was programmed for January 7, at 23:30:09, with a total burn time of 11.35 s ($\approx$11 m/s). Results of the maneuver as seen in the two-way doppler data from DSS 11 are presented in Fig. 63. As can be seen in the data, the midcourse maneuver resulted in a doppler shift over DSS 11 of approximately +40 Hz.

3. Post-midcourse phase doppler tracking. All post-midcourse orbit computations used only two-way doppler from the prime stations, DSS 51, DSS 42, DSS 61, and DSS 11. Two-way doppler data ranging from very good to excellent were returned during this period. The DSS 11 two-way doppler residuals during the first pass (post-midcourse) show a standard deviation of 0.0035 Hz—a quite nominal figure for a combination of 60-s and 10-s count data. Second pass two-way doppler residuals show a somewhat high standard deviation of 0.0065 Hz—a result of three bad doppler resolver points. Third pass two-way doppler residuals from DSS 11 show a characteristic drift that, probably, can be attributed to near-moon trajectory model errors. Uniformly good two-way doppler data were taken by DSS 42 during the second and third passes; these data showed a standard deviation of 0.004 Hz. Third pass data from DSS 51 showed a nominal standard deviation of 0.0045 Hz. Finally, DSS 61 took uniformly excellent two-way doppler data during the second and third passes; these data produced a standard deviation of 0.002 Hz. Two-way doppler residuals for all four principal tracking stations for these passes are shown in Fig. 71.

4. Touchdown phase doppler data. Final inflight calculations by the orbit determination group indicated a retroignition time of 01:02:16 GMT, January 10, 1968. A soft landing occurred at 01:05:28 after a flight of 66 h, 35 min, 27 s. The results of the retroengine burn as seen in the one-way doppler data at DSS 11 are presented in Fig. 66.

B. Comparison of Inflight and Postflight Results

The orbit determination inflight results can be evaluated by comparing them to the results obtained from the postflight computations. The degree to which these results agree is influenced primarily by the success attained in detecting and eliminating bad or questionable tracking data from the inflight computations, and accounting for all trajectory perturbations. Of these, the largest variations are usually caused by bad or questionable data resulting from equipment malfunction, incorrect time information, or incorrect frequency information. Other than gross blunder points, these data are not easily detected unless two-way doppler data are available from more than one station. That is, the least squares method used to fit data in the ODP gives no information on constant data biases when data are available from only one station; a comparison can be made only when data from more than one station are available. Furthermore, data must be available from three or more stations in order to isolate bad blocks of data.

The most meaningful comparison between inflight and postflight orbit determination results can be made by examining the critical target parameters—namely, the unbraked impact time and impact location. These results are summarized in Table 65. In the table, it can be seen that *the inflight premaneuver impact point was in error by 0.073 deg in latitude and 0.022 deg in longitude.* This is well within the uncertainty associated with the inflight estimate. The inflight postmaneuver impact point associated with the orbit solution (5 POM YD) used for the terminal attitude maneuver computations was in error by 0.041 deg in latitude and 0.041 deg in longitude. It should be noted that these errors are also within the stated uncertainties associated with the inflight estimates. The inflight predicted unbraked impact time used to provide the AMR backup was in error by 0.680 s, which was within the 1σ stated uncertainty of 0.700 s.

The best estimate of the landing point determined by transit tracking data (i.e., current best postmaneuver

Fig. 72. *Surveyor VII* landing location

Table 65. Summary of target impact parameters

Source	Estimated impact or landed location		Uncertainty about estimated impact point (1σ dispersion ellipse)			Estimated unbraked impact time, GMT (Jan. 10, 1968)	1σ uncertainty in estimated unbraked impact time, s
	Latitude, (deg)	Longitude, (deg)	SMAA, (km)	SMIA, (km)	THETA, (deg)		
Premaneuver uncorrected							
Inflight OD	−5.936	5.392	25.0	9.0	112.7	01:02:53.534	5.630
Postflight OD	−6.009	5.4144	15.0	5.0	107.1	01:02:52.983	2.771
Postmaneuver transit							
Inflight OD	−41.161	348.808	11.7	5.5	68.22	01:02:47.393	0.700
Postflight OD (5POM YD)	−41.202	348.767	2.5	1.0	32.91	01:02:47.914	0.500
Observed unbraked impact time	—	—	—	—	—	01:02:48.31	0.050
Post landing							
Postflight OD (adjusted)	−41.021	348.560					
Jaffe (*Lunar Orbiter*)	−40.95	348.560					
Post touch-down OD	−40.86	348.473					

orbit) and the landing points determined by independent observations are presented in Table 65. One of the independent observations was obtained by processing tracking data from the landed spacecraft; the other one was obtained via optical methods, by correlating *Surveyor VII* television photos of surrounding lunar horizon features with the *Lunar Orbiter* photos of the same lunar region. In Fig. 72 it can be seen that the estimated location based on the preliminary analysis of the landed spacecraft tracking data falls within the 3σ dispersion ellipse associated with the transit location. The estimate based on the *Lunar Orbiter* photos is also within the 3σ uncertainty of the transit estimate. The inflight unbraked impact time and impact time predicted by the current best postmaneuver orbit solution differ by 0.521 s.

Based on the results of the comparison between inflight and postflight results, it may be concluded that all OD requirements were met.

XVI. Analysis of Air Force Eastern Test Range (AFETR) Tracking Data, *Surveyor VII*

The AFETR supported the *Surveyor* missions by computing injection conditions and classical orbital elements for the parking orbit, the spacecraft transfer orbit, and the *Centaur* post-retromaneuver orbit. The injection conditions computed by the AFETR were relayed to the SFOF in Pasadena where they could be used as the initial values for early JPL orbit computations. The AFETR also transmitted initial acquisition information to the SFOF, from which it could be relayed to the Deep Space Stations. The input for the AFETR calculations is the *Centaur* C-band tracking data obtained from various AFETR and MSFN tracking stations. The locations of these stations are given in Table 66.

Table 66. AFETR station locations used for JPL inflight transfer orbit, *Surveyor VII*

Station	Radar type	Geocentric radius, km	Geocentric latitude, deg	Longitude, deg
Carnarvon	FPQ-6	6374.464	−24.7508	113.71608
Tananarive	FPS-16	6377.2402	−18.882671	47.315050
Pretoria	MPS-25	6375.7617	−25.7960	28.35670
Twin Falls	FPS-16	Coordinates given below		
Ascension	TPQ-18	6377.9609	−7.9223	345.59729
Antigua	FPQ-6	6376.3798	17.0349	298.20663
Bermuda	FPS-16	6372.099	32.1744	295.34620
Grand Turk	TPQ-18	6375.3547	21.3313	288.86751

Coordinates of *Twin Falls* ship as reported on launch day were: 23.7°S lat (geodetic); 4.0°E lon.

Table 67. Transfer orbit solutions computed on Pretoria C-band data

Geocentric position and velocity	AFETR inflight solution	Epoch Jan. 7, 1968, 07:27:00.000 GMT		JPL postflight solution		
		JPL inflight solution	Best JPL inflight DSS solution	1	2	3
x, km	9447.7483	9447.7557	9448.6578	9447.3996	9446.6157	9447.7667
y, km	−6126.8163	−6125.0613	−6126.9896	−6125.1094	−6122.4572	−6126.8950
z, km	−4455.7700	−4464.8462	−4458.0533	−4453.8871	−4454.2424	−4449.7067
Dx, km/s	7.9178403	7.9198404	7.9198541	7.9182465	7.9172418	7.9183976
Dy, km/s	1.4094392	1.4091096	1.4086390	1.4107089	1.4128928	1.4097481
Dz, km/s	0.10407639	0.098247365	0.10225866	0.10571085	0.10597140	0.10845327
Encounter parameters						
B, km	2947.30	2040.01	2075.45	2842.22	3250.06	2859.92
B • TT, km	2926.51	1993.36	2044.16	2826.31	3234.74	2850.97
B • RT, km	349.46	433.77	359.04	300.32	315.27	226.00
SMAA (1σ), km	—	1625.89	39.97	65.24	438.56	236.97
Latitude, deg	−5.789	−7.414	−5.936	−4.873	−5.170	−3.510
Longitude, deg	28.814	4.389	5.392	25.562	38.846	26.143
Unbraked Impact on 1/10/68, GMT	01:39:48.400	00:58:08.146	01:02:53.534	01:39:57.637	02:00:48.550	01:41:41.260

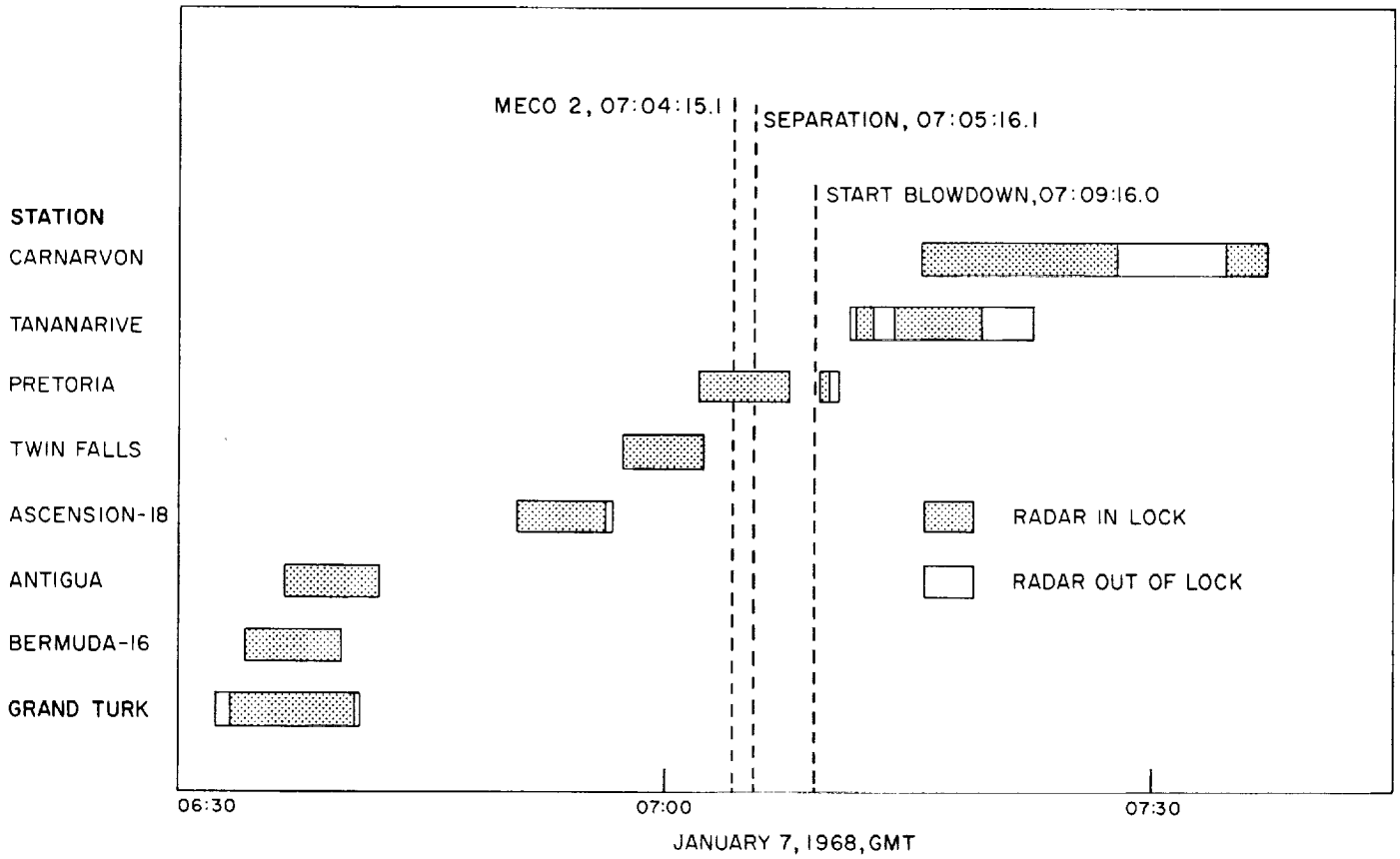

Fig. 73. *Surveyor VII* AFETR tracking coverage

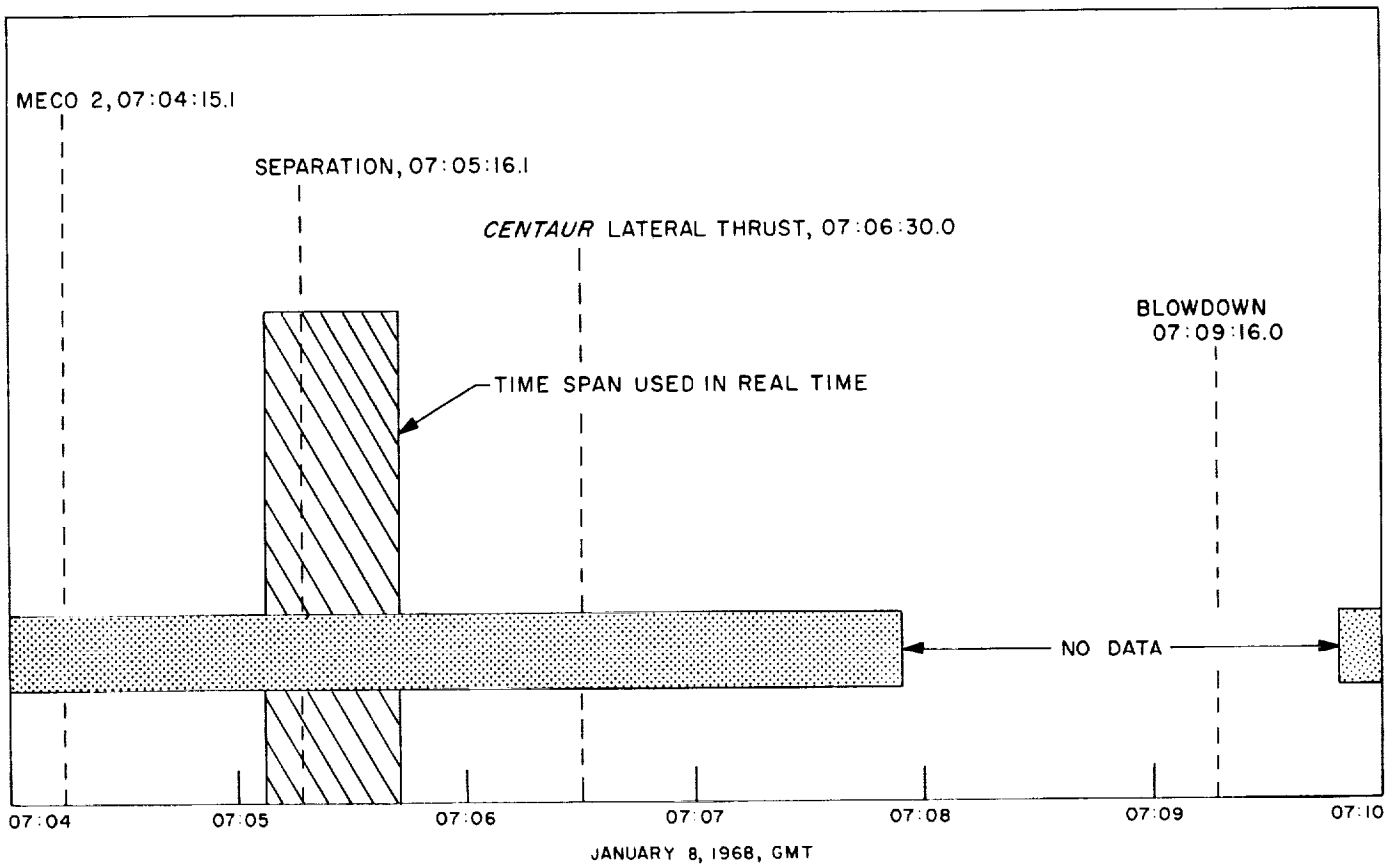

Fig. 74. Transfer orbit data for *Surveyor VII*

In addition to fulfilling these requirements, the AFETR transmitted the C-band tracking data taken during the transfer orbit and the *Centaur* post-retromaneuver orbit to the SFOF. The transfer orbit data was used to compute an early JPL transfer orbit based solely on the C-band data. This early JPL orbit was used as a backup, should unusual circumstances cause a failure of the AFETR orbit computation system. Under normal conditions, the early JPL orbit is used as a quick check on the AFETR transfer orbit. The *Centaur* post-retromaneuver orbit was made available to verify the *Centaur* retromaneuver was performed properly, ensuring that the *Centaur* will not impact the moon and that the spacecraft would be separated from the booster sufficiently to prevent the Canopus sensor on board the spacecraft from locking up on the *Centaur*. The AFETR tracking coverage for *Surveyor VII* is shown in Fig. 73.

A. Analysis of Transfer Orbit Data

For *Surveyor VII*, Pretoria was the source of transfer orbit C-band data. Figure 74 gives a time-history of the spacecraft's pass over Pretoria; the starts of various spacecraft events are also shown. Pretoria provided data during the time span nominally used for C-band transfer orbit solutions (from MECO 2 to spacecraft–*Centaur* separation). There was a 2 min loss of data shortly after the start of *Centaur* lateral thrust, but the earlier data was available, so this loss was not critical.

Table 67 shows all the transfer orbit solutions computed on the Pretoria C-band data. In addition, the best inflight solution based on pre-midcourse DSS tracking data is given. This solution is presented for comparison purposes.

The AFETR inflight solution shown was based on Pretoria data from 07:04:18 to 07:07:15 GMT. If the short arc of data used is considered, this solution compares rather well to the best inflight solution based on pre-midcourse DSS tracking data.

The JPL inflight solution presented in this table was based on Pretoria data between 07:05:06 and 07:05:42 GMT. This very short time span of data yields a solution

very close to the best inflight solution based on pre-midcourse DSS tracking data. The difference in GMT of unbraked impact is less than 5 min, and the impact point of the DSS solution is well within the impact uncertainty ellipse of the C-band solution. The tracking data residuals for JPL inflight solution are shown in Fig. 75.

During postflight analysis, three different C-band data solutions were tried. The data span and data statistics for the JPL inflight solutions and postflight solutions are shown in Table 68.

Postflight solution 1 used all Pretoria C-band data from MECO 2 until the start of *Centaur* blowdown. This solution yielded the smallest uncertainty in the various parameters merely because it contained the most data points. However, use of all the C-band data seemed to degrade the solution somewhat from the inflight solution. This can be judged by comparing encounter parameters and GMT of unbraked impact with the best inflight DSS solution.

Postflight solution 2 used all Pretoria C-band data from MECO 2 until spacecraft–*Centaur* separation. After the

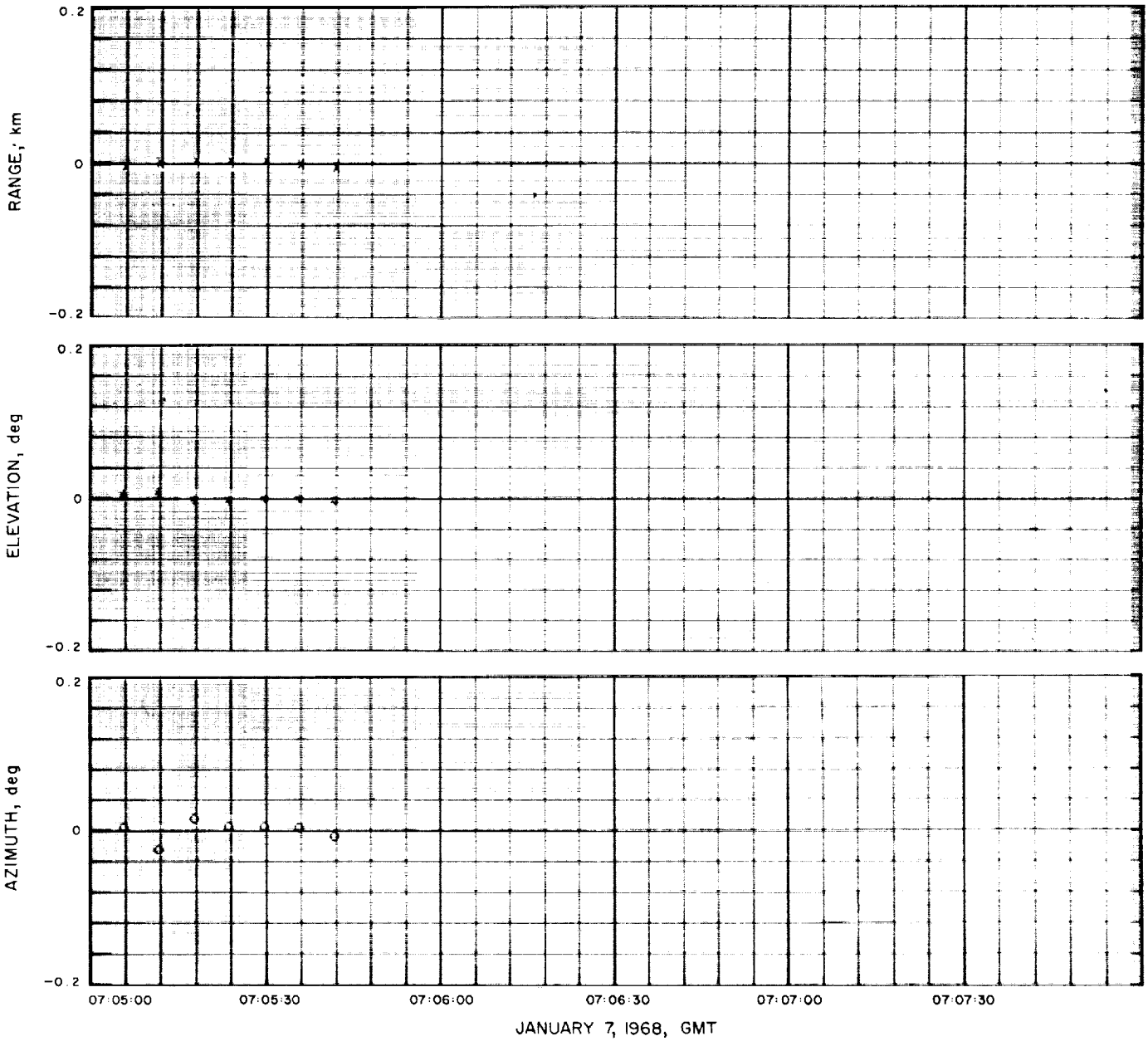

Fig. 75. Pretoria tracking data residuals for inflight transfer orbit solution, *Surveyor VII*

Table 68. Data spans and data statistics for JPL C-band transfer orbit solutions

Solution	Data type	Data span, GMT		Number of points	Standard deviation	Mean error
		Start	End			
JPL inflight	Range, km	07:05:06	07:05:42	7	0.00337	0.0000207
	Azimuth, deg	07:05:06	07:05:42	7	0.0121	−0.000264
	Elevation, deg	07:05:06	07:05:42	7	0.00359	−0.000149
JPL postflight 1	Range, km	07:04:18	07:07:54	37	0.00926	−0.000816
	Azimuth, deg	07:04:18	07:07:54	37	0.0632	0.00647
	Elevation, deg	07:04:18	07:07:54	37	0.0241	0.00328
JPL postflight 2	Range, km	07:04:18	07:05:18	11	0.00614	−0.000920
	Azimuth, deg	07:04:18	07:05:18	11	0.107	0.0150
	Elevation, deg	07:04:18	07:05:18	11	0.0126	0.0119
JPL postflight 3	Range, km	07:05:24	07:07:54	26	0.00686	−0.000232
	Azimuth, deg	07:05:24	07:07:54	26	0.0155	−0.000193
	Elevation, deg	07:05:24	07:07:54	26	0.0258	−0.00315

spring separation between the spacecraft and *Centaur*, the C-band radars actually track the C-band transponder on the *Centaur*, not the spacecraft. It was felt that because of the bias introduced through the spring separation and, also because of subsequent maneuvers by the *Centaur* that use of data before separation, only, might improve the transfer orbit solution. However, such use again degraded the solution from the JPL inflight solution.

Postflight solution 3 used all Pretoria C-band data from spacecraft–*Centaur* separation until start of *Centaur* blowdown. For reasons discussed above, it was expected that this solution would not yield as good a solution as the JPL inflight solution. This run was made for the sake of completeness and the results were as expected.

B. Conclusions From the Postflight Analysis of the Transfer Orbit Data

Pretoria was an excellent source of C-band transfer orbit data for the *Surveyor VII* mission. By use of a short span of data near spacecraft–*Centaur* separation, it was possible to attain an inflight solution that compared very favorably with the best inflight pre-midcourse DSS solution. On only one other *Surveyor* mission (that of *Surveyor II*) was the C-band data of sufficient quality to yield as good an inflight solution.

Three different postflight solutions were tried with different time spans of the Pretoria C-band data. All three postflight solutions compare less favorably to the best inflight DSS solution. It appears from the postflight analysis that the time span of data used for the inflight C-band transfer orbit solution was an optimum. Other than the missing 2 min of C-band data, there was no problem in using the Pretoria data to yield a solution consistent with the best inflight pre-midcourse DSS solution.

C. Analysis of Post-Retromaneuver Orbit Data

Centaur C-band tracking data from Carnarvon and Tananarive were available for post-retromaneuver orbit computations. Although Carnarvon provided about 21 min of data, about 7 min of this data was unusable (see Fig. 73) because the radar lost lock on the C-band transponder. Tananarive provided about 9 min of data, but the last 4 min were out-of-lock.

The AFETR inflight post-retromaneuver orbit solution was computed on Carnarvon data only. The data time span used was from 07:16:0.00 to 07:22:54.00 GMT. Several different JPL postflight solutions were tried with different combinations of the data.

Some solutions are presented in Table 69. In addition, the data spans used for the JPL postflight solutions and the associated statistics of the tracking data residuals are shown in Table 70.

Postflight solution 1 used all in-lock *Centaur* C-band data available from both Carnarvon and Tananarive. These data yielded a solution in good agreement with the AFETR inflight solution. An examination of the tracking data residuals shown in Fig. 76 shows that the Tananarive elevation and azimuth angles seem to be slightly biased in this solution. While some bias between the stations is to be expected, a bias of 0.1 deg in the Tananarive angle data seems somewhat high.

Postflight solution 2 used only the Tananarive data. While the biases in the Tananarive angle data were

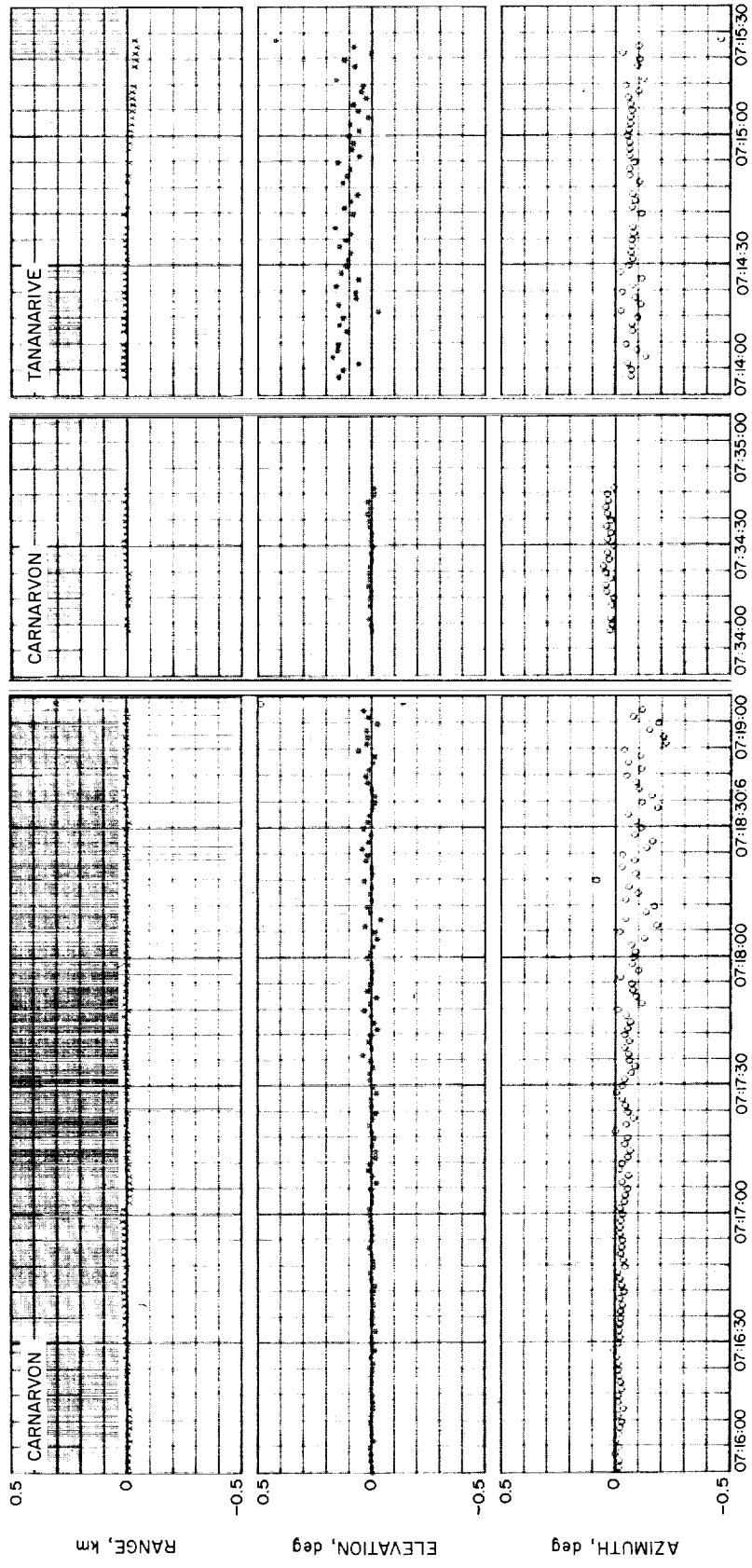

Fig. 76. Carnarvon and Tananarive tracking data residuals for postflight post-retromaneuver solution 1, *Surveyor VII*

Table 69. Post-retromaneuver orbit solutions (Epoch January 7, 1968, 07:17:00.000 GMT)

Geocentric inertial position and velocity	Solution				
	AFETR inflight	Postflight 1	Postflight 2	Postflight 3	Postflight 4
x, km	4274.9996	4274.4569	4274.6375	4273.8462	4275.4616
y, km	−6618.2484	−6618.5905	−6629.6963	−6617.9521	−6619.9740
z, km	−4270.8594	−4269.6775	−4266.0137	−4270.8592	−4266.9568
Dx, km/s	9.3019849	9.3023066	9.3017521	9.3022977	9.3024942
Dy, km/s	0.025501502	0.025384672	0.017247394	0.024557972	0.025599959
Dz, km/s	−0.83395367	−0.83196172	−0.83134001	−0.83296669	−0.82816187
Encounter parameters					
B, km	24427.05	24542.30	21962.84	24621.68	24503.33
B • TT, km	24403.34	24519.45	21934.46	24599.92	24481.96
B • RT, km	1075.90	1058.77	1116.25	1035.25	1023.20
Closest approach 1/10/68, GMT	13:19:15.000	13:23:59.672	12:11:15.205	13:23:45.987	13:26:31.740

Table 70. Data spans and data statistics for JPL post-retromaneuver orbit solutions

Solution	Station	Data type	Data span, GMT		Number of points	Mean error	Standard deviation
			Start	End			
Postflight 1	Carnarvon	Azimuth, deg	07:16:00	07:36:54	141	−0.0442	0.0545
		Elevation, deg	07:16:00	07:36:54	141	0.000740	0.0142
		Range, km	07:16:00	07:36:54	141	−0.00118	0.00698
	Tananarive	Azimuth, deg	07:14:18	07:19:24	48	−0.0753	0.0245
		Elevation, deg	07:14:18	07:19:24	48	0.0945	0.0442
		Range, km	07:14:18	07:19:30	45	−0.00377	0.0180
Postflight 2	Tananarive	Azimuth, deg	07:16:00	07:19:24	48	0.0000392	0.0255
		Elevation, deg	07:16:00	07:19:24	48	−0.00139	0.0419
		Range, km	07:16:00	07:19:30	45	−0.000178	0.00561
Postflight 3	Carnarvon	Azimuth, deg	07:16:00	07:36:54	141	−0.00641	0.0368
		Elevation, deg	07:16:00	07:36:54	142	−0.00280	0.0185
		Range, km	07:16:00	07:36:54	142	−0.0000254	0.0260
Postflight 4	Carnarvon	Range, km	07:16:00	07:36:54	141	−0.00208	0.00663
	Tananarive	Range, km	07:14:18	07:19:30	45	−0.00119	0.00543

removed, the latter part of the Carnarvon azimuth data now appeared to be of bad quality. The Carnarvon azimuth data gained in noise level and jumped from a negative bias to a positive bias.

Postflight solution 3 used only the Carnarvon data. Since there was about three times as much Carnarvon data as Tananarive, the Carnarvon data dominated postflight solution 1 (which contained all data). Thus, postflight solutions 1 and 3 are in close agreement; but by weighting out the Tananarive data, it was not possible to observe anything but a small bias in the weighted out data.

Postflight solution 4 used only the range data from Carnarvon and Tananarive. Since there appeared to be problems with the angle data from both stations, it was thought the best solution would be one that excluded all angle data.

D. Conclusions on the Post-Retromaneuver Orbit Data

The *Centaur* C-band post-retromaneuver orbit data was very clean (with few blunder points) in comparison with earlier *Surveyor* missions. However, there definitely was a problem with the Carnarvon azimuth data. The early part of these data was slightly negatively biased, then jumped to a slight positive bias. The Tananarive angle data seemed biased by about 0.1 deg. Because of the problems with the angle data, it was felt the best post-retromaneuver orbit solution was one based on range data, only.

References

1. Warner, M. R., and Nead, M. W., *SPODP—Single Precision Orbit Determination Program,* Technical Memorandum 33-204. Jet Propulsion Laboratory, Pasadena, Calif., Feb. 15, 1965.
2. White, R. J., et al., *SPACE—Single Precision Cowell Trajectory Program,* Technical Memorandum 33-198. Jet Propulsion Laboratory, Pasadena, Calif., Jan. 15, 1965.
3. Kizner, W., *A Method of Describing Miss Distances for Lunar and Interplanetary Trajectories,* External Publication 674. Jet Propulsion Laboratory, Pasadena, Calif., Aug. 1, 1959.
4. Clarke, V. C., Jr., "Constants and Related Data for Use in Trajectory Calculations," Technical Report No. 32-604. Jet Propulsion Laboratory, Pasadena, Calif., Mar. 6, 1964.
5. Vegos, C. J., and Trask, D. W., "*Ranger* Combined Analysis, Part II: Determination of the Masses of the Earth and Moon from Radio Tracking Data," *The Deep Space Network,* Space Programs Summary 37-44, Vol. III, pp. 11–28. Jet Propulsion Laboratory, Pasadena, Calif., Mar. 31, 1967.
6. Surveyor Project Staff, *Surveyor V Mission Report, Part I. Mission Description and Performance,* Technical Report 32-1246. Jet Propulsion Laboratory, Pasadena, Calif., Mar. 15, 1968.
7. Surveyor Project Staff, *Surveyor VI Mission Report, Part I. Mission Description and Performance,* Technical Report 32-1262. Jet Propulsion Laboratory, Pasadena, Calif. (To be published)
8. Surveyor Project Staff, *Surveyor VII Mission Report, Part I. Mission Description and Performance,* Technical Report 32-1264. Jet Propulsion Laboratory, Pasadena, Calif. (To be published)
9. O'Neil, W. J., Labrum, R. G., Wong, S. K., and Reynolds, G. W., *The Surveyor III and Surveyor IV Flight Paths and Their Determination from Tracking Data,* Technical Report 32-1292. Jet Propulsion Laboratory, Pasadena, Calif., Sept. 15, 1968.
10. Sjogren, W. L., "*Lunar Orbiter V* Doppler Data Characteristics Using the Doppler Resolver," *The Deep Space Network,* Space Programs Summary 37-47, Vol. III, pp. 11–12. Jet Propulsion Laboratory, Pasadena, Calif., Sept. 30, 1967.

Appendix A

Definition of Doppler Data Types

Three types of doppler data were obtained by the DSN tracking stations – one-way, two-way, and three-way doppler. The following sketches and definitions distinguish the methods.

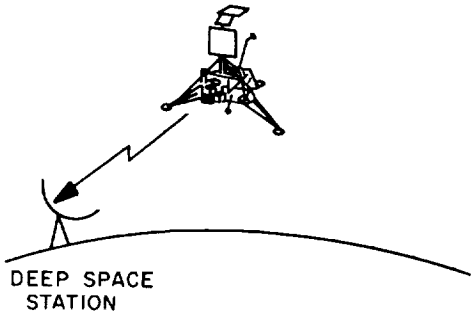

ONE-WAY DOPPLER

The spacecraft transmits to the ground station. The ground station operates in receive mode, only.

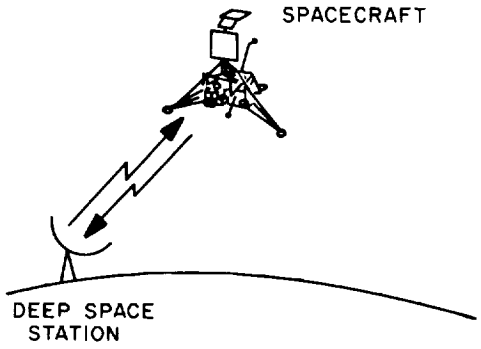

TWO-WAY DOPPLER

The ground station transmits to the spacecraft; the spacecraft retransmits signal to the same ground station. The ground station operates in both transmit and receive modes.

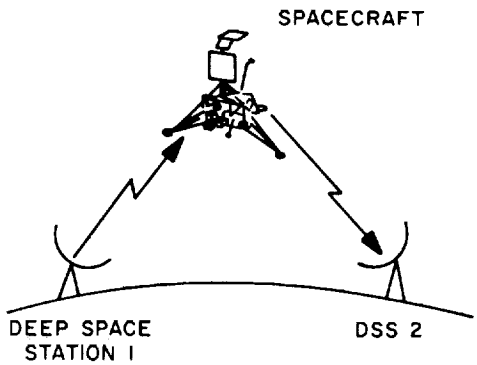

THREE-WAY DOPPLER
(NONCOHERENT)

The first ground station transmits a signal to the spacecraft; the spacecraft retransmits the signal to the second ground station. Station 1 does *not* transmit a reference frequency to station 2.

Appendix B

Definition of the Miss Parameter B

The miss parameter **B** is used at JPL to measure miss distances for lunar and interplanetary trajectories; it is described by W. Kizner in Ref. B-1. The parameter has the desirable feature of being very nearly a linear function of changes in injection conditions.

The osculating conic at closest approach to the target body is used in defining **B**, which is the vector from the target's center of mass, perpendicular to the incoming asymptote. Let $\mathbf{S}_I$ be a unit vector in the direction of the incoming asmyptote. The orientation of **B** in the plane normal to $\mathbf{S}_I$ is described in terms of two unit vectors, **R** and **T**, normal to $\mathbf{S}_I$. Unit vector **T** is taken parallel to a fixed *reference plane*, and **R** completes a right-handed orthogonal system. Figure B-1 illustrates the system.

For *Surveyor*, two reference planes have been used: the plane of the earth's equator **TQ** or the plane of the moon's equator **TT**.

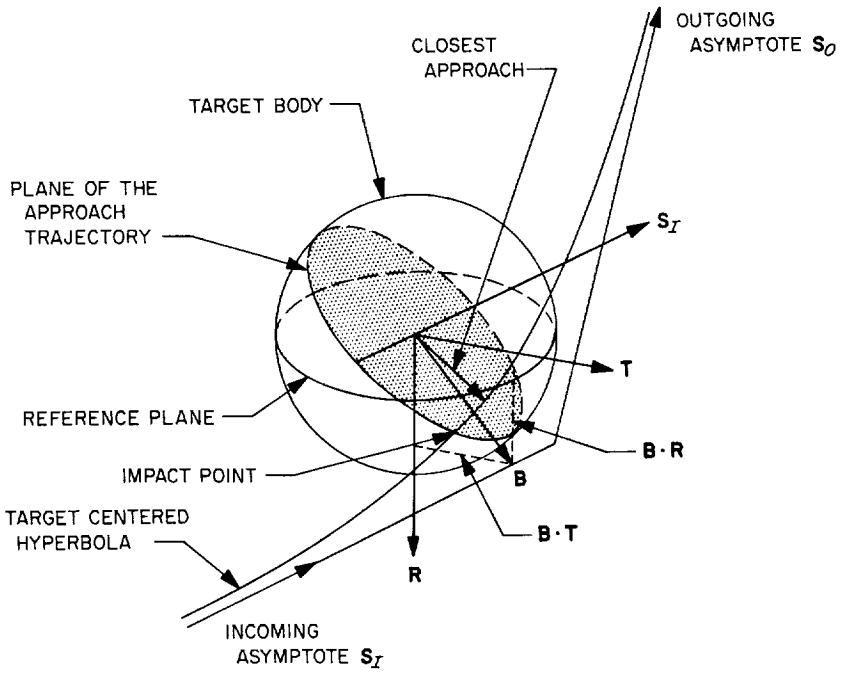

Fig. B-1. Definition of B·T, B·R system